DISSERTATION

AN EXPLORATION OF VIRAL RNA-MEDIATED STRATEGIES TO STALL AND

REPRESS THE CELLULAR EXORIBONUCLEASE XRN1

Submitted by

Phillida A Charley

Department of Microbiology, Immunology, and Pathology

In partial fulfillment of the requirements

For the Degree of Doctor of Philosophy

Colorado State University

Fort Collins, Colorado

Fall 2018

Doctoral Committee:

    Advisor: Jeffrey Wilusz

    Mark Zabel
    Rushika Perera
    Anireddy Reddy

ABSTRACT

AN EXPLORATION OF VIRAL RNA-MEDIATED STRATEGIES TO STALL AND

REPRESS THE CELLULAR EXORIBONUCLEASE XRN1

The regulation of mRNA decay plays a vital role in determining both the level and quality control of cellular gene expression in eukaryotes. Since they are likely recognized as foreign/unwanted transcripts, viral RNAs must also successfully navigate around the cellular host RNA decay machinery to establish a productive infection. This bypass of the cellular RNA decay machinery can be accomplished in many ways, including the sequestering of regulatory proteins or inactivating enzymatic components. One attractive way for RNA viruses to undermine the cellular RNA decay machinery is to target the cellular exoribonuclease XRN1 since this enzyme plays a major role in mRNA decay, appears to coordinate transcription rates with RNA decay rates, and is localized to the cytoplasm and thus readily accessible to cytoplasmic RNA viruses.

We have previously shown that many members of *Flaviviridae* (e.g. Dengue, West Nile, Hepatitis C and Bovine Viral Diarrhea viruses) use RNA structures in their 5' or 3' untranslated regions (UTRs) to stall and repress XRN1. This results in the stabilization of viral RNAs while also causing significant dysregulation of cellular RNA stability (and thus dysregulation of overall cellular gene expression). In this dissertation we first extend this observation to another member of the *Flaviviridae*, Zika virus, by demonstrating that structures in the 3' UTR of the viral genomic RNA can stall and repress XRN1. Significantly, we also demonstrate that the 3' UTR of the N mRNA of the

ambisense segment of Rift Valley Fever virus, as well as two other phleboviruses of the *Phenuiviridae,* also can effectively stall and repress XRN1. This observation establishes XRN1 stalling in an additional family of RNA viruses, in this case in the order *Bunyavirales*. We have mapped the region responsible for XRN1 stalling to a G-rich core of ~50 nucleotides and provide evidence that the formation of a G-quadruplex is contributing to stalling of XRN1.

In addition to phleboviruses, we also detected RNA regions that stall XRN1 in the non-coding regions of two other virus families. The 3' UTRs of all four ambisense transcripts of Junin virus, an arenavirus, stall and repress XRN1. This observation was extended to two additional arenaviruses, suggesting that XRN1 stalling may be a conserved property of the 3' UTRs in the *Arenaviridae*. Finally, we demonstrate that the non-coding RNA from beet necrotic yellow vein virus RNA segment 3 is produced by XRN1 stalling and requires a conserved sequence called the coremin motif. Collectively, these observations establish XRN1 stalling and repression as a major strategy used by many virus families to effectively interface with the cellular RNA decay machinery during infection.

We performed two proof of principle studies to extend the significance of the observation of XRN1 stalling during RNA virus infections. First, since XRN1 stalling may be associated with successful viral gene expression as well as cytopathology, we explored whether we could identify a small molecule compound that could interfere with the knot-like three helix RNA junction structure that stalls XRN1 in the 3' UTR of flaviviruses. We tested several triptycene-based molecules, compounds that have been previously shown to intercalate into three helix junctions and identified four triptycene

derivatives that interfere with XRN1 stalling. Lastly, we explored whether there might be a cellular exoribonuclease that could navigate through the well-characterized flavivirus structure that effectively stalls XRN1. Our efforts focused on the mammalian Dom3z/DXO enzyme which contains both 5' decapping and 5'-3' exoribonuclease activity. Interestingly, recombinant Dom3z/DXO enzyme did not stall on RNAs containing the 3' UTR of either Dengue virus or the Rift Valley Fever Virus N mRNA. This may suggest that there is a molecular arms race of sorts between the cell and the virus for supremacy of regulating the 5'-3' decay of RNA during infection.

ACKNOWLEDGEMENTS

letting me practice my prelim. oral presentation with him. Dr. Joe Russo, who I like to think of as my third advisor in the lab, taught me to do several different experiments. Adam Heck helped to make my graphs pretty, provided statistical analysis, and assisted with protein pull-downs. Dr. Annie Zhang Bargsten provided overall support - including carpooling for a semester. Dr. Aimee Jalkanen always gave me rides home after events like ASV 2014 and for overall support too. Also, I wish to thank the new members of the lab (Cary, Tavo, Dan, and most recently Laura) for discussing science and making the lab a lively place again because for a couple of years I was the only person in the lab.

Lastly, I would like to thank my family for their support throughout graduate school. My sisters for always watching my son while I was working in the lab. My son for understanding the effort I needed to expend to obtain the highest degree I can achieve. My parents and brothers for their personal and financial support. Finally, I'd like to thank all the friends I made over the years who supported me.

TABLE OF CONTENTS

Chapter 1: Introduction

This first chapter will be a review of the literature and is broken into four different sections. Section I will give an overview of the RNA decay pathway and various factors involved in regulating the different pathways. Section II is an overview of how various DNA and RNA viruses interact with the cellular RNA decay machinery. Section III gives evidence of alternative RNA structures that can stall the XRN family of enzymes. Section IV gives insight into the virus families used in this study and why they are good candidates to generate RNAs that could stall and repress XRN1.

Section I: Cellular RNA decay machinery

In all eukaryotic organisms, the cellular messenger RNA (mRNA) decay machinery plays an important role in determining the quality and quantity of gene expression. The RNA decay machinery (Figure 1) is critically responsible for the removal of unwanted, aberrant, or spent transcripts. This section will give insight on how mRNAs are typically degraded.
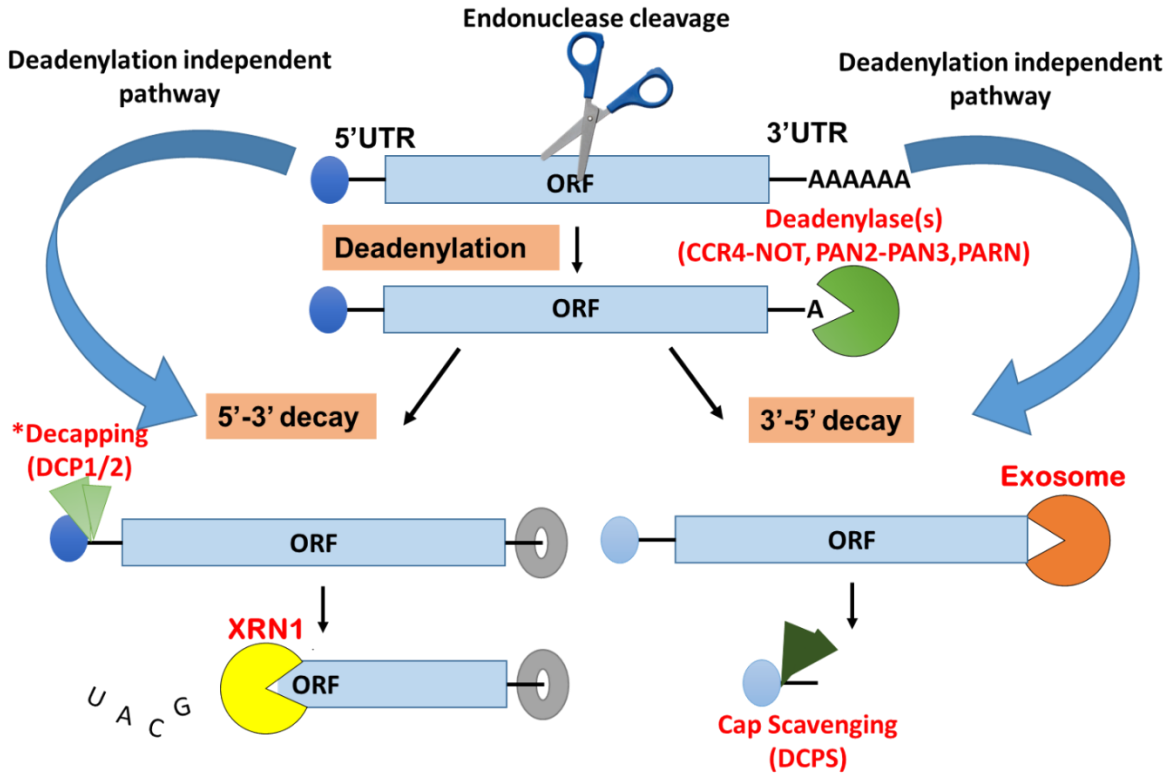
Figure 1. Two major pathways in messenger RNA decay. An mRNA typically has a 5' 7-methyl cap (dark blue oval), an open reading frame (ORF), and a 3' poly(A) tail. mRNA decay will usually begin with deadenylation and then proceed down either the 5'-3' decay pathway (which requires decapping for the major exonuclease (XRN1) to gain access to the transcript) or the 3'-5'decay pathway (in which decay is mediated by the exosome complex). The blue arrows indicate the deadenylation-independent pathway where an endonucleolytic cleavage occurs in the body of the transcript and is directly fed into the 5'-3' or 3'-5' decay pathway. The gray donut represents the Lsm1-7 complex that interacts with the 3' end of deadenylated mRNAs and helps to target the transcript for decapping.

Deadenylation-dependent RNA decay

An mRNA marked for decay will most likely go down the deadenylation-dependent mRNA decay pathway. In this pathway, the first step is deadenylation (Anderson and Parker, 1998). Deadenylation is the process of shortening of the poly(A) tail of the mRNA and is oftentimes the rate-limiting step in the decay of an mRNA (Muhlrad and Parker, 1992; Shyu et al., 1989). Several deadenylases can be involved in the process, but two enzymes - Carbon catabolite repression 4/negative on TATA-less

(CCR4-NOT)/ CCR4 associated factor (CAF1) (Albert et al., 2000; Chen et al., 2001) and poly (A) binding protein-stimulated poly (A) ribonuclease (PAN2-PAN3) (Boeck et al., 1996; Brown et al., 1996) - are generally considered to be the major players. Additional deadenylases that are involved in poly(A) shortening include the poly(A)-specific ribonuclease (PARN) (Körner and Wahle, 1997; Li et al., 2001), nocturnin (Baggs and Green, 2003; Blanco et al., 2017; Delis et al., 2016; Grönke et al., 2009), and most recently the target of EGR1 protein 1 (TOE1, also known as CAF1Z) which is responsible for removing a poly(A) tail from small non-coding RNA during 3' end processing (Table1) (Lardelli et al., 2017; Wagner et al., 2007).

Table 1. Major Deadenylase Enzymes.

Protein name:	Abbreviation:	Function:	References:
Poly (A) binding protein-stimulated poly (A) ribonuclease complex	PAN2-PAN3 complex	Trims poly (A) tails	(Boeck et al., 1996; Brown et al., 1996)
Carbon catabolite repression 4/negative on TATA-less/CCR4 associated factor complex	CCR4-NOT complex	After timming then removes remaining adenosine	(Albert et al., 2000; Chen et al., 2001)
Target of EGR1 protein 1	TOE1 or CAF1Z	Removal of Poly (A) tail from small RNAs	(Lardelli et al., 2017; Wagner et al., 2007)
Nocturnin	NOCT	poly(A) tail regulation of mRNAs associated with circadian responses	(Baggs and Green, 2003; Blanco et al., 2017)
Poly (A)-specific ribonuclease	PARN	Involved in RNA processing and deadenylating AU-rich mRNAs	(Berndt et al., 2012; Helfer et al., 2012; Ishikawa et al., 2016; Shukla and Parker, 2017)

The CCR4-Not and PAN2-PAN3 complex

Current models of deadenylation by the PAN2-PAN3 and CCR4-NOT complex

indicate that poly(A) tail shortening happens in two phases. The first phase requires the

PAN2-PAN3 complex. PAN2 is the subunit that is thought to be involved in the initial

trimming of the poly(A) tail (Yamashita et al., 2005) and PAN3 is the cofactor/regulatory

subunit (Brown et al., 1996; Wolf et al., 2014). PAN3 will form a homodimer that will

then bind to PAN2 to make the complex complete (Schäfer et al., 2014). In humans

there are two isoforms of PAN3 (PAN3S and PAN3L) that can respectively either

promote or suppress PAN2 activity (Chen et al., 2017). PAN3L will diminish the

deadenylase activity of PAN2 and PAN3S has the opposite effect by stimulating

deadenylase activity (Chen et al., 2017). Interestingly, the PAN2-PAN3 complex is

activated by the polyadenylate-binding protein (Pab1) (Boeck et al., 1996), but *in vitro*

can be active without it (Schäfer et al., 2014). After the PAN2-PAN3 complex trims the

poly(A) tail, this allows the CCR4-NOT complex to finish deadenylation in the second

phase in a more processive fashion.

Carbon catabolite repression 4/negative on TATA-less (CCR4-NOT)/ CCR4

associated factor (CAF1) complex is responsible for the majority of deadenylation in

mammalian cells (Albert et al., 2000). Several RNA binding proteins can recruit the

CCR4-NOT complex to mRNAs for deadenylation, such as DDX6 (Ozgur et al., 2015),

Tristetraprolin (TTP) (Fabian et al., 2013; Lykke-Andersen and Wagner, 2005; Sandler

et al., 2011), BTG (Prévôt et al., 2001; Rouault et al., 1998), Pumilio and fem-3 binding

factor (PUF) proteins with Nanos (Nos) (Van Etten et al., 2012; Kadyrova et al., 2007;

Suzuki et al., 2014; Weidmann et al., 2014), and GW182 via specific miRNAs

(Chekulaeva et al., 2011; Fabian et al., 2011; Kuzuoğlu-Öztürk et al., 2016). The CCR4-NOT complex is composed of eight different subunits (NOT1, NOT2, NOT3, NOT4, CCR4, CAF1, CAF40, and MMI1) and all are required for function (Ukleja et al., 2016). The CCR4-NOT subunit 1 is the main scaffold of this multi-component complex and deletion of this protein will induce apoptosis (Ito et al., 2011; Yamaguchi et al., 2018). The Carbon Catabolite Repressor Protein 4 Homolog (also called CCR4 and CNOT6) and the CCR4-associated factor 1 (CAF1) (also known CNOT7) have enzymatic roles in RNA decay. CNOT6 is the major the 3' to 5' catalytically active component (Mittal et al., 2011). CNOT7 has minor catalytically activity for poly(A) tails (Daugeron et al., 2001; Tucker et al., 2001), yet it still appears to be functionally significant in certain instances. In dendritic cells, it was shown CNOT7 regulates mRNA transport, local translation, and synaptic plasticity of cultured cells. The same study also showed that decrease of CNOT7 will lead to impaired cognitive functions (McFleder et al., 2017). A second isoform of CNOT7 was identified called CNOT7v2 that is made through alternative splicing (Chapat et al., 2017). It has no deadenylase activity and does not bind the BTG protein. This isoform can interact with the CCR4-NOT complex and regulate PRMT1-dependent arginine methylation (Chapat et al., 2017). Furthermore, another example of regulation is during germ cell development. The RNA binding protein DND1 is involved in recruitment of the CCR4-NOT complex for survival of primordial germ cells (PGCs) and loss of DND1 will result in loss of PGCs (Yamaji et al., 2017). In addition, deletion of the subunit 3 of the CCR4-NOT complex will lead to lethal cardiomyopathy by dysregulation of the key autophagy regulator ATG7 (Yamaguchi et al., 2018).

Target of EGR1 protein 1 (TOE1, also known as CAF1Z)

The target of EGR1 protein 1 (TOE1) was found to have deadenylase activity on small non-coding RNAs and is localized in the nucleus but can be shuttled to the cytoplasm (Son et al., 2018; Wagner et al., 2007). Recent data suggest that TOE1 is not a major player in the main mRNA decay pathway, but rather is involved in the biogenesis of small nuclear RNA (snRNA) by trimming adenylated 3' ends (Lardelli et al., 2017). TOE1 will also help prevent the degradation of the immature snRNA (Son et al., 2018).

Nocturnin

Nocturnin is a specialized deadenylase involved in poly(A) tail regulation of mRNAs associated with circadian responses (Baggs and Green, 2003; Blanco et al., 2017; Green and Besharse, 1996). Multiple studies in mice have shown optimal expression of nocturnin occurs in a circadian fashion (Garbarino-Pico et al., 2007; Kojima et al., 2010; Wang et al., 2001b) and is regulated by the heterodimeric transcription factor CLOCK/BMAL (Li et al., 2008). Interestingly, a knockout of nocturnin in mice causes resistance to diet-induced obesity, whereas mice over-expressing nocturnin are obese (Green et al., 2007). In goldfish, nocturnin has two isoforms - nocturnin A increases after feeding while nocturnin B expression remains constant (Blanco et al., 2017). In zebrafish, nocturnin B is expressed more in retinal photoreceptor layers and is important for regulating retinal circadian rhythmicity (Yang et al., 2017). In *Arabidopsis thaliana,* nocturnin is called AtHesperin (AtHESP) and plays

a role in stress responses as knockouts of *AtHESP* improve light absorption (Delis et al., 2016).

Poly (A)-specific ribonuclease (PARN)

      Poly (A)-specific ribonuclease (PARN) is located in the nucleus but has the capability to be shuttled into the cytoplasm (Son et al., 2018). This deadenylase has a preference for targeting mRNAs containing AU-rich elements (Helfer et al., 2012; Lin et al., 2007). PARN activity can be enhanced by binding the mRNA 5' cap (Gao et al., 2000; Niedzwiecka et al., 2016; Nilsson et al., 2007; Virtanen et al., 2013; Wu et al., 2009). In addition to a potential role in mRNA deadenylation, PARN is also involved in the processing of Y RNA (Shukla and Parker, 2017), 18S rRNA (Ishikawa et al., 2016; Montellese et al., 2017), snoRNA (Berndt et al., 2012; Dhanraj et al., 2015), telomerase RNA component (TERC) (Boyraz et al., 2016; Moon et al., 2015a; Shukla et al., 2016; Tummala et al., 2015), and scaRNA (Berndt et al., 2012). PARN also displays interesting roles in plant biology. A root-colonizing fungus called *Piriformospora indica* secretes cellotriose which benefits the plant by inducing growth as well as resistance to abiotic stress and biotic diseases. This symbiotic relationship is affected when a single mutation occurs in the gene encoding PARN (Johnson et al., 2018). In humans, mutations in PARN can cause diseases such as familial pulmonary fibrosis, bone marrow failure, and hypomyelination (Dhanraj et al., 2015; Newton et al., 2016; Tummala et al., 2015).

The 3' to 5' decay pathway

The exosome

One of the routes of RNA decay is the 3' to 5' decay pathway. A multi-subunit protein complex called the exosome will bind the deadenylated 3' end of a mRNA and start degrading the body of the transcript (Anderson and Parker, 1998; Mitchell et al., 1997). The exosome has been implicated in processing of small non-coding RNA (Allmang et al., 1999), ribosomal maturation (Schuller et al., 2018), and degrading aberrant RNAs (Kadaba et al., 2004; Sayani and Chanfreau, 2012). The exosome core component is made up of nine non-nucleolytically active subunits and will bind to the RRP44 subunit (also known as DIS3), which is the active nuclease (Kowalinski et al., 2016; Zinder et al., 2016). The six-subunit PH-like ring (RRP46-RRP45, RRP41-RRP42, RRP43- MTR3) forms a core structure via three heterodimers that bridges to the S1/KH ring (RRP40, RRP4, and CSL4) (Liu et al., 2006). The RRP6 protein will also bind to the S1/KH ring to activate the nuclear RNA exosome (Wasmuth and Lima, 2017; Zinder et al., 2016). In yeast, the SKI-complex will funnel RNA through the exosome (Halbach et al., 2013). RBM7, ZCCHC8 and MTR4 are three other co-factors required for effective RNA targeting by the exosome (Puno and Lima, 2018; Wasmuth et al., 2017). In humans, RRP44 (DIS3) has two alternatively spliced isoforms that are both catalytically active (Robinson et al., 2018). Multiple myeloma patient samples, as well as other cells from cancer patients, tend to have higher levels of one isoform than the other, which could be a possible way to identify the disease since healthy cells have similar of levels of both isoforms (Robinson et al., 2018). Once the exosome degrades the mRNA to the 5' cap of the mRNA, a scavenger decapping enzyme (DcpS) will

hydrolyze the cap to complete the degradation of the mRNA (Liu et al., 2002, 2008; Wang and Kiledjian, 2001).

RNA uridylation

In humans, DIS3-like exoribonuclease 2 (DIS3L2) (Malecki et al., 2013) is a member of DIS3 family of proteins that is independent from the exosome and targets poly(U) tails but can also degrade poly(A) tails (Chang et al., 2013; Lubas et al., 2013; Ustianenko et al., 2013). The Lin28-let-7 pathway is responsible for uridylation of the pre-let-7 miRNA by recruiting 3′ terminal uridylyl transferases (TUTase), Zcchc11 (TUT4) and Zcchc6 (TUT7), to inhibit dicer-mediated pre-miRNA processing (Hagan et al., 2009; Heo et al., 2008, 2009; Piskounova et al., 2011; Thornton et al., 2012). This led to the discovery that TUT/DIS3L2 is a surveillance system for aberrant small non-coding and ribosomal RNAs (Ishikawa et al., 2018; łabno et al., 2016; Pirouz et al., 2016; Reimão-Pinto et al., 2016; Ustianenko et al., 2013, 2016). In humans, mutations in DIS3L2 have been associated with Perlman syndrome (Astuti et al., 2012). Furthermore, DIS3L2 is essential for regulation of cell growth and division (Higashimoto et al., 2013).

The 5' to 3' decay pathway

The 5'-3' decay pathway is currently considered to be the major route of mRNA decay. After deadenylation, the mRNA will go through decapping to generate an access

point for 5'-3' exoribonucleases to come in and degrade the RNA. Information on decapping and several 5'-3' exoribonucleases is presented below.

Decapping

Decapping is an important part of RNA decay and require enhancers such as the LSM 1-7 protein complex (Bouveret et al., 2000; Tharun et al., 2000; Vindry et al., 2017), DCP1 (Beelman et al., 1996; Charenton et al., 2016; Mugridge et al., 2018), PATL1 (Pat1) (Fourati et al., 2014; Vindry et al., 2017), DDX6 (Dhh1) (Mas et al., 2006; Wurm et al., 2016), LSM14 (Scd6) (Fromm et al., 2012; Miller et al., 2018), and a set of EDC proteins (Harigaya et al., 2010; Kshirsagar and Parker, 2004; Mugridge et al., 2018; Wurm et al., 2016). The decapping enzymes are responsible for hydrolyzing the 5' 7-methylguanosine cap by releasing 7-methylguanosine 5′-diphosphate, thus creating a monophosphate on the 5' end of the mRNA (van Dijk et al., 2003; Dunckley and Parker, 1999; Lykke-Andersen, 2002; Song et al., 2010; Wang et al., 2002). Two characterized enzymes responsible for the decapping reaction, DCP2 and NUDT16, are part of the Nudix superfamily of hydrolases (Li et al., 2011; Song et al., 2013). Activation of DCP2 requires binding of DCP1 to the N-terminal regulatory domain (NRD) to create the DCP1-DCP2 complex (Vindry et al., 2017). These enzymes generally prefer to work on a certain set of transcripts. NUDT16, for example, will decap short unmethylated dinucleotide capped RNAs (Grzela et al., 2018). This opens the possibility that other decapping enzymes exist in the cell. In recent years, several other enzymes have also been identified to have decapping activity (NUDT2, NUDT3, NUDT12, NUDT15,

NUDT17, and NUDT19) (Song et al., 2010). The relative contribution to decapping of cellular transcripts remains to be explored.

5'-3'exoribonuclease XRN1

The major decay enzyme in the 5'-3' decay pathway are members of the XRN family of exoribonucleases. Messenger RNAs will be degraded by the XRN family after decapping has occurred. Information on several XRNs and graphical amino acid alignment (Figure 2) from different organisms is presented below.

Figure 2. Graphical alignment of amino acid sequence of several XRNs from varies of species. Amino acid alignment of XRN from different species with Geneious version 11.1.5. The black represents similarities between the difference amino acid sequences. Amino acid sequences used are *Homo sapiens* (NCBI accession number: NP_061874), *Kluyveromyces lactis* (NCBI accession number: CAG98788), *Saccharomyces cerevisiae* XRN1 (NCBI accession number: AAA35219), *Culex quinquefasciatus* (NCBI accession number:EDS29953), *Drosophila melanogaster* (NCBI accession number: CAB43711), *Mus musculus* (NCBI accession number: NP_036046), *Arabidopsis thaliana* (NCBI accession number: AAG40731), and *Saccharomyces cerevisiae* RAT1 (NCBI accession number: NP_014691).

Saccharomyces cerevisiae XRN1 (KEM1, SKI1, SEP1)

To date, most information on the 5'-3' exoribonuclease XRN1 has been obtained from studies in *Saccharomyces cerevisiae*. XRN1 is responsible for degrading 5' monophosphorylated RNA transcripts (Jinek et al., 2011) in the cytoplasm, for example the products of decapping (Hsu and Stevens, 1993; Muhlrad et al., 1994). Yeast XRN1 is a highly processive enzyme that has a practical use in the molecular biology laboratory – it is used to remove ribosomal RNAs from total RNA samples for RNA-seq studies (He et al., 2010). In addition to its role in mRNA decay, XRN1 is responsible for the removal of a wide range of unwanted RNAs in the cell including aberrantly spliced mRNAs (Harigaya and Parker, 2012), long non-coding RNAs (e.g. XRN1-sensitive unstable transcripts (XUTs) (Van Dijk et al., 2011; Wery et al., 2016, 2018) and tRNA introns (Whipple et al., 2011; Wu and Hopper, 2014). Deletion of cytoplasmic XRN1 is not lethal in yeast but does have significant physiological ramifications (Heyer et al., 1995; Kenna et al., 1993) such as reduced growth rate (Larimer and Stevens, 1990), microtubule destabilization (Interthal et al., 1995), reduced sporulation (Tishkoff et al., 1991), and defects in filamentous growth (Kim and Kim, 2002). Lastly, XRN1 also plays a role in transcriptional buffering - a communication that occurs in yeast between RNA decay rates and RNA synthesis rates to maintain homeostasis of gene expression. (Abernathy et al., 2015; Sun et al., 2013). Thus, this enzyme is clearly a key player in cell biology.

Drosophila XRN1 (Pacman)

In Drosophila, the homolog of XRN1 is called Pacman (Till et al., 1998) and it is essential for numerous aspects of fly development. Pacman localizes to cytoplasmic particles and is required for normal spermatogenesis (Zabolotskaya et al., 2008). Pacman is responsible for interacting with the protein called Puckered, a phosphatase involved in the JNK (c-Jun N-terminal kinase) pathway (Grima et al., 2008). Puckered is critical for thorax development, dorsal closure, and wound healing, therefore mutations in Pacman will lead to inability of wound healing in the fly and generation of small thorax variants (Grima et al., 2008). Another phenotype seen in Drosophila with mutant Pacman is that imaginal discs (wings) are not formed correctly. Four mRNAs that have been linked to small imaginal disc formation, insulin-like peptide (Dilp8), neuropeptide-like precursor 2 (Nplp2) (Jones et al., 2016), pro-apoptotic hid, and reaper mRNA (Waldron et al., 2015), are usually degraded by Pacman to tightly regulate their abundance during development (Jones et al., 2013b, 2016; Waldron et al., 2015).

Plant XRN4

In plants, the active homolog of the XRN1 enzyme is called XRN4 and is found in the cytoplasm. Not surprisingly, XRN4 also plays major roles in numerous aspects of plant biology. XRN4 is responsible for regulating 25% of the *Arabidopsis* seedling transcriptome (Merret et al., 2013) and is key for the removal of certain mRNAs required to establish dormancy or germination (Basbouss-Serhal et al., 2017; Rymarquis et al., 2011). Knockdown of XRN4 leads to suppression of oleosin isoprotein (OLE1), a major membrane protein required to create oil bodies in plants (Hayashi et al., 2012). XRN4

has also been implicated in the ethylene response pathway that regulates a wide range of developmental processes in plants (Potuschak et al., 2006). The addition of ethylene leads to an increase of XRN4, which in turn antagonizes the negative feedback regulation of a key transcription factor (EIN3) mediating ethylene-regulated gene expression (Olmedo et al., 2006; Potuschak et al., 2006; Souret et al., 2004; Weber et al., 2008). Finally, XRN4 has been shown to have antiviral activity in plants. Overexpression of XRN4 led to a decrease in pathogen replication during rice stripe and tobacco mosaic viral infections (Jiang et al., 2018).

XRN2 (Rat1) and Rai1

The cytoplasmic XRN1 enzyme has a counterpart found in the nucleus called XRN2 (also known as Rat1 in yeast, XRN2/3 in plants). In yeast, XRN2/Rat1 interacts with Rat1p interacting protein 1 (Rai1) (Xue et al., 2000) and this interaction enhances XRN2 function because Rai1 has 5' pyrophosphohydrolase activity (Jiao et al., 2010). Rai1 is selective and targets unmethylated cap mRNAs (Chang et al., 2012), thus assisting the quality control function of XRN2.

XRN2/Rai1 are localized near the transcriptional complex in the nucleus and are ready for recognition of aberrant mRNA (Davidson et al., 2012). XRN2 plays a key role in transcription termination by degrading downstream nascent RNA after the pre-mRNA is cleaved by the polyadenylation signal (PAS) endonuclease CPSF73 (Eaton et al., 2018; El Hage et al., 2008; Kim et al., 2004; Park et al., 2015). XRN2 quickly hops on the downstream fragment and is thought to eventually contact RNA polymerase II to induce termination in a torpedo-like mechanism (Sansó et al., 2016; West et al., 2004).

In addition to its role in mRNA biogenesis and quality control in yeast, XRN2 mutants also demonstrate accumulation of pre-5.8S ribosomal RNA (Henry et al., 1994) and pre-25S ribosomal RNA (Geerlings et al., 2000). Biochemical analyses have shown that XRN2 is important for trimming the excess 5' end of pre-5.8S ribosomal RNA (Axt et al., 2014; Granneman et al., 2011), which is required for ribosomal RNA biogenesis.

Human XRN1 and Disease

In humans, XRN1 has been linked to several diseases such as intranuclear inclusion body disease (INIBD) and osteogenic sarcoma. In INIBD, XRN1 is found in neuronal and glial nuclear inclusions, co-localizing with ubiquitin (Mori et al., 2018). This results in sequestration of this major cellular exoribonuclease, leading to a decrease in its activity in the cell and perhaps contributing to the pathogenesis of INIBD. In osteogenic sarcoma, several patient samples and cell lines were shown to possess a mutation in the human XRN1 gene which leads to downregulation of XRN1 mRNA and protein expression (Zhang et al., 2002). Downregulation of XRN1 could lead to stabilization of many oncogene mRNAs, resulting in uncontrolled cellular proliferation. However clearly establishing cause and effect requires further study.

Other 5'-3' exoribonucleases

Advances in technologies have allowed the discovery of additional proteins/enzymes that may be involved in RNA decay. The identification of non-canonical 5' caps, for example, has fueled the discovery for the enzymes responsible

for their decay (Jiao et al., 2017). The next section will provide a brief overview of two recently described enzymes that possess 5'-3' exoribonuclease activity in mammalian cells.

Yeast Dxo1

In yeast, a protein called Dxo1 has both decapping activity as well as 5'-3' exoribonuclease activity and is found in the cytoplasm (Chang et al., 2012). The decapping activity works on both methylated and unmethylated caps. This implies that if 5'-end capping occurs in the absence of methyltransferase activity, Dxo1 is likely responsible for the removal of these incorrectly capped mRNAs. Unlike its counterpart Rai1, Dxo1 does not have 5' end pyrophosphohydrolase (PPH) activity – thus its decapping activity appears to occur through an independent mechanism, (Chang et al., 2012).

Mammalian DOM3z/DXO

The mammalian DOM3z (also known as DXO) is a weak homolog of yeast DXO1 (Jiao et al., 2013). It is an important protein for 5' end quality control because it recognizes incompletely capped pre-mRNAs and is responsible for their degradation (Jiao et al., 2013). Mammalian DOM3z is predominantly found in the nucleus but a small amount is present in the cytoplasm. Removal of the DOM3Z nuclear localization signal causes the protein to be relocated into the cytoplasm (Picard-Jean et al., 2018). Recently, DOM3z was also demonstrated to recognize mRNAs with nicotinamide

adenine dinucleotide (NAD+) caps and will degrade these transcripts with non-canonical 5' ends (Jiao et al., 2017). In *Caenorhabditis elegans*, the homolog of mammalian DOM3z is called EOL-1 and has been linked to regulating learning in URX sensory neurons (Shen et al., 2014). Replacement of EOL-1 with the mammalian DOM3Z can also regulate learning in worms.

Deadenylation-independent pathways of mRNA decay

Deadenylation-independent pathways of mRNA decay also exist in cells. This can occur, for example, if the mRNA is first cleaved by an endonuclease (Müller et al., 2010) such as the RISC complex (using siRNAs or shRNAs) (Orban and Izaurralde, 2005), or the gammaherpesvirus SOX protein (Lee et al., 2017a; Richner et al., 2011). In other instances, RNAs can be targeted to this pathway by first getting decapped without prior deadenylation (Mishima et al., 2012). Once the mRNA is cleaved, it will then get degraded by standard exonucleolytic pathways, including XRN1 and/or the exosome.

Nonsense-mediated decay (NMD)

Nonsense mediated decay (NMD) is important in quality control by triggering decay of aberrant mRNAs with a premature termination codon (PTC) (Amrani et al., 2004). Transcripts that are targeted for NMD often contain one or multiple premature termination codons (PTC) (Nagy and Maquat, 1998) and/or long 3' untranslated regions (Peccarelli et al., 2014). Furthermore, enhancement of NMD is based on the position of

the exon-exon junction site from the PTC because it has to be at least 50 to 55 nucleotides downstream from the PTC (Nagy and Maquat, 1998; Thermann et al., 1998). Up-frameshift proteins 1, 2, and 3 (UPF1, UPF2, and UPF3) are regulators of NMD (Chamieh et al., 2008). SMG1, UPF1, eRF1, and eRF3, also known as the SURF complex, is bound to the ribosome and ribosome stalling makes the complex connect with the EJC complex (with UPF2 and UPF3) called DECID (Chamieh et al., 2008; Hug and Cáceres, 2014). Then UPF1 is phosphorylated by the SMG1/SMG8/SMG9 complex, causing UPF1 to dissociate from eRF1 and eRF3 (Deniaud et al., 2015; Kashima et al., 2006; Ohnishi et al., 2003; Yamashita et al., 2001). Once UPF1 phosphorylation creates a binding platform to recruit SMG6, SMG5, and SMG7 (Cho et al., 2013; Eberle et al., 2009; Okada-Katsuhata et al., 2012), decay of the transcript will start with either SMG6-dependent endonucleolytic cleavage or by SMG5-SMG7 recruitment of exonucleolytic decay factors (e.g. XRN1) and/or deadenylases (Eberle et al., 2009; Loh et al., 2013; Okada-Katsuhata et al., 2012).

RNA granules

Processing body (P body)

One major cytoplasmic granular-like structure that is composed of RNA and proteins are called processing bodies (P bodies). In a low salt concentration environment promotes formation of P bodies occurs by liquid-liquid phase separation (LLPS) and exist as liquid droplets (Brangwynne et al., 2009, 2011; Gallo et al., 2008; Schutz et al., 2017). While XRN1 was the first protein identified in P bodies (Bashkirov et al., 1997), today over 125 proteins have been identified in the P body proteome

(Hubstenberger et al., 2017). P body proteins are generally associated with mRNA fate determination – i.e. translation, silencing, or decay. Along these lines, P body factor relevant to this study include the DCP1/2 complex, LSM1-7, GW182, and DDX6 (Cougot et al., 2004; Ingelfinger et al., 2002; Sheth and Parker, 2003). Sheth and Parker (2003) originally demonstrated that mRNA decay intermediates can be localized to P bodies, leading to the model that P bodies are major sites of the 5'-3 mRNA decay. More recent data, however, suggest that the vast majority of mRNA decay may actually be co-translational (Hu et al., 2009, 2010; Radhakrishnan et al., 2016; Webster et al., 2018). Thus, P bodies may be more appropriately considered as sites for mRNA storage or sequestration of partially degraded mRNA intermediates. Consistent with this notion, P bodies also contain translation repressor protein such as DDX6, LSM14A, LSM14B, and IGF2BP2 (Aizer et al., 2014; Bhattacharyya et al., 2006; Brengues et al., 2005; Cougot et al., 2012; Hubstenberger et al., 2017).

Stress granules (SG)

In the presence of cellular stress, the number of RNA granules referred to as stress granules (SGs) increase dramatically in the cell cytoplasm. SGs typically contain translation initiation factors (eIFs) (eIF4E, eIF4G, eIF4A, eIF4B, and eIF3), poly(A) binding protein (PABP), 40S ribosomal subunit, and poly (A)+ mRNA (along with a variable assortment of other proteins) (Grousl et al., 2009; Kedersha, 2002; Kedersha et al., 1999; Kimball et al., 2003; Mazroui et al., 2006; Wheeler et al., 2016). Two RNA binding proteins that are important for formation of SGs are T-cell-restricted intracellular antigen 1 (TIA-1) and the RasGAP SH3-domain binding protein 1 (G3BP 1) (Gilks et al.,

2004; Tourrière et al., 2003). SG formation appears to be important for preventing decay of targeted mRNAs while ensuring their translational arrest (Mokas et al., 2009) during times of environmental stress. Common stresses that induce SGs include oxidative stress (Emara et al., 2012; Kedersha et al., 1999; Shenton et al., 2006), heat shock (Gallouzi et al., 2000; Kedersha et al., 1999; Nover et al., 1989), hypoxia (Van Der Laan et al., 2012; Lokdarshi et al., 2016), nutrient deprivation (Cassola et al., 2007; Jones et al., 2013a), and some viral infections (Khaperskyy et al., 2014; McInerney et al., 2005; Raaben et al., 2007).

There are two main subclasses of stress granules: canonical or noncanonical SGs. Canonical SG formation involves the phosphorylation of the translation initiation factor eIF2α (Kedersha, 2002; Kedersha et al., 1999; McInerney et al., 2005) but noncanonical SG formation occurs independently of eIF2α phosphorylation (Emara et al., 2012; Fujimura et al., 2012). Viral infection can trigger SG formation at early times post viral entry as a cellular antiviral defense mechanism (Ng et al., 2013; Piotrowska et al., 2010; Reineke and Lloyd, 2015; Reineke et al., 2015; Zhai et al., 2018).

In conclusion, cellular mRNA decay is vital for the removal of unwanted RNAs and aberrant RNAs. RNA decay is a tightly controlled process and the CCR4-NOT complex, decapping proteins, and the exonucleases (exosome complex and XRN1) are the key players. Defects in RNA decay enzymes in the major pathway can cause diseases in humans and are often lethal in early development. Thus, the focus of our study was on how RNA viruses influence the activity of RNA decay enzymes – in particular the XRN1 exoribonuclease.

Section II: Viral interactions with the host RNA decay machinery

In this section the focus will be on viruses that interact with different aspects of the cellular RNA decay machinery. Viruses have evolved to either bypass or alter the host RNA decay machinery to establish a productive infection. Mechanistic examples include the use of viral endonucleases to reprogram RNA decay, protein sponging to dysregulate decay, or direct inactivation of RNA decay enzymes in a viral infection (Table 2).

Table 2. Summary of the viruses discussed in this section.

Virus name:	Virus family:	Interaction with RNA decay	Reference:
Viral endonuclease and protease			
Kaposi's sarcoma-associated herpesvirus (KSHV) and Epstein-Barr virus (EBV)	*Herpesviridae*	The viral protein SOX cleaves mRNAs, which accelerates mRNA decay	(Covarrubias et al., 2011; Dahlroth et al., 2009; Lee et al., 2017a)
Herpes simplex virus (HSV)	*Herpesviridae*	The virion host shut off (VHS) protein also cleaves mRNAs to accelerated RNA decay	(Fenwick and Everett, 1990; Kwong and Frenkel, 1987)
Influenza A virus (IAV)	*Orthomyxoviridae*	The viral PA-X protein cleaves transcripts promoting accelerated RNA decay	(Bavagnoli et al., 2015; Desmet et al., 2013; Khaperskyy et al., 2016)
Severe acute respiratory syndrome (SARs) coronavirus	*Coronaviridae*	The viral NSP1 protein also cleaves mRNA to accelerating RNA decay	(Kamitani et al., 2006; Narayanan et al., 2008)
Poliovirus, foot-and-mouth diease virus, coxsackievirus, and human rhinovirus	*Picornaviridae*	Several viral proteases that cleaves RNA decay factors	(Cathcart and Semler, 2014; Dougherty et al., 2011, 2015)
Viral cap-snatching from host mRNA			
Orthomyxoviruses	*Orthomyxoviridae*	The subunit (PA) has enzymatic activity to host mRNA capped to prime its viral transcription	(Dias et al., 2009; Yuan et al., 2009)

Arenaviruses	*Arenaviridae*	The viral RNA dependent RNA polymerase N terminal with the help of viral nucleocapsid protein cleaves the host mRNA to use host cap to prime its transcription	(Fernández-García et al., 2016; Raju et al., 1990)
Bunyaviruses	Order: *Bunyavirales*	Uses similar mechanism as arenaviruses	(Fernández-García et al., 2016; Jeeva et al., 2017; Reguera et al., 2010)
Sequestering of host proteins			
Alphaviruses	*Togaviridae*	Binding of the host protein HUR to stabilize the viral transcript	(Barnhart et al., 2013; Garneau et al., 2008; Sokoloski et al., 2010)
Rabies virus (RABV)	*Rhaboviridae*	The viral glycoprotein mRNA binds the host protein PCBP2 to regulates its stability	(Palusa et al., 2012)
Picornaviruses	*Picornaviridae*	Utilize host proteins PCBP2 and PTB to regulate viral translation and replication	(Blyn et al., 1997; Choi et al., 2004; Gamarnik and Andino, 1997)
Brome mosaic virus (BMV)	*Bromoviridae*	Binds the LSM complex to promote viral replication and translation	(Galão et al., 2010; Jungfleisch et al., 2015)
Hepatitis C virus (HCV)	*Flaviviridae*	Interacts with several host proteins (LSM complex, DDH1, PAT1, PTB and HuR)	(Ariumi et al., 2011; Scheller et al., 2009; Shwetha et al., 2015)
West Nile virus (WNV)	*Flaviviridae*	Recruit P bodies and stress granules factors to viral replication sites	(Chahar et al., 2013; Emara and Brinton, 2007)
Flock house virus (FHV)	*Nodaviridae*	Bind host protein LSM complex, PAT1, and DDH1	(Giménez-Barcons et al., 2013)
Viral interaction with the nonsense mediated decay pathway			
Alphaviruses	*Togaviridae*	Host factors UPF1, SMG5, and SMG7 restrict viral replication	(Balistreri et al., 2007, 2014;

			Wernet et al., 2014)
Potato virus X (PVX)	*Alphaflexviridae*	Host factor UPF1 restricts viral replication	(Garcia et al., 2014)
Rous sarcoma virus (RSV)	*Retroviridae*	Uses a RNA stability element to evade the NMD pathway	(Balagopal and Beemon, 2017; Ge et al., 2016; Withers and Beemon, 2010)
Human T-cell leukemia virus type-1 (HTLV-1)	*Retroviridae*	Viral protein TAX binds UPF1 prevents activation of NMD pathway	(Fiorini et al., 2018)
Human immunodeficiency virus type 1 (HIV-1)	*Retroviridae*	Sequesters and utilize UPF1 to promote viral expression	(Ajamian et al., 2008; Rao et al., 2018)
Repression of decay enzyme			
Flaviviruses	*Flaviviridae*	Uses complex structures in the 5' or 3'UTR to stall XRN1	(Moon et al., 2012, 2015b; Pijlman et al., 2008)
Red clover necrotic mosaic virus	*Tombusviridae*	Uses the translation-enhancer element of dianthovirus RNA 1 (TE-DR1) sequence to stall XRN1	(Iwakawa et al., 2008; Steckelberg et al., 2018)

Viral endonucleases and proteases

Gammaherpesvirus nuclease SOX protein

Herpesviruses are a part of the *Herpesviridae* family (Lefkowitz et al., 2018) and its DNA genome is maintained in episomes to produce latent or lytic infections. Herpesviruses are large, enveloped double-stranded DNA viruses which are taxonomically divided into three sub-families: the alpha (α), beta (β), and gamma (γ) herpesvirinae (Lefkowitz et al., 2018). Only eight herpesviruses can infect humans. Two gammaherpesviruses, Kaposi's sarcoma-associated herpesvirus (KSHV or HHV8) and Epstein-Barr virus (EBV or HHV4), can cause cancer in humans (Dahlroth et al., 2009;

Sei et al., 2015). Below is an example of how a gammaherpesvirus interacts with the cellular RNA decay machinery.

All gammaherpesviruses encode a viral nuclease called SOX (for EBV it is called BGLF5) that targets host mRNAs for degradation (Dahlroth et al., 2009; Lee et al., 2017a) and possesses DNase activity (Bagnéris et al., 2011). During an active lytic gammaherpesvirus infection, the production of the SOX protein leads to rapid decay of cellular mRNA (Covarrubias et al., 2011; Lee et al., 2017a). Transcript cleavage will occur at RNA sequences that possess some general conserved features (Gaglia et al., 2015). SOX cleaves both viral and host transcripts, thus allowing the processive XRN1 and the exosome to rapidly degrade targeted RNAs (Abernathy et al., 2015; Lee et al., 2017a). Interestingly, this increase in host cellular mRNA decay causes a change in cellular transcription rates that will allows the virus to establish its viral gene expression (Abernathy et al., 2015). A couple of host mRNAs, including IL-6 and GADD45B, have been identified to escape SOX cleavage due either to the presence of ill-defined elements in their 3' UTRs called SOX resistance element (SRE) (Muller and Glaunsinger, 2017) or via protection by the cellular RNA binding protein nucleolin (Muller et al., 2015).

Herpes Simplex Virus virion host shutoff (VHS) protein

Herpes simplex virus (HSV) is a member of the subfamily *Alphaherpesvirinae* in the *Herpesviridae* family (Lefkowitz et al., 2018). Two types of HSV members infect humans and most of the time infections are asymptomatic. Symptoms associated with

lytic HSV infections are painful blisters or cold sores around either the mouth (HSV-1) or genital area (HSV-2).

HSV encodes an endoribonuclease on the UL41 gene called the virion host shutoff (VHS) protein (Fenwick and Everett, 1990; Kwong and Frenkel, 1989; Smibert et al., 1992; Taddeo and Roizman, 2006; Taddeo et al., 2006). In HSV infected cells, both viral and host mRNAs are destabilized due to the UL41 gene (Kwong and Frenkel, 1987, 1989; Strom and Frenkel, 1987). Experiments with purified VHS protein confirmed that the protein was indeed a powerful endoribonuclease. VHS protein is responsible for disrupting host translation by triggering decay of mRNAs (Fenwick and Clark, 1982; Fenwick and McMenamin, 1984; Fenwick and Owen, 1988; Fenwick and Walker, 1978; Kwong and Frenkel, 1987; Oroskar and Read, 1989; Strom and Frenkel, 1987). Its endoribonuclease activity is stimulated by host cell translation factors eIF4B and eIF4H (Doepker et al., 2004; Lu et al., 2001; Sarma et al., 2008; Shiflett and Read, 2013). Silencing of the host protein eIF4H, for example, will hinder VHS protein nuclease activity during infection (Sarma et al., 2008; Shiflett and Read, 2013). In terms of viral cofactors, VHS protein accumulation requires VP16 and VP22, but only VP22 is required at late times post-infection to simulate VHS activity (Elliott et al., 2018; Korom et al., 2008; Taddeo et al., 2007). VHS will cleave single stranded RNA at cytidine and uridine or uridine and adenine residues (Taddeo and Roizman, 2006). The host protein tristetraprolin recruits the VHS protein to the AU-rich elements (Shu et al., 2015); therefore, this means VHS targets AU-rich mRNAs (Taddeo et al., 2006, 2013). VHS also causes a disruption of stress granule formation, perhaps simply because there is

little mRNA remaining to store during times of stress (Burgess and Mohr, 2018; Finnen et al., 2016).

Influenza A Virus PA-X protein

Influenza A virus (IAV) is in the genus *Alphainfluenzavirus* in the family *Orthomyxoviridae* (Lefkowitz et al., 2018). IAV has eight segments that comprise its RNA genome and each segment is in the negative sense orientation (Mccauley and Mahy, 1983). IAV can infect a vary of mammalian species such as humans (Imai et al., 2017), dogs (Luo et al., 2018), horses (Sreenivasan et al., 2018), and pigs (Neira et al., 2018). Reassortment of IAV genomic RNA segments can generate a huge variety of IAV strains (Briand et al., 2018; Westgeest et al., 2014; Zhang et al., 2018a). Interestingly, IAV is another virus that uses an endonuclease to enhance mRNA decay to suppress cellular protein expression and perhaps create a cellular environment more conducive to support its own viral mRNAs.

Segment 3 of IAV generates the PA mRNA that encodes the PA protein, a subunit of the viral RNA-dependent RNA polymerase complex that is responsible for cleaving capped RNA from pre-mRNA and small non-coding RNAs (such as U1 and U2 snRNAs) to be used for viral transcription (Dias et al., 2009; Gu et al., 2015; Hara et al., 2006; Yuan et al., 2009). PA mRNA contains a second open reading frame called PA-X (Jagger et al., 2012; Muramoto et al., 2013) that creates a novel PA-X protein by ribosomal frameshifting (Firth et al., 2012). PA-X has endonuclease activity and suppresses protein expression by cleaving mRNA from RNA polymerase II transcripts, which contributes to host cell shut-off during infection (Bavagnoli et al., 2015; Desmet et

al., 2013; Khaperskyy et al., 2016). The N-terminal region of PA-X has endonuclease

activity and its C-terminal domain is regulatory in nature (Hayashi et al., 2016; Xu et al.,

2016). Furthermore, C-terminal truncated PA-X protein can inhibit IFN-1 mRNA

expression by promoting its decay and truncated PA-X protein is mainly nuclear

(Hayashi et al., 2016; Xu et al., 2016). In addition to its endonuclease activity, PA-X

plays a role in enhancing viral replication by increasing virus polymerase activity and

pathogenicity by suppressing the immune response early during infection (Lee et al.,

2017b).

Severe acute respiratory syndrome (SARS) coronavirus NSP1

Severe acute respiratory syndrome (SARS) coronavirus (SCoV) is a part of the

genus *Betacoronaviruses* in the *Coronaviridae* family (Lefkowitz et al., 2018). SCoV

infection symptoms include high fever, body aches, and mild respiratory illness (e.g. dry

cough) which can lead to death in humans (Booth et al., 2003; Lee et al., 2003b). SCoV

has an endoribonuclease called NSP1 and it is encoded in gene 1. NSP1 was shown to

suppress host gene expression by promoting decay of mRNAs such as interferon β

mRNA (Kamitani et al., 2006; Narayanan et al., 2008) by cleaving the transcript, leading

to degradation of mRNA fragments by XRN1 or the exosome (Gaglia et al., 2012).

Kamitani et al., (2009) showed that NSP1 inhibits host translation by interacting with the

host 40S ribosomal subunit and rendering it inactive. The NSP1-40S complex will

render the mRNA inactive by cleaving the 5' cap off; therefore, the mRNA cannot be

translated (Kamitani et al., 2009). Furthermore, NSP1 can target other RNAs that

contain a different 5' end such as internal ribosome entry site (IRES) elements. NSP1

cleaves picornavirus mRNAs that contain an IRES element in the 5' UTR three

nucleotides after the start codon (AUG). SCoV mRNAs are protected from nsp1

cleavage by the leader sequence that is present on the 5' UTR of all viral mRNAs

(Huang et al., 2011). Interaction between the stem loop 1 in the 5' UTR of SCoV and

NSP1 is important for cleavage evasion and stabilization SCoV mRNAs (Tanaka et al.,

2012).

Picornavirus 2A and 3C/3CD proteinase

Poliovirus, foot-and-mouth disease virus, coxsackievirus B, and human rhinovirus

are members of the *Picornaviridae* family (Lefkowitz et al., 2018) and can cause a

variety of common childhood illnesses. Symptoms include respiratory illness,

myocarditis, meningitis, and sepsis (which can result in death) (Abedi et al., 2018; Jartti

et al., 2004; Pires et al., 2017; Thi et al., 2018). The picornavirus genome consists of a

positive sense, single stranded RNA (Boothroyd et al., 1981; Van Dyke et al., 1982;

Kitamura et al., 1981; van der Werf et al., 1981).

Poliovirus, coxsackievirus B, and human rhinovirus (members of the genus

Enterovirus) infections will cause the relocalization of the host protein AUF1 from the

nucleus to the cytoplasm (Rozovics et al., 2012; Spurrell et al., 2005; Wong et al., 2013)

Interestingly, AUF1 relocalization occurs in a viral protease 2A-dependent manner

(Cathcart et al., 2013). Silencing of AUF1 will actually increase viral translation and

titers; therefore, AUF1 is an inhibitor of enteroviruses (Cathcart et al., 2013). This

apparent conundrum of a viral factor relocalizing an antiviral factor to the cellular

compartment of viral replication can be resolved by considering what happens to AUF1

when it shuttles to the cytoplasm. The viral precursor protease 3CD actively cleaves

AUF1 (Cathcart et al., 2013; Rozovics et al., 2012). Curiously, encephalomyocarditis

virus (EMCV), which is in the genus *Cardiovirus* in the *Picornaviridae* family, does not

cleave AUF1 but still causes the relocalization from the nucleus to the cytoplasm

(Cathcart and Semler, 2014). Perhaps as an alternative means is used by the virus to

inactivate this regulator of mRNA decay.

AUF1 is of course not the only target of the picornavirus proteases and several

additional mRNA decay proteins are among the cellular factors targeted by viral

enzymes. P bodies are absent during poliovirus infection and it was discovered that

XRN1, PAN3, and DCP1a are targeted for degradation. DCP1a is direct target of the

poliovirus 3C protease and XRN1 is cleaved by poliovirus 2A protease (Dougherty et

al., 2011). Furthermore, cleavage of PAN3 leads to the impairment of deadenylation

(Dougherty et al., 2011). Stress granules (SG) are also disrupted during poliovirus

infection and this phenomenon is also mediated through the action of viral proteases in

a dynamic fashion (Fung et al., 2013; Piotrowska et al., 2010; White et al., 2007).

Picornavirus 2A protease will induce formation of SG by cleaving eIF4GI to sequester

host mRNAs and not viral RNA, which help facilitate viral translation (Wu et al., 2014;

Yang et al., 2018). However, once viral 3C protease is expressed, it in turn cleaves

factors like G3BP, thus disrupting formation of SGs (Dougherty et al., 2015; Fung et al.,

2013; Piotrowska et al., 2010; White et al., 2007; Yang et al., 2018; Ye et al., 2018).

Viral cap-snatching from host mRNA

Several negative sense RNA viruses use the method of cap-snatching from host RNAs to prime transcription of viral mRNAs as a way to trick the host RNA decay machinery and produce capped viral mRNAs for translation. The multi-segmented RNA viruses that use this as a mechanism are the *Arenaviridae, Orthomyxoviridae* families, and viruses from the order *Bunyavirales* (Reguera et al., 2016; Sikora et al., 2017).

The mechanism of cap snatching was first observed in the *Orthomyxoviridae* family. The *Orthomyxoviridae* RNA dependent RNA polymerase requires three subunits; polymerase basic protein 1 (PB1), polymerase basic protein 2 (PB2), and polymerase acidic protein (PA) (Hengrung et al., 2015; Pflug et al., 2014; Reich et al., 2014; Shih and Krug, 1996). The subunit responsible for binding host 5' RNA caps is PB2 (Constantinides et al., 2018; Guilligay et al., 2008; Pautus et al., 2013; Severin et al., 2016). The PA subunit uses enzymatic activity in its N terminal domain to cleave RNAs to release the cap. (Dias et al., 2009; Yuan et al., 2009). Cleavage occurs 10-15 nucleotides downstream of the 5' cap and generally happens after a purine residue (Beaton and Krug, 1981; Koppstein et al., 2015; Krug et al., 1980; Plotch et al., 1979, 1981; Rao et al., 2003). PB1 is the main polymerase component and has domains that include a nucleotide recognition site for RNA synthesis (Binh et al., 2014). The polymerase does not transcribe naked RNA templates but rather relies on an interaction between the viral nucleoprotein (NP) of the encapsidated helical RNA segment and the PB1/PB2 subunits for function (Biswas et al., 1998).

Arenaviruses encode one RNA dependent RNA polymerase (L), which also has endoribonuclease activity associated with its N-terminal domain that is involved in cap

snatching (Cheng and Mir, 2012; Djavani et al., 1997; Lelke et al., 2010; Morin et al., 2010; Reguera et al., 2016; Singh et al., 1987). The L protein cleaves the host 5' cap along with up to 4 nucleotides for priming transcription (Raju et al., 1990). The C-terminal domain of the L protein is less conserved and is involved in viral mRNA synthesis (Lehmann et al., 2014). The L protein works in conjunction with the nucleocapsid (NP) protein in a more active way in cap snatching than was described above for the orthomyxoviruses (D'Antuono et al., 2014; Iwasaki et al., 2015; Kerber et al., 2011; Lee et al., 2000). NP binds to the 5' cap of the cytoplasmic cellular mRNA, leading to a conformational change in the protein which causes the NP protein to bind the L protein to start cap snatching and viral transcription (Fernández-García et al., 2016). Furthermore, the NP protein was also reported to have nuclease activity involve in repressing the interferon response (Qi et al., 2010).

Lastly, members of the order *Bunyavirales* also use host 5' cap snatching for priming viral transcription (Reguera et al., 2010, 2016). Bunyavirus RNA dependent RNA polymerase is homologous to the N terminal domain of the PA subunit of orthomyxovirus and arenavirus enzymes (Reguera et al., 2010). Also, the N terminal domain of the bunyavirus polymerase has endonuclease function and will cleave 9-22 nucleotides downstream from the 5' cap (Marklewitz et al., 2013; Rothenberger et al., 2016). The nucleocapsid protein (N) of bunyaviruses has been shown to interact with the 5' cap of host mRNAs by mimicking the cellular cap-binding complex (Jeeva et al., 2017).

Sequestering of host proteins as a strategy to evade the cellular RNA decay machinery

RNA binding proteins are important for post transcriptional regulation and play a major role in the fate of mRNAs. RNA viruses rely heavily on host proteins for many aspects of their life cycle due to the limited coding capacity of the viral genome. One way for viruses to escape the cellular RNA surveillance system is to disguise the viral transcript with host RNA binding proteins.

Alphaviruses are a part of the *Togaviridae* family (Lefkowitz et al., 2018) and are transmitted by mosquitoes (Menchaca-Armenta et al., 2018; Severini et al., 2018). Certain alphaviruses (Venezuelan equine encephalitis (VEEV), western equine encephalitis (WEE), eastern equine encephalitis (EEE) chikungunya (CHIKV), Ross River (RRV), o'nyong-nyong (ONNV), and Sindbis (SINV) viruses) can infect humans and cause symptoms such as fever, rash, headache, or encephalitis. The alphavirus genome is a single-stranded, positive sense RNA which is capped and polyadenylated. Alphaviruses have three repeat sequence elements (RSE) and a conserved U-rich region called the U-Rich Element/Conserved Sequence Element (URE/CSE) near the end of their 3' UTR (Faragher and Dalgarno, 1986; Zhang et al., 2013). The alphavirus 3' UTR has the ability to repress deadenylation of viral transcripts via interaction with the host HuR protein (Garneau et al., 2008; Sokoloski et al., 2010). HuR is a known stabilizing factor of mRNAs that contain an adenylate/uridylate-rich element (ARE) which serves as the binding site for the protein (Bakheet et al., 2018; Bolognani et al., 2012; Vreeland et al., 2014; Zhang and Wang, 2018; Zybura-Broda et al., 2018). Normally, HuR is mainly localized in the nucleus, but in an alphavirus infection (or

simply in the presence of large amounts of the SINV 3' UTR in the cytoplasm) HuR is

relocalized to the cytoplasm (Barnhart et al., 2013). This relocalization affects nuclear

alternative polyadenylation and splicing (Barnhart et al., 2013). Curiously, this

mechanism of HuR interaction and relocalization is conserved among all the

alphaviruses (Dickson et al., 2012; Sokoloski et al., 2010), suggesting that it is

fundamentally important to virus-host interactions.

Rabies virus from the genus Lyssavirus in the *Rhabdoviridae* family in the order

Mononegavirales order can infect a range of animals including bats (Bourhy et al., 1992;

Morimoto et al., 1996; Streicker et al., 2010), coyotes/dogs (McQuiston et al., 2001;

Rohde et al., 1997; Sidwa et al., 2005), foxes (Black and Lawson, 1970; Sidwa et al.,

2005), raccoons (Guerra et al., 2003; Szanto et al., 2008) and skunks (Guerra et al.,

2003; Leslie et al., 2006). Humans generally get infected by the virus via a bite from an

infected animal (Constantine and Woodall, 1966; Hampson et al., 2015; Tang et al.,

2005) or in rare cases an organ transplant from an infected person (Houff et al., 1979;

Srinivasan et al., 2005). Rabies virus infection has symptoms such as fever, headache,

nausea, vomiting, excessive salivation, and difficulty swallowing which lead to death

(Leach and Johnson, 1939). The rabies virus genome consists of a single stranded

RNA molecule in the negative sense orientation (Oem et al., 2013; Tang et al., 2014;

Zhao et al., 2014). Five different messenger RNAs are made of the genomic RNA which

are capped and polyadenylated (Coslett et al., 1980; Holloway and Obijeski, 1980;

Wunner et al., 1980). The glycoprotein mRNA contains a short poly (A) tail ranging from

7 to 13 adenosines (Wu et al., 2007a) and is highly expressed during infection when

compared to the other four viral mRNAs (Palusa et al., 2012), particularly in the context

of the 'start-stop' model of polar transcription that occurs on rabies viral RNA templates. Palusa et al. (2012) previously showed that stabilization of the glycoprotein mRNA of rabies viruses is likely regulated by the binding of the host cell poly(rC) binding protein 2 (PCBP2). Several known PCBP2 functions include regulating mRNA stability (Chen et al., 2018; Holcik and Liebhaber, 1997; Thiele et al., 2004; Weiss and Liebhaber, 1994, 1995) and translation (Blyn et al., 1997; Gamarnik and Andino, 1997).

Picornaviruses have also been shown to utilize host cell proteins to promote viral translation and RNA replication. The 5' UTR of picornaviruses contains a cloverleaf structure and an internal ribosome entry site (IRES) element (Klinck et al., 1997; Nomoto et al., 1977; Witwer et al., 2001). Picornaviruses use host proteins poly (rC) binding protein 1/2 (PCBP1/2), and polypyrimidine tract-binding protein (PTB) to modulate viral translation and RNA replication (Blyn et al., 1997; Choi et al., 2004; Gamarnik and Andino, 1997; Walter et al., 1999). PCBP2 will bind to the 5' cloverleaf, which will protect the 5' end from 5' exoribonucleases and stabilize the viral mRNA (Kempf and Barton, 2008; Murray et al., 2001). After infection, PTB and PCBP2 will promote early viral translation until viral proteins accumulate - especially the viral proteases. Picornavirus viral 3C and 3CD proteases will then cleave PCBP2 and PTB to modulate the switch from translation to RNA replication on picornavirus RNA templates (Back et al., 2002; Chase and Semler, 2014; Perera et al., 2007). Cleaved PCBP2 can form a complex with 3CD and mutations that prevent this interaction affect the virus infectivity and growth rates (Chase et al., 2014; Parsley et al., 1997; Sean et al., 2009; Toyoda et al., 2007). Therefore, host proteins PCBP2 and PTB are important for picornaviruses translation and RNA synthesis.

Brome mosaic virus (BMV), a member of the *Bromoviridae* family (Lefkowitz et al., 2018), infects plants from the *Poaceae* family (Lane, 1974). BMV contains three positive single-stranded RNA genomic segments and produce one subgenomic RNA during infection (Ahlquist and Janda, 1984; Ahlquist et al., 1984; Miller et al., 1985). BMV has a tRNA-like structure (TLS) in the 3' UTR of its genomic segments and deletions in the TLS decrease viral replication, translation and encapsidation of viral RNA (Barends et al., 2004; Bujarski et al., 1985; Choi and Rao, 2003; Dasgupta and Kaesberg, 1977; Joshi et al., 1983; Rietveld et al., 1983). *Saccharomyces cerevisiae* has been used as a model system to study the molecular biology of plants viruses like BMV (Janda and Ahlquist, 1993; Price et al., 1996). In yeast, deletion of the LSM1 protein suppresses BMV replication as well as the generation of the subgenomic RNA (Diez et al., 2000). Deletions of other LSM proteins as well as the PAT1 translation/RNA stability factor have the same effect (Noueiry et al., 2003). Furthermore, DHH1 (DDX6) also has a role in the BMV replication but, curiously, other decapping enhancers (i.e. EDC1 and ECD2) have very little effect on BVM replication (Mas et al., 2006). Mutational analysis on the BMV RNA 3 3' UTR revealed that the LSM complex binds to the TLS in the 3' UTR of BMV RNA 3 (Galão et al., 2010) and interacts with the viral 1a protein to promote replication and translation of the BMV RNAs (Jungfleisch et al., 2015).

Hepatitis C virus (HCV), is a member of the genus *Hepacivirus* in the *Flaviviridae* family (Lefkowitz et al., 2018). HCV has a positive sense single-stranded RNA genome, which is used to produce one polyprotein that is cleaved by viral NS3 (Grakoui et al., 1993b, 1993a). Interestingly, HCV genomic RNA has been shown to interact with

several host proteins to promote viral replication and translation. Scheller et al. (2009) showed that silencing of LSM1, DDH1, and PAT1 reduces the amount of HVC replicon RNA synthesis as well as the generation of infectious virus particles. HCV was shown to bind the LSM1-7 complex in both the viral 5' and 3' UTRs (Ariumi et al., 2011; Pager et al., 2013; Pérez-Vilaró et al., 2012; Scheller et al., 2009). Therefore, aspects of the RNA decay machinery are critical in the biology of an HCV infection. However, the silencing of DCP2 and XRN1 does not affect virus production. Another host protein that is usurped by HCV is HuR. Knockdown of HuR will reduce HCV replication (Harris et al., 2006). Mechanistically, HuR will relocalize to the cytoplasm in an HCV infection and is responsible for displacing polypyrimidine tract binding protein (PTB) protein from the viral RNA. This is then thought to allow La protein to bind the 3' UTR, which enhances viral replication (Shwetha et al., 2015).

West Nile virus (WNV) is another member of the *Flaviviridae* family and has been shown to recruit P body components to viral replication sites. After 12 hours post WNV infection, it was observed that P bodies are disrupted, and different factors are recruited to replication sites. Recruited factors include GW182, LSM1, DDX3, DDX6 and XRN1. Furthermore, silencing of LSM1, DDX3, and GW182 impairs viral replication (Chahar et al., 2013). Additionally, P body factors are not the only ones recruited and sequestered by HCV. T cell intracellular antigen-1 (TIA-1) and the related protein TIAR (stress granules factors) are also recruited to replication sites of WNV and DENV-2 (Emara and Brinton, 2007). Therefore, disruption of P bodies and stress granules will allow viral RNA access to different RNA binding factors and likely prevents activation of targeted anti-viral pathways.

Flock house virus (FHV), a member of the *Nodaviridae* family, also utilizes the host proteins LSM1-7, PAT1, and DHH1 (Giménez-Barcons et al., 2013) during infection. FHV has two positive sense single stranded RNA genomic segments and generates one subgenomic RNA from RNA 1 during infection (Guarino et al., 1984; Krishna and Schneemann, 1999; Scotti et al., 1983). In yeast, silencing of LSM1, PAT1 and DHH1 increased the generation of the FHV subgenomic RNA (which is called RNA 3) and had little effect on RNA1 (Giménez-Barcons et al., 2013).

Viral interaction with the nonsense mediated decay pathway

Positive sense RNA viruses

Several studies have shown the NMD pathway can restrict positive-sense viruses, such as Semliki Forest virus (SFV), Sinbis virus (SINV), and Potato virus X (PVX), in mammalian cells, insect, and plants (Balistreri et al., 2014; Garcia et al., 2014; Wernet et al., 2014). Positive stranded RNA viruses can have premature termination codons (PTC), upstream open reading frames (hORF), long 3' untranslated regions or unconventional 5' or 3' ends (5' cap or 3' poly A tail). The RNA genome of alphaviruses contains two open reading frames which encoding for the structural and non-structural genes. After the RNA genome is released into the cytoplasm,the non-structural proteins (includes the viral polymerase) are translated first from the genomic mRNA. The NMD machinery likely views these genomic mRNAs as having a very long 3' UTR. Once there is enough accumulation of the viral non-structual proteins, then a subgenomic RNA encoding the structural viral proteins are made from negative sense anti-genomic RNA template. Balistreri et al., (2014) performed an siRNA screen on Semliki Forest

virus (SFV) and Sindbis virus (SINV) cellular infections to identify potential host cell

restriction factors and identified three cellular NMD proteins (UPF1, SMG5 and SMG7).

In the presense of SFV infection, the silencing of UPF1, SMG5, or SMG7 showed

increase in viral replication (Balistreri et al., 2007, 2014). Silencing of UPF1 in

Drosophila resulted in a 3.5X increase in SINV particles (Wernet et al., 2014).

In plants, the role of UPF1 as a viral restriction factor was shown by studying

potato virus X (PVX) infection in *Arabidopsis* and *N. benthamiana* (Garcia et al., 2014).

PVX has a positive sense RNA genome which contains multiple internal translation

termination codons. Overall, PVX is similar to the alphaviruses because it generates

subgenomic RNAs with one open reading frame during RNA synthesis, which will be the

template for translation of one viral protein. The viral RNA genome, which contains

multiple stop codons, is the main target of NMD pathway. Therefore, knockdown of

UPF1 leads to an increase in viral genome and 3 of the four subgenomic RNAs

(subgenomic RNA 4 shows no change) (Garcia et al., 2014).

Retroviruses

Retroviruses are a part of the *Retroviridae* family and use reverse transcriptase

to produce a DNA version of their RNA genomes that is then inserted into the host cell

chromosomes (Goodman and Spiegelman, 1971; Lefkowitz et al., 2018). Once the viral

DNA is integrated, it is used to produce one unspliced mRNA and a plethora of spliced

viral mRNAs (Arrigo and Beemon, 1988). The mRNAs of retroviruses have relatively

long 3' UTRs, implying that the transcripts should be targets of NMD. An RNA stability

element (RSE), located 400 nucleotides downstream from the gag stop codon, was

identified in Rous sarcoma virus (RSV) as a structured domain in the retroviral RNA

required to evade NMD (Barker and Beemon, 1994; Weil and Beemon, 2006; Weil et

al., 2009; Withers and Beemon, 2010). Mutational analysis done on the RSE shows that

a minimal sequence of 155 nucleotides is required to evade NMD (Withers and

Beemon, 2010), including pyrimidine-rich stretches which bind the polypyrimidine tract

binding protein 1 (PTBP1) (Ge et al., 2016). PTBP1 prevents recruitment of UPF1 -

thereby promoting stabilization of RSV RNAs (Ge et al., 2016). Recently, a study

showed that the RSE will inhibit deadenylation as well as impair decapping and 5'-3

XRN1 mediated decay (Balagopal and Beemon, 2017).

Human T-cell leukemia virus type-1 (HTLV-1) employs an alternative strategy by

using viral proteins TAX and REX to inhibit NMD (Fiorini et al., 2018; Mocquet et al.,

2012; Nakano et al., 2013). TAX binds to the central domain of UPF1, thereby

decreasing UPF1 binding affinity for RNA (Fiorini et al., 2018) and causing displacement

of the translation initiation factor INT6/eIL3E from UPF1 to prevent activation of the

NMD pathway. HTLV-1 REX is another viral protein that inhibits NMD resulting in the

stabilization of cellular IL-6, MAP3K14, and FYN mRNAs and other known NMD targets

(Nakano et al., 2013). Overall, HTLV-1-mediated inhibition of the NMD pathway also

results in the global stabilization of cellular RNAs which are normally regulated by NMD

(Mocquet et al., 2012).

Human immunodeficiency virus type 1 (HIV-1) is another retrovirus that interacts

with UPF1 (Ajamian et al., 2008, 2015; Rao et al., 2018; Serquina et al., 2013). UPF1

was identified to be a component of an HIV-1 ribonucleoprotein complex that contains

the unspliced viral full-length RNA, DDX3, viral protein REV, CRM1, and p62 (Ajamian

et al., 2008). In HIV-1 infected cells, depletion of UPF1 reduces viral expression and

reactivation while overexpression of the NMD factor dramatically increases viral

expression (Ajamian et al., 2008; Rao et al., 2018). In contrast, overexpression of UPF2

and SMG6 both decrease viral expression, perhaps by sequestering UPF1 (Ajamian et

al., 2015; Rao et al., 2018). It has indeed been demonstrated that UPF2 and UPF3aL

block the binding of the UPF1 on the viral RNA, resulting in a reduction of nucleus-

cytoplasmic transport of full length transcript (Ajamian et al., 2015). Therefore, in

contrast to other retroviruses, UPF1 is a positive regulator for HIV-1 expression and

HIV-1 virions made in the absence of UPF1 are also less infectious (Serquina et al.,

2013).

Repression of an RNA decay enzyme

Flaviviruses

Increase in world travel has led to the spread of many infectious pathogens such

as RNA viruses. One RNA virus family which uses arthropods as vectors are the

members of the *Flaviviridae* (e.g. Dengue 1-4 virus, West Nile virus, Zika virus, etc.).

There are four genera in the *Flaviviridae* family: Flavivirus, Hepacivirus, Pegivirus, and

Pestivirus (Lefkowitz et al., 2018). Flaviviruses are enveloped viruses that contain a

single positive sense, single-stranded, RNA viruses that can cause a range of

symptoms. These include hemorrhagic fevers, mild fevers, rashes, headaches, and

myalgia in humans.

Flaviviruses interface with the RNA decay machinery by stalling and repressing a

key decay enzyme. Arthropod-borne flaviviruses rely on the highly processive

exoribonuclease XRN1 to generate a non-coding RNA called subgenomic flaviviral RNA (sfRNA), which has been mapped to viral 3' UTRs (Funk et al., 2010; Moon et al., 2012; Pijlman et al., 2008; Silva et al., 2010). Furthermore, hepaciviruses (HCV) and pestiviruses (BVDV) of the *Flaviviridae* family also stall XRN1 in the 5' UTR in a region associated with the Internal Ribosome Entry Site (IRES) element (Moon et al., 2015b). Early studies of sfRNAs indicated that a conserved pseudoknot is important for XRN1 stalling as deletion of the pseudoknot prevent sfRNA formation (Funk et al., 2010; Silva et al., 2010). Chapman et al (2014b), the authors were able to crystalize a 68-nucleotide sequence of 3' UTR of Murray Valley Encephalitis virus (another member of the *Flaviviridae*) that stalls XRN1 and show that the RNA forms a three-helix junction RNA structure. The RNA folds into a ring-like structure in which the 5' end of the RNA passes through the middle of ring (Chapman et al., 2014a). Based on structural modeling, the viral RNA dependent RNA polymerase will have no problem passing through the structure from the 3'-5' direction, but XRN1 coming from the 5'-3' direction is stalled by the knot-like fold. Recently, an XRN1 stalling region of the 3' UTR of Zika virus has been crystalized and shown to have a similar structure to that of the Murray Valley Encephalitis virus element (Akiyama et al., 2016).

In addition, XRN1 stalling on these viral structures can also cause repression of enzymatic activity (Moon et al., 2012, 2015b). It is hypothesized that XRN1 repression happens due to slow release of the stalled enzyme from the viral RNA decay intermediate. Interestingly, this reversible XRN1 repression affects other enzymes throughout the 5'-3' decay pathway as well. Thus, the accumulation of sf/xr (XRN1-

Resistant) RNAs leads to the dysregulation of host mRNA stability (Moon et al., 2012, 2015b).

RNA binding proteins a play important role in determining the fate of the mRNA and viruses can sponge host RNA binding protein to bypass the RNA decay machinery. Not only do flaviviruses generate sfRNAs, but these decay intermediates also appear to interact with numerous host cell proteins (Manokaran et al., 2015). To date, several RNA binding proteins have been confirmed to interact with sfRNAs of DEN-2 virus. These proteins include G3BP1, G3BP2, Caprin1, and TRIM25. The host tripartite motif 25 (TRIM25) protein requires deubiquitylation by ubiquitin-specific peptidase 15 (USP15) to activate expression of the retinoic acid–inducible gene 1 (RIG-I) (Pauli et al., 2014). In a dengue virus infection, the host TRIM25 protein will bind to the sfRNA of DEN-2 virus and thus prevent activation of RIG-I expression (Manokaran et al., 2015). G3BP1, GCBP2, and Caprin1 are required for activation of the several interferons stimulated genes. In a dengue virus infection, the production of sfRNA will sequester these three proteins by reducing the activation level of interferon stimulated genes (Bidet et al., 2014). sfRNAs have also have been shown to interact with the antiviral RNA interference pathway in mosquitoes and mammalian cells (Moon et al., 2015c; Schnettler et al., 2012). Schnettler et al. 2012, showed that West Nile virus (WNV) sfRNA will prevent dicer from cleaving double stranded RNA and this prevents dicer from activating the RNA-induced silencing complex (RISC). Moon et al. 2015c, showed that both dicer and Ago2 will associate with the 3' UTR of Kunjin virus (a WNV variant). Non-coding RNA that sponge dicer and Ago are likely contributing to the mild repression of the RNAi pathway observed in West Nile virus infected cells and mosquitoes.

Tombusviruses

Red clover necrotic mosaic virus (RCNMV) from the genus Dianthovirus is a member of the *Tombusviridae* family (Lefkowitz et al., 2018). The genome consists of two RNA segments which encode for four proteins: p27, p88, CP, and MP (Okuno et al., 1983; Stuart et al., 2004). Additionally, the RNA genome has no cap structure or poly(A) tail to protect its 5' or 3' ends (Mizumoto et al., 2003). Iwakawa et al., (2008) showed that the 3'UTR of RNA 1, which contains a translation-enhancer element of dianthovirus RNA1 (TE-DR1) -mediated cap-independent translation sequence, can stall XRN1. Interestingly, the non-coding RNA decay intermediate is also packaged into the virion (Iwakawa et al., 2008). Furthermore, recently the structure of the 3' UTR that stalls XRN1 has been identified to have a fold that is unique relative to the stalling structures identified in the 3' UTR of flaviviruses (Steckelberg et al., 2018).

The interface between other members of the *Tombusviridae* and the XRN family of enzymes appears to be more complicated. Several studies have shown knockdown of XRN4 leads to the accumulation and recombination of other tombusvirus RNAs (Jaag and Nagy, 2009; Peng et al., 2011). In contrast, overexpression of XRN4 was shown to enhance Bamboo mosaic virus (BMV) replication and silencing of XRN4 lead to decrease in BMV RNAs (Lee et al., 2016).

In conclusion, evidence is accumulating that all RNA viruses must successfully interact with the RNA decay machinery early on in order to establish a productive infection. A plethora of strategies and targets appears to be in place – and understanding the molecular details of these mechanisms will likely not only provide

important insights into viral-host interactions but may also reveal unforeseen aspects of the cellular RNA decay machinery itself.

Section III: Evidence of alternative RNA structures that can stall XRN1

A main focus of this dissertation is to provide evidence of the range of RNA structures that can stall and repress XRN family enzymes. Thus, this section will provide an overview of past work into other ways that XRN1 can be stalled on RNA substrates. These include poly(G) sequences that were used 20 years ago to help delineate mRNA decay pathways in yeast as well as protein-RNA complexes that form a measurable impediment to XRN1 movement on the targeted RNA. Finally, XRN1 stalling is not something that is restricted to viral RNAs. It is important to note that XRN1 stalling is naturally involved in cellular RNA processing events such as 5' end maturation of snoRNAs and ribosomal RNAs. Thus, the view of XRN1 as simply an unstoppable 'terminator' exoribonuclease is clearly not accurate as the enzyme appears to have a much more dynamic interplay with select RNA substrates.

Poly(G) insertions in yeast mRNAs stall XRN1

The addition of poly guanosine (poly(G)) into the body of a mRNA will produce measurable decay intermediates when assessed in *Saccharomyces cerevisiae* cells or when the RNA substrate is incubated with recombinant yeast XRN1 (Poole and Stevens, 1997). As alluded to above, the initial mapping of RNA decay pathways benefited greatly from poly(G) insertions strategically placed into the 5' or 3 UTRs of

reporter mRNAs (Decker and Parker, 1993; Dunckley and Parker, 1999; Muhlrad and

Parker, 2005; Poole and Stevens, 1997). For example, the insertion of a poly(G) tract

into the 3' UTR of the EDC1 mRNA helped to determine that the decay of this mRNA

occurs through a deadenylation-independent pathway (Muhlrad and Parker, 2005).

Insertion of poly(G) stretches, however, failed to reproducibly generate measurable

mRNA decay intermediates when used in many other eukaryotic systems (Li et al.,

2006; Opyrchal et al., 2005). Thus, the utility of poly(G) to block XRN1 appears to the

limited and perhaps even transcript-specific or context-specific. Thus, the biological

relevance of poly(G)-mediated XRN1 stalling was not clear, a point that will be

addressed by the phlebovirus section of this dissertation.

Protein complexes can also stall XRN1

The MS2 tagging system has been used to study mRNA localization as well as a

fundamental component in the tethering of proteins to reporter RNAs to assess function.

The MS2 tagging system inserts multiple copies of a stem loop structure derived from

bacteriophage MS2 which binds the MS2 coat protein very specifically and with high

affinity (Peabody, 1993). Interestingly, the addition of MS2 protein and MS2 protein

complexes to a mRNA can apparently also influence its degradation in unexpected

ways. In 2015, Garcia and Parker showed that the presence of MS2 stem loops in a

reporter RNA resulted in a measurable accumulation of downstream fragments due to

the protein/protein complex blocking XRN1 from degrading the portion of the mRNA

lying 3' to the MS2 binding sites (Garcia and Parker, 2015).

XRN enzymes stall during 5' end processing of small nucleolar RNAs

Small nucleolar RNAs (snoRNAs) are non-coding RNAs required for site-directed modifications to RNAs (in particular rRNAs) and are concentrated in the nucleoli or Cajal bodies (Wu et al., 2016). The majority of box C/D and H/ACA snoRNAs are made from introns of splicing mRNAs and require the use of members of the XRN family of enzymes to generate a mature 5' end. In yeast, mutations in either XRN1 or XRN2 will lead to accumulation in the pre-snoRNAs that get relocalized to the cytoplasm to be degraded (Lee et al., 2003a). The XRN enzyme trims the 5' end of pre-snoRNAs to form the mature snoRNA (Kiss and Filipowicz, 1995). Dicistronic RNAs (e.g pre-snoR190-U14) require the Rnt1 endonuclease to cleave the RNA to liberate monocistronic RNAs (Grzechnik et al., 2018).

XRN enzymes stall during 5' end processing of ribosomal RNA

The 60S ribosomal RNA is processed from a precursor rRNA (pre-rRNA) which contains the 18S, 5.8S, and 25S (yeast)/28S (mammals). XRN2 involvement in ribosomal processing has been reported in yeast (Amberg et al., 1992; Fang et al., 2005; Petfalski et al., 1998), ciliates (Couvillion et al., 2012), plants (Zakrzewska-Placzek et al., 2010), and mammals (Wang and Pestov, 2011). The sequences in pre-rRNA not found in mature rRNA are called external transcribed spacer (5' or 3' ETS) or internal transcribed spacer (ITS1 and ITS2) sequences. XRN2 is responsible for removal of the 5' ETS works in parallel with another 5'-3' exonuclease RRP17 in trimming the 5' ends (Oeffinger et al., 2009). The ITS1 and 2 are cleaved by the nuclear RNase MRP to allow access for the exosome and XRN2 to trim the 3' and 5' ends

respectively (Fang et al., 2005). In mammals, knockdown of XRN2 causes accumulation of the 5.8S and 28S transcripts with extended 5' ends (Wang and Pestov, 2011). Furthermore, when XRN2 is knocked down, then XRN1 can compensate (Fang et al., 2005; Henry et al., 1994; Johnson, 1997). The mechanism of how XRN2 just trims and does not degrade the whole ribosomal RNA has yet to be uncovered. Based on observations presented here as well as in the literature noted above, we hypothesize that terminal rRNA structure and/or rRNA protein interactions may play a key role.

In conclusion, this section shows XRN1 stalling is a natural part of the lifecycle of some RNAs and that there appears to be several ways to stall this exoribonuclease. Thus, XRN1 stalling is not limited to viral RNAs and insights gained towards understanding underlying mechanisms of blocking progression of this normally very processive exoribonuclease may have major implications to cellular biology as well as virology.

Section IV: Introduction of virus families used in this study

This section will give an overview of the four different families of viruses used in this study with an emphasis on what is known regarding RNA structures in the 3' untranslated region of these viral transcripts.

Overview of Phleboviruses

Phleboviruses are in the genus Phlebovirus, part of *Phenuiviridae* family (formally *Bunyaviridae* family) within the order *Bunyavirales* (Lefkowitz et al., 2018).

Phleboviruses are transmitted by sandflies (Badakhshan et al., 2018), ticks (Sakamoto et al., 2016), or mosquitoes (Talavera et al., 2018; Vloet et al., 2017). These viruses can cause fevers which can be deadly in humans (Nakouné et al., 2016). In livestock, phleboviruses can cause high rates of abortions, resulting in significant economic losses for the agriculture industry (Mutua et al., 2017; Nakouné et al., 2016; Nderitu et al., 2011). It is important to understand phleboviruses (as well as all RNA viruses) at the molecular level to potentially reveal novel anti-viral targets for rational drug design. The three phleboviruses used in this study are Rift Valley fever virus (RVFV), Sandfly Naples virus, and Heartland virus.

Phlebovirus gene expression

Phleboviruses are enveloped viruses with a genome consisting of three single stranded RNA segments named S (small), M (medium), and L (large) (Figure 3). The L segment is in the negative sense orientation and encodes for the viral RNA-dependent polymerase (Accardi et al., 1993; Elliott et al., 1992; Muller et al., 1992, 1994). The M segment is also of negative polarity and encodes the viral glycoprotein (Grò et al., 1997; Mochi et al., 1997). Interestingly, the S segment uses an ambisense gene expression strategy in which both the genomic and anti-genomic RNA segments are utilized independently to produce two different mRNAs encoding either the nucleocapsid protein or a non-structural protein (Brennan et al., 2014; Marriott et al., 1989; Muller et al., 1992; Perrone et al., 2007).

L segment
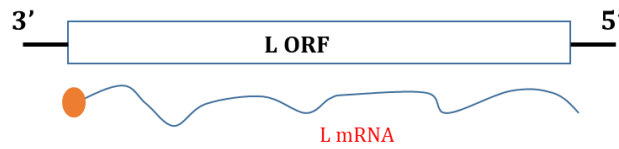
M segment
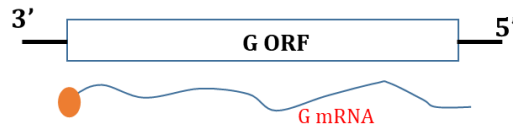
S segment

AMBISENSE
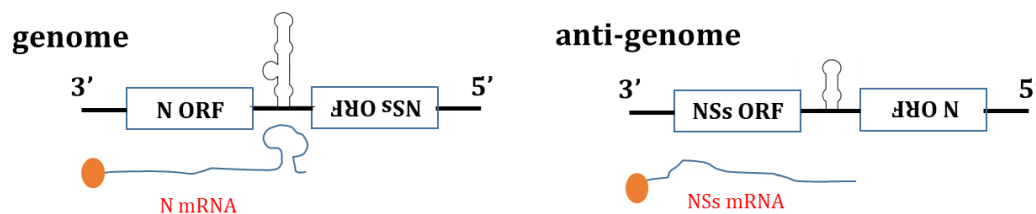
Figure 3: Diagram of Phlebovirus gene expression. The L segment encodes for the RNA-dependent RNA polymerase (L). The M segment encodes for the glycoprotein precursor protein (G). The ambisense S segment genome encodes for the nucleocapsid (N) in the negative sense orientation and viral anti-genome encodes the non-structural (NSs) protein in a positive sense orientation. The orange circle represents the 5' cap and the viral transcripts are not polyadenylated.

Structure in the 3' UTRs of phlebovirus RNAs

The area between the two delineated open-reading frames of the S segment has a highly structured area called the intergenic region (Emery and Bishop, 1987; Giorgi et al., 1991). The predicted structure of the intergenic region is one huge stem loop that serves as to help terminate transcription (Emery and Bishop, 1987). In the intergenic region of the S segment contains a conserved set of CGUCG pentanucleotides that serves are the termination site for the viral RNA polymerase to generate mRNAs. Before this CGUCG sequence contains either a G-rich (3' UTR of the nucleocapsid

mRNA) or C-rich sequence (3' UTR of the nonstructural mRNA) (Brennan et al., 2017; Ikegami et al., 2007; Lara et al., 2011). This G-rich region will become a focus of this dissertation project as described in the results section.

Overview of Arenaviruses

Arenaviruses are a part of the *Arenaviridae* family (Lefkowitz et al., 2018) and are transmitted by rodents (Mariën et al., 2017, 2018). Arenaviruses can be sorted into Old World (e.g. Lassa virus, Lujo virus) or New World arenaviruses (e.g. Junin virus, Machupo virus, etc.) (Fehling et al., 2012). In humans, arenaviruses can cause hemorrhagic fevers which can be deadly (Hass et al., 2004; Hidalgo et al., 2017; Mariën et al., 2018). This study will focus on Junin virus as well as two novel snake arenaviruses.

Arenaviruses gene expression

Arenaviruses are enveloped viruses containing two segments of single-stranded genomic RNA (Figure 4). Both segments utilize the ambisense coding strategy in which both the viral genome and anti-genome RNA segments are used to produce independent mRNAs (Auperin and McCormick, 1989; Singh et al., 1987).The L segment generates the mRNA that encodes for the viral RNA-dependent RNA polymerase (Lukashevich et al., 1997) and the anti-genomic L segment generates the mRNA that encodes for the RING finger Z protein (Cornu et al., 2001; Djavani et al., 1997; Fehling et al., 2012). The S genomic RNA segment generates the mRNA that encodes for the

nucleocapsid protein (Auperin and McCormick, 1989; Iapalucci et al., 1991) while the S

anti-genomic segment encodes for the mRNA that generates the precursor glycoprotein

mRNA (Ghiringhelli et al., 1991; Pinschewer et al., 2003).
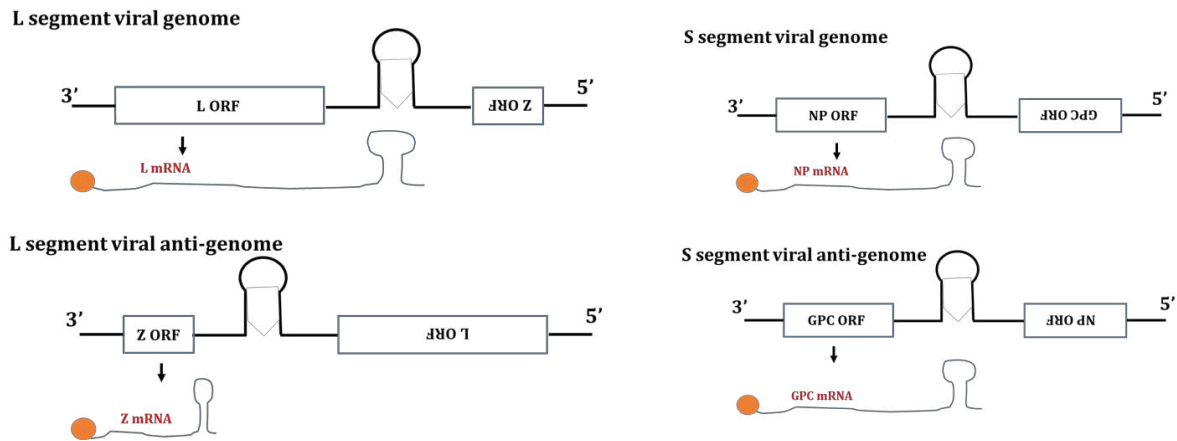
Figure 4. Diagram of arenaviruses gene expression. The ambisense L segment encodes
the RNA-dependent RNA polymerase (L) in the negative sense orientation and the matrix
protein (Z) from the viral anti-genome in the positive sense orientation. The amibsense S
segment encodes for the nucleoprotein (NP) in the negative sense orientation and
glycoprotein precursor (GPC) in the positive sense orientation from the anti-genome.

Structure in the 3' untranslated regions of arenavirus RNAs

Arenaviruses have an intergenic region, which contains one (Auperin et al., 1984;

Charrel et al., 2001; López and Franze-Fernández, 2007), two (Ghiringhelli et al., 1991),

or three (Gonzalez et al., 1996) stable stem loops located between the two open-

reading frames on either the S and L genome segments (Auperin and McCormick,

1989; Clegg et al., 1991; Iapalucci et al., 1989, 1991; Moncayo et al., 2001;

Romanowski and Bishop, 1985; Salvato and Shimomaye, 1989; Wilson and Clegg,

1991). One of the functions of the intergenic region is to serve as a transcription

termination site/signal (Iapalucci et al., 1991; López and Franze-Fernández, 2007;

Pinschewer et al., 2005). In several studies, it was observed that partial deletion of the

intergenic region caused attenuation of the virus (Golden et al., 2017; Iwasaki et al., 2016; Pinschewer et al., 2005).

Overview of Coronaviruses

Coronaviruses are in the *Coronaviridae* family within the order *Nidovirales* (Lefkowitz et al., 2018) and can cause a range common respiratory and enteric diseases in a variety of mammalians and domestic species. Two emerging coronaviruses, severe acute respiratory syndrome coronavirus (SARS-CoV) and Middle East respiratory syndrome coronavirus (MERS-CoV), cause life-threating diseases in humans (Wong et al., 2015; Xiao et al., 2017). MERs-CoV and the 3' UTR of its mRNAs was the focus a part of this study.

Coronaviruses gene expression

Coronaviruses contain a single-stranded, positive-sense genomic RNA which is capped and polyadenylated (Bouvet et al., 2010; Peng et al., 2016; Spagnolo and Hogue, 2000; Wu et al., 2013). The genome can range from 27 to 32 kilobases in size, making it the largest RNA virus studied to date (Boursnell et al., 1987; Eleouet et al., 1995b, 1995a; Lee et al., 1991). The virus generates a number of subgenomic mRNAs that contain the same 5' leader sequence and 3' UTR but different open reading frames (Hsue and Masters, 1997; Sethna et al., 1991; Williams et al., 1999). The genomic RNA contains over 10 different open reading frames, two of which are accessed by ribosomal frame shifting for the RNA-depend-RNA polymerase (Bredenbeek et al., 1990). The

subgenomic RNAs are made during viral replication by discontinuous RNA synthesis (Bentley et al., 2013; Dufour et al., 2011; van Marle et al., 1999; Pasternak et al., 2001; Sethna et al., 1989; Zúñiga et al., 2004).

A conserved structure in the 3' UTR of coronavirus mRNAs

A conserved pseudoknot and multiple stem-loop with bulges are found the in the 3' UTR of coronaviruses (Goebel et al., 2004a). These structures can interact with other parts of RNA genome and are essential for viral replication (Goebel et al., 2004a, 2004b). The pseudoknot structure is only partially stable in solution, as demonstrated best using the pseudoknot region from murine hepatitis virus (MHV). Thus, any structure associated with the pseudoknot may require viral or host proteins to stabilize it (Stammler et al., 2011).

Overview of Benyviruses

Many plant viruses can cause significant losses to agriculture. Benyviruses are in the genus Benyvirus in the *Benyviridae* family (Gilmer et al., 2017; Lefkowitz et al., 2018) and consist of non-enveloped, rod shape particles (Putz, 1981). The particles can range in length from 65 to 390 nanometers (Putz, 1981). The best studied virus from the *Benyviridae* is beet necrotic yellow vein viruses (BNYVV) which causes rhizomania disease in sugar beets (Heidel et al., 1997). BNYVV is transmitted by a soil protozoan, *Polymyxa betae* (family *Plasmodiophoraceae*) and a protein called P75 is important for transmission (Tamada et al., 1996).

53

Benyvirus gene expression

The benyavirus genome consist of two main RNA segments and three optional segments (Putz, 1981). The genomic segments are linear, positive-sense, single stranded RNAs that are capped and polyadenylated. RNA 1 has one large open reading frame encoding for replication-associated proteins. RNA 2 has six open reading frames encoding for the coat protein (responsible for coating the RNA), p75 (mentioned above) (Tamada et al., 1996), p14 (a post-transcriptional suppressor) (Chiba et al., 2012) and other proteins associated with cell-to-cell movement (Crutzen et al., 2009; Gilmer et al., 1992). RNA 3, the focus of this study, will be reviewed in the next paragraph. RNA 4 encodes for p31 which increases the transmission rate by *Polymyxa betae* (D'Alonzo et al., 2012). RNA 5 encodes for the p26 protein which may modulate the type of symptoms in viral infection (Peltier et al., 2012).

BNYVV subgenomic RNA 3

Beet necrotic yellow vein virus (BNYVV) RNA 3 is 1773 nucleotides long and contains three open reading frames (p25, N, p4.6). BNYVV RNA 3 is responsible for the systemic movement of the virus and thus is a major factor in generating disease symptoms in plants (Lauber et al., 1998; Peltier et al., 2012). Interestingly, Peltier et al., 2012 showed the accumulation of a subgenomic RNA from RNA 3 in both a natural plant infection as well as in yeast transfections. 5' RACE analysis mapped the proximal end of the sub genomic RNA to a conserved sequence called the coremin motif (Peltier et al., 2012). The coremin motif is also found in RNA 5 which also generates a subgenomic RNA.

Project Rationale

The cellular RNA decay machinery is important for the recognition and removal of 'unwanted' RNAs in the cell. Transcripts from RNA viruses certainly fall into the 'unwanted' category, but these viruses clearly have evolved ways to avoid or successfully interact with this machinery. Previously in our lab, we have established that flavivirus transcripts successfully interface with the RNA decay machinery by targeting the major decay enzyme XRN1. Flaviviruses generate a non-coding RNA (sfRNA or xrRNA) by the stalling of XRN1, resulting in the incomplete degradation of the genomic RNA. Notably, the strategy of XRN1 stalling and repression is conserved throughout the *Flaviviridae* and represents an important aspect of the virus life cycle (Moon et al., 2012, 2015b; Pijlman et al., 2008). XRN1 stalling in the 3' UTR of arthropod-borne flaviviruses is caused by an RNA structure with a three-helix junction at its core, producing a slipknot of sorts that is difficult for enzymes moving in the 5' to 3' direction to penetrate (Chapman et al., 2014a). Stalling of XRN1 at this structure also results in the slow release of XRN1 from the RNA substrate, resulting in a reversible inhibition of enzymatic activity (Moon et al., 2012; 2015b). This disruption of XRN1 activity resulting in a major dysregulation of mRNA turnover in infected cells.

Based on the attractiveness of targeting an accessible cytoplasmic enzyme whose repression will have major effects on cellular gene expression, we hypothesized that other virus families may have evolved the ability to stall and repress XRN1. To investigate this possibility, we focused in this study on several virus families that have complex structures in the 3' UTRs of their transcripts. In the course of this work, we investigated the following three hypotheses:

55

(1) Conserved sequences from phleboviruses, arenaviruses, coronaviruses, and a benyvirus may stall and repress the cellular exoribonuclease XRN1.

(2) Small molecules that are known to intercalate into three helix junction containing RNA structures may be capable of inhibiting sfRNA generation from flavivirus RNAs

(3) All 5' to 3' exonucleases may not be as susceptible as XRN1 to stalling at flavivirus 3' UTR structures. To test this hypothesis, we focused on the mammalian DOM3Z/DXO exoribonuclease.

Chapter 2: Methods

Plasmids and templates for *in vitro* transcription

DNA templates to produce RNAs by *in vitro* transcription were generated by cloning PCR products into pGEM4 (Promega) or pGEMA60 (Garneau et al., 2008) vectors. The plasmid to produce the RNA containing the upstream portion of the DENV-2 3' UTR was described previously (Moon et al., 2015b) and sequence information is listed in Table 4. PCR products from the 3' UTRs of the RVFV L, G, NSs, and N mRNAs, as well as the 3' UTRs from the Junín Virus GPC, NP, Z, and L mRNAs, were obtained from Dr. Brian Gowen (Utah State University). PCR products from the arenavirus SN90 Z and SN68 L 3' UTRs were generated by using primers: 68FW-AGAGAAGCTTTAGAAGACTAGATCGCCGGG, 68RV-GAGACTGCAG GCCCTGAGAAGCCAGCAGCA, 90FW-AGAGAAGCTTGAGTCTAGAGGTCCTCCAACCCAG, and 90RV-GAGACTGCAGATCGACGATGACTGAGGGGGA, from plasmids received from Dr. Mark Stenglein (Colorado State University) (Stenglein et al., 2012). The MERS-CoV 3' UTR was obtained by RT-PCR from total infected cell RNA (obtained from Tony Schountz) using the primers 5'-GCCTGGTCCAATGATTGATGTTA and 5'-TTTTGCAAATCATCTAATTAGCCTAATCTA. DNA oligonucleotides containing the 3' UTRs of the Sandfly Naples and Heartland virus N mRNA were obtained from Integrated DNA technologies (IDT). DNA oligonucleotides containing the 3' UTRs of Zika virus (Wildtype (WT) contains sequence: 10,380…10,807; point mutations were inserted to disrupt sfRNA formation – Mutant 1-MUT1- 10,416 - C→G; Mutant 2-MUT2- 10,496 - C→G; Double Mutant-DM- 10,416 - C→G AND 10,496 - C→G) were obtained

from Thermo Fisher Scientific GeneArt. Information on all the sequences of these oligonucleotides and PCR products that were generated is listed in Table 4. All but one of the PCR products were inserted into pGEMA60 or pGEM-4 at the PstI and HindIII sites. This generates an RNA with a 5' plasmid-derived 'leader' sequence of 50 nucleotides. The RVFV G 3' UTR was inserted into pGEMA60 at the PstI and SphI sites because of an incompatibility with the HindIII restriction site. In addition, the RVFV N 3' UTR PCR products was also subcloned into the NotI site of peGFP-N1 (Clontech). A portion of the eGFP 3' UTR (1402–1520 nucleotides, GenBank: U55762.1) was subcloned from peGFP-N1 into the EcoRI and HindIII sites of pGEM4 to generate peGFP-UTR. This plasmid was used to generate a probe for northern blotting. Plasmids were isolated using the Zymo-PURE Plasmid Maxiprep Kit per the manufacturer's instructions (Zymo Research). Plasmids were all verified by Sanger sequencing. For *in vitro* transcription templates, the plasmids were linearized with restriction enzymes as listed in Table 2.

DNA template used for RNA ladder was amplified by PCR from the pGEM-4 plasmid as the template. The forward primer in the PCR reaction was the same but the reverse primers are different (Table 3). PCR products were gel purified and then mixed. This was done by John Anderson.

Table 3- Primers for RNA ladder template

Size (bases)	Forward Primer 5'-3'	Reverse primer 5'-3'
100	TACACATACGATTTAGGTGA	TCGAAATTAATACGACTCAC
200		ACCGAGCGCAGCGAGTCAGT
300		GCCTTTTGCTCACATGTTCT

400		TCTGACTTGAGCGTCGATTT
500		AGGTATCCGGTAAGCGGCAG
750		GAACTCTGTAGCACCGCCTA
1000		AAATCCCTTAACGTGAGTTT

Table 4- Information on all sequences used in this study.

Name:	Virus strain:	NCBI Accession Number:	Sequence 5'-3'	Restriction enzymes used for linearization of plasmids
Control-pGEM		X65303.1	1…61 1…168 1…390	Report RNA: HindIII Control and competitor RNA: Ear1 Control RNA (Figure 2): Sml1
Zika 3' UTR	PRVABC-59	KX377337	10,380…10,807 MUT1- 10,416 - C→G MUT2- 10,496 - C→G DM- 10,416 - C→G AND 10,496 - C→G	HindIII
Zika 5' half of 3' UTR	PRVABC-59	KX377337	10,380…10,551	Ear1
RVFV L 3'UTR	ZH-501	DQ375406	6282…6404	HindIII
RVFV G 3'UTR	ZH-501	DQ380200	3605…3847	SphI
RVFV NSs 3' UTR	ZH-501	DQ380149	783…936	HindIII
RVFV N 3' UTR	ZH-501	DQ380149	930…730	HindIII Northern probe: EcoRI

Sandfly Naples N 3' UTR		HM566170	1062…984	Ear1
Heartland N 3' UTR	TN	KJ740146	1020…921	Ear1
JUNV GP 3'UTR	Rumero	JN801476	1519…1859	HindIII
JUNV N 3'UTR	Rumero	JN801476	1637…1420	HindIII
JUNV Z 3'UTR	Rumero	AY619640	349…542	HindIII
JUNV L 3'UTR	Rumero	AY619640	492…306	HindIII
SN90 Z 3' UTR			AACCCGAGTCTAGAGGTCCTCCAACCCAGGAGGCCACCAA ACCAACCCCACCCAGCAAACAACCAAACCAACACCCCAGA CCACCGGGGACGGCGCCGCCGTCCCCGGTGGTCTGGGGTC ATCGAGGGCAGTCTCGGGACCATGTCCCCCTCAGTCAT	HindIII
SN-68 L 3' UTR			ATCGCCGGGCCACACTCCAGAACCCCCCAGACCGCCGAGG AGAGCGCTGCTCTCCTCGGCGGTCTGGGTTGTTCCTTGCT CTTGTCCTTTCCGGGTTTTCTGTTGTTGTCCCTCTGCTCT GCTGCTGGCTTC	HindIII
DENV-2 5' half of the 3' UTR	Jamaica/N. 1409	M20558	10273…10491	Ear1
BNYVV-55mer	Isolate S	NC_003516	1222…1278	HindIII For competition assay: Ear1

| MERs-CoV 3' UTR | HCoV-EMC | NC_01984 3 | 29774…30109 | HindIII |
| | | | | For Northern Blot: EcoR1 |

In vitro transcription

The protocol used for generating RNA from plasmid templates with internally radiolabeled nucleotides is as follows: 1 µg linearized plasmid, 1 µL 5X transcription buffer (Thermo Fisher Scientific), 0.5 µL RiboLock RNase inhibitor (Thermo Fisher Scientific), 1 µL riboNTPs (5 mM ATP, CTP; 0.5 mM GTP, UTP), 1µL 5mM guanosine monophosphate (GMP), 4.5 µL α-^{32}P-UTP (800 Ci/mmol), and 1µL SP6 polymerase (Thermo Fisher Scientific). Four changes to this standard protocol were done to generate radiolabeled probes for northern blots and RNA ladder: the riboNTP concentration was changed to 5 mM ATP, CTP, GTP; 0.5 mM UTP, GMP was omitted, T7 polymerase was used instead of SP6 polymerase (Thermo Fisher Scientific), and 1µL of nuclease-free water was added to bring the final reaction volume to 10 µL. To generate larger amounts of lightly-radiolabeled RNA for use in competition assays 4 µg linearized plasmid, 8 µL 5X transcription buffer, 1 µL RiboLock RNase inhibitor (Thermo Fisher Scientific), 4 µL 5 mM GMP, 4µL riboNTPs (5 mM ATP, CTP, UTP; 0.5 mM GTP), 8µL 1:25 dilution of α-^{32}P-UTP (800 Ci/mmol), 4 µL SP6 polymerase, and nuclease-free water were mixed to generate a final reaction volume of 40 µL. Finally, the MEGAscript® SP6 transcription kit (Life Technologies) was used to generate unlabeled RNAs for use in the 5' mapping of RVFV N mRNA 3' UTR decay intermediates. All RNAs were made with guanosine monophosphate as a way for XRN1 to target these RNAs (Jinek et al., 2011).

Reactions were incubated for three hours at 37ºC then extracted using phenol/chloroform/isoamyl alcohol (25:24:1) and ethanol precipitated. RNA pellets were washed with 70% ethanol, dried and resuspended in 10 µL RNA loading dye (8M urea,

20 mM EDTA, 100 mM Tris-HCl pH 7.6, 0.06% bromophenol blue, and 0.06% xylene cyanol) containing urea or for RNA ladder 20 µL nuclease-free water. RNAs were heated at 90° for 30 seconds and run on a 5% polyacrylamide gel containing 7M urea. Radiolabeled bands were imaged by X-ray film and unlabeled RNA bands was identified by UV shadowing. The band containing the RNA was excised, placed into 400 µL high salt column buffer (HSCB- 400 mM NaCl, 25 mM Tris-HCl pH 7.6, and 0.1% SDS) and eluted overnight at room temperature. The buffer was then placed in a fresh tube, 400 µL of phenol/chloroform isoamyl alcohol (25:24:1) was added, vortexed, and centrifuged for one minute in a microfuge. The top aqueous layer was transferred to a new microfuge tube, 1ml of 100% ethanol was added and mixtures were incubated for at least 20 minutes in the -80°C freezer. Tubes were then centrifuged for 10 minutes at max speed in a microfuge to pellet the RNA. The ethanol supernatant was removed, and the pellet was washed in 150 µL 70% ethanol. Following a brief centrifugation, the ethanol wash was removed, and the pellet dried for about two minutes at room temperature. RNA pellets were resuspended in 11 or 21 µL of nuclease-free water and 1 µL was taken and put into three mL of ScintiSafe Econo liquid and counted in a liquid scintillation counter. RNAs for cell free decay assays were adjusted to 100,000 counts per minute (CPM)/uL and competitor RNAs were set to 200 femtomoles per microliter, then added to final concentration listed in the reaction below.

Recombinant *K. lactis* XRN1 and DOM3z protein purification

BL21 (DE3) cells transformed with pET26b-XRN1 (Chang et al., 2011) were obtained from Dr. Jeff Kieft (CU Medical School) and pET28a-DXO(DOM3z) plasmid

(Picard-Jean et al., 2018) was obtain from Dr. Brian Geiss (Colorado State University). pET28a-DXO was transformed into BL21 cells. An isolated colony was inoculated into 15 mL of LB containing kanamycin (40 µg/mL) and incubated overnight at 37°C. A 100 µL aliquot was saved at this step (as well as after all other steps) to run on a SDS-PAGE gel for quality control assessment at a later time. The remaining culture was added to 500 mL of LB containing kanamycin (40 µg/mL) and incubated until the culture reached an OD_{600} = 0.3. At this stage the temperature was lowered to 20°C and incubation continued until the OD_{600} of the culture reached 0.6. Isopropyl β-D-1-thiogalactopyranoside (IPTG) was then added to the final concentration of 0.4 mM to induce recombinant protein expression and the culture was incubated overnight. The bacteria were then pelleted at 5,000 rpm (Sorvall Evolution RC / SLA-3000 rotor) for 10 minutes. The supernatant was carefully decanted, and the pellets resuspended in 10 mL of lysis buffer (20 mM Tris-Cl pH 7.6, 500 mM NaCl, 2 mM DTT, 10% glycerol, 1 complete tab of protease inhibitor (Roche)) and transferred to a 50 mL conical tube. Using a Sonic Dismembrator Model 100 sonicator set to "7"; the sample was then sonicated on ice for three one-minute cycles (30 seconds on / 30 seconds off). The lysate was centrifuged (Sorvall Evolution RC / SS-34 rotor) at 16,000 rpm for 20 minutes at 4ºC and the cleared supernatant transferred into new 50 mL conical tube. Then 2 mL of a 50% slurry of nickel beads and 20 mM imidazole was added to the sample and the mixture was rotated for two hours at 4ºC to allow the protein to bind to the beads. The beads were pelleted by centrifugation at 500 rpm for 10 minutes on a table top Fisher Scientific accuSpin™ 3R and the supernatant was discarded. 10 mL of wash buffer (20 mM Tris-Cl pH 7.6, 500 mM NaCl, 2 mM DTT, 10% glycerol, and 40

mM imidazole) was added, mixed to wash the beads, and the beads were pelleted at 500 rpm for 10 minutes. This wash procedure was repeated at least four times. After the last wash, 2 mL of elution buffer (20 mM Tris-Cl, pH 8.0, 150 mM NaCl, 2 mM DTT, 10% glycerol, and 200 mM imidazole) was added and rotated for one hour at 4ºC. The mixture was centrifuged at 500 rpm for 10 minutes and the supernatant was transferred into a 15 mL conical tube on ice. The supernatant containing the recombinant protein was dialyzed in the elution buffer without the imidazole and aliquoted and stored at -80ºC. Samples were run on an 8 % SDS-PAGE gel and imaged by coomassie staining to evaluate protein purity and quality.

Cell free RNA decay assays

RNA decay assays using recombinant XRN1: 2 µL (100,000 cpm/ uL) of internally radiolabeled RNA substrate, 1 µL RiboLock RNase inhibitor (Thermo Fisher Scientific), 2 µL 10X NEBuffer 3 (1000 mM NaCl, 500 mM Tris-HCl, 100 mM $MgCl_2$, 10 mM DTT at pH 7.9), and 14 µL of nuclease-free water were mixed to bring the total reaction volume to 19 µL. Lastly, 1µL (0.06 µg/µl) of purified recombinant XRN1 was added. Reaction mixtures were placed at 37ºC and 4 µL aliquots were taken at designated time points and placed into 200 µL HSCB to stop the reaction prior to phenol/chloroform extraction and ethanol precipitation.

Recombinant XRN1 RNA decay assays in the presence of RNA competitors or triptycene compounds: Reactions were performed as described above with the addition of 1800 fmol (RVFV N, JUNV L, SN90, BNYVV-55mer) or 1400 fmol (Zika virus) of lightly radiolabeled (for accurate quantification) RNA and 2 µL internally radiolabeled

reporter RNA (100,000 cpm/ μL). Alternatively, triptycenes were added at the designated concentrations. The volume of nuclease-free water was adjusted to maintain a final volume of 20 μL.

Cell-free RNA decay assay – Lithium and Potassium. These reactions were performed in a similar fashion as the XRN1 assays described above using 10X NEBuffer 3 (500 mM Tris-HCl, 100 mM $MgCl_2$, 10 mM DTT at pH 7.9) without the NaCl. The addition of 1 μl of 1M lithium chloride (LiCl) or potassium chloride (KCl) was included in the reaction and the nuclease-free water was adjusted to bring to final volume to 20μL.

*DOM3Z/DXO RNA decay assay*s. These reactions were performed in a similar fashion as the XRN1 assays described above using 2 μL of 10X IVDA-2 buffer (100 mM Tris-HCl, pH 7.6, 1000 mM KOAc, 20 mM $MgCl_2$, 0.50 mM $MnCl_2$, 20 mM DTT, and 20 mM spermidine) and 1 μL(.07μg/μL) of recombinant mammalian DOM3Z/DXO.

Cytoplasmic extract-mediated RNA decay assays: 2μL (100,000 cpm/uL) of internally radiolabeled RNA, 2 μL phosphocreatine and adenosine triphosphate (PC-ATP) (final concentration: 250 mM PC, 12.5mM ATP), 6.5 μL 10% polyvinyl alcohol (PVA), 1 μL RiboLock RNase inhibitor (Thermo Fisher Scientific), and 16 μL HeLa (protein concentrations about 4.8 μg/μL) or C6/36 extract (protein concentration range from 6.2 μg/μL to 8.5 μg/μL) (Ford and Wilusz, 1999; Sokoloski et al., 2008) were combined and incubated at 37°C for the indicated times. At each time point, 6 μL was removed from the reaction and added to 200 μL HSCB prior to phenol/chloroform extraction.

To process samples for analysis, 200 µL of phenol/chloroform/ isoamyl alcohol (25:24:1) was added, samples were vortexed, and centrifuged for one minute at max speed in a microfuge to separate the phases. 150 µL of the upper aqueous phase was carefully transferred into a new 1.5 ml microfuge tube. 350 µL of 100% ethanol and 1 µL glycogen (as a carrier to add in RNA precipitation) was added and samples were placed at -80°C for at least 20 minutes. RNA was pelleted by centrifugation for 20 minutes at max speed, washed with 150 µl 70% ethanol, air dried for about three minutes, and resuspended in 8 µL urea RNA loading dye. Reaction samples were run on a 5% polyacrylamide gel containing 7M urea. Gels were dried on a slab dyer, exposed to a phosphorimage screen, and analyzed using a Typhoon Trio phosphorimager.

5' mapping of the RVFV n 3' UTR RNA decay intermediate

For mapping the 5' end of decay intermediates, 5 µg of unlabeled RNA substrate containing the 3' UTR of N mRNA of RVFV was incubated with recombinant XRN1 for 15 minutes at 37°C in reaction conditions as described above. Reactions were stopped by addition of 400 µL of HSCB followed by phenol/chloroform extraction and ethanol precipitation. RNA products were separated on a 5% polyacrylamide gel containing 7M urea and stained for one hour with SYBR Gold Nucleic Acid Gel Stain (Thermo Fisher Scientific) at room temperature. The indicated decay intermediate band was purified from the gel by soak elution overnight and the RNA was circularized using T4 RNA ligase (NEB). Ligation products were reverse-transcribed using a reverse primer (5'-AGCATGATGGGGAGAAA), and products were then amplified using Pfu Ultra II Fusion HS DNA polymerase (Agilent) and cloned into the pGEM T-Easy vector (Promega) for

68

transformation of DH5α cells. Colony screens were performed by PCR with Pfu Ultra II

Fusion HS DNA polymerase using RVFV-N-specific primers 5'-

AGCCTTAACCTCTAATCA and 5'-CTCCAATCCCAGATGTTGAG to amplify the

junction region that resulted from ligation of the 3' and 5' ends of the original RNA. Ten

positive clones were sequenced and the 5' ends were aligned to the RVFV-N 3' UTR.

Cell culture

Human embryonic kidney 293T (HEK293T) were maintained in Dulbecco's

Modified Eagle's medium (DMEM; Mediatech-Corning) supplemented with 10% fetal

bovine serum (FBS; Peak Serums) and 1% streptomycin/penicillin (Fisher Scientific-

Hyclone) at 37ºC in the presence of 5% CO_2. Cells were routinely passage by washing

the monolayer with cold phosphate buffered saline (PBS; Corning) followed by

incubation at 37ºC with a 0.25% trypsin solution (Fisher Scientific-Hyclone) until the

cells detached. Cells and buffer were then transferred to a 15mL conical tube and

centrifuged at 500 rpm for five minutes. The cell pellet was resuspended in fresh media

by pipetting and routinely passaged at a 1/10 dilution.

Plasmid transfections

GFP reporter plasmids were routinely treated for endotoxin removal

(MiraCLEAN, Mirus Bio) prior to transfection into HEK293T cells with jetPRIME

(Polyplus) according to the manufacturer's recommendations using 3 µg eGFP plasmid

and 1 µg shRNA. Cells were collected 48 hours after transfection.

RNA extraction

Total RNA was extracted from infected/transfected cells using TRIzol reagent (Life Technologies) according to the manufacturer's recommendations. DNase I treatment (Thermo Fisher) was performed for 20 minutes at 37°C to remove genomic DNA and RNA was recovered by phenol/chloroform/ isoamyl alcohol (25:24:1) extraction and ethanol precipitation. Total RNA from transfected cells were isolated by column-based RNA purification (Zymo Research). Total RNA yield was measured using a Nanodrop instrument (Thermo Fisher).

Northern Blot

For the detection of stable decay intermediates from eGFP reporter transfections or Rift Valley fever virus (MP-12 strain) infected cells, 5 µg of total cellular RNA was separated on a 5% polyacrylamide gel containing 7M urea. The electrophoresed RNAs were transferred onto a nylon membrane (Hybond-XL; GE Healthcare) using a tank transfer unit. The blots were UV cross-linked and pre-washed with high stringency buffer (0.1X SSC, 0.1% SDS) for one hour at 60°C. Blots were then prehybridized for one hour at 60°C in hybridization buffer (50% formamide, 1 mg/mL bovine serum albumin, 750 mM sodium chloride, 75 mM sodium citrate, 0.1 mg/mL salmon sperm DNA, 1% SDS, 1 mg/mL polyvinylpyrrolidone, 1 mg/mL ficoll). *In vitro* transcribed, internally radiolabeled RNA probes complementary to the 3' UTR of GFP (which both GFP constructs have in common) or the N 3' UTR of RVFV were gel purified were used to detect stable decay intermediates by incubating with the blot in hybridization buffer overnight at 60°C. Blots were washed three times with low stringency wash solution (2X

SSC, 0.1% SDS) and three times with stringent wash solution (0.2X SSC, 0.1% SDS)

for 15 minutes each at 60ºC. Hybridized RNAs were visualized by exposing the blot to

phosphor screens and imaging on the Typhoon Trio Imager (GE Healthcare).

Chapter 3: Results

Section I: A variety of viruses can stall and repress the cellular exoribonuclease XRN1

Zika sfRNA is produced by XRN1-mediated decay

Previous research has shown members of the *Flaviviridae* produce subgenomic RNAs due to XRN1 stalling in their 5' untranslated region (UTR) (e.g. Hepatitis C virus and Bovine viral diarrhea virus) or 3' UTR (e.g. Dengue 2 virus, Japanese encephalitis virus, West Nile virus) (Moon et al., 2012, 2015b). These stable decay intermediates generated from XRN1 stalling in the 3' UTR are called subgenomic flavivirus RNA (sfRNA) (Pijlman et al., 2008). The generation of these 300-500 base sfRNAs is responsible for global stabilization of cellular mRNAs, resulting in a significant reprogramming of host cell gene expression (Moon et al., 2012, 2015b). Furthermore, sfRNAs are also required for efficient virus transmission in mosquitoes (Göertz et al., 2016; Pompon et al., 2017). Recently, the structure of Murray Valley encephalitis virus (another member of the *Flaviviridae*) sfRNA was determined using X-ray crystallography. This study determined that a knot-like three-helix junction structure is primarily responsible for XRN1 stalling (Akiyama et al., 2016; Chapman et al., 2014b, 2014a). Importantly, this structure is conserved throughout the *Flaviviridae* - therefore XRN1 stalling on the 3' UTR of flaviviruses should also be conserved (Moon et al., 2012; Pijlman et al., 2008). Thus, we first wanted to formally demonstrate that the 3' UTR of Zika virus was capable of forming sfRNAs due to XRN1 stalling.

A definitive approach to demonstrating RNA-mediated XRN1 stalling is to reconstitute the activity in a purified system. To demonstrate specific stalling of purified XRN1 exoribonuclease on either a non-specific RNA generated from p-GEM4 sequence (control lanes) or a positive control RNA (the 5' half of the 3' UTR of Dengue-2 virus (DENV lanes) (Moon et al., 2012)), was incubated with recombinant XRN1 (rXRN1). As seen in Figure 5, two sfRNAs accumulated specifically from the DENV-2 RNAs while the exoribonuclease rapidly degraded the control RNAs. XRN1 stalls at two sites in the DENV-2 RNA since it contains tandem three helix junction structures (Chapman et al., 2014b, 2014a) and XRN1 apparently can degrade through the first three helix junction structure, likely due to structural heterogeneity. Similar XRN1 read through and stalling at downstream structures is also observed *in vivo* (Pjilman et al, 2008). Collectively, these data demonstrate the validity of our *in vitro* reconstituted XRN1 degradation assay as an approach to identify RNA structures that can stall the progression of the 5'-3' exoribonuclease.
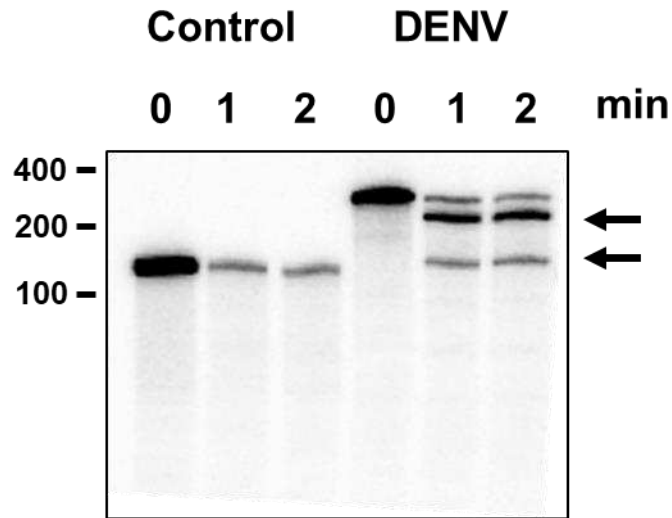
Figure 5. The 3' UTR of DENV-2 generates stable decay intermediates (sfRNA) by XRN1-mediated decay. Radiolabeled RNA containing a 5' monophosphate was incubated with recombinant XRN1 for the times indicated. The control RNA was derived from pGEM-4 vector sequence and the DENV RNA was derived from the DENV-2 viral 5' half of the 3' UTR inserted into the polylinker of pGEM-4. Reaction products were separated on a 5% polyacrylamide gel containing urea and visualized by phosphorimaging. The gel shown is representative of >3 independent experiments.

Zika virus is another member of the Flaviviridae that has recently emerged as a significant public health concern (Rosenberg et al., 2018; Zanluca et al., 2015). Sequence alignment analysis among over a dozen flavivirus genomes indicated a set of highly conserved sequences adjacent to the P1, L2 and P3/L3 regions of the structure that form key interactions in the three-helix junction structure that stalls XRN1 (Chapman et al., 2014a). Interestingly, the 3' UTR of ZIKV also maintains this same sequence conservation at appropriately spaced regions in two places at the proximal end of its 3' UTR (sfRNA1: GUCAG 10384-10388 and UGCxxxCUG 10413- 10420; sfRNA2: GUCAG 10468-10472; UGCxxxCUG 10503-10511) – indicating that ZIKV likely generates two sfRNA species by XRN1 stalling. This conservation of sequence and predicted structure strongly suggests that two highly stable knot-like structures will form consecutively at the proximal side of the 3' UTR of the ZIKV RNA just like it does in other insect-borne arboviruses. In addition, we hypothesize that targeted mutation of the conserved sequence blocks will disrupt the structure (as it does for WNV and DENV-2 sfRNA structures (Chapman et al., 2014a) and result in the lack of sfRNA formation.

To formally determine if the sfRNAs are generated by XRN1-mediated stalling at these two structures in the ZIKV 3' UTR, internally radiolabeled RNA containing either pGEM-4 sequence (control) or viral 3' UTRs (WT- the full length 3' UTR of Zika, MUT1- has a point mutation that disrupts the first predicted sfRNA structure, MUT2 - has a point mutation that disrupts the second sfRNA structure, and DM - has both point mutations and thus disrupts both three helix junctions) were incubated with HeLa cytoplasmic extract (Figure 6A), recombinant XRN1 (Figure 6B), or C6/36 (made from Aedes albopictus) cytoplasmic extract (Figure 6C). As seen in Figure 6, the wild-type 3'

UTR of Zika generated two sfRNAs by XRN1-mediated decay. As predicted, mutants 1

and 2 RNAs only generated one sfRNA each by XRN1-mediated decay and the double

mutant did not generate any sfRNAs like the control RNA. As this work was in progress,

the Kieft lab also demonstrated sfRNA generation by the Zika virus 3' UTR (Akiyama et

al., 2016). Collectively, these data demonstrate that Zika virus, like other insect-borne

flaviviruses, contains structures in its 3' UTR capable of stalling XRN1.
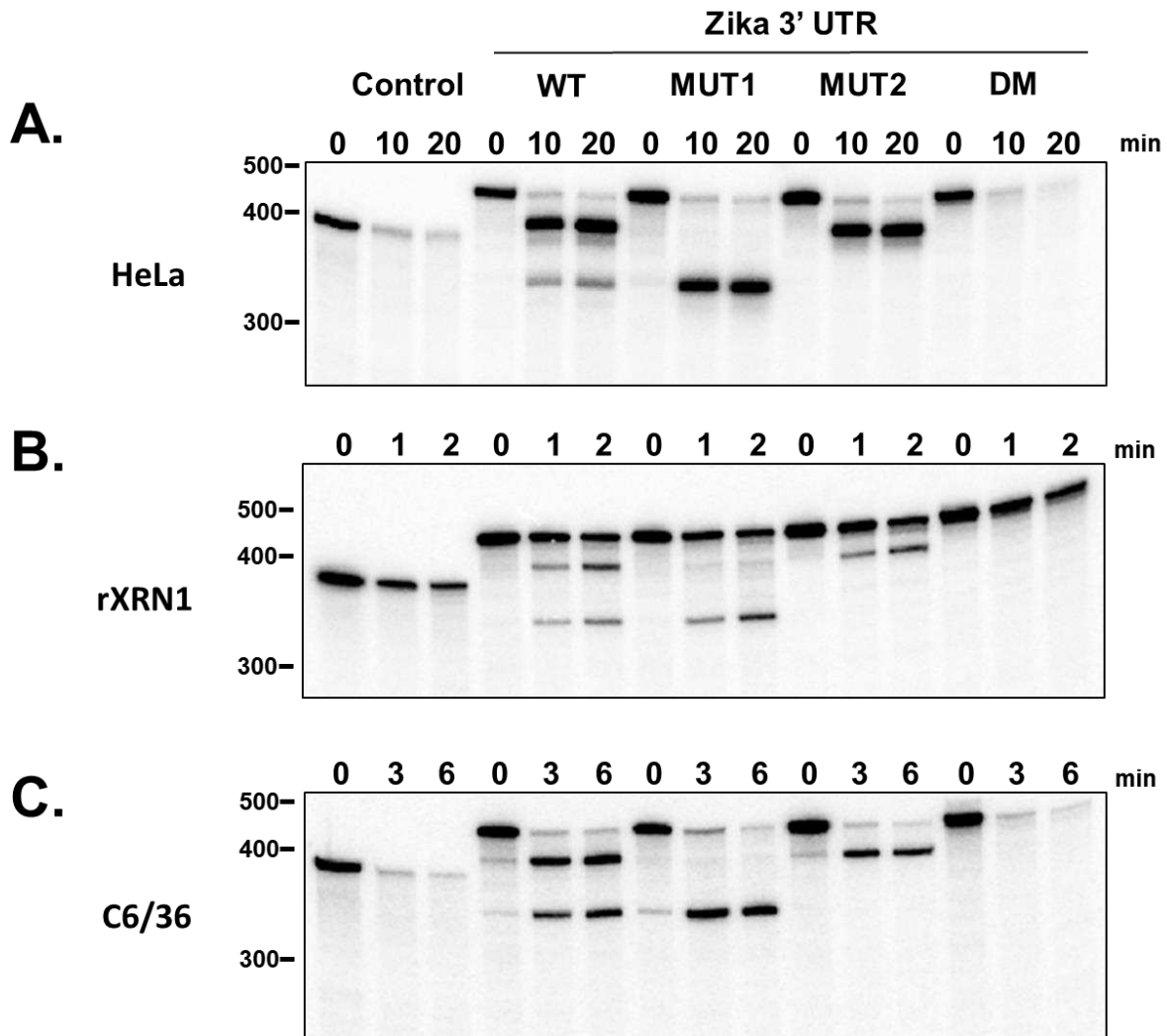
Figure 6. Zika sfRNA is generated by XRN1-mediated decay. Radiolabeled RNAs containing pGEM-4 vector-derived sequence (Control), or the Zika virus 3' UTR (either WT (wild type), MUT1 (which destroys the structure generating the 5' proximal knot-like structure), MUT2 (which destroys the structure generating the second (distal) knot-like structure), or DM (a Double Mutant which contains mutations that inhibit formation of both knot-like structures) were incubated for the times indicated with either Hela cytoplasmic extract (A), recombinant XRN1 (B), or C6/36 cytoplasmic extract (C) under conditions to favor 5'-3' decay. All RNAs contained a 5' monophosphate to ensure that they served as effective substrates for XRN1. Reaction products were separated on 5% polyacrylamide gels containing urea and visualized by phosphorimaging.

Generation of Zika sfRNA represses XRN1

XRN1 is the major enzyme in the 5'-3' decay pathway and possesses a highly processive exoribonuclease activity. Therefore, when XRN1 stalls on a flaviviral 3' UTR it appears from previous work to be released rather slowly, resulting in a transient but measurable repression of the enzyme (Moon et al., 2012; 2015). To determine if the sfRNA-generating portion of the 3' UTR of Zika virus can also repress XRN1, a monophosphate radiolabeled reporter RNA (to assess XRN1 activity over time) was incubated with recombinant XRN1 in the presence of a 16-fold molar excess of monophosphate competitor RNA. The competitor RNAs included a non-specific control, the sfRNA-generating portion of the DENV- 2 3' UTR as a positive control, or the sfRNA-generating portion of the 3' UTR of Zika virus. As seen in Figure 7, both the DENV-2 and ZIKV 3' UTR competitor RNAs repressed XRN1 activity when compared to the control. Intriguingly, the ZIKV 3' UTR did not cause as robust a repression of XRN1 as the DENV-2 3' UTR. This may be due to a faster release of the enzyme when it is stalled on the ZIKV 3' UTR compared to when it is stalled on the DENV-2 3' UTR. The ZIKV 3' UTR double mutant that fails to generate sfRNAs (Figure 6), also failed to repress XRN1 (data not shown). Thus, we conclude that the structured 3' UTR of ZIKV stalls and represses XRN1 like the RNAs of other insect-borne flaviviruses tested to date. Given the apparent differences in repression rates of XRN1 in reconstitution assays noted above, it will be interesting to assess and compare the impact of ZIKV and DENV-2-mediated XRN1 stalling on the relative stability of host cell mRNAs during infection in future studies.
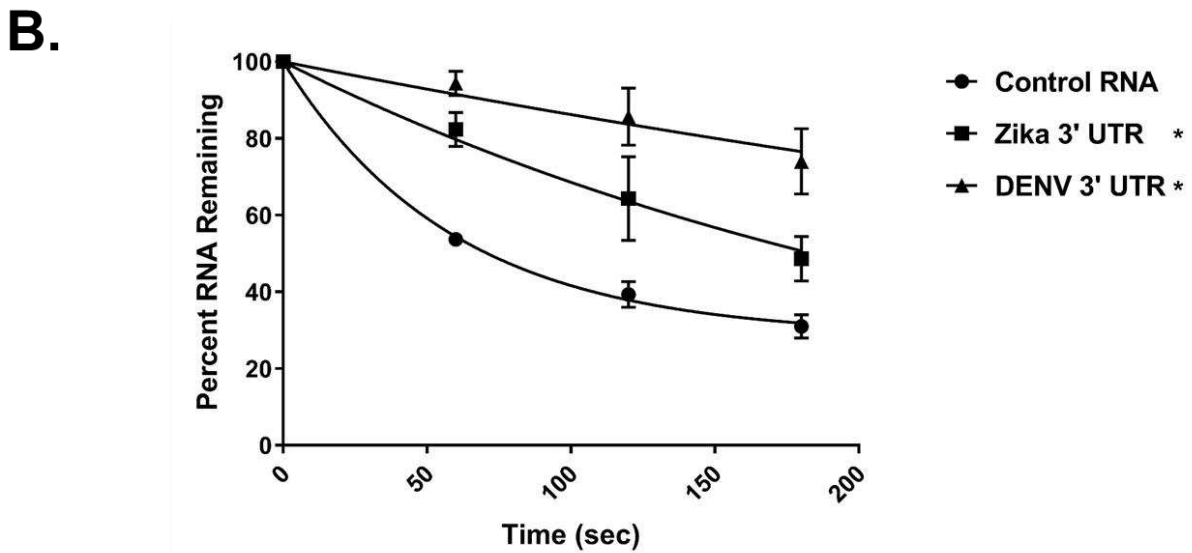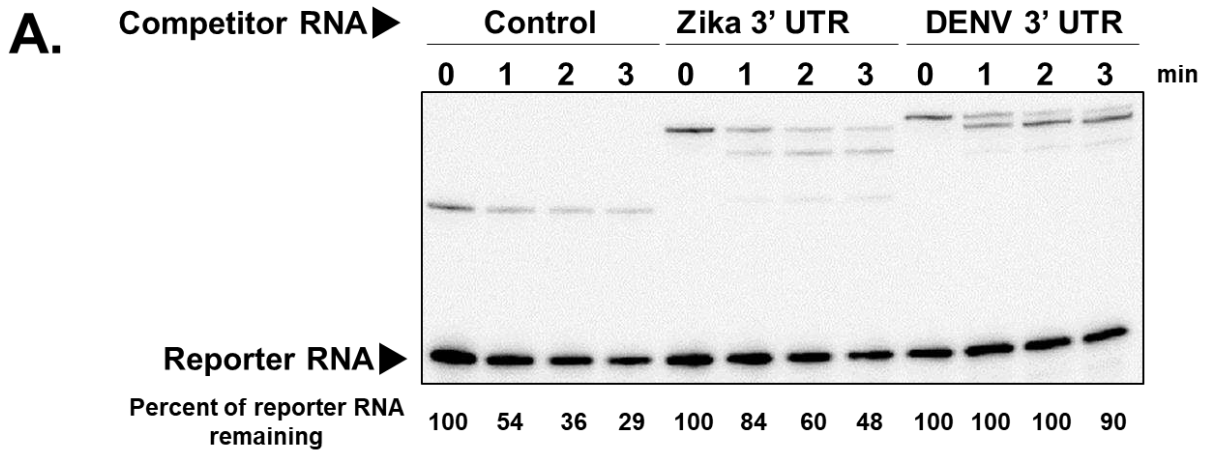
Figure 7. Generation of Zika virus sfRNA represses XRN1 activity in a reconstituted system.
Panel A: A radiolabeled reporter RNA (derived from pGEM-4 vector sequence) was incubated for the times indicated with recombinant XRN1 as well as with a 16-fold excess of competitor RNA (radiolabeled at a very low specific activity) containing either the Zika viral 5' half of 3'UTR (Zika 3' UTR lanes), the DENV-2 5' half of 3' UTR (DENV 3' UTR lanes) or a control sequence from pGEM-4 (Control lanes). Reaction products were resolved on a 5% polyacrylamide gel containing urea and visualized by phosphorimaging. Representative data of three independent experiments is shown. Panel B: Quantification of the efficiency of XRN1 activity in the presence of the indicated competitor RNA. The results of three independent experiments were used to generate the graph. The asterisk represents a p value of < 0.05 at all three time points for the viral 3' UTR/fragments compared to the control as determined using a two-way ANOVA and Holm-Sidak post-hoc analysis.

The 3' untranslated region of the N mRNA of Rift Valley fever virus stalls XRN1

Next, we wanted to expand our search to see if other virus families could stall XRN1. Rift Valley fever virus (RVFV) has a tripartite genome containing large (L), medium (M), and small (S) segments. The large and medium segments are in the negative-sense orientation. The small segment, on the other hand, uses an ambisense coding strategy in which both the viral and anti-viral S segments are used to produce two different messenger RNAs (Figure 8). Since many regulatory elements are normally located in the 3' UTR, we focused on the end of the open reading frame through the 3' UTR in our studies (Figure 8).

To determine if the 3' UTR of the four mRNAs of RVFV can produce stable decay intermediates via stalling of the XRN1 exoribonuclease, radiolabeled RNAs containing either the pGEM4 sequence or a 3' UTR from an RVFV mRNA were incubated in HeLa extract under conditions that favor 5'-3' decay. As seen in Figure 9A, only the 3' UTR of the nucleocapsid (N) mRNA of RVFV produced a decay intermediate. To assess whether the decay intermediate generated from the RVFV N 3' UTR was indeed a product of XRN1-mediated decay, RNAs were incubated with purified recombinant XRN1. As seen in Figure 9B, only the N 3' UTR of RVFV produced a decay intermediate, whereas the other three 3' UTRs were completely degrade similar to the control transcript. Finally, since RVFV is naturally transmitted by mosquitoes, we wanted assess whether the N 3' UTR was also capable of specifically stalling mosquito XRN1. As seen in Figure 9C, the 3' UTR of N mRNA of RVFV produced a decay intermediate in C6/36 cytoplasmic extracts. Lastly, to formally demonstrate that the size of the decay intermediate is similar regardless of the source of XRN1, decay

intermediates generated by RNA incubation with either cytoplasmic extract or recombinant protein were all run on a single 5% polyacrylamide gel containing urea. As seen in Figure 9D, the RVFV decay intermediate is the same size regardless of the source of XRN1. Thus, we conclude that the mRNA generated from the ambisense genomic segment of RVFV can stall XRN1 and generate a stable decay intermediate in reconstituted RNA decay assays.

Next, we wanted to determine if the RVFV N mRNA decay intermediate could also be detected in transfected or infected cells. To test this, the N 3' UTR of RVFV was subcloned into a GFP reporter construct and this construct was used to transfect HEK293T cells. In some experiments, a shRNA which targets the open reading of GFP was added to decrease the innate stability of the reporter mRNA and more readily allow for detection of RNA decay intermediates. As seen in Figure 10A, northern blot analysis showed the predicted decay intermediate from XRN1 stalling on the RVFV 3'UTR inserted sequence is indeed present in transfected cells. To determine if the N 3' UTR decay intermediate is detectable in an RVFV infection, Vero cells were infected at a MOI of 0.01 with the RVFV MP-12 strain and total RNA was collected 48 hour post infection. As seen in Figure 10B, northern blot analysis identified a decay intermediate of ~85 nucleotides, consistent with the size predicted from cell-free decay assays. Collectively, these data identify a novel RVFV N mRNA decay intermediate.
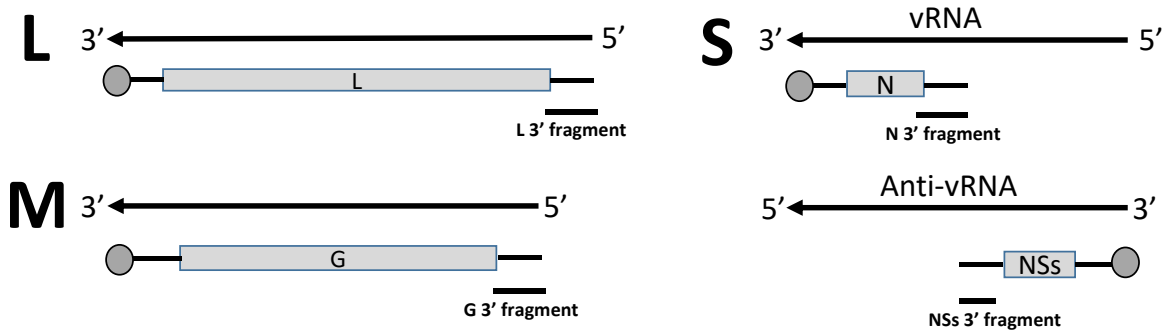
Figure 8. The genomes and mRNAs of Rift Valley Fever Virus. Diagrammatic description of the mRNAs generated from the three segments of Rift Valley Fever virus, a phlebovirus of the *Phenuiviridae.* The L segment is 6.4 kb; the M is 3.89 kb; and the S segment is 1.69 kb in size. Genomic (vRNA) and the antigenomic RNA (Anti-vRNA) from the S segment that serve as templates for mRNAs are indicated by the *arrows*. The 5′ and 3′ designations refer to the ends of the genomic or antigenomic RNAs and indicate their orientation as templates from which mRNAs are generated. The *circles* at the 5′ ends of the mRNA represent host cell-derived cap structures. The location of the small RNA fragments used in Figure 9 are indicated by the lines under the capped mRNAs.
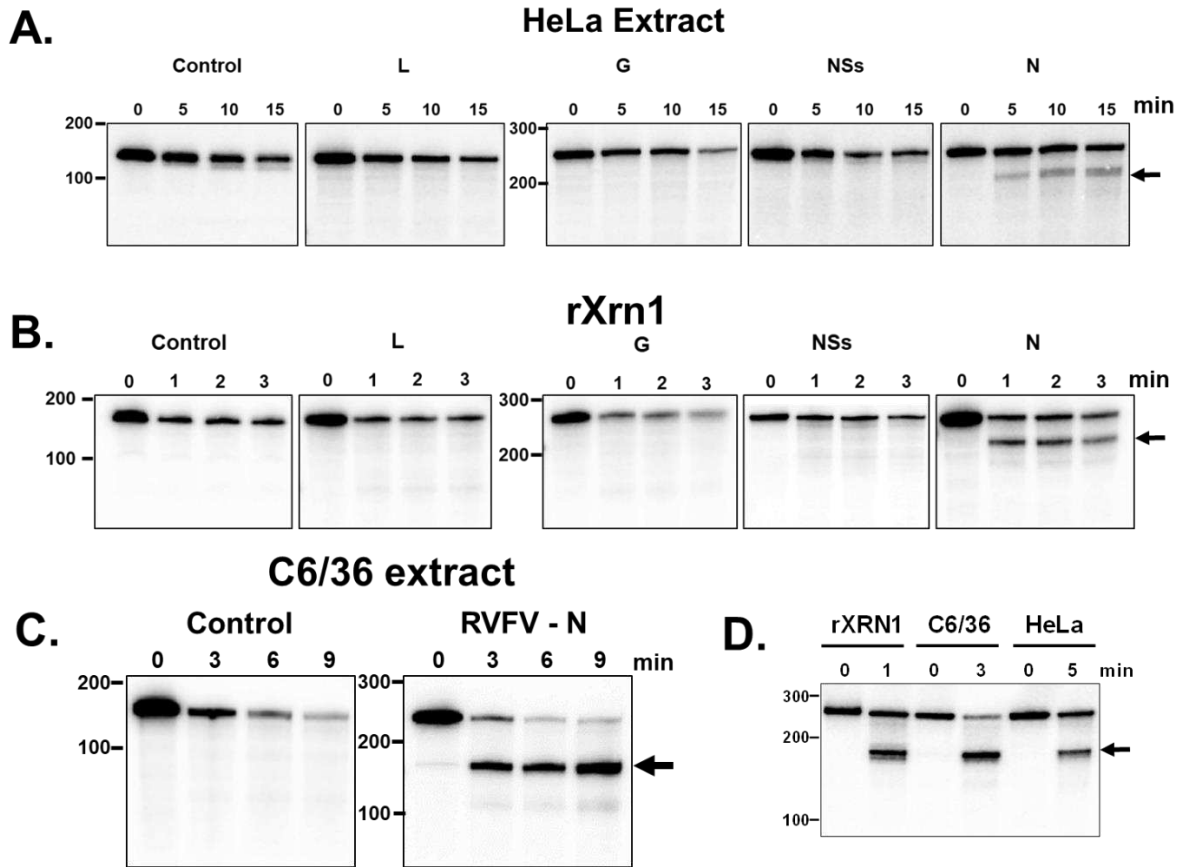
Figure 9. The 3' UTR of RVFV nucleocapsid (N) mRNA generates a stable decay intermediate by stalling XRN1. Radiolabeled, 5' monophosphorylated RNAs containing either pGEM-4 sequence (Control) or the 3' UTR of the indicated RVFV mRNA were incubated with Hela cytoplasmic extract (A), recombinant XRN1 (B), or C6/36 cytoplasmic extract (C) for the times indicated. Reaction products were separated on 5% polyacrylamide gels containing urea and visualized by phosphorimaging. In panel D, radiolabeled, 5' monophosphorylated RNAs containing the RVFV N 3' UTR were incubated with either recombinant XRN1 or the indicated cytoplasmic extract as described above. Reaction products were resolved on a single 5% denaturing polyacrylamide gel to compare the relative sizes of the decay intermediates that were generated. All gels are representative of >3 independent experiments.
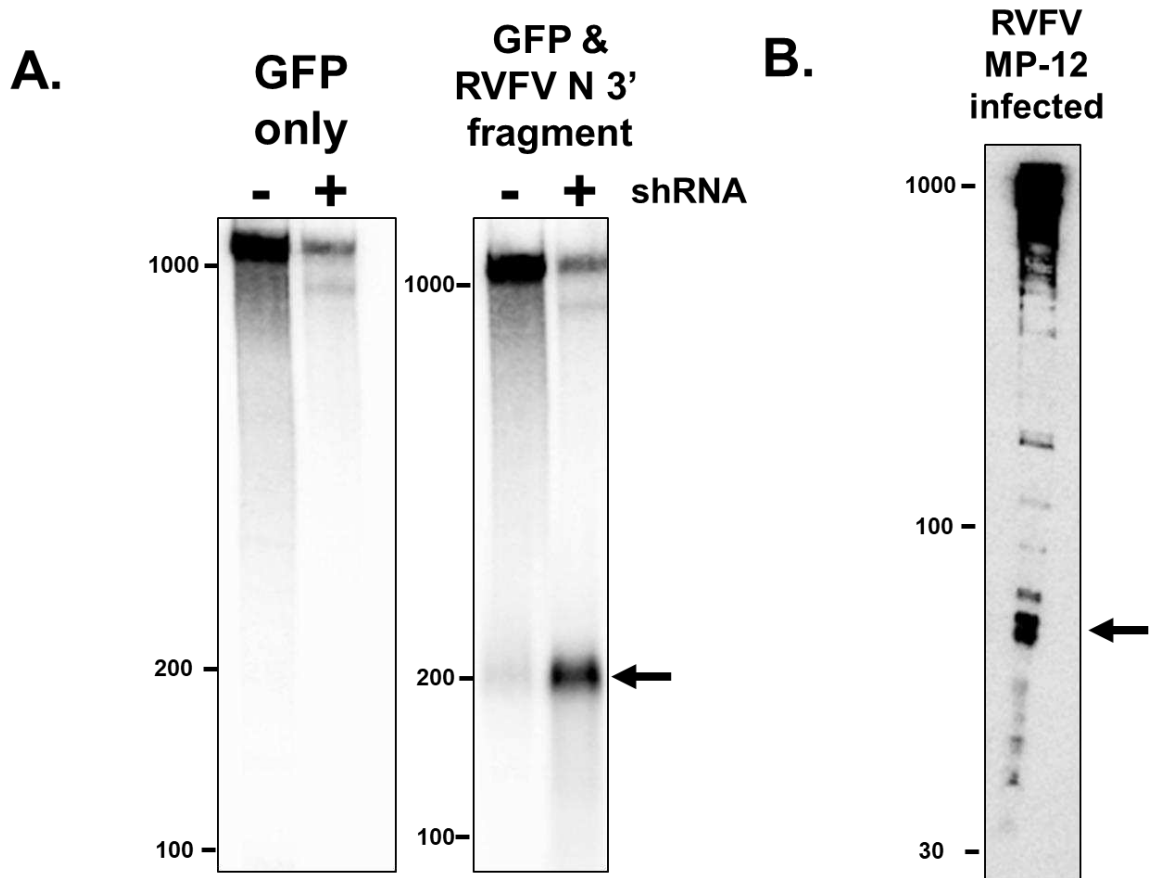
Figure 10.Stable RNA decay intermediates derived from the 3' UTR of the RVFV N mRNA are observable in transfected cells as well as cells infected with the RVFV MP-12 strain. Panel A: HEK293T cells were transfected with either an eGFP-expressing plasmid (GFP only lanes) or a plasmid expressing an eGFP-encoding mRNA containing the N 3'UTR of RVFV (GFP & RVFV N 3' fragment). To enhance the decay rate of the relatively stable eGFP mRNAs, shRNA targeting the eGFP open reading frame was co-transfected into the cells. Panel B: Vero cells were infected at an MOI of 0.01 pfu/cell with the strain MP-12 of RVFV in collaboration with Nicholas Bergren and Rebekah Kading. To assess for the presence of RNA decay intermediates, total RNA was isolated 48 h post-transfection and infection, separated on a 5% polyacrylamide gel containing urea, transferred to a membrane, and visualized using radioactive probes which hybridize to either a common sequence in the GFP 3' UTR (Panel A) or to the N 3' UTR of RVFV (Panel B). Results were visualized by phosphorimaging and gels are representative of at least three experiments. Arrows on the right of the gels indicate the identified decay intermediate.

XRN1 stalling is conserved among phleboviruses

Since XRN1 stalling is conserved among members of the *Flaviviridae,* we wished

to determine whether the 3' UTR of the N mRNA from other phleboviruses also have the

ability to stall XRN1. To test this, we choose the 3' UTRs of the N mRNAs of Sandfly

Naples virus (SFNV) and Heartland virus (HLV). Radiolabeled RNAs containing either a

control pGEM4-derived sequence or the SFNV or HLV 3' UTRs were incubated with

C6/36 cytoplasmic extract (Figure 11, top panel) or recombinant XRN1 (Figure 11,

bottom panel). As determined by the presence of decay intermediate, both of the 3'

UTRs SFNV or HLV N mRNAs have the ability to stall XRN1. These data clearly

indicate that XRN1 stalling is conserved among multiple phleboviruses.
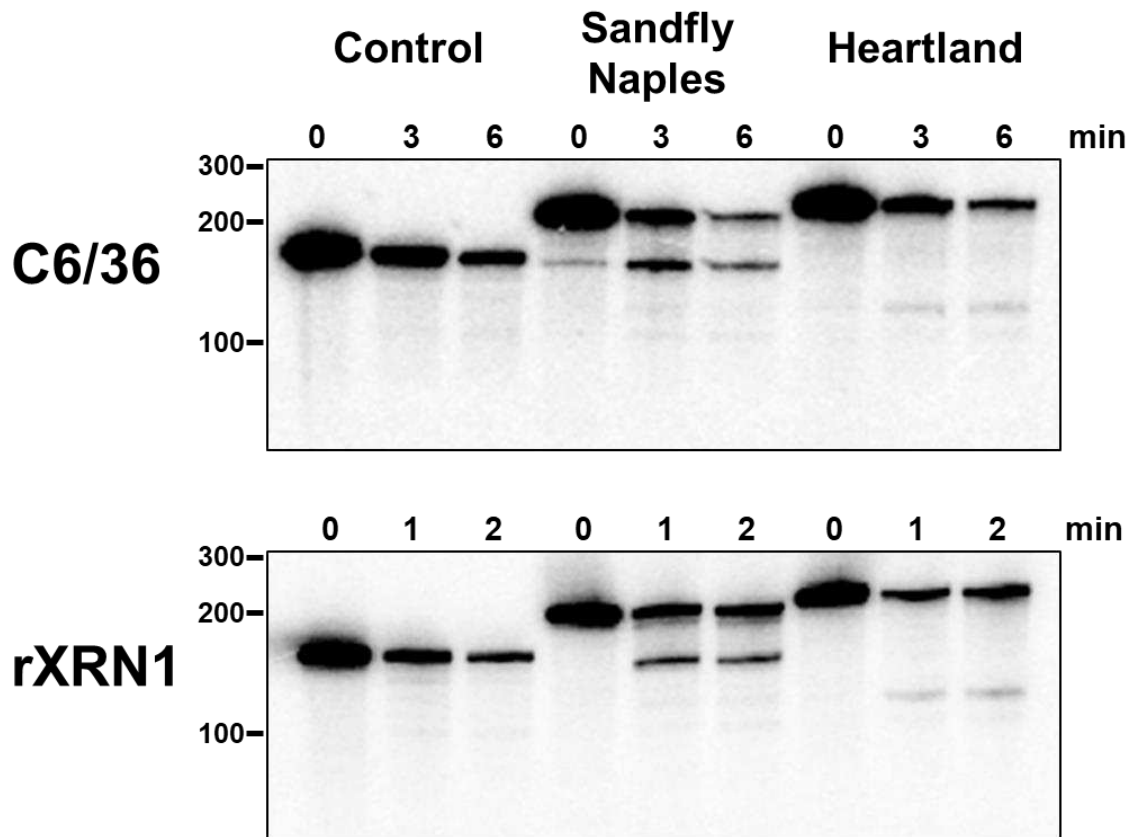
Figure 11. The 3' UTR of the nucleocapsid (N) mRNA from other phleboviruses can also stall XRN1.Radiolabeled, 5' monophosphorylated RNAs containing either pGEM-4 sequence (Control) or viral N 3′ UTRs of the Sandfly Naples virus (Sandfly Naples lanes) or Heartland virus (Heartland lanes) were incubated with C6/36 mosquito cell cytoplasmic extract (top panel) or recombinant XRN1 (bottom panel) for the times indicated. Reaction products were resolved on 5% polyacrylamide gels containing urea and visualized by phosphorimaging. All gels are representative of at least 3 independent experiments.

The 3' UTR of the nucleocapsid mRNA of RVFV has the ability to repress XRN1

Next, we wished to determine if the 3' UTR of N mRNA of RVFV has the ability to repress XRN1 as we have demonstrated with flaviviruses (e.g. Figure 7, above). Using a competition assay containing 20-fold molar excess of competitor RNA and following the decay efficiency of a radiolabeled reporter RNA by recombinant XRN1. The RVFV N 3' RNA fragment was able to repress XRN1 similarly to the sfRNA-generating portion of the 3' UTR of DENV-2 (Figure 12).
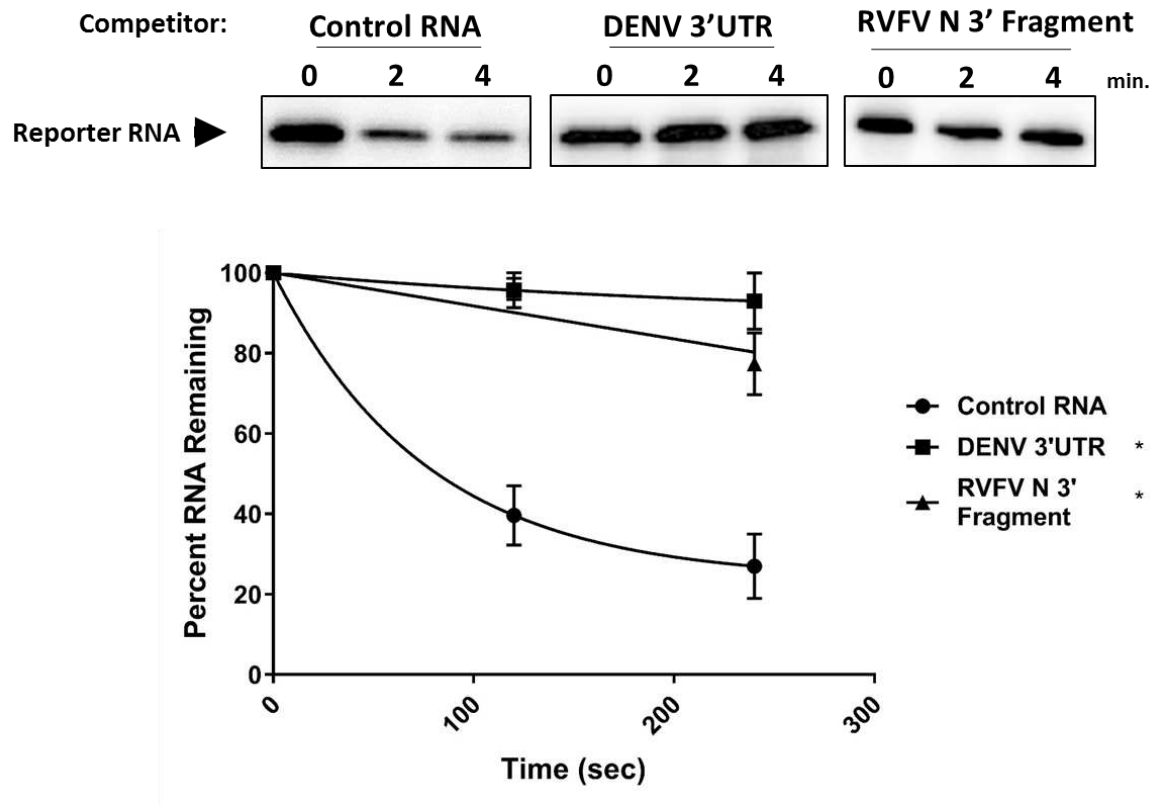
Figure 12.The N 3' UTR of RVFV represses XRN1 similarly to the DENV-2 3' UTR in a reconstituted system. A radiolabeled reporter RNA (derived from pGEM-4 vector sequence) was incubated for the times indicated with recombinant XRN1 in the presence of a 20-fold molar excess of competitor RNA containing either pGEM-4 sequence (Control RNA lanes), the N 3' UTR of RVFV (RVFV N 3' Fragment lanes) or the 5' half of the 3' UTR of DENV-2 (DENV 3'UTR lanes). Reaction products were run on a 5% acrylamide gel contain urea and visualized by phosphorimaging (top panel). Quantification of three independent experiments is shown in the graph (bottom panel). The asterisk represents a p value of < 0.001 at both time points for the two viral 3' UTR competitor RNA fragments compared to the control as determined by a two-way ANOVA and a Turkey's multiple comparison test as post-hoc analysis.

Mapping the XRN1 stall site of the RVFV decay intermediate

In order to begin to elucidate the structural requirements for stalling XRN1 on the

3' UTR of the RVFV N mRNA, we determined the 5' end of the decay intermediate to

map the stall site. RNA containing the 3' UTR of N mRNA of RVFV was incubated with

recombinant XRN1 for 15 minutes to maximize the amount of decay intermediate that

was generated. The decay intermediate was then gel purified, reverse transcribed, the

junction region was PCR amplified, and cloned into T-easy pGEM vector. Ten

independent colonies were sent for sequencing of the junction fragment, one colony

was inclusive. As seen in Figure 13, the RVFV N 3' UTR decay intermediate is

predicted to be about 178 nucleotides based on migration relative to an RNA (Figure 13,

upper). The 5' stall sites as determined from the nine independent clones are clustered

in this region of the RNA (Figure 13, bottom). Interestingly, the area around the stall site

is very G-rich suggesting that a specialized G-quadruplex structure could be involved in

XRN1 stalling on this RNA substrate. G-quadruplexes are known to be more stable in a

potassium environment than a lithium environment (Havrila et al., 2017; You et al.,

2017). To determine if the predicted structure is indeed a G-quadruplex, the monovalent

cations in the XRN1 decay assays were altered. As seen in Figure 14, stalling of XRN1

by the three-helix junction structure of DENV-2 (which is predicted to fold independently

of monovalent cations) was similar whether potassium chloride or lithium chloride was

added to the reaction. The situation with the RVFV N 3' UTR RNA, however, was

substantially different. In the presence of lithium chloride – which disfavors G-

quadruplex formation, the amount of stable RVFV N 3' UTR decay intermediate formed

was reduced to 36% of the remaining input RNA when compared to the 52% of the

remaining input RNA when potassium chloride is added (Figure 14, right). Thus, we

conclude that it is highly likely the RNA structure contributing to the XRN1 stalling for

the RVFV decay intermediate involves a G-quadruplex, a novel structure in terms of

natural viral RNA-mediated XRN1 stalling.

RVFV-N

300 —
200 — ← 178 nts
100 —

CAAGACAGCAGCCTAAGTGGCTGCCCAGGGGGTTGGGGGGAAGGGGAGTTGGGGTTACGGT
CGGGATTGGGGGGTGGGGGGTGGGGCAGCCTTAACCTCTAATCAACCTCAACAAATCCATC
ATCATCACTCTCCTCCTCTGATTCCATCTCAACATCTGGGATTGGAGGAATAACTGGAATC
CAGTTGTTTCTCCCCATCATGCT
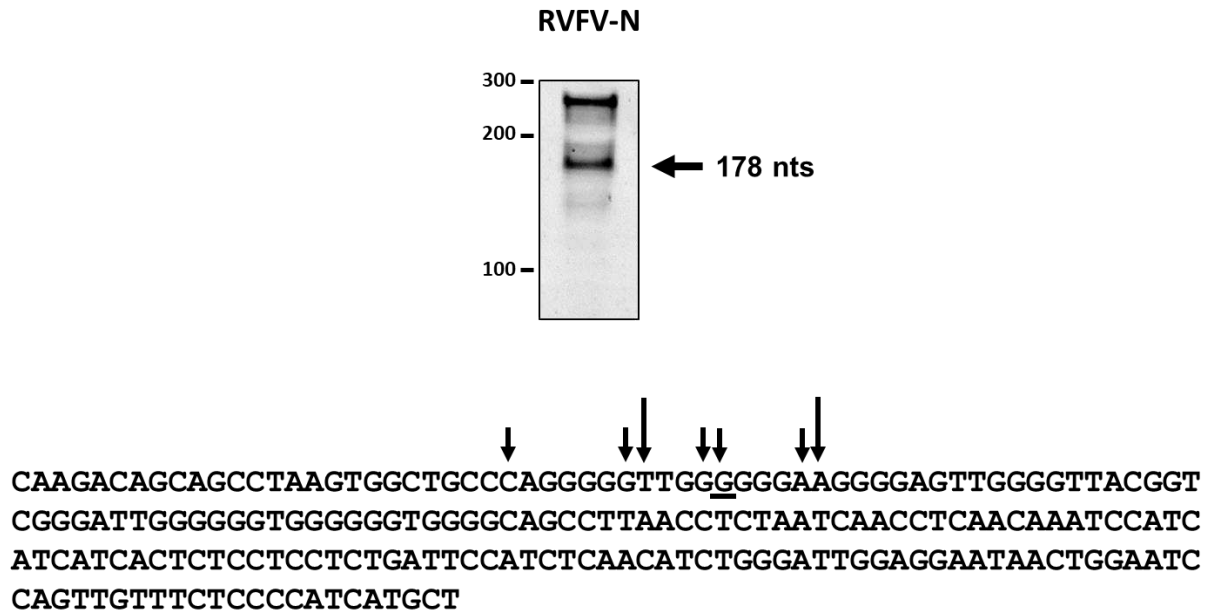
Figure 13. Determination of the XRN1 stall sites in the 3' UTR of the N mRNA of RVFV. Top Panel: 5 µg of unlabeled RNA containing the N 3′ UTR of RVFV was incubated with recombinant XRN1 for 15 min and reaction products were resolved on a 5% polyacrylamide gel containing urea and visualized by SYBR Green staining. The arrow at right indicates the size of the stable decay intermediate in nucleotides (nts) as calculated by migration relative to size markers from multiple gels. Bottom Panel: RNA decay intermediates from the top panel were excised, circularized, and reverse-transcribed to generate cDNA copies. The 5′–3′ junction fragment was cloned, and nine independent plasmids were sequenced. The positions of the 5′ end of the decay intermediates (i.e. the XRN1 stall site) in the sequenced clones are indicated by the arrows above the sequence of the N 3' UTR region of RVFV. The larger arrows at two sites indicate two independent clones that resulted from XRN1 stalling at those sites. The underlined nucleotide is the approximate stall site indicated by sizing of decay intermediates on acrylamide gels as described in the top panel.
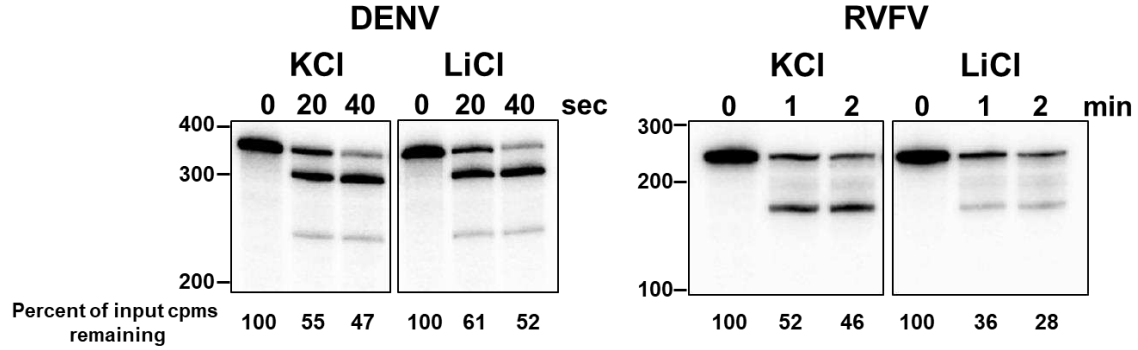
Figure 14. A G-quadruplex structure contributes to XRN1 stalling in N 3' UTR of RVFV. Radiolabeled, 5' monophosphorylated RNAs containing the 5' half of 3' UTR of DENV-2 (DENV panel) or the N 3' UTR of RVFV (RVFV panel) were incubated with recombinant XRN1 in the presences of 100 mM of potassium chloride (KCl lanes) or lithium chloride (LiCl lanes) for the times indicated. The number below the gels are the quantitative measure of total RNA decay (i.e. the amount of the input RNA that remaining on the gel) over time. Reaction products were separated on 5% urea polyacrylamide gels and visualized by phosphorimaging. Gels are representative of three independent experiments.

The 3' UTRs of arenaviruses also have the ability to stall XRN1

It was intriguing that the only mRNA 3' UTR region of the phleboviruses that stalled XRN1 was in the major ambisense coding genomic RNA fragment of the viruses. We therefore hypothesized that perhaps additional ambisense viral RNAs may be capable of stalling XRN1 since they are known to contain stable structural hairpins and perhaps other elements in their non-coding regions (Auperin et al., 1986; Clegg et al., 1991; López and Franze-Fernández, 2007; Wilson and Clegg, 1991). To assess this idea, we turned our attention to the other major family of mammalian RNA viruses that uses the ambisense coding strategy. The members of the *Arenaviridae* family are bi-segmented RNA viruses in which both genomic segments use the ambisense coding strategy to encode mRNAs from both the genomic and anti-genomic RNA species (Figure 15A). Furthermore, the intergenic region of these RNA species, which encodes the 3' UTR of the resultant mRNAs, is known to be highly structured (Ghiringhelli et al., 1991; Iapalucci et al., 1991; Salvato and Shimomaye, 1989). To determine if 3' UTRs of all four mRNAs of a model arenavirus, Junin virus (JUNV), produces XRN1 decay intermediates, we incubated radiolabeled RNAs containing each of the 3' UTRs of the viral mRNAs (L, N, Z, or GPC) with recombinant XRN1 (Figure 15B) or HeLa extract (Figure 15C). As seen in Figure 15, the 3' UTRs of all four JUNV mRNAs generated stable decay intermediates during XRN1-mediated decay. Therefore, we conclude that RNA structures associated with the ambisense coding strategy may also be moonlighting as XRN1 stall sites, expanding the biological implications of this strategy of viral gene expression.
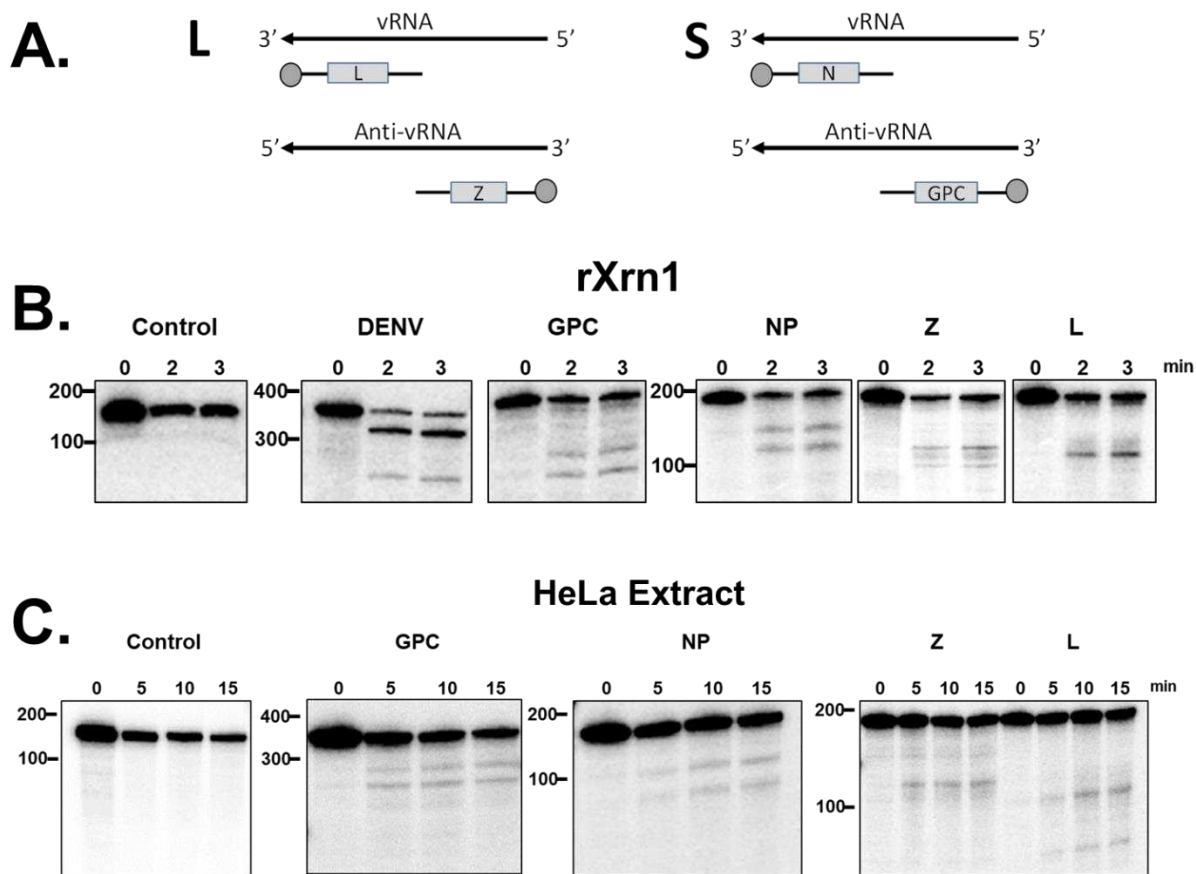
Figure 15. The 3' UTRs of the four independent mRNAs of Junin virus (JUNV) generate stable decay intermediates by XRN1-mediated stalling. Panel A: A diagram of arenavirus gene expression. Note that mRNAs are generated in an ambisense strategy from both genomic (vRNA) and antigenomic (Anti-vRNA) from both segments. Panels B and C: Radiolabeled, 5' monophosphorylated RNAs containing pGEM-4 sequence (Control lanes), the DENV-2 3' UTR (DENV lanes in panel B) or a 3' UTR region from the indicated Junin virus mRNA (GPC, NP, Z or L lanes) was incubated with recombinant XRN1 (Panel B) or Hela cytoplasmic extract (Panel C) for the times indicated. Reaction products were separated on 5% polyacrylamide gels containing urea and visualized by phosphorimaging. All gels are representative of >3 independent experiments.

XRN1 stalling is conserved among arenaviruses

Since the inclusion of structures that stall XRN1 appear to be conserved in all the

insect-borne flaviviruses as well as many if not all phleboviruses, we hypothesized that

the 3' UTRs of mRNAs from all arenavirus species may share the ability to stall XRN1.

To address this hypothesis, we isolated the 3' UTR region from mRNAs of two recently

described snake arenaviruses (SN-68 L or SN-90 Z) and incubated these transcripts

with recombinant XRN1 to search for stable decay intermediates. As seen in Figure 16,

both of the 3' UTRs of SN-68 L and SN-90 Z snake arenaviruses were able to stall

XRN1 and to produce decay intermediates. These data strongly suggest that XRN1

stalling may in fact be a conserved feature throughout the *Arenaviridae*.
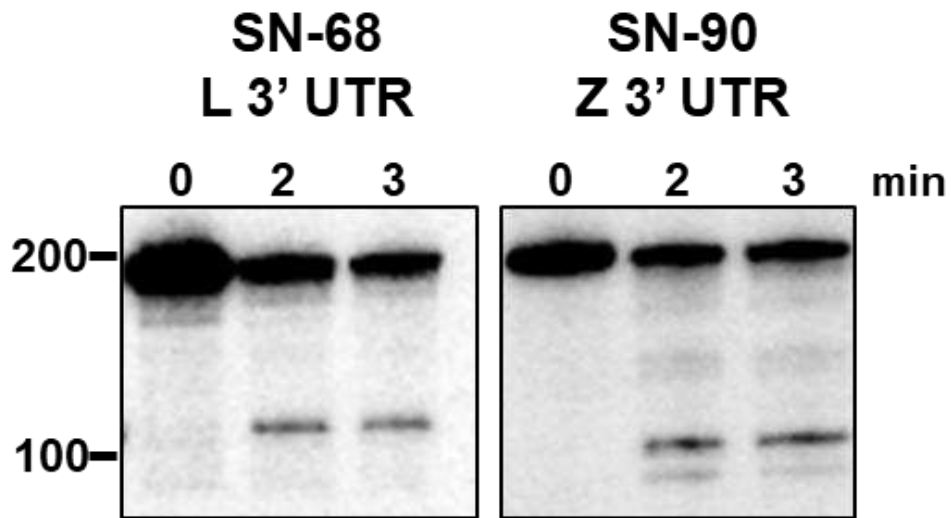
Figure 16. 3' UTRs derived from mRNAs of two novel snake arenaviruses also generate stable decay intermediates during XRN1-mediated decay. Radiolabeled, 5' monophosphorylated RNAs containing the 3' UTR of the L mRNA of SN-68 arenavirus (left panel) or the 3' UTR of the Z mRNA of SN-90 arenavirus (right panel) were incubated with recombinant XRN1 for the times indicated. Reaction products were separated on 5% polyacrylamide gels containing urea and visualized by phosphorimaging. All gels are representative of >3 independent experiments.

Arenaviruses can also repress XRN1 activity

We next wished to determine if stalling in the 3' UTR of arenavirus mRNAs can also repress XRN1, likely due to a relatively slow rate of release of the enzyme from the substrate. To address this, we used a radiolabeled reporter RNA to track the activity of the recombinant XRN1 enzyme in the presence of 20-fold molar excess of various competitor RNAs. As seen Figure 17, the 3' UTRs of the JUNV L mRNA as well as the Z mRNA of the snake arenavirus SN90 were able to repress XRN1 activity when compared to the control RNA. The lower efficiency of repression observed with the SN90 Z competitor RNA may be related to a faster off rate of the stalled enzyme on this transcript. This suggests that the structure(s) in the 3' UTR of arenavirus mRNAs share the ability to both stall and repress XRN1 like was observed with flavivirus and phlebovirus 3'UTR structures.
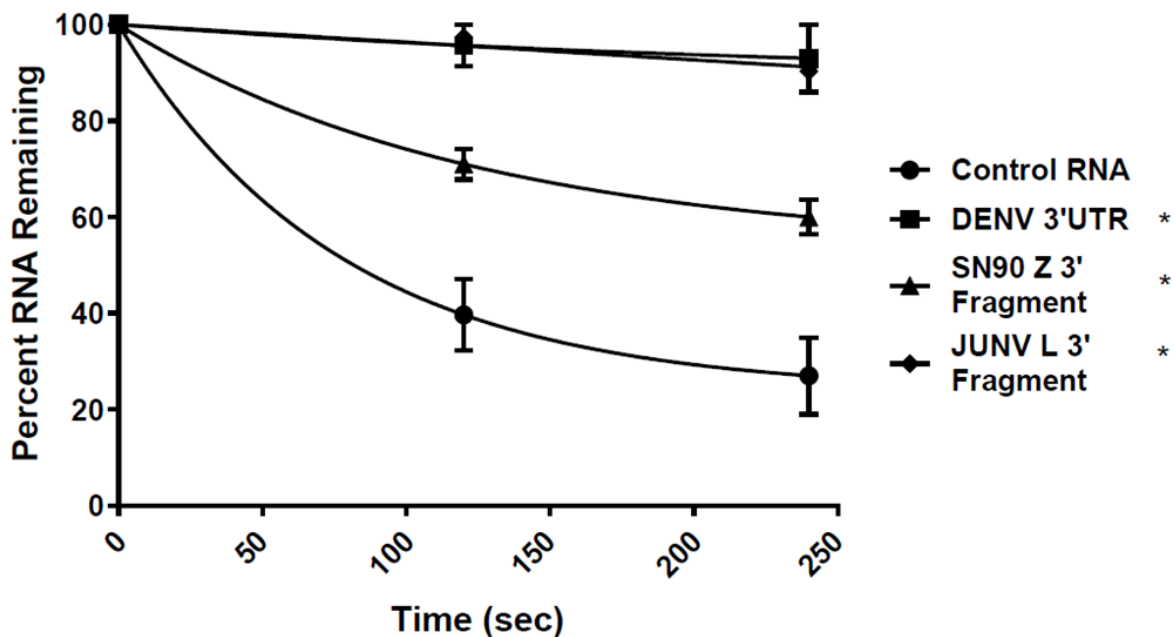
Figure 17. The 3' UTR of the L mRNA of JUNV as well as the 3' UTR of the Z mRNA of SN90 virus repress XRN1 activity in a reconstituted system. A radiolabeled reporter RNA (derived from pGEM-4 sequence) was incubated with recombinant XRN1 in the presence of a 20-fold molar excess of competitor RNAs containing either the 5' half of the 3' UTR of DENV-2, the Z 3' UTR of SN90 virus, the L 3' UTR of JUNV, or pGEM-4 derived sequences (Control RNA) for the times indicated. Reaction products were run on a 5% acrylamide gel containing urea and visualized and quantified by phosphorimaging. Quantification of three independent experiments is shown in the graph. The asterisk represents a p value of < 0.001 at both time points for all three viral 3' UTR competitor RNA fragments compared to the control RNA as determined by a two-way ANOVA and a Turkey's multiple comparison test as post-hoc test.

A region of the RNA 3 segment of Beet Necrotic Yellow Vein Virus (BNYVV) can stall and repress XRN1

So far in this dissertation, we have extended the strategy of RNA-mediated XRN1 stalling and repression to two additional families of mammalian RNA viruses. We now wished to explore whether some plant RNA viruses may also use a similar strategy to interface with the cellular RNA decay machinery. In particular, beet necrotic yellow vein virus (BNYVV), a multi-segmented RNA virus which is a part of the genus Benyvirus (Lee et al., 2001; Ratti et al., 2009), has recently been determined to produce a non-coding RNA with a 5' end that is generated post-transcriptionally, perhaps through the action of XRN1 (Peltier et al., 2012). Interestingly, this non-coding RNA is generated from the RNA 3 segment of the virus that is responsible for viral dissemination throughout the plant (Flobinus et al., 2016). A conserved 20 base 'coremin' sequence at the 5' end of this non-coding RNA has been shown to be indispensable for its generation (Peltier et al., 2012).

To determine if the BNYVV RNA 3 non-coding RNA is indeed generated by XRN1, a 55-nucleotide sequence containing the conserved coremin sequence of BNYVV (Figure 19, top) was inserted into pGEM4 to produce an RNA containing a 53-nucleotide leader (to serve as a landing site for XRN1) followed by the BNYVV sequence. RNAs were incubated with recombinant XRN1 or C6/36 extract (in conditions that favor 5'-3' decay). As seen in Figure 18, the RNA containing the BNYVV-55mer produced a stable decay intermediate by both recombinant XRN1 and in C6/36 extracts, consistent with RNA-mediated stalling of XRN1. In order to determine the minimal sequence region required for stalling XRN1, we created a set of three deletion variants

99

(Figure 19). While the 55 base B3 variant produced an XRN1 decay intermediate, the other variants containing less BNYVV sequence did not (Figure 19). This suggests that a 55-base fragment is sufficient to stall XRN1

Based on our mammalian virus work and XRN1 stalling, the next logical step was to determine if the BNYVV-55mer also has the ability to repress XRN1. XRN1 decay assays were run in the presence of 20-fold molar excess of viral 3' UTR-containing or control competitor RNAs. As seen in Figure 20, the BNYVV-55mer was able to repress XRN1 in a similar fashion to the well-characterized DENV-2 3' UTR. These data indicate that select plant RNA viruses also use the strategy of XRN1 stalling/repression and that this novel viral RNA-host interaction could contribute to plant virus-induced cytopathology.
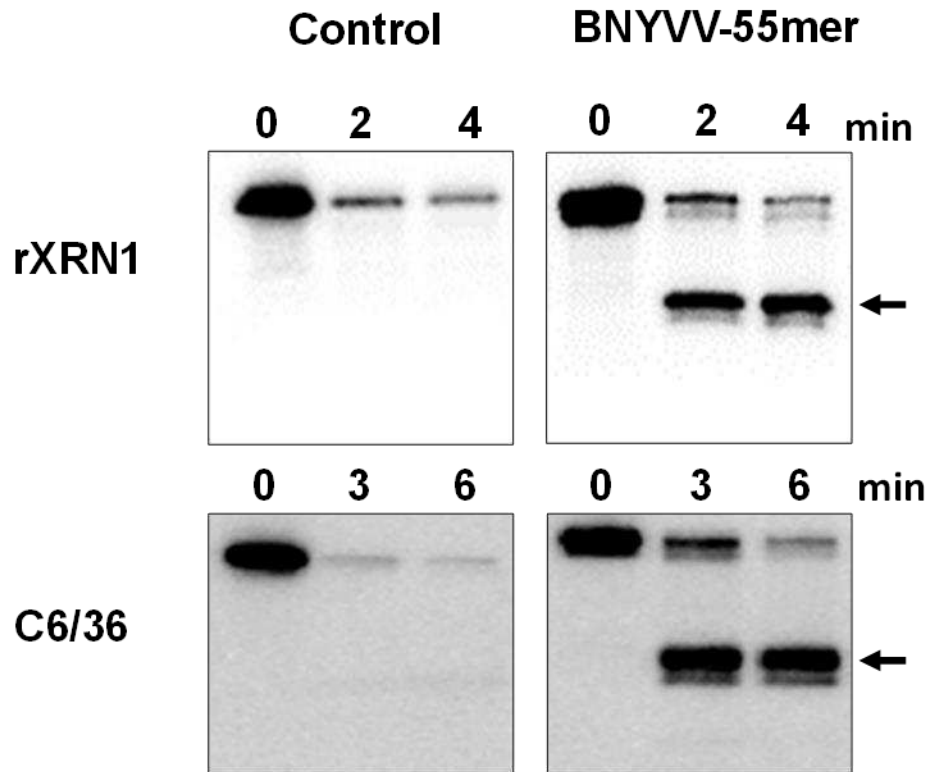
Figure 18. A 55 base fragment derived from the RNA 3 segment of BNYVV generates a stable decay intermediate during XRN1-mediated decay. Radiolabeled, 5' monophosphorylated RNA containing either pGEM-4 derived sequence (control lanes) or a 55-nucleotide fragment from the 3' UTR of the RNA 3 segment of beet necrotic yellow vein virus was incubated with recombinant XRN1 (top panel) or C6/36 cytoplasmic extract (bottom panel) for the times indicated. Reaction products were separated on 5% polyacrylamide gels containing urea and visualized by phosphorimaging. The decay intermediate generated by XRN1 stalling is indicated by the black arrows on the right. All gels are representative of at least three independent experiments.
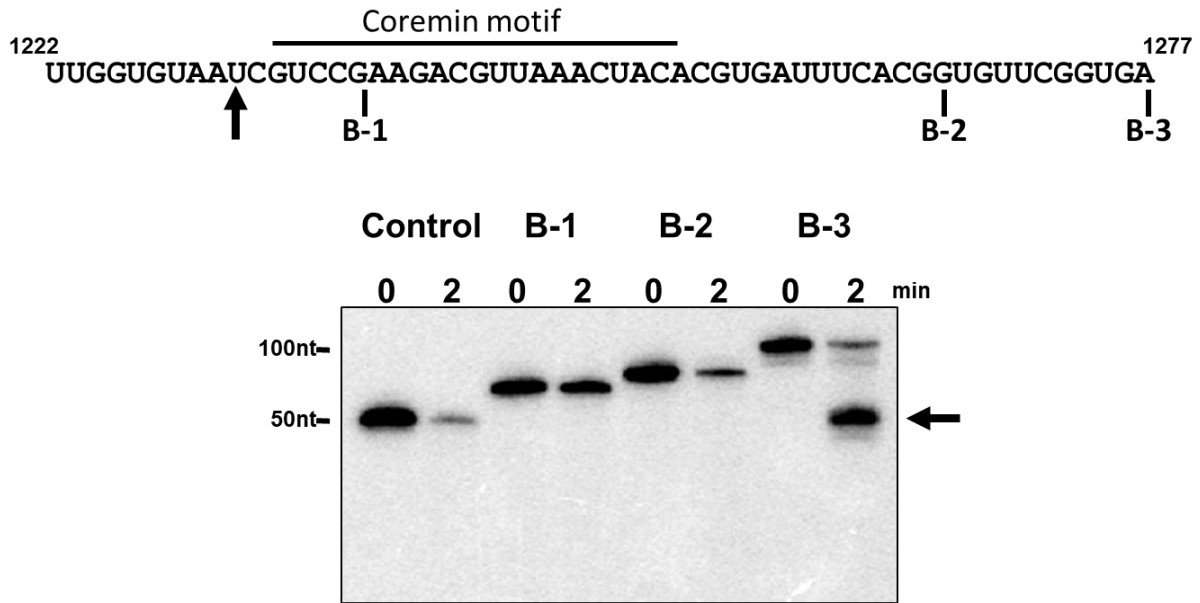
Figure 19. Mutational analysis of the BYNVV RNA fragment indicates a 55-base fragment is necessary for XRN1 stalling. Top Panel: The 55-base sequence of BNYVV RNA derived from the 3' UTR of the RNA 3 segment. B-1, B-2 and B-3 variant RNAs begin at position 1222 and have their 3' end at the position indicated by the bars. The black arrows indicates the start of the 5' decay fragment begins. Bottom Panel: Radiolabeled, 5' monophosphorylated RNAs containing either control sequences derived from pGEM4 (Control lanes) or the B-1, B-2 and B-3 sequences indicated above were incubated with recombinant XRN1 for the times indicated. Reaction products were resolved on a 5% acrylamide gel containing urea and viewed by phosphorimaging. The decay intermediate generated by XRN1 stalling is indicated by the black arrow on the right. The gel is representative of at least three independent experiments.
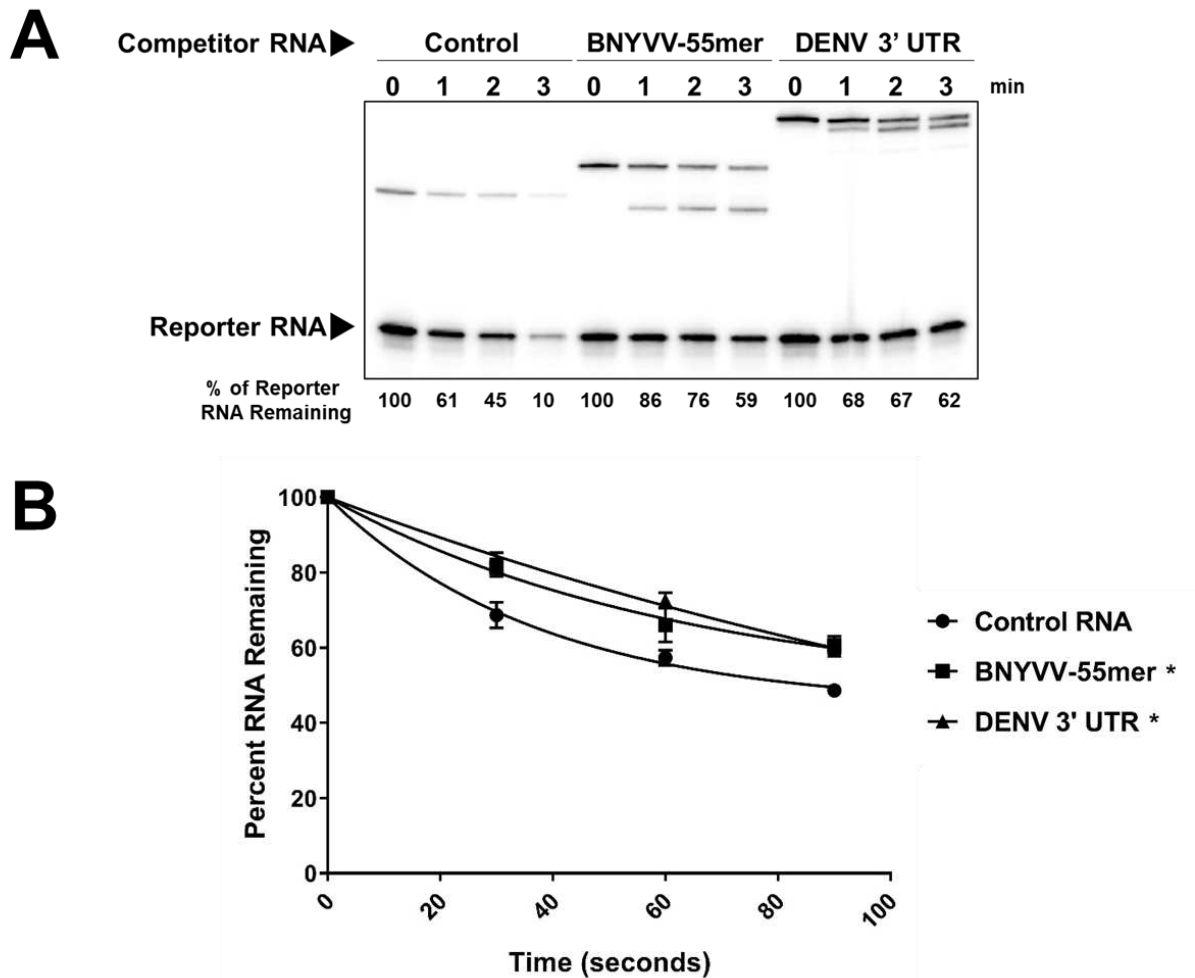
Figure 20. The BNYVV-55mer RNA represses XRN1 activity. Panel A: A reporter RNA (derived from pGEM-4 sequence) was incubated with recombinant XRN1 in the presence of a 20-fold molar excess of a competitor RNA containing either a viral 3'UTR (the 55-nucleotide fragment of the 3' UTR of BNYVV (BNYVV-55mer lanes) or the 5' half of the 3' UTR of DENV-2 (DENV 3' UTR lanes), or sequence from pGEM-4 (Control lanes) for the times indicated. Reaction products were run on a 5% acrylamide gel containing urea and visualized by phosphorimaging. Panel B: Quantification of three independent experiments performed as described in Panel A is shown in the graph. The asterisk represents a p value of < 0.001 at all three-time points for the viral 3' UTR competitor RNAs compared to the control RNA competitor as determined by a two-way ANOVA and a Turkey's multiple comparison test as post-hoc test.

Coronavirus that contain a conserved pseudoknot in the 3' UTR does not stall XRN1

Given that RNA structures in the non-coding regions of flaviviruses, phleboviruses, arenaviruses and a benyvirus have the ability to stall XRN1, we wondered if any conserved viral RNA structure could stall the exoribonuclease. Thus, we next tested a conserved, pseudoknot-containing RNA structure in the 3' UTR of coronaviruses mRNAs (Figure 21A). RNAs containing the 3' UTR of mRNAs made by Middle Eastern respiratory syndrome coronavirus (MERS-CoV) were incubated with recombinant XRN1 to assess the generation of degradation intermediates. As seen in Figure 21B, the MERs-CoV 3' UTR did not generate any decay intermediates similar to the control RNAs. In addition, northern blot analysis on total RNA from MERs-CoV infected cells showed no sign of a decay intermediate (Figure 21C). These data suggest that not all conserved viral RNA structures can stall XRN1.
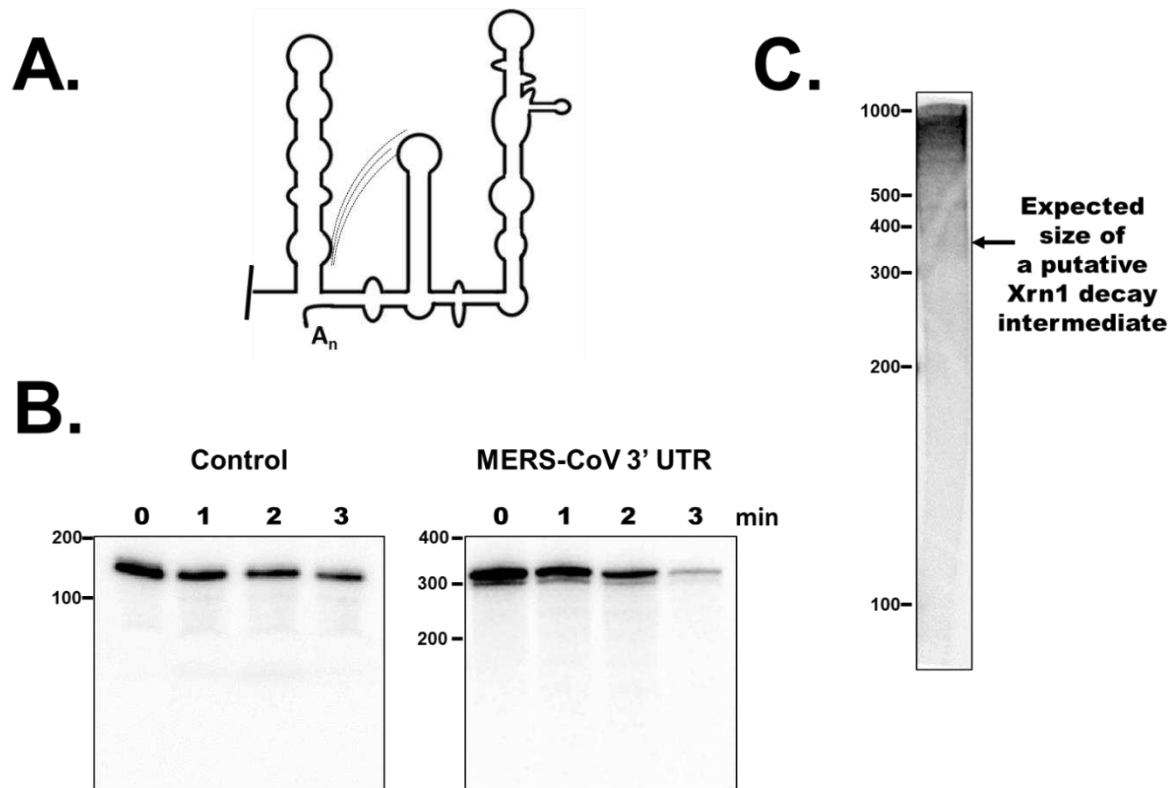
Figure 21. The 3′ UTR of Middle Eastern Respiratory Syndrome Coronavirus (MERS-CoV) which contains a conserved pseudoknot structure fails to stall XRN1. Panel A: diagrammatic representation of the conserved pseudoknot structure present in the 3′ UTR of the mRNAs of the *Coronaviridae*. Panel B: Radiolabeled, 5' monophosphorylated RNA containing pGEM4 sequence (control lanes) or the MERS-CoV 3′ UTR (MERS-CoV 3′ UTR lanes) was incubated with recombinant XRN1 for the times indicated. Reaction products were resolved on a 5% polyacrylamide gel containing urea and visualized by phosphorimaging. Panel C: Vero cells were infected at Middle Eastern Respiratory Syndrome Coronavirus in collaboration with Tony Schountz. To assess for the presence of RNA decay intermediates, total RNA was isolated 48 h post-transfection and infection, separated on a 5% polyacrylamide gel containing urea, transferred to a membrane, and visualized using radioactive probes which hybridize to the 3' UTR of MERS-CoV. Data shown are representative of three independent experiments.

Section II: Triptycene-based molecules disrupt the ability of the knot like three-helix junction structure in DEN-2 sfRNA to stall XRN1

For years, triptycene-based molecules have been used in cancer treatments (Perchellet et al., 1999; Wang et al., 2001a, 2006) and sometimes drugs can be repurposed. Triptycene-based molecules are created from using triptycene (resembles a paddle wheel) as the base and the addition of different chemical groups are added to it to create different analogs. The triptycene base is made up of three rings that produce a scaffold which has the ability for diversification of up to 14 positions (Barros and Chenoweth, 2014). In Figure 22A illustrates the 14 positions addition of different functional groups (such as aldehyde, haloalkane, ester, and amide) can diverse binding function (Yoon et al., 2016). In Figure 22B is an example of one of the chemical structures used in this study.

X-ray crystallography of the portion of the 3' UTRs of Murray Valley encephalitis virus (MVEV) and Zika virus that stall XRN1 has identified a stabilized three-helix junction structure as a key component of the stall site (Akiyama et al., 2016; Chapman et al., 2014a). Recent independent studies have shown some triptycene-based molecules can specifically bind to three-helix junctions in DNA and RNA (Barros and Chenoweth, 2014; Yoon et al., 2016). Thus, we wished to test if these triptycene-based molecules (Figure 22B) might be able to disrupt the three-helix junction structure in the 3' UTR of flavivirus RNAs and allow XRN1 to effectively degrade the entire mRNA, thereby reducing the amount sfRNA produced. We surveyed a set of independent triptycene-based compounds (Figure 22B) for their ability to reduce the amount of

sfRNA generated by XRN1 off a flavivirus RNA substrate. Radiolabeled RNAs containing the 3' UTR structure of DENV-2 that stalls XRN1 was incubated with recombinant enzyme in the presence of a variety of triptycene-based molecules. As seen in Figure 23, triptycene 1, 5, 6, and 10 all had an effect on sfRNA generation. Thus, we chose these 4 compounds to follow up in more depth to gain insight into their mechanism of action.
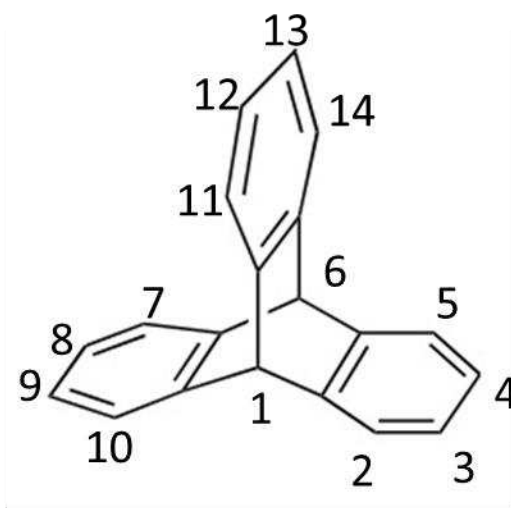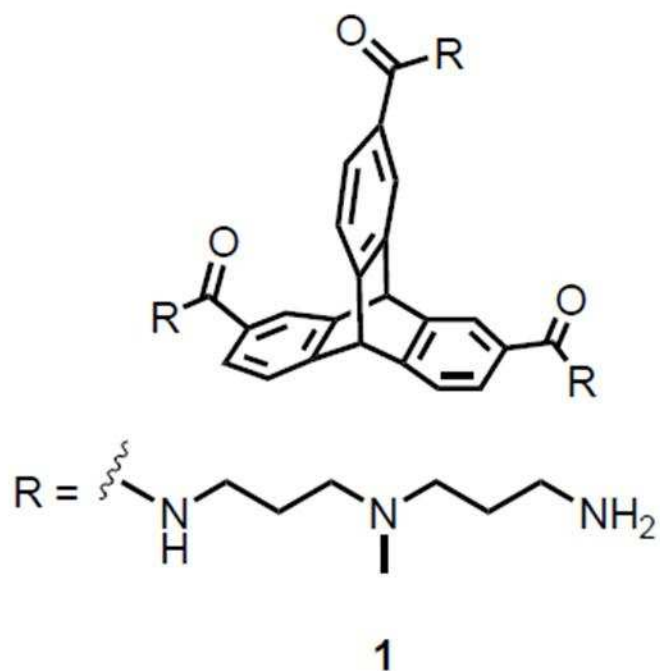
Figure 22. The chemical structure of triptycenes based molecule. Panel A: The basic chemical triptycene structure. Panel B: The chemical structure of one of the ten triptycenes based molecules used in this study (Images taken from Barros and Chenoweth, 2014). Provide by David M. Chenoweth lab (University of Pennsylvania).
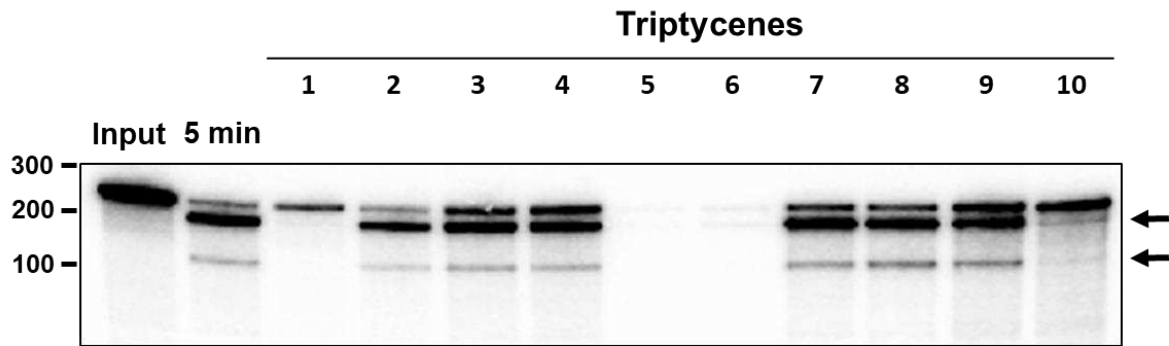
Figure 23. Select triptycene derivatives disrupt sfRNA generation by XRN1-mediated decay. Radiolabeled, 5' monophosphorylated RNA containing the 5' half of 3' UTR of DENV-2 was incubated with recombinant XRN1 in the presences of 250 μM of 10 triptycene derivatives for five minutes. Reaction products were separated on a 5% polyacrylamide gel containing urea and visualized by phosphorimaging. The decay intermediates generated by XRN1 stalling are indicated by the black arrows on the right. The gel is representative of at least three independent experiments.

Some triptycene compounds cause RNAs to partition with the organic phase during phenol extraction

As seen in Figure 23, the addition of triptycenes 5 and 6 to XRN1 decay assays resulted in a dramatic reduction in the amount of input RNA recovered following incubation, phenol extraction, and ethanol precipitation. We suspected that in the presence of these small molecules, the radiolabeled RNA substrates were either being non-selectively degraded or were being pulled into the organic phase via intercalation of the triptycene compounds into the RNAs. To determine if the triptycene - RNA complexes were being pulled into the organic phase during phenol/chloroform extraction, the organic extraction step was omitted following XRN1 treatment and the RNA products were directly ethanol precipitated and analyzed by gel electrophoresis. As seen in Figure 24, treatment with triptycenes 1, 5, 6, and 10 not only blocked sfRNA generation by XRN1, they all now resulted in similar levels of RNA recovery. This suggests that in addition to binding and disrupting the three-helix junction structure to allow XRN1 read-through, triptycenes 5 and 6 give the RNA-drug complex sufficient hydrophobic character to draw the RNA into the organic phase during phenol/chloroform extraction.
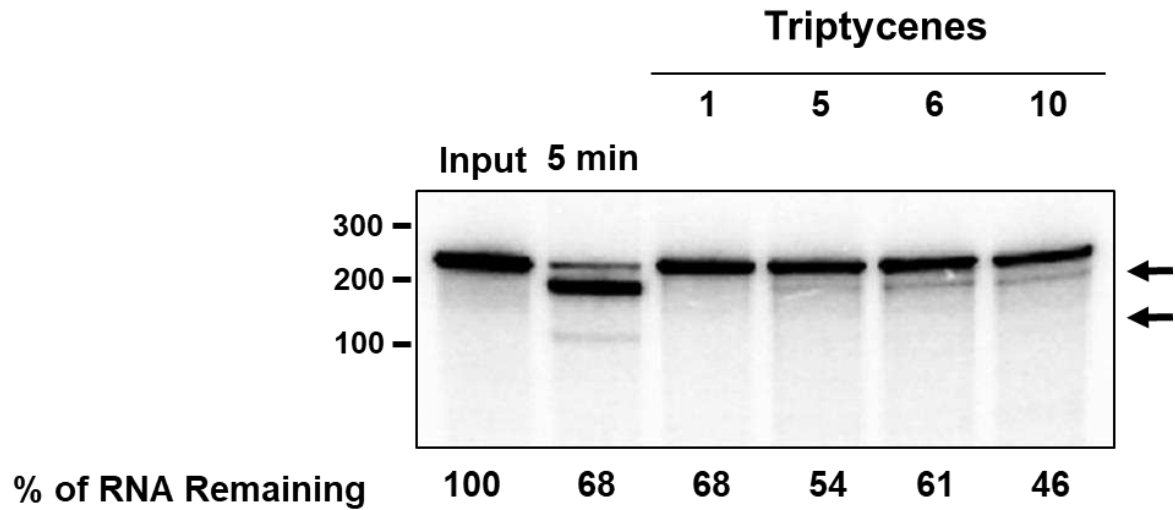
Figure 24. Triptycene 1, 5, 6, and 10 disrupt generation by XRN1-mediated decay.
Radiolabeled, 5' monophosphorylated RNA containing the 5' half of the 3' UTR of DENV-2 was incubated with recombinant XRN1 in the presences of 250 µM of the indicated triptycenes for five minutes. Following incubation, the standard phenol extraction clean up step was omitted and samples were directly ethanol precipitated and loaded onto the gel. Reaction products were separated on 5% polyacrylamide gel containing urea and visualized by phosphorimaging. The decay intermediate generated by XRN1 stalling is indicated by the black arrows on the right.

Triptycenes 1 and 10 inhibit XRN1 stalling by the knot-like flavivirus 3' UTR structures in a dose-dependent fashion

Finally, we focused our attention on triptycenes 1 and 10 since they appear to disrupt the generation of sfRNA without substantially affecting the extractability of the RNA substrate (Figure 23 and 24). To confirm that triptycene 1 can inhibit XRN1-mediated sfRNA generation, we performed a controlled time course. As seen in Figure 25A, the addition of triptycene 1 to an XRN1 decay assay slightly reduced overall XRN1 activity as well as blocked the generation of sfRNA. Next, we titered in the compound to determine the effective range of concentrations to inhibit sfRNA generation by XRN1. As seen in Figure 25B, 50 µM of triptycene 1 is sufficient to disrupt sfRNA generation under our standard in vitro reaction conditions. Similar data were obtained for inhibition of sfRNA generation by the triptycene 10 compound (Figure 26). Finally, since all experiments to date with this compound used the DENV-2 3' UTR sfRNA-generating RNA fragment as substrate, we wanted to assess whether the triptycene 1 could block XRN1 stalling by other flavivirus 3' UTR structures. As seen in Figure 27, 125 uM triptycene 1 effectively blocked the stalling of XRN1 by the Zika virus 3' UTR. Collectively, these data identify triptycenes 1 and 10 as repressors of flavivirus RNA-mediated XRN1 and suggest that this class of compounds may represent a chemical backbone for the future development of broad spectrum anti-flaviviral therapeutics.
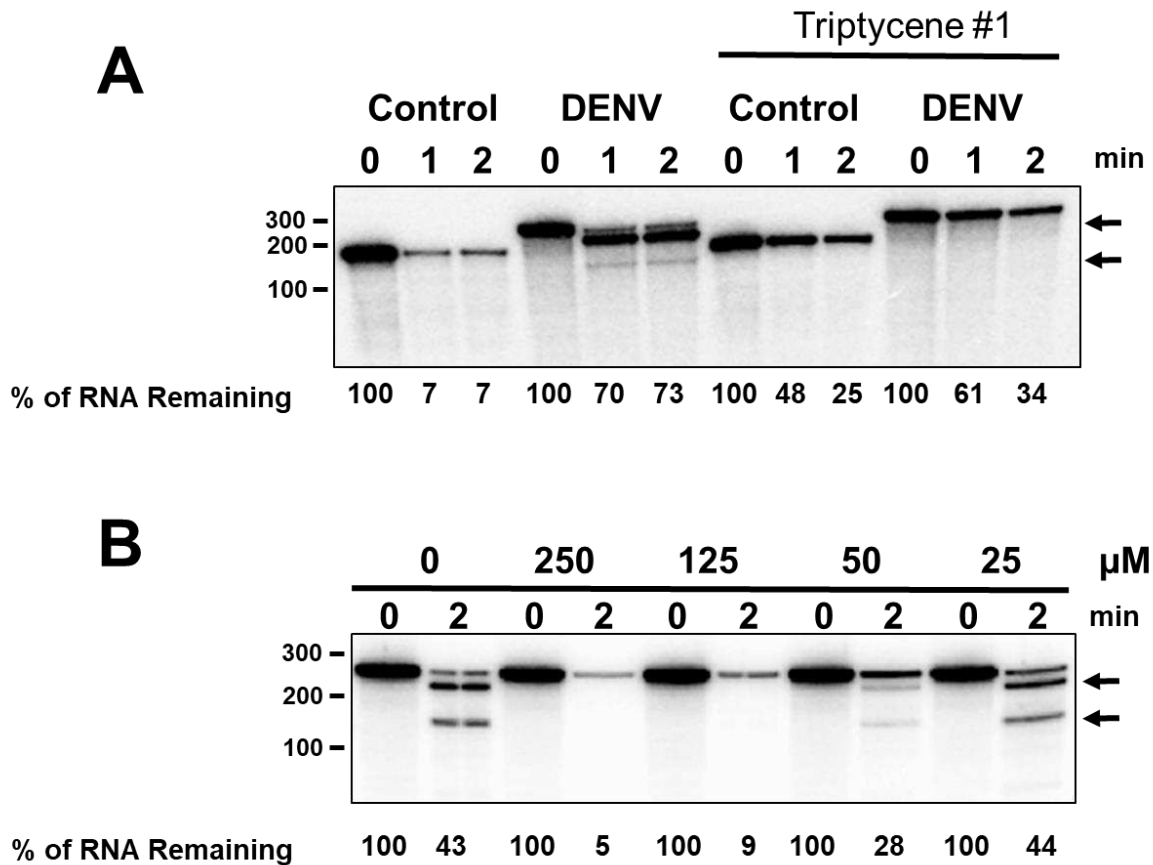
Figure 25. Triptycene 1 disrupt DENV-2 sfRNA generation by XRN1-mediated decay.
Panel A: Radiolabeled, 5' monophosphorylated RNAs containing the pGEM-4 sequence
(Control lanes) or the 5' half of the 3' UTR of DENV-2 (DENV lanes) were incubated with
recombinant XRN1 in the presence of 250 μM of triptycene 1 (triptycene #1 lanes) for the times
indicated. Panel B: A titration of triptycene 1 from 0 μM to 250μM was tested in the XRN1 decay
assay as described in Panel A. Reaction products were separated on 5% polyacrylamide gels
containing urea and visualized by phosphorimaging. The rate of the decay was measured as
the percent of total input RNA remaining on the gel and is indicated under the lanes of both
panels.
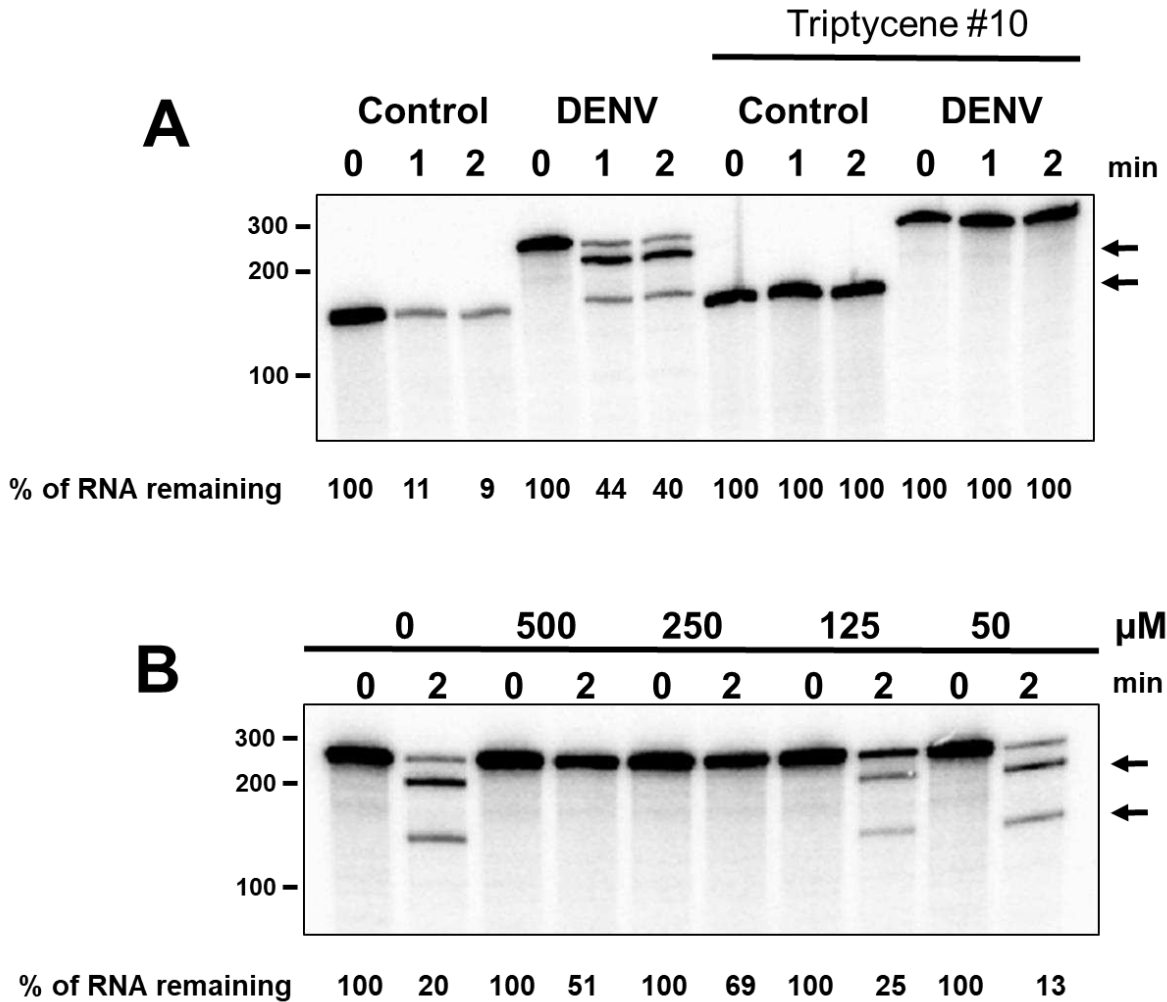
Figure 26. Triptycene 10 inhibits overall XRN1 enzymatic activity. Panel A: Radiolabeled, 5' monophosphorylated RNAs containing the pGEM-4 sequence (Control lanes) or the 5' half of the 3' UTR of DENV-2 (DENV lanes) were incubated with recombinant XRN1 in the presence (right side) or absence (left side) of 250μM of triptycene 10 for the times indicated. Panel B: Radiolabeled, 5' monophosphorylated RNA containing the 5' half of the 3' UTR of DENV-2 was incubated with recombinant XRN1 in the presence of the indicated concentrations of triptycene 10. Reaction product were separated on 5% polyacrylamide gel containing urea and visualized by phosphorimaging. The rate of the decay was measured as the percent of total input RNA remaining on the gel and is indicated under the lanes in both panels.

114
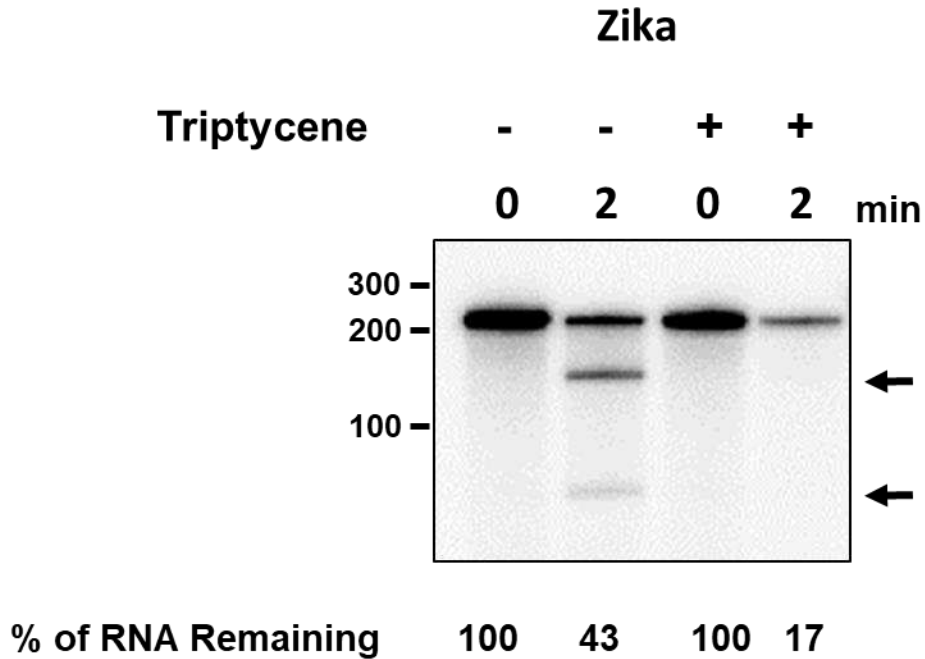
Figure 27. Triptycene 1 also disrupt XRN1-mediated sfRNA generation from the Zika virus 3' UTR. Radiolabeled, 5' monophosphorylated RNA containing the 5' half of the 3' UTR of Zika virus was incubated with recombinant XRN1 in the presence of 125μM of triptycene 1 for the times indicated. Reaction products were separated on a 5% polyacrylamide gel containing urea and visualized by phosphorimaging. The rate of the decay was measured as the percent of total input RNA remaining on the gel and is indicated under the lanes.

Section III: The mammalian DOM3z/DXO 5'-3' exoribonuclease does not appear to stall on flavivirus 3' UTRs like XRN1

DOM3z/DXO is a multi-functional enzyme that possesses both decapping as well as 5'-3' exoribonuclease activity (Jiao et al., 2013). The main cellular function identified to date for DOM3z/DXO is the decapping and degradation of defective pre-mRNA (Jiao et al., 2013, 2017). Recently, DOM3z/DXO has been implicated as a factor that specifically targets flaviviral RNAs during infection (Dr. Brian Geiss, personal communication). To determine if the mammalian DOM3z/DOX exoribonuclease can stall and contribute to the generation of flaviviral sfRNAs, we assessed the activity of the purified recombinant enzyme in reconstituted 5'-3' RNA decay assays as described above for XRN1. As seen in Figure 28, DENV-2 or RVFV- N 3' UTR-containing RNAs generated stable decay intermediates with XRN1 as expected from our earlier results. Incubation of the same RNAs with DOM3z/DXO, however, failed to generate stable decay intermediates from either the DENV-2 or RVFV-N RNA substrates. These data suggest that the mammalian DOM3z/DXO enzyme, unlike XRN1, may have the ability to degrade through either the knot-like three helix junction or G-quadraplex based structures to degrade the RNA.
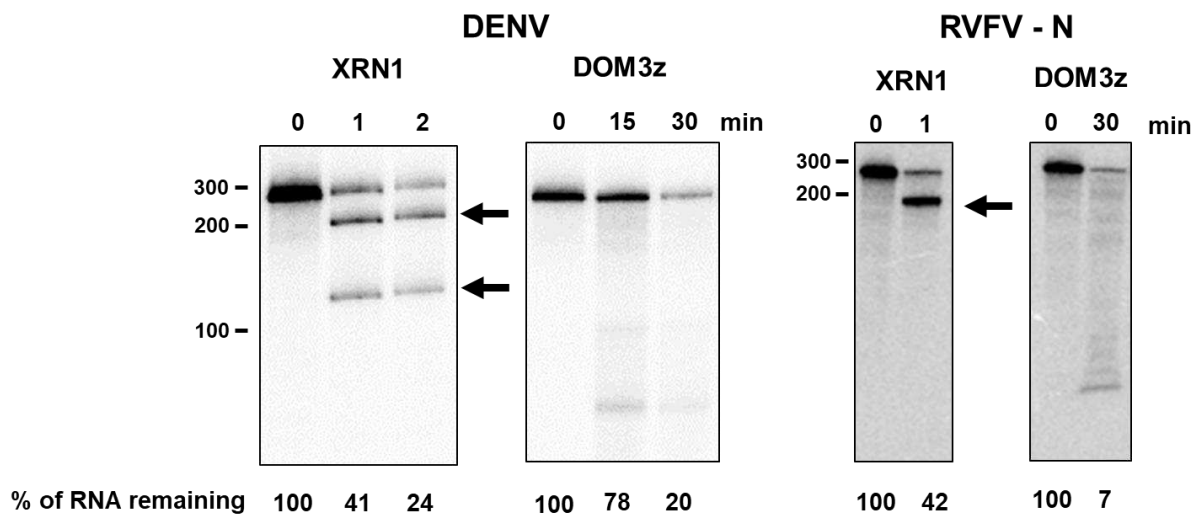
Figure 28. Unlike XRN1, the mammalian DOM3Z/DXO 5'-3' exoribonuclease does not stall on structural elements in DENV-2 or RVFV 3' UTRs. Radiolabeled, 5' monophosphorylated RNAs containing the 5' half of the 3' UTR of DENV (left side) or N 3' UTR of RVFV (right side) were incubated with either recombinant XRN1 or DOM3Z/DXO for the times indicated. Reaction products were separated on 5% polyacrylamide gels containing urea and visualized by phosphorimaging. The arrows indicate XRN1-generated decay intermediates. The rate of the decay was measured as the percent of total input RNA remaining on the gel and is indicated under the lanes.

117

Chapter 4: Discussion

Summary of Results

In this study, we have made seven key observations that represent a significant increase in our understanding of the interaction between viral RNAs and the cellular RNA decay machinery. First, we were able to reproduce that another member of the *Flaviviridae*, Zika virus, generates two sfRNAs via the stalling and subsequent repression of XRN1. Second, the 3' UTR of the RVFV N mRNA, as well as the N mRNAs of two other phleboviruses, generates a decay intermediate due to XRN1 stalling. We narrowed the sequence in the 3' UTR of RVFV N mRNA required for stalling of XRN1 to a G-rich region that is capable of forming a possible G-quadruplex structure. Third, all four of the 3' UTRs of the mRNAs generated by the ambisense JUNV RNA genome stall XRN1 and produce decay intermediates. This may be a highly conserved feature of arenaviruses as we observed similar efficiencies of XRNA 1 stalling by the 3' UTRs of mRNAs from two novel snake arenaviruses. Fourth, we also established XRN1 stalling as a strategy used by plant RNA viruses. We demonstrated that the BNYVV RNA 3 generates a non-coding RNA fragment via XRN1-mediated decay. The minimal sequence for the BNYVV was 55nt in our assays, which includes the previously established coremin motif. Fifth, we used the pseudoknot region of the 3' UTR of MERS-CoV to demonstrate that there is selectivity in RNA structures that can stall XRN1. Thus, not all highly conserved, knot-like structures, have the ability to stall XRN1. Sixth, we provided proof-of-principle data to suggest that structures that stall XRN1 may be valid targets for small molecule drugs. We identified four potential triptycene-based molecules which have the ability to disrupt DENV-2 sfRNA generation

by XRN1. Lastly, we provided evidence that all cellular 5'-3' exoribonucleases may not be susceptible to stalling by the viral RNA structures that we identified. The human (mammalian) DOM3z/DXO enzyme, for example, fails to produce sfRNA decay intermediates from flaviviral 3' UTRs and efficiently degrades the entire transcript. This might be an example of the molecular arms race between the virus and the host as the cell may have evolved DOM3z/DXO to at least in part effectively remove viral RNAs from the cell. Overall, the work reported here, and previously published literature on flavivirus-mediated XRN1 stalling, demonstrates that XRN1 stalling and repression is a strategy used by five independent virus families (*Phenuiviridae, Arenaviridae, Benyviridae, Flaviviridae*, and *Tombusviridae*).

Could XRN1-generated viral RNA fragments be functional small non-coding RNAs?

Pathogen-specific small non-coding RNAs, transcripts $\leq$ 200 nucleotides long, have been previously identified from both DNA and RNA viruses. Epstein-Barr virus (EBV) encodes several ~22 nucleotide (nt) miRNAs which are generated from the apoptosis regulator BHRF1 gene along with two clusters within the BART gene (Kang et al., 2015; Qiu et al., 2011; Skalsky et al., 2012). Recently, EBV miRNA-BART16 has been demonstrated to target the 3' UTR of viral latent membrane protein (LMP) 1 mRNA and modulate its expression (Zhang et al., 2018b). This was tested by transfecting BART16 mimics into GT38 and GT39 gastric epithelial cell lines which are positive for Epstein-Barr virus. Addition of 50 nM of the BART16 mimic caused a decrease in the levels of LMP1 mRNA and protein. In addition, EBV also encodes two

non-coding RNAs called Epstein-Barr virus Encoded RNA (EBER) 1 and 2 (Lerner et al., 1981). EBER 1 (167 nt) and EBER 2 (172 nt) are transcribed by host cell RNA polymerase III (Howe and Shu, 1988; Lerner et al., 1981). EBERs have been shown to interact with several host protein; the La protein (Lerner et al., 1981), double-stranded RNA-activated protein kinase R (PKR) (Clarke et al., 1991), ribosomal protein L22 (Toczyski et al., 1994), hnRNP-D/AUF1 (Lee et al., 2012), and retinoic acid inducible gene I (RIG-I) (Samanta et al., 2008). The EBERs are proposed to form complexes with these factors as a way to sequester them and preventthem from properly doing their jobs. Deletion of both EBERs resulted in slower transformation potential of B-cells when compared to wildtype EBV infection (Yajima et al., 2005). It was shown the EBER 2 is important for B-cell growth /transformation and interacts with interleukin 6 (IL-6), but additional work is necessary to determine the exact mechanism (Wu et al., 2007b). Another DNA virus family, the adenoviruses, encodes for a 160nt non-coding RNA called VA1 that is expressed at the late stage of the lytic cycle (Bhat and Thimmappaya, 1983). Adenovirus utilize the host RNA polymerase III to transcribe VA1 (Jennings and Molloy, 1987). VA1 has been shown to inhibit RNA interference (RNAi) by binding Dicer (Bennasser et al., 2011; Lu and Cullen, 2004) and well as antagonize the interferon response by binding but not activating PKR (Mathews, 1990). Rabies virus (RABV), vesicular stomatitis virus (VSV), and many other negative sense RNA viruses produce a leader RNA (leRNA) at the beginning of infection whose length ranges from 56 to 58nt (Colonno and Banerjee, 1978; Kurilla et al., 1984). While previous research has suggested that the leRNA interacts with the viral unphosphorylated nucleoprotein to participate in the transition from transcription to replication in the virus life cycle (Yang et

al., 1999). The function of these non-coding leRNAs in virus-cell interactions is currently unclear. There is evidence, however, that the leRNAs may be playing a role in the virus-host interactions. For example, wildtype RABV does not activate dendritic cells because of low levels of the leRNA and instead relies on its glycoprotein to interface with the cell (Yang et al., 2015). Several RNA binding proteins have been shown to interact with leRNAs, including La (Kurilla et al., 1984; Wilusz et al., 1983) and heat shock cognate 70 kDa protein (Hsc 70) (Zhang et al., 2017).

In this study, we have identified several small non-coding RNAs that are generated by XRN1 acting on viral mRNAs (e.g. Figure 9 and Figure 15). Therefore, we hypothesize that these stable RNA decay intermediates that accumulate in infected cells may represent functional small non-coding RNAs. One possibility that should be pursued in future studies is whether these XRN1 decay intermediates are precursor for viral microRNAs. Interestingly, Sabin et al., (2013) identified the presence of what they termed viral small interfering RNAs (vsiRNA) in RVFV infected cells, but they did not identify the mechanism of their biogenesis. However, it should be noted that they used C6/36 cells in their study, which are defective in RNAi. Thus, other factors rather than conventional RNAi proteins (such as DICER, AGO2, and RNA-induced silencing complex (RISC)) must be involved in the production of these putative RVFV vsiRNA (Sabin et al., 2013). Since we have shown the presence of a putative RNA decay intermediate in both RVFV MP-12 strain infections (Figure 12) as well as in RVFV 3'UTR containing reporter transfections (Figure 10), these structured RNAs might represent precursor molecules for further processing. To test this possibility, we would look for RNAs in the 21-22 nucleotide range and then hopefully the sequence could be

matched to our RVFV decay intermediate. These RVFV stable RNA decay intermediates could be interacting with Dicer or Argonaute proteins (as has been shown for flavivirus sfRNAs (Moon et al., 2015c)).

Another possible function of these small non-coding RNAs is they could serve as a sponge for host RNA binding proteins. Since RNA binding proteins play important roles in cellular biology, their sponging by stable XRN1 decay intermediates could disrupt a variety of cellular functions. Flavivirus sfRNAs have to date been shown to bind several host proteins, including G3BP1, G3BP2, Caprin1, and TRIM25 (Bidet et al., 2014; Manokaran et al., 2015). Interaction with these proteins helps to prevent the activation of the interferon response and RIG-I signaling (Bidet et al., 2014; Manokaran et al., 2015). Alphavirus RNAs sponge the host protein HuR by dephosphorylation of the HuR protein and cause its relocation from the nucleus into the cytoplasm (Dickson et al., 2012). This sequestration and relocalization of the HuR RNA binding protein causes dramatic changes in host mRNA stability, polyadenylation, and splicing (Barnhart et al., 2013). Therefore, we hypothesize that the small RNAs we have identified that are generated by XRN1 stalling in a variety of viral infections may also serve to sequester important cellular RNA binding proteins and disrupt post-transcriptional processes. In a preliminary protein pull-down experiment, we were able to identify 32 proteins that interact with the RVFV N 3'UTR RNA fragment. We have confirmed one of these interactions – the La protein. Future explorations into the interaction and functional consequences of host RNA binding protein interactions with stable XRN1 generated viral RNA fragments may yield novel insights into viral-host molecular interactions and mechanisms of pathogenesis

Identification of arenavirus decay intermediates in viral infection

There is evidence of subgenomic RNAs that are created in transfected cells with a reporter plasmid using arenaviral highly structure intergenic regions. Pinschewer et al., (2005) used two reporter constructs containing the 5' and 3' UTR (with the intergenic region-IGR) of lymphocytic choriomeningitis virus (LCMV) or one without the IGR, to study the effects on virus propagation. The IGR construct was observed to create subgenomic RNAs, while deletion of the intergenic region (IGR) did not. Furthermore, the reporter construct lacking the IGR did not produce virus particles as efficiently as the construct with the IGR. Other studies have shown that variants which contain deletions of the IGR do not produce virus particles as efficiently, resulting in overall viral attenuation (Golden et al., 2017; Iwasaki et al., 2016). For our study, we used the 3' UTRs of the four mRNAs of the pathogenic Junin virus (JUNV) Romero strain in cell-free RNA decay assays. This Romero strain is highly regulated by the CDC/NIH due to its possible use as a bioweapon because it causes Argentina hemorrhagic fever in humans (Borio et al., 2002; Davis, 2004). We demonstrated that multiple members of the *Arenaviridae* (JUNV and two novel snake viruses) generate RNA decay intermediates in our cell-free assays (Figure 16 and 15), but have yet to demonstrate XRN1 stalling on arenavirus 3' UTRs in live cells or during infection. In the future, we plan to use a reporter construct with the 3' UTR of the JUNV nucleoprotein mRNA to establish if arenavirus 3' UTRs generate a decay intermediate in cellular transfections. Furthermore, we plan to study the effect on host mRNA stability with this reporter construct by transfecting it into HEK293T cells with an siRNA or shRNA targeting the GFP open reading frame.

Possible implications of XRN1 stalling on the pathology/cytopathology of arenavirus and bunyavirus infections

Several non-coding RNAs are important for the life cycles of DNA (e.g. Epstein-Barr virus and adenovirus) and RNA viruses. The viral non-coding RNAs studied in this project can also impact host-virus interactions by producing symptoms which can be linked to its pathology/cytopathology. First, beet necrotic yellow vein virus (BNYVV) requires non-coding RNA 3 for dissemination of the virus throughout the plant. Additionally, RNA 3 is found in the lesions of the infected plant and is directly associated with the accumulation of the non-coding RNA as well as viral-induced pathology (Peltier et al., 2012; Ratti et al., 2009). Furthermore, replacement of three nucleotides at the top of the predicted stem-loop of the coremin sequence of RNA 3 prevents accumulation of the non-coding RNA 3 and this alleviates symptoms on the plant (Peltier et al., 2012). Second, we have previously observed in our lab through plaque assays that accumulation of the sfRNA is required for cytopathology associated with Kunjin virus infection. Mutations in the 3' UTR that prevent the formation of sfRNA produce very small plaques when compared to wildtype. Furthermore, sfRNA is important for transmission of the virus in human and mosquitoes cell culture as sfRNA- viral mutants are unable to be effectively transmitted (Göertz et al., 2016).

These two examples discussed in the paragraph above indicate how non-coding RNAs can be important for the virus life cycle by showing symptoms on the plant or effects on viral replication as seen in plaque assays. Whether the novel non-coding RNAs we identified in this project play a functional role remains to be determined in future studies. For arenaviruses, however, it has already been observed that deletions

in the intergenic region can affect virus propagation (Pinschewer et al., 2005). Thus, there is some albeit circumstantial evidence to suggest that there may be functional roles for these small, XRN1-resistant RNAs. To test this, we could create mutant viruses with either deletions or substituted nucleotides in the 3' UTRs of the arenaviruses or phleboviruses and determine if there are changes in viral RNA replication and/or plaque formation. This would be a first step in the identification of possible mechanisms by which the small RNAs generated by XRN1 stalling on arenavirus and phlebovirus transcripts may have cytopathological effects. However, interpretation of these data may be significantly complicated by the fact that these viruses also perform 'cap-snatching' on cellular mRNAs via targeted endonucleolytic cleavage. Thus, the landscape of factors that reprogram mRNA stability in these infections is complex.

XRN1 is important for cellular homeostasis

XRN1 has an important role in the regulation of gene expression and silencing of this protein in more complex organisms can result in death. Therefore, suppression of XRN1 could enhance viral replication by dysregulation of cellular processes. One such example is XRN1's role in activation of apoptosis by activating the reap and hid proteins which are important for activation of apoptosis (Waldron et al., 2015). This could be linked to how RNA viruses (e.g. flaviviruses, phleboviruses, and arenaviruses) prevent XRN1 from properly doing its job thus preventing the activation of apoptosis. To test this, we can used infected cellular total RNA to look at the expression of the mRNA of these pro-apoptotic factors. Furthermore, in *S. pombe* and *S. cerevisae*, deletion of XRN1 has been linked to increased cell size and doubling time, which causes the

stabilization of cellular mRNAs and this can be seen also in a flavivirus infection

(Larimer and Stevens, 1990; Moon et al., 2012; Szankasi and Smith, 1996). Therefore,

there is a strong evidence supporting the idea that XRN1 is important for basic cellular

process, such as cellular growth and proliferation. Thus, when XRN1 is repressed by

structured viral RNA this could wreak havoc on a variety of cellular processes.

A conserved coremin motif is in multiple plant virus families

The coremin motif is a short, 20 nucleotide sequence paramounts for stalling

XRN1 in the BNYVV non-coding RNA 3. For BNYVV, it is present in the 3' UTR of RNA

3 and in the 3' UTR of RNA 5 (Peltier et al., 2012). The *Bromoviridae* and one

Betaflexiviridae families contain the coremin motif in the 3' UTRs of their genome.

Furthermore, both the subgroup II of the genus cucumoviruses (e.g. cucumber mosaic

virus, peanut stunt virus, and tomato aspermy virus) and the *Bromoviridae* contain a

coremin motif in the 3' UTRs of the viral genome (Thompson et al., 2008). Scaevola

virus A, is a member of the *Betaflexiviridae*, that was identified in a metagenomic study

which also contains a coremin motif found in the 3' UTR (Wylie et al., 2012). We aligned

multiple 3' UTRs to the coremin motif to demonstrate this similarity among the various

viruses (Figure 29; Peltier et al., 2012). We observed that peanut stunt virus has one

nucleotide difference in the coremin motif when compared to the others. The most

represented virus in subgroup II for cucumoviruses is cucumber mosaic virus (CMV).

CMV has three positive sense RNA genomes and is a part of the *Bromoviridae* family. It

would be interesting to test whether RNAs from these other viruses with the coremin

sequence generate a decay intermediate in our cell-free decay assays. Furthermore, a

tRNA-like structure is found downstream from the coremin motif (Joshi et al., 1983). De

Wispelaere and Rao (2009), showed an RNA (called RNA 5) is produced during CMV

plant infection and is not the byproduct of replication. They further observed that RNA 5

is not capped and deletion of the RNA box 1 (coremin motif) alters the generation of

RNA 5 (de Wispelaere and Rao, 2009). In figure 18, we showed a smaller portion of the

BNYVV non-coding RNA 3 (a 55nt sequence) does create a decay intermediate, which

indicates biogenesis of the BNYVV non-coding RNA 3 (which is important for the

movement of the virus throughout the plant, but the exact mechanism needs further

study (Flobinus et al., 2016; Peltier et al., 2012)) relies on XRN1. It would be interesting

to follow this up by first testing if the other viral 3' UTRs with the coremin motif create

non-coding RNAs. BNYVV RNA 5 has been shown to produce a non-coding RNA;

however, it was not as abundant as the one from RNA 3 (Peltier et al., 2012).

Interestingly, the RNAs from the *Bromoviridae* which have been shown to use the tRNA-

like structure bind several host proteins (e.g. LSM1-7) and regulate their translation

(Barends et al., 2004). It could be hypothesized that these plant viruses also produce

non-coding RNAs that act as sponges for endogenous proteins during plant infection.

To test this, we could produce wildtype or mutant virus with mutation in 3' UTR and

study protein-RNA interactions by UV cross linking using plant extracts. Another way to

test this is to silence the proteins which have been already establish and check the

effects on viral translation and replication.
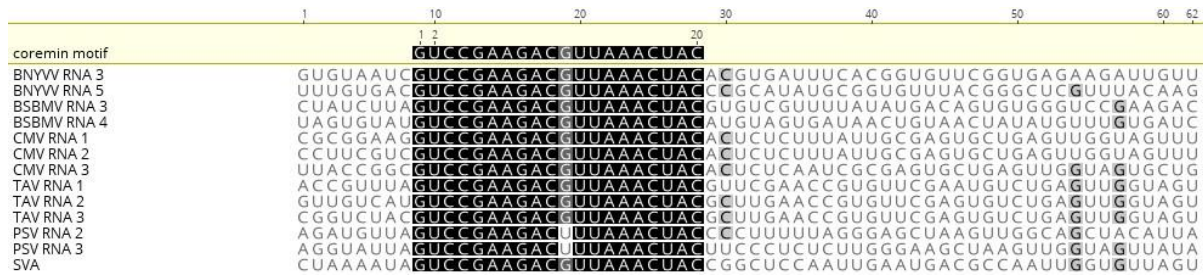
Figure 29. Nucleotide alignment of coremin motif to varies plant viruses. Black highlights the similarities to the reference sequence: coremin motif. Beet necrotic yellow vein virus (BNYVV- RNA 3 accession number: NC_003516; RNA 5 accession number: NC_003513), Beet soil-borne mosaic virus (BSBMV- RNA 3 accession number; NC_039224; RNA 4 accession number: NC_039227), cucumber mosaic virus (CMV- RNA 1 accession number: AF416899; RNA 2 accession number: AF416900; and RNA 3 accession number: AF127976), Peanut stunt virus (PSV- RNA 2 accession number: EU570237; RNA 3: EU570238), Tomato aspermy virus (TAV- RNA 1 accession number: NC_003837; RNA 2 accession number: NC_003838; and RNA 3 accession number: NC_003836), and Scaevola virus A (SVA - accession number: JN127346) using Geneious version 11.1.5 (Kearse et al., 2012)

Could endogenous RNA stall and repress XRN1?

In the context of viruses, we have shown multiple virus families use XRN1 stalling and repression as a mechanism. It is also possible for cellular transcripts to have XRN1-resistent elements in the untranslated regions. The use of cap-independent translation in times of stress has been observed as a way for the cell to maintain translation. Park et al., (2005) showed that the endothelium-specific receptor tyrosine kinase (called Tie2) is translated under hypoxic conditions using an IRES-mediated element. These IRES structures are highly conserved in the non-coding regions and variation has been associated with several diseases (Ward and Kellis, 2012). The encyclopedia of DNA elements (ENCODE) project has made it possible to track disruption to regulatory regions, which are in the non-coding region (e.g. untranslated regions) (Davis et al., 2018). In addition, a previous study observed that many transcripts have different abundance levels of their 3' UTRs verses their associated

128

open reading frames (Mercer et al., 2011). A recent study in zebrafish revealed that the

translation start/stop sites and 3' UTRs of their mRNA contain higher order secondary

structure (Kaushik et al., 2018). Furthermore, influenza A virus contains secondary

structures in the mRNAs that change in the event of a temperature change. This

dynamic conformational change in RNA structure allows the virus to adapt to the colder

temperature (Chursov et al., 2012). Thus, considering these finding we could predict

there are endogenous mRNA with the structures to have the ability to stall XRN1 and

create non-coding RNAs that have a purpose down the line. We could test several

mRNAs that have been established to have IRES element such as the apoptotic

protease activating factor (Apaf-1) (Coldwell et al., 2000) or the ubiquitous transcription

factor NF-κB repressing factor (NRF) (Oumard et al., 2000). We could also use the viral

structures that were crystallized in Figure 30 to predict if endogenous RNAs have

similar RNA structures. A limitation to studying these endogenous RNAs could be these

RNAs might be only detected at times of stress.
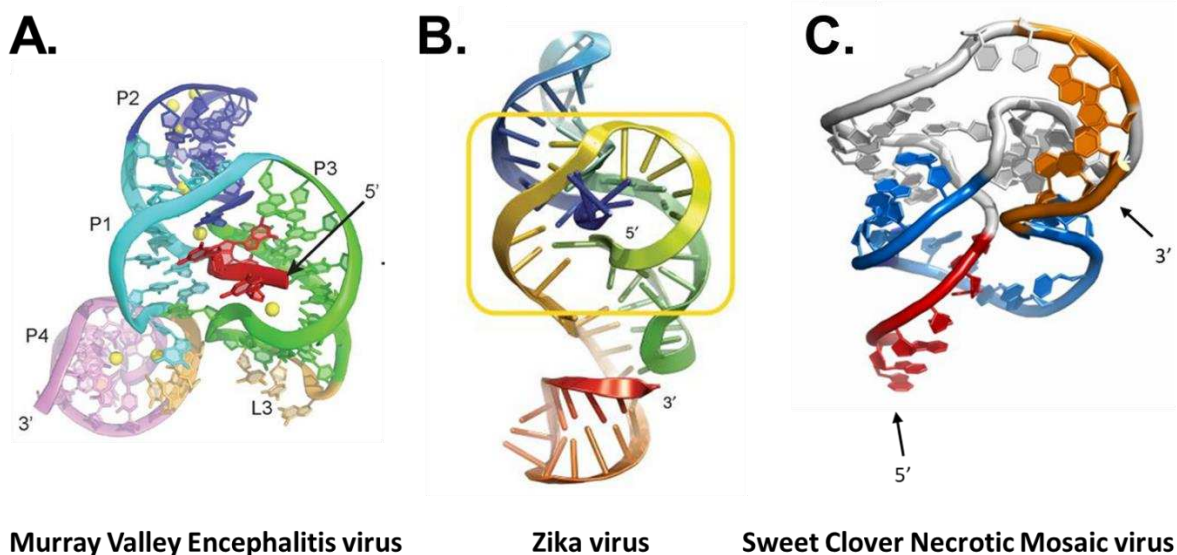
Figure 30. XRN1 resistant RNAs structures crystallized. Panel A: Crystal structure of Murray Valley Encephalitis virus sf/xr RNA. The 5' end is in red and the black arrow indicates where it starts. Yellow dots are Mg^{2+}, and light purple is the 3' end. Panel B: is the ribbon crystal structure of Zika virus sf/xr RNA. The blue is the 5' end and the reddish orange is 3' end. The yellow square represents highlights the ring-like structure in the RNA. Panel C: The model of the pseudoknot formation to create the xrRNA of the sweet clover necrotic mosaic virus. The black arrows indicate where the 5' and 3' ends are located. The red color is the 5' end and the orange is the 3' end which interacts with the pseudoknot to create a ring like structure. Images were taken from Chapman et al. 2014a, MacFadden et al. 2018, and Steckelberg et al. 2018.

Triptycene-based molecules

Small molecules can be used as a source of treatment for certain diseases like cancer (Mas-Moruno et al., 2010). Some of these small molecule drugs can be repurposed for potential antiviral therapies. Barrros et al., (2016) used a triptycene-based small molecule to modulate the *E. coli* temperature sensor mRNA called rpoH, which encodes the σ32 protein (a regulator of the heat shock response). The mRNA of rpoH uses complex secondary structure to regulate proper translation. At lower temperatures, the rpoH mRNA creates several three-helix junctions. Heat shock will cause the mRNA secondary structure to change, thus allowing for translation to proceed. The addition of the triptycene-based molecule at the lower temperature causes

it to bind the rpoH mRNA and prevents the heat shock response from being activated

(Barros et al., 2016). The identification of tripytcene-based molecules which can bind a

three-helix junction structure led us to investigate these compounds further. In this study

we have identified four out of twenty tripytcene-based molecules that have the ability to

disrupt the generation of sfRNA from the 3' UTR of DENV-2 or Zika virus. The four

triptycene-based molecules have the same base and the R-groups are in the same

positions (carbon 4, 8, and 13). Three out of the four triptycenes have pyrimidine rings

in their R-groups that could interact with other parts of the three-helix junction (Figure

31B). We are currently exploring cellular toxicity assessments of these four compounds

because triptycenes have been used as an anti-cancer drug (Barros and Chenoweth,

2014). One technical issue that should be kept in mind during studies with triptycenes is

that some triptycenes appear in our assays to be pulling the RNA/triptycene complex

into the organic phase during phenol/chloroform extraction. In the future, we would like

to test the binding affinity of triptycene to the structured RNA. It would also be

interesting to crystallize the triptycene/RNA complex to understand why one triptycene-

based molecule binds more efficiently than the others. This could open up the possibility

of producing a triptycene probe by adding a florescent tag to a different carbon, if it does

not interfere with the binding. The probe could then be used to identity endogenous

transcripts that have three-helix junction in their 3' UTRs. Next, several RNA binding

proteins have been shown to interact with DENV-2 sfRNAs. One possible use of

triptycenes could be as a competitor to interactions of the native RNA binding proteins

on the sfRNA. Finally, an additional challenge in these studies is that the synthesis of

the triptycene-based molecules requires several days and produce low yields.
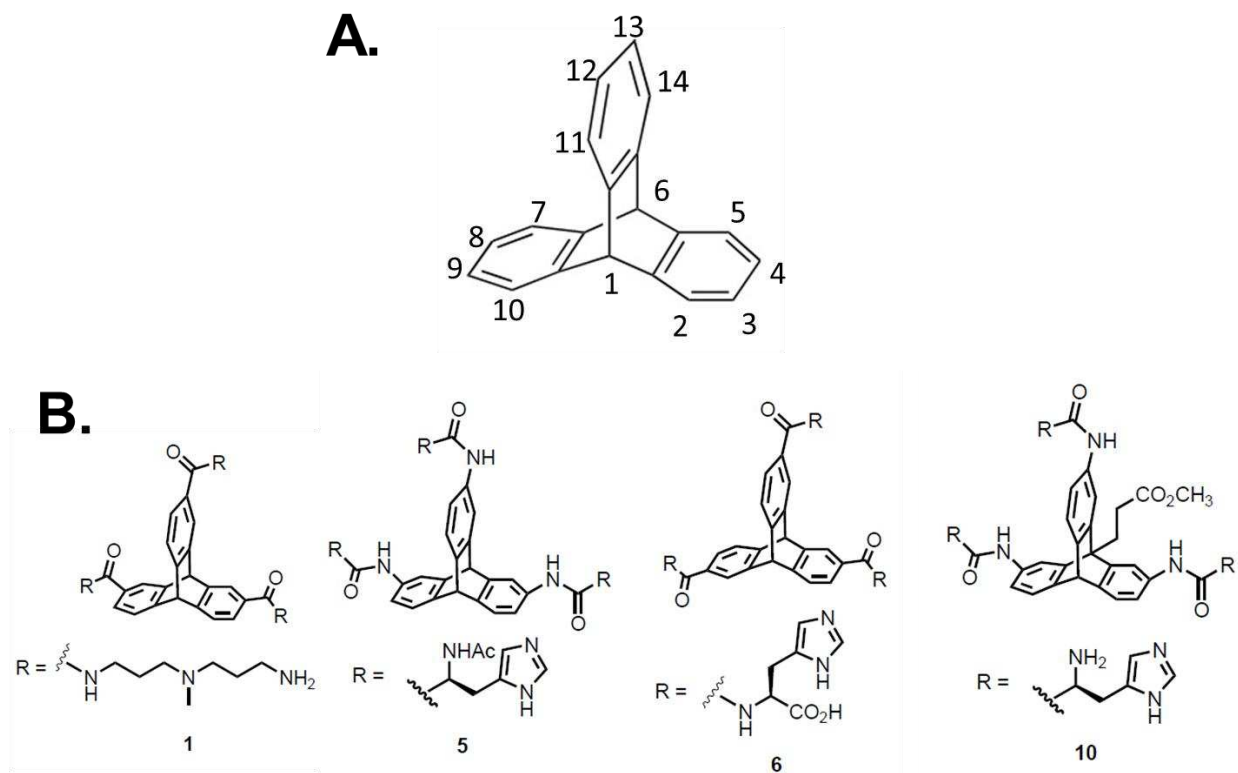
Figure 31. Chemical structure of the four triptycene based molecules we have shown that disrupt XRN1 stalling. Panel A: Triptycene with the carbons numbered on the bases. Panel B: Diagrammatic representation of the four triptycenes with the ability to disrupt the three helix junction in the 3' UTR of Dengue and Zika virus to allow XRN1 to degrade the RNA.

Differences between the DOM3z/DXO and XRN1

In this study we used recombinant mammalian DOM3z/DXO and *K. lactis* XRN1, which were purified using the same method (see Experimental Methods section above). These recombinant proteins are different sizes; DOM3z/DXO is about 45kDa and XRN1 is about 130kDa. Additionally, the recombinant DOM3z/DXO protein was cloned with the full open reading frame (Picard-Jean et al., 2018), whereas the recombinant K. lactis XRN1 is missing 209 amino acids from the C-terminal (Chang et al., 2011). Another

major difference is that DOM3z/DXO has its own decapping ability whereas XRN1 relies on the DCP1/2 complex to decap the mRNA which allows exonucleolytic decay to proceed (Jiao et al., 2013). The homolog of the mammalian DOM3z/DXO in yeast is called DXO1. MacFadden et al., (2018) tested the xrRNA 2 of the Kunjin strain of West Nile virus with recombinant yeast DXO1 to check if it will stall in this 3'UTR region like XRN1. While DXO1 did generate sfRNA in their assays, it was much less robust than the XRN1(MacFadden et al., 2018). Figure 31 illustrates the differences between the amino acid sequence alignment of yeast DXO1 and the human DOM3z/DXO using Geneious version 11.1.5 (Kearse et al., 2012). These two proteins have only 10 percent similarity and differences of 46-amino acids in size. Furthermore, it would be interesting to compare the XRN1 catalytic domain with the DOM3x/DXO catalytic domain to tease out if these proteins are truly different. This might help explain why the mammalian DOM3z/DXO was able to degrade through different structured viral RNAs while XRN1 was stalled (Figure 28). Future studies will carefully compare the yeast DXO1 and mammalian DOM3z in our *in vitro* assays. This will help us to understand any differences of activity on RNAs between these proteins. This future study might also reveal how mammalian organisms have evolved to use other 5'-3' exoribonuclease in the battle against RNA viruses, even though the enzymes is not as highly processive as XRN1. As seen in Figure 28, mammalian Dom3z/DXO degrades through the 3' UTR of DENV-2 and RVFV N, whereas XRN1 generates a decay intermediate. One limitation in our data at this time that we cannot formally rule out is the possibility of nuclease contamination (despite the fact that we have observed read-through by Dom3z/DXO using multiple independent enzyme preparations.

Figure 32. Amino acid sequence alignment between mammalian DOM3z/DXO and yeast DXO1. The black highlights the similarities between the sequences. Amino acid sequences used are human DOM3z/DXO (NCBI accession number: O77932.2) and yeast DXO1 (NCBI accession number: Q063449.1). Alignment was done using Geneious version 11.1.5 (Kearse et al., 2012).

In addition, we will also be studying the role of DOM3z/DXO1 role in a viral infection, which will be performed in collaboration with Dr. Brian Geiss' lab. We plan to study how DOM3Z interacts with the flavivirus RNA in the context of viral infection. One possibility that recent studies have shown is that DOM3z is localized primarily to the nucleus during homeostasis (Amador-Cañizares et al., 2018; Picard-Jean et al., 2018). It would be interesting to check if more the DOM3x/DXO protein relocalizes to the cytoplasm during a virus infection.

References

Abedi, G.R., Watson, J.T., Nix, W.A., Oberste, M.S., and Gerber, S.I. (2018). Enterovirus and Parechovirus Surveillance - United States, 2014-2016. MMWR. Morb. Mortal. Wkly. Rep. *67*, 515–518.

Abernathy, E., Gilbertson, S., Alla, R., and Glaunsinger, B. (2015). Viral nucleases induce an mRNA degradation-transcription feedback loop in mammalian cells. Cell Host Microbe *18*, 243–253.

Accardi, L., Grò, M.C., Di Bonito, P., and Giorgi, C. (1993). Toscana virus genomic L segment: molecular cloning, coding strategy and amino acid sequence in comparison with other negative strand RNA viruses. Virus Res. *27*, 119–131.

Ahlquist, P., and Janda, M. (1984). cDNA cloning and in vitro transcription of the complete brome mosaic virus genome. Mol. Cell. Biol. *4*, 2876–2882.

Ahlquist, P., Dasgupta, R., and Kaesberg, P. (1984). Nucleotide sequence of the brome mosaic virus genome and its implications for viral replication. J. Mol. Biol. *172*, 369–383.

Aizer, A., Kalo, A., Kafri, P., Shraga, A., Ben-Yishay, R., Jacob, A., Kinor, N., and Shav-Tal, Y. (2014). Quantifying mRNA targeting to P-bodies in living human cells reveals their dual role in mRNA decay and storage. J. Cell Sci. *127*, 4443–4456.

Ajamian, L., Abrahamyan, L., Milev, M., Ivanov, P. V, Kulozik, A.E., Gehring, N.H., and Mouland, A.J. (2008). Unexpected roles for UPF1 in HIV-1 RNA metabolism and translation. RNA *14*, 914–927.

Ajamian, L., Abel, K., Rao, S., Vyboh, K., Garcï¿½a-de-Gracia, F., Soto-Rifo, R., Kulozik, A.E., Gehring, N.H., and Mouland, A.J. (2015). HIV-1 recruits UPF1 but excludes UPF2 to promote nucleocytoplasmic export of the genomic RNA. Biomolecules *5*, 2808–2839.

Akiyama, B.M., Laurence, H.M., Massey, A.R., Costantino, D.A., Xie, X., Yang, Y., Shi, P.-Y., Nix, J.C., Beckham, J.D., and Kieft, J.S. (2016). Zika virus produces noncoding RNAs using a multi-pseudoknot structure that confounds a cellular exonuclease. Science *354*, 1148–1152.

Albert, T.K., Lemaire, M., van Berkum, N.L., Gentz, R., Collart, M.A., and Timmers, H.T. (2000). Isolation and characterization of human orthologs of yeast CCR4-NOT complex subunits. Nucleic Acids Res. *28*, 809–817.

Allmang, C., Kufel, J., Chanfreau, G., Mitchell, P., Petfalski, E., and Tollervey, D. (1999). Functions of the exosome in rRNA, snoRNA and snRNA synthesis. EMBO J. *18*, 5399–5410.

Amador-Cañizares, Y., Bernier, A., Wilson, J.A., and Sagan, S.M. (2018). miR-122 does not impact recognition of the HCV genome by innate sensors of RNA but rather protects the 5′ end from the cellular pyrophosphatases, DOM3Z and DUSP11. Nucleic Acids Res. *46*,5139-5158

Amberg, D.C., Goldstein, A.L., and Cole, C.N. (1992). Isolation and characterization of RAT1: An essential gene of Saccharomyces cerevisiae required for the efficient nucleocytoplasmic trafficking of mRNA. Genes Dev. *6*, 1173–1189.

Amrani, N., Ganesan, R., Kervestin, S., Mangus, D.A., Ghosh, S., and Jacobson, A. (2004). A faux 3′-UTR promotes aberrant termination and triggers nonsense-mediated mRNA decay. Nature *432*, 112–118.

Anderson, J.S.J., and Parker, R. (1998). The 3' to 5' degradation of yeast mRNAs is a general mechanism for mRNA turnover that requires the SK12 DEVH box protein and 3' to 5' exonucleases of the exosome complex. EMBO J. *17*, 1497–1506.

Ariumi, Y., Kuroki, M., Kushima, Y., Osugi, K., Hijikata, M., Maki, M., Ikeda, M., and Kato, N. (2011). Hepatitis C Virus Hijacks P-Body and Stress Granule Components around Lipid Droplets. J. Virol. *85*, 6882–6892.

Arrigo, S., and Beemon, K. (1988). Regulation of Rous sarcoma virus RNA splicing and stability. Mol. Cell. Biol. *8*, 4858–4867.

Astuti, D., Morris, M.R., Cooper, W.N., Staals, R.H.J., Wake, N.C., Fews, G.A., Gill, H., Gentle, D., Shuib, S., Ricketts, C.J., et al. (2012). Germline mutations in DIS3L2 cause the Perlman syndrome of overgrowth and Wilms tumor susceptibility. Nat. Genet. *44*, 277–284.

Auperin, D.D., and McCormick, J.B. (1989). Nucleotide sequence of the Lassa virus (Josiah strain) S genome RNA and amino acid sequence comparison of the N and GPC proteins to other arenaviruses. Virology *168*, 421–425.

Auperin, D.D., Galinski, M., and Bishop, D.H.L. (1984). The sequences of the N protein gene and intergenic region of the S RNA of pichinde arenavirus. Virology *134*, 208–219.

Auperin, D.D., Sasso, D.R., and McCormick, J.B. (1986). Nucleotide sequence of the glycoprotein gene and intergenic region of the Lassa virus S genome RNA. Virology *154*, 155–167.

Axt, K., French, S.L., Beyer, A.L., and Tollervey, D. (2014). Kinetic analysis demonstrates a requirement for the Rat1 exonuclease in cotranscriptional pre-rRNA cleavage. PLoS One *9*, e85703.

Back, S.H., Kim, Y.K., Kim, W.J., Cho, S., Oh, H.R., Kim, J.-E., and Jang, S.K. (2002). Translation of polioviral mRNA is inhibited by cleavage of polypyrimidine tract-binding proteins executed by polioviral 3C(pro). J. Virol. *76*, 2529–2542.

Badakhshan, M., Yaghoobi-Ershadi, M.R., Moin-Vaziri, V., Charrel, R., Hanafi-Bojd, A.A., Rezaei, F., Akhavan, A.A., Rassi, Y., and Oshaghi, M.-A. (2018). Spatial Distribution of Phlebotomine Sand Flies (Diptera: Psychodidae) as Phlebovirus Vectors in Different Areas of Iran. J. Med. Entomol. 1–9.

Baggs, J.E., and Green, C.B. (2003). Nocturnin, a deadenylase in Xenopus laevis retina: A mechanism for posttranscriptional control of circadian-related mRNA. Curr. Biol. *13*, 189–198.

Bagnéris, C., Briggs, L.C., Savva, R., Ebrahimi, B., and Barrett, T.E. (2011). Crystal structure of a KSHV-SOX-DNA complex: Insights into the molecular mechanisms underlying DNase activity and host shutoff. Nucleic Acids Res. *39*, 5744–5756.

Bakheet, T., Hitti, E., Al-Saif, M., Moghrabi, W.N., and Khabar, K.S.A. (2018). The AU-rich element landscape across human transcriptome reveals a large proportion in introns and regulation by ELAVL1/HuR. Biochim. Biophys. Acta - Gene Regul. Mech. *1861*, 167–177.

Balagopal, V., and Beemon, K.L. (2017). Rous sarcoma virus RNA stability element inhibits deadenylation of mRNAs with long 3'UTRs. Viruses *9,* 204

Balistreri, G., Caldentey, J., Kaariainen, L., and Ahola, T. (2007). Enzymatic Defects of the nsP2 Proteins of Semliki Forest Virus Temperature-Sensitive Mutants. J. Virol. *81*, 2849–2860.

Balistreri, G., Horvath, P., Schweingruber, C., Zünd, D., McInerney, G., Merits, A., Mühlemann, O., Azzalin, C., and Helenius, A. (2014). The host nonsense-mediated mRNA decay pathway restricts mammalian RNA virus replication. Cell Host Microbe *16*, 403–411.

Barends, S., Barends, S., Rudinger-Thirion, J., Rudinger-Thirion, J., Florentz, C., Giege, R., Pleij, C.W., Pleij, C.W., Kraal, B., and Kraal, B. (2004). tRNA-like structure regulates translation of Brome mosaic virus RNA. J. Virol. *78*, 4003–4010.

Barker, G.F., and Beemon, K. (1994). Rous sarcoma virus RNA stability requires an open reading frame in the gag gene and sequences downstream of the gag-pol junction. Mol. Cell. Biol. *14*, 1986–1996.

Barnhart, M.D., Moon, S.L., Emch, A.W., Wilusz, C.J., and Wilusz, J. (2013). Changes in cellular mRNA stability, splicing, and polyadenylation through HuR protein sequestration by a cytoplasmic RNA virus. Cell Rep. *5*, 909–917.

Barros, S.A., and Chenoweth, D.M. (2014). Recognition of nucleic acid junctions using triptycene-based molecules. Angew. Chemie - Int. Ed. *53*, 13746–13750.

Barros, S.A., Yoon, I., and Chenoweth, D.M. (2016). Modulation of the E. coli rpoH Temperature Sensor with Triptycene-Based Small Molecules. Angew. Chemie - Int. Ed. *55*, 8258–8261.

Basbouss-Serhal, I., Pateyron, S., Cochet, F., Leymarie, J., and Bailly, C. (2017). 5′ to 3′ mRNA Decay Contributes to the Regulation of Arabidopsis Seed Germination by Dormancy. Plant Physiol. *173*, 1709–1723.

Bashkirov, V.I., Scherthan, H., Solinger, J.A., Buerstedde, J.M., and Heyer, W.D. (1997). A mouse cytoplasmic exoribonuclease (mXRN1p) with preference for G4 tetraplex substrates. J. Cell Biol. *136*, 761–773.

Bavagnoli, L., Cucuzza, S., Campanini, G., Rovida, F., Paolucci, S., Baldanti, F., and Maga, G. (2015). The novel influenza A virus protein PA-X and its naturally deleted variant show different enzymatic properties in comparison to the viral endonuclease PA. Nucleic Acids Res. *43*, 9405–9417.

Beaton, A.R., and Krug, R.M. (1981). Selected host cell capped RNA fragments prime influenza viral RNA transcription in vivo. Nucleic Acids Res. *9*, 4423–4436.

Beelman, C.A., Stevens, A., Caponigro, G., LaGrandeur, T.E., Hatfield, L., Fortner, D.M., and Parker, R. (1996). An essential component of the decapping enzyme required for normal rates of mRNA turnover. Nature *382*, 642–646.

Bennasser, Y., Chable-Bessia, C., Triboulet, R., Gibbings, D., Gwizdek, C., Dargemont, C., Kremer, E.J., Voinnet, O., and Benkirane, M. (2011). Competition for XPO5 binding between Dicer mRNA, pre-miRNA and viral RNA regulates human Dicer levels. Nat. Struct. Mol. Biol. *18*, 323–327.

Bentley, K., Keep, S.M., Armesto, M., and Britton, P. (2013). Identification of a Noncanonically Transcribed Subgenomic mRNA of Infectious Bronchitis Virus and Other Gammacoronaviruses. J. Virol. *87*, 2128–2136.

Berndt, H., Harnisch, C., Rammelt, C., Stohr, N., Zirkel, A., Dohm, J.C., Himmelbauer, H., Tavanez, J.-P., Huttelmaier, S., and Wahle, E. (2012). Maturation of mammalian H/ACA box snoRNAs: PAPD5-dependent adenylation and PARN-dependent trimming. RNA *18*, 958–972.

Bhat, R.A., and Thimmappaya, B. (1983). Two small RNAs encoded by Epstein-Barr virus can functionally substitute for the virus-associated RNAs in the lytic growth of adenovirus 5. Proc. Natl. Acad. Sci. U. S. A. *80*, 4789–4793.

Bhattacharyya, S.N., Habermacher, R., Martine, U., Closs, E.I., and Filipowicz, W. (2006). Relief of microRNA-Mediated Translational Repression in Human Cells Subjected to Stress. Cell *125*, 1111–1124.

Bidet, K., Dadlani, D., and Garcia-Blanco, M.A. (2014). G3BP1, G3BP2 and CAPRIN1 are required for translation of interferon stimulated mRNAs and are targeted by a dengue virus non-coding RNA. PLoS Pathog. *10*, e1004242.

Binh, N.T., Wakai, C., Kawaguchi, A., and Nagata, K. (2014). Involvement of the N-terminal portion of influenza virus RNA polymerase subunit PB1 in nucleotide recognition. Biochem. Biophys. Res. Commun. *443*, 975–979.

Biswas, S.K., Boutz, P.L., and Nayak, D.P. (1998). Influenza virus nucleoprotein interacts with influenza virus polymerase proteins. J Virol *72*, 5493–5501.

Black, J.G., and Lawson, K.F. (1970). Sylvatic rabies studies in the silver fox (Vulpes vulpes). Susceptibility and immune response. Can. J. Comp. Med. *34*, 309–311.

Blanco, A.M., Gómez-Boronat, M., Madera, D., Valenciano, A.I., Alonso-Gómez, A.L., and Delgado, M.J. (2017). First Evidences of Nocturnin in Fish: Two Isoforms in Goldfish Differentially Regulated by Feeding. Am. J. Physiol. Integr. Comp. Physiol. *314*, R304-R312.

Blyn, L.B., Towner, J.S., Semler, B.L., and Ehrenfeld, E. (1997). Requirement of poly(rC) binding protein 2 for translation of poliovirus RNA. J. Virol. *71*, 6243–6246.

Boeck, R., Tarun, S., Rieger, M., Deardorff, J.A., Müller-Auer, S., and Sachs, A.B. (1996). The yeast Pan2 protein is required for poly(A)-binding protein-stimulated poly(A)-nuclease activity. J. Biol. Chem. *271*, 432–438.

Bolognani, F., Gallani, A.I., Sokol, L., Baskin, D.S., and Meisner-Kober, N. (2012). MRNA stability alterations mediated by HuR are necessary to sustain the fast growth of glioma cells. J. Neurooncol. *106*, 531–542.

Booth, C.M., Matukas, L.M., Tomlinson, G.A., Rachlis, A.R., Rose, D.B., Dwosh, H.A., Walmsley, S.L., Mazzulli, T., Avendano, M., Derkach, P., et al. (2003). Clinical Features and Short-term Outcomes of 144 Patients with SARS in the Greater Toronto Area. J. Am. Med. Assoc. *289*, 2801–2809.

Boothroyd, J.C., Highfield, P.E., Cross, G.A., Rowlands, D.J., Lowe, P.A., Brown, F., and Harris, T.J. (1981). Molecular cloning of foot and mouth disease virus genome and nucleotide sequences in the structural protein genes. Nature *290*, 800–802.

Borio, L., Inglesby, T., Peters, C.J., Schmaljohn, A.L., Hughes, J.M., Jahrling, P.B., Ksiazek, T., Johnson, K.M., Meyerhoff, A., O'Toole, T., et al. (2002). Hemorrhagic fever viruses as biological weapons: Medical and public health management. J. Am. Med. Assoc. *287*, 2391–2405.

Bourhy, H., Kissi, B., Lafon, M., Sacramento, D., and Tordo, N. (1992). Antigenic and molecular characterization of bat rabies virus in Europe. J. Clin. Microbiol. *30*, 2419–2426.

Boursnell, M.E., Brown, T.D., Foulds, I.J., Green, P.F., Tomley, F.M., and Binns, M.M. (1987). The complete nucleotide sequence of avian infectious bronchitis virus: analysis of the polymerase-coding region. Adv Exp Med Biol *218*, 15–29.

Bouveret, E., Rigaut, G., Shevchenko, A., Wilm, M., and Séraphin, B. (2000). A Sm-like protein complex that participates in mRNA degradation. EMBO J. *19*, 1661–1671.

Bouvet, M., Debarnot, C., Imbert, I., Selisko, B., Snijder, E.J., Canard, B., and Decroly, E. (2010). In vitro reconstitution of SARS-coronavirus mRNA cap methylation. PLoS Pathog. *6*, e1000863.

Boyraz, B., Moon, D.H., Segal, M., Muosieyiri, M.Z., Aykanat, A., Tai, A.K., Cahan, P., and Agarwal, S. (2016). Posttranscriptional manipulation of TERC reverses molecular hallmarks of telomere disease. J. Clin. Invest. *126*, 3377–3382.

Brangwynne, C.P., Eckmann, C.R., Courson, D.S., Rybarska, A., Hoege, C., Gharakhani, J., Jülicher, F., and Hyman, A.A. (2009). Germline P granules are liquid droplets that localize by controlled dissolution/condensation. Science. *324*, 1729–1732.

Brangwynne, C.P., Mitchison, T.J., and Hyman, A.A. (2011). Active liquid-like behavior of nucleoli determines their size and shape in Xenopus laevis oocytes. Proc. Natl. Acad. Sci. *108*, 4334–4339.

Bredenbeek, P.J., Pachuk, C.J., Noten, A.F.H., Charité, J., Luytjes, W., Weiss, S.R., and Spaan, W.J.M. (1990). The primary structure and expression of the second open reading frame of the polymerase gene of the coronavirus MHV-A59; a highly conserved polymerase is expressed by an efficient ribosomal frameshifting mechanism. Nucleic Acids Res. *18*, 1825–1832.

Brengues, M., Teixeira, D., and Parker, R. (2005). Movement of Eukaryotic mRNAs Between Polysomes and Cytoplasmic Processing Bodies. Science. *310*, 486–489.

Brennan, B., Welch, S.R., and Elliott, R.M. (2014). The Consequences of Reconfiguring the Ambisense S Genome Segment of Rift Valley Fever Virus on Viral Replication in Mammalian and Mosquito Cells and for Genome Packaging. PLoS Pathog. *10*, e1003922.

Brennan, B., Rezelj, V. V, and Elliott, R.M. (2017). Mapping of Transcription Termination within the S Segment of SFTS Phlebovirus Facilitated Generation of NSs Deletant Viruses. J. Virol. *91*, e00743-17.

Briand, F.X., Niqueux, E., Schmitz, A., Hirchaud, E., Quenault, H., Allée, C., Le Prioux, A., Guillou-Cloarec, C., Ogor, K., Le Bras, M.O., et al. (2018). Emergence and multiple reassortments of French 2015–2016 highly pathogenic H5 avian influenza viruses. Infect. Genet. Evol. *61*, 208–214.

Brown, C.E., Tarun, S.Z., Boeck, R., and Sachs, A.B. (1996). PAN3 encodes a subunit of the Pab1p-dependent poly(A) nuclease in Saccharomyces cerevisiae. Mol. Cell. Biol. *16*, 5744–5753.

Bujarski, J.J., Dreher, T.W., and Hall, T.C. (1985). Deletions in the 3'-terminal tRNA-like structure of brome mosaic virus RNA differentially affect aminoacylation and replication in vitro. Proc. Natl. Acad. Sci. U. S. A. *82*, 5636–5640.

Burgess, H.M., and Mohr, I. (2018). Defining the role of stress granules in innate immune suppression by the HSV-1 endoribonuclease VHS. J. Virol. JVI.00829-18.

Cassola, A., De Gaudenzi, J.G., and Frasch, A.C. (2007). Recruitment of mRNAs to cytoplasmic ribonucleoprotein granules in trypanosomes. Mol. Microbiol. *65*, 655–670.

Cathcart, A.L., and Semler, B.L. (2014). Differential restriction patterns of mRNA decay factor AUF1 during picornavirus infections. J. Gen. Virol. *95*, 1488–1492.

Cathcart, A.L., Rozovics, J.M., and Semler, B.L. (2013). Cellular mRNA Decay Protein AUF1 Negatively Regulates Enterovirus and Human Rhinovirus Infections. J. Virol. *87*, 10423–10434.

Chahar, H.S., Chen, S., and Manjunath, N. (2013). P-body components LSM1, GW182, DDX3, DDX6 and XRN1 are recruited to WNV replication sites and positively regulate viral replication. Virology *436*, 1–7.

Chamieh, H., Ballut, L., Bonneau, F., and Le Hir, H. (2008). NMD factors UPF2 and UPF3 bridge UPF1 to the exon junction complex and stimulate its RNA helicase activity. Nat. Struct. Mol. Biol. *15*, 85–93.

Chang, H.M., Triboulet, R., Thornton, J.E., and Gregory, R.I. (2013). A role for the Perlman syndrome exonuclease Dis3l2 in the Lin28-let-7 pathway. Nature *497*, 244–248.

Chang, J.H., Xiang, S., Xiang, K., Manley, J.L., and Tong, L. (2011). Structural and biochemical studies of the 5'→3' exoribonuclease Xrn1. Nat. Struct. Mol. Biol. *18*, 270–276.

Chang, J.H., Jiao, X., Chiba, K., Oh, C., Martin, C.E., Kiledjian, M., and Tong, L. (2012). Dxo1 is a new type of eukaryotic enzyme with both decapping and 5′-3′ exoribonuclease activity. Nat. Struct. Mol. Biol. *19*, 1011–1019.

Chapat, C., Chettab, K., Simonet, P., Wang, P., De La Grange, P., Le Romancer, M., and Corbo, L. (2017). Alternative splicing of CNOT7 diversifies CCR4-NOT functions. Nucleic Acids Res. *45*, 8508–8523.

Chapman, E.G., Costantino, D.A., Rabe, J.L., Moon, S.L., Wilusz, J., Nix, J.C., and Kieft, J.S. (2014a). The structural basis of pathogenic subgenomic flavivirus RNA (sfRNA) production. Science *344*, 307–310.

Chapman, E.G., Moon, S.L., Wilusz, J., and Kieft, J.S. (2014b). RNA structures that resist degradation by Xrn1 produce a pathogenic Dengue virus RNA. Elife *3*, e01892.

Charenton, C., Taverniti, V., Gaudon-Plesse, C., Back, R., Séraphin, B., and Graille, M. (2016). Structure of the active form of Dcp1-Dcp2 decapping enzyme bound to m 7 GDP and its Edc3 activator. Nat. Struct. Mol. Biol. *23*, 982–986.

Charrel, R.N., De Lamballerie, X., De Micco, P., and Fulhorst, C.F. (2001). Nucleotide sequence of the pirital virus (family Arenaviridae) small genomic segment. Biochem. Biophys. Res. Commun. *280*, 1402–1407.

Chase, A.J., and Semler, B.L. (2014). Differential cleavage of IRES trans-acting factors (ITAFs) in cells infected by human rhinovirus. Virology *449*, 35–44.

Chase, A.J., Daijogo, S., and Semler, B.L. (2014). Inhibition of Poliovirus-Induced Cleavage of Cellular Protein PCBP2 Reduces the Levels of Viral RNA Replication. J. Virol. *88*, 3192–3201.

Chekulaeva, M., Mathys, H., Zipprich, J.T., Attig, J., Colic, M., Parker, R., and Filipowicz, W. (2011). MiRNA repression involves GW182-mediated recruitment of CCR4-NOT through conserved W-containing motifs. Nat. Struct. Mol. Biol. *18*, 1218–1226.

Chen, C., Lei, J., Zheng, Q., Tan, S., Ding, K., and Yu, C. (2018). Poly(rC) binding protein 2 (PCBP2) promotes the viability of human gastric cancer cells by regulating CDK2. FEBS Open Bio *8*, 764–773.

Chen, C.Y.A., Zhang, Y., Xiang, Y., Han, L., and Shyu, A. Bin (2017). Antagonistic actions of two human Pan3 isoforms on global mRNA turnover. RNA *23*, 1404–1418.

Chen, J., Rappsilber, J., Chiang, Y.-C., Russell, P., Mann, M., and Denis, C.L. (2001). Purification and Characterization of the 1 . 0 MDa CCR4-NOT Complex Identifies Two Novel Components of the Complex. J. Mol. Biol. *314*, 683–694.

Cheng, E., and Mir, M.A. (2012). Signatures of Host mRNA 5' Terminus for Efficient Hantavirus Cap Snatching. J. Virol. *86*, 10173–10185.

Chiba, S., Hleibieh, K., Delbianco, A., Klein, E., Ratti, C., Ziegler-Graff, V., Bouzoubaa, S.E., and Gilmer, D. (2012). The benyvirus RNA silencing suppressor is essential for long-distance movement, requires both Zn-finger and NoLS basic residues but not a nucleolar localization for its silencing suppression activity. Mol. Plant-Microbe Interact. *26*, 168-181.

Cho, H., Han, S., Choe, J., Park, S.G., Choi, S.S., and Kim, Y.K. (2013). SMG5-PNRC2 is functionally dominant compared with SMG5-SMG7 in mammalian nonsense-mediated mRNA decay. Nucleic Acids Res. *41*, 1319–1328.

Choi, Y.G., and Rao, A.L.N. (2003). Packaging of Brome Mosaic Virus RNA3 Is Mediated through a Bipartite Signal. J. Virol. *77*, 9750–9757.

Choi, K., Kim, J.H., Li, X., Paek, K.Y., Ha, S.H., Ryu, S.H., Wimmer, E., and Jang, S.K. (2004). Identification of cellular proteins enhancing activities of internal ribosomal entry sites by competition with oligodeoxynucleotides. Nucleic Acids Res. *32*, 1308–1317.

Chursov, A., Kopetzky, S.J., Leshchiner, I., Kondofersky, I., Theis, F.J., Frishman, D., and Shneider, A. (2012). Specific temperature-induced perturbations of secondary mRNA structures are associated with the cold-adapted temperature-sensitive phenotype of influenza A virus. RNA Biol. *9*, 1266–1274.

Clarke, P.A., Schwemmle, M., Schickinger, J., Hilse, K., and Clemens, M.J. (1991). Binding of epstein-barr virus small RNA EBER-1 to the double-stranded RNA-activated protein kinase DAI. Nucleic Acids Res. *19*, 243–248.

Clegg, J.C.S., Wilson, S.M., and Oram, J.D. (1991). Nucleotide sequence of the S RNA of Lassa virus (Nigerian strain) and comparative analysis of arenavirus gene products. Virus Res. *18*, 151–164.

Coldwell, M.J., Mitchell, S.A., Stoneley, M., MacFarlane, M., and Willis, A.E. (2000). Initiation of Apaf-1 translation by internal ribosome entry. Oncogene. *19*, 899–905.

Colonno, R.J., and Banerjee, A.K. (1978). Complete nucleotide sequence of the leader RNA synthesized in vitro by vesicular stomatitis virus. Cell. *15*, 93–101.

Constantine, D.G., and Woodall, D.F. (1966). Transmission experiments with bat rabies isolates: reactions of certain Carnivora, opossum, rodents, and bats to rabies virus of red bat origin when exposed by bat bite or by intrasmuscular inoculation. Am. J. Vet. Res. *27*, 24–32.

Constantinides, A., Gumpper, R., Severin, C., and Luo, M. (2018). High-resolution structure of the Influenza A virus PB2cap binding domain illuminates the changes induced by ligand binding. Acta. Cryst. *74*, 122–127.

Cornu, T.I., De, J.C., and Torre, L. (2001). RING Finger Z Protein of Lymphocytic Choriomeningitis Virus (LCMV) Inhibits Transcription and RNA Replication of an LCMV S-Segment Minigenome. J. Virol. *75*, 9415–9426.

Coslett, G.D., Holloway, B.P., and Obijeski, J.F. (1980). The structural proteins of rabies virus and evidence for their synthesis from separate monocistronic RNA species. J. Gen. Virol. *49*, 161–180.

Cougot, N., Babajko, S., and Séraphin, B. (2004). Cytoplasmic foci are sites of mRNA decay in human cells. J. Cell Biol. *165*, 31–40.

Cougot, N., Cavalier, A., Thomas, D., and Gillet, R. (2012). The dual organization of P-bodies revealed by immunoelectron microscopy and electron tomography. J. Mol. Biol. *420*, 17–28.

Couvillion, M.T., Bounova, G., Purdom, E., Speed, T.P., and Collins, K. (2012). A Tetrahymena Piwi Bound to Mature tRNA 3' Fragments Activates the Exonuclease Xrn2 for RNA Processing in the Nucleus. Mol. Cell. *48*, 509–520.

Covarrubias, S., Gaglia, M.M., Kumar, G.R., Wong, W., Jackson, A.O., and Glaunsinger, B.A. (2011). Coordinated destruction of cellular messages in translation complexes by the gammaherpesvirus host shutoff factor and the Mammalian Exonuclease Xrn1. PLoS Pathog. *7*, e1002339.

Crutzen, F., Mehrvar, M., Gilmer, D., and Bragard, C. (2009). A full-length infectious clone of beet soil-borne virus indicates the dispensability of the RNA-2 for virus survival in planta and symptom expression on Chenopodium quinoa leaves. J. Gen. Virol. *90*, 3051–3056.

D'Alonzo, M., Delbianco, A., Lanzoni, C., Autonell, C.R., Gilmer, D., and Ratti, C. (2012). Beet soil-borne mosaic virus RNA-4 encodes a 32kDa protein involved in symptom expression and in virus transmission through Polymyxa betae. Virology. *423*, 187–194.

D'Antuono, A., Loureiro, M.E., Foscaldi, S., Marino-Buslje, C., and Lopez, N. (2014). Differential Contributions of Tacaribe Arenavirus Nucleoprotein N-Terminal and C-Terminal Residues to Nucleocapsid Functional Activity. J. Virol. *88*, 6492–6505.

Dahlroth, S.L., Gurmu, D., Haas, J., Erlandsen, H., and Nordlund, P. (2009). Crystal structure of the shutoff and exonuclease protein from the oncogenic Kaposi's sarcoma-associated herpesvirus. FEBS J. *276*, 6636–6645.

Dasgupta, R., and Kaesberg, P. (1977). Sequence of an oligonucleotide derived from the 3' end of each of the four brome mosaic viral RNAs. PNAS *74:11*, 4900–4904.

Daugeron, M.C., Mauxion, F., and Séraphin, B. (2001). The yeast POP2 gene encodes a nuclease involved in mRNA deadenylation. Nucleic Acids Res. *29*, 2448–2455.

Davidson, L., Kerr, A., and West, S. (2012). Co-transcriptional degradation of aberrant pre-mRNA by Xrn2. EMBO J. *31*, 2566–2578.

Davis, R.G. (2004). The ABCs of bioterrorism for veterinarians, focusing on Category B and C agents. J. Am. Vet. Med. Assoc. *224*, 1096–1104.

Davis, C.A., Hitz, B.C., Sloan, C.A., Chan, E.T., Davidson, J.M., Gabdank, I., Hilton, J.A., Jain, K., Baymuradov, U.K., Narayanan, A.K., et al. (2018). The Encyclopedia of DNA elements (ENCODE): Data portal update. Nucleic Acids Res. *46*, D794–D801.

Decker, C.J., and Parker, R. (1993). A turnover pathway for both stable and unstable mRNAs in yeast: Evidence for a requirement for deadenylation. Genes Dev. *7*, 1632–1643.

Delis, C., Krokida, A., Tomatsidou, A., Tsikou, D., Beta, R.A.A., Tsioumpekou, M., Moustaka, J., Stravodimos, G., Leonidas, D.D., Balatsos, N.A.A., et al. (2016). AtHESPERIN: A novel regulator of circadian rhythms with poly(A)-degrading activity in plants. RNA Biol. *13*, 68–82.

Deniaud, A., Karuppasamy, M., Bock, T., Masiulis, S., Huard, K., Garzoni, F., Kerschgens, K., Hentze, M.W., Kulozik, A.E., Beck, M., et al. (2015). A network of SMG-8, SMG-9 and SMG-1 C-terminal insertion domain regulates UPF1 substrate recruitment and phosphorylation. Nucleic Acids Res. *43*, 7600–7611.

Desmet, E.A., Bussey, K.A., Stone, R., and Takimoto, T. (2013). Identification of the N-Terminal Domain of the Influenza Virus PA Responsible for the Suppression of Host Protein Synthesis. J. Virol. *87*, 3108–3118.

Dhanraj, S., Gunja, S.M.R., Deveau, A.P., Nissbeck, M., Boonyawat, B., Coombs, A.J., Renieri, A., Mucciolo, M., Marozza, A., Buoni, S., et al. (2015). Bone marrow failure and developmental delay caused by mutations in poly(A)-specific ribonuclease (PARN). J. Med. Genet. *52*, 738–748.

Dias, A., Bouvier, D., Crépin, T., McCarthy, A.A., Hart, D.J., Baudin, F., Cusack, S., and Ruigrok, R.W.H. (2009). The cap-snatching endonuclease of influenza virus polymerase resides in the PA subunit. Nature. *458*, 914–918.

Dickson, A.M., Anderson, J.R., Barnhart, M.D., Sokoloski, K.J., Oko, L., Opyrchal, M., Galanis, E., Wilusz, C.J., Morrison, T.E., and Wilusz, J. (2012). Dephosphorylation of HuR protein during alphavirus infection is associated with HuR relocalization to the cytoplasm. J. Biol. Chem. *287*, 36229–36238.

Diez, J., Ishikawa, M., Kaido, M., and Ahlquist, P. (2000). Identification and characterization of a host protein required for efficient template selection in viral RNA replication. Proc. Natl. Acad. Sci. *97*, 3913–3918.

van Dijk, E., Le Hir, H., and Seraphin, B. (2003). DcpS can act in the 5'-3' mRNA decay pathway in addition to the 3'-5' pathway. Proc. Natl. Acad. Sci. *100*, 12081–12086.

Van Dijk, E.L., Chen, C.L., Daubenton-Carafa, Y., Gourvennec, S., Kwapisz, M., Roche, V., Bertrand, C., Silvain, M., Legoix-Ne, P., Loeillet, S., et al. (2011). XUTs are a class of Xrn1-sensitive antisense regulatory non-coding RNA in yeast. Nature. *475*, 114–119.

Djavani, M., Lukashevich, I.S., Sanchez, A., Nichol, S.T., and Salvato, M.S. (1997). Completion of the Lassa fever virus sequence and identification of a RING finger open reading frame at the L RNA 5' end. Virology. *235*, 414–418.

Doepker, R.C., Hsu, W.-L., Saffran, H.A., and Smiley, J.R. (2004). Herpes simplex virus virion host shutoff protein is stimulated by translation initiation factors eIF4B and eIF4H. J. Virol. *78*, 4684–4699.

Dougherty, J.D., White, J.P., and Lloyd, R.E. (2011). Poliovirus-Mediated Disruption of Cytoplasmic Processing Bodies. J. Virol. *85*, 64–75.

Dougherty, J.D., Tsai, W.C., and Lloyd, R.E. (2015). Multiple poliovirus proteins repress cytoplasmic RNA granules. Viruses. *7*, 6127–6140.

Dufour, D., Mateos-Gomez, P.A., Enjuanes, L., Gallego, J., and Sola, I. (2011). Structure and Functional Relevance of a Transcription-Regulating Sequence Involved in Coronavirus Discontinuous RNA Synthesis. J. Virol. *85*, 4963–4973.

Dunckley, T., and Parker, R. (1999). The DCP2 protein is required for mRNA decapping in Saccharomyces cerevisiae and contains a functional MutT motif. EMBO J. *18*, 5411–5422.

Van Dyke, T.A., Rickles, R.J., and Flanegan, J.B. (1982). Genome-length copies of poliovirion RNA are synthesized in vitro by the poliovirus RNA-dependent RNA polymerase. J. Biol. Chem. *257*, 4610–4617.

Eaton, J.D., Davidson, L., Bauer, D.L.V., Natsume, T., Kanemaki, M.T., and West, S. (2018). Xrn2 accelerates termination by RNA polymerase II, which is underpinned by CPSF73 activity. Genes Dev. *32*, 127–139.

Eberle, A.B., Lykke-Andersen, S., Mühlemann, O., and Jensen, T.H. (2009). SMG6 promotes endonucleolytic cleavage of nonsense mRNA in human cells. Nat. Struct. Mol. Biol. *16*, 49–55.

Eleouet, J.F., Rasschaert, D., Lambert, P., Levy, L., Vende, P., and Laude, H. (1995b). Complete genomic sequence of the transmissible gastroenteritis virus. Adv Exp Med Biol. *380*, 459–461.

Eleouet, J.F., Rasschaert, D., Lambert, P., Levy, L., Vende, P., and Laude, H. (1995a). Complete Sequence (20 Kilobases) of the Polyprotein-Encoding Gene 1 of Transmissible Gastroenteritis Virus. Virology. *206*, 817–822.

Elliott, G., Pheasant, K., Ebert-Keel, K., Stylianou, J., Franklyn, A., and Jones, J. (2018). Multiple post-transcriptional strategies to regulate the herpes simplex virus type 1 vhs endoribonuclease. J. Virol. JVI.00818-18.

Elliott, R.M., Dunn, E., Simons, J.F., and Pettersson, R.F. (1992). Nucleotide sequence and coding strategy of the Uukuniemi virus L RNA segment. J. Gen. Virol. *73*, 1745–1752.

Emara, M.M., and Brinton, M.A. (2007). Interaction of TIA-1/TIAR with West Nile and dengue virus products in infected cells interferes with stress granule formation and processing body assembly. Proc. Natl. Acad. Sci. *104*, 9041–9046.

Emara, M.M., Fujimura, K., Sciaranghella, D., Ivanova, V., Ivanov, P., and Anderson, P. (2012). Hydrogen peroxide induces stress granule formation independent of eIF2α phosphorylation. Biochem. Biophys. Res. Commun. *423*, 763–769.

Emery, V.C., and Bishop, D.H.L. (1987). Characterization of Punta Toro S mRNA species and identification of an inverted complementary sequence in the intergenic region of Punta Toro phlebovirus ambisense S RNA that is involved in mRNA transcription termination. Virology. *156*, 1–11.

Van Etten, J., Schagat, T.L., Hrit, J., Weidmann, C.A., Brumbaugh, J., Coon, J.J., and Goldstrohm, A.C. (2012). Human pumilio proteins recruit multiple deadenylases to efficiently repress messenger RNAs. J. Biol. Chem. *287*, 36370–36383.

Fabian, M.R., Cieplak, M.K., Frank, F., Morita, M., Green, J., Srikumar, T., Nagar, B., Yamamoto, T., Raught, B., Duchaine, T.F., et al. (2011). MiRNA-mediated deadenylation is orchestrated by GW182 through two conserved motifs that interact with CCR4-NOT. Nat. Struct. Mol. Biol. *18*, 1211–1217.

Fabian, M.R., Frank, F., Rouya, C., Siddiqui, N., Lai, W.S., Karetnikov, A., Blackshear, P.J., Nagar, B., and Sonenberg, N. (2013). Structural basis for the recruitment of the human CCR4-NOT deadenylase complex by tristetraprolin. Nat. Struct. Mol. Biol. *20*, 735–739.

Fang, F., Phillips, S., and Butler, J.S. (2005). Rat1p and Rai1p function with the nuclear exosome in the processing and degradation of rRNA precursors. RNA .*11*, 1571–1578.

Faragher, S.G., and Dalgarno, L. (1986). Regions of conservation and divergence in the 3′ untranslated sequences of genomic RNA from Ross River virus isolates. J. Mol. Biol. *190*, 141–148.

Fehling, S.K., Lennartz, F., and Strecker, T. (2012). Multifunctional nature of the arenavirus RING finger protein Z. Viruses. *4*, 2973–3011.

Fenwick, M.L., and Clark, J. (1982). Early and delayed shut-off of host protein synthesis in cells infected with herpes simplex virus. J. Gen. Virol. *61*, 121–125.

Fenwick, M.L., and Everett, R.D. (1990). Inactivation of the shutoff gene (UL41) of herpes simplex virus types 1 and 2. J. Gen. Virol. *71*, 2961–2967.

Fenwick, M.L., and McMenamin, M.M. (1984). Early virion-associated suppression of cellular protein synthesis by herpes simplex virus is accompanied by inactivation of mRNA. J. Gen. Virol. *65*, 1225–1228.

Fenwick, M.L., and Owen, S.A. (1988). On the control of immediate early (α) mRNA survival in cells infected with herpes simplex virus. J. Gen. Virol. *69*, 2869–2877.

Fenwick, M.L., and Walker, M.J. (1978). Suppression of the synthesis of cellular macromolecules by herpes simplex virus. J. Gen. Virol. *41*, 37–51.

Fernández-García, Y., Reguera, J., Busch, C., Witte, G., Sánchez-Ramos, O., Betzel, C., Cusack, S., Günther, S., and Reindl, S. (2016). Atomic Structure and Biochemical Characterization of an RNA Endonuclease in the N Terminus of Andes Virus L Protein. PLoS Pathog. *12*, e1005635.

Finnen, R.L., Zhu, M., Li, J., Romo, D., and Banfield, B.W. (2016). Herpes Simplex Virus 2 Virion Host Shutoff Endoribonuclease Activity Is Required To Disrupt Stress Granule Formation. J. Virol. *90*, 7943–7955.

Fiorini, F., Robin, J.P., Kanaan, J., Borowiak, M., Croquette, V., Le Hir, H., Jalinot, P., and Mocquet, V. (2018). HTLV-1 Tax plugs and freezes UPF1 helicase leading to nonsense-mediated mRNA decay inhibition. Nat. Commun. *9*, 431.

Firth, A.E., Jagger, B.W., Wise, H.M., Nelson, C.C., Parsawar, K., Wills, N.M., Napthine, S., Taubenberger, J.K., Digard, P., and Atkins, J.F. (2012). Ribosomal frameshifting used in influenza A virus expression occurs within the sequence UCC-UUU-CGU and is in the +1 direction. Open Biol. *2*, 120109.

Flobinus, A., Hleibieh, K., Klein, E., Ratti, C., Bouzoubaa, S., and Gilmer, D. (2016). A viral noncoding RNA complements a weakened viral RNA silencing suppressor and promotes efficient systemic host infection. Viruses *8*, 272.

Ford, L.P., and Wilusz, J. (1999). An in vitro system using HeLa cytoplasmic extracts that reproduces regulated mRNA stability. Methods A Companion to Methods Enzymol. *17*, 21–27.

Fourati, Z., Kolesnikova, O., Back, R., Keller, J., Charenton, C., Taverniti, V., Plesse, C.G., Lazar, N., Durand, D., Van Tilbeurgh, H., et al. (2014). The C-terminal domain from S. cerevisiae Pat1 displays two conserved regions involved in decapping factor recruitment. PLoS One *9*, e96828.

Fromm, S.A., Truffault, V., Kamenz, J., Braun, J.E., Hoffmann, N.A., Izaurralde, E., and Sprangers, R. (2012). The structural basis of Edc3-and Scd6-mediated activation of the Dcp1:Dcp2 mRNA decapping complex. EMBO J. *31*, 279–290.

Fujimura, K., Sasaki, A.T., and Anderson, P. (2012). Selenite targets eIF4E-binding protein-1 to inhibit translation initiation and induce the assembly of non-canonical stress granules. Nucleic Acids Res. *40*, 8099–8110.

Fung, G., Ng, C.S., Zhang, J., Shi, J., Wong, J., Piesik, P., Han, L., Chu, F., Jagdeo, J., Jan, E., et al. (2013). Production of a dominant-negative fragment due to G3BP1 cleavage contributes to the disruption of mitochondria-associated protective stress granules during CVB3 infection. PLoS One. *8*, e79546.

Funk, A., Truong, K., Nagasaki, T., Torres, S., Floden, N., Balmori Melian, E., Edmonds, J., Dong, H., Shi, P.-Y., and Khromykh, A.A. (2010). RNA structures required for production of subgenomic flavivirus RNA. J. Virol. *84*, 11407–11417.

Gaglia, M.M., Covarrubias, S., Wong, W., and Glaunsinger, B.A. (2012). A Common Strategy for Host RNA Degradation by Divergent Viruses. J. Virol. *86*, 9527–9530.

Gaglia, M.M., Rycroft, C.H., and Glaunsinger, B.A. (2015). Transcriptome-Wide Cleavage Site Mapping on Cellular mRNAs Reveals Features Underlying Sequence-Specific Cleavage by the Viral Ribonuclease SOX. PLoS Pathog. *11*, e1005305.

Galão, R.P., Chari, A., Alves-Rodrigues, I., Lobão, D., Mas, A., Kambach, C., Fischer, U., and Díez, J. (2010). LSm1-7 complexes bind to specific sites in viral RNA genomes and regulate their translation and replication. RNA. *16*, 817–827.

Gallo, C.M., Munro, E., Rasoloson, D., Merritt, C., and Seydoux, G. (2008). Processing bodies and germ granules are distinct RNA granules that interact in C. elegans embryos. Dev. Biol. *323*, 76–87.

Gallouzi, I.E., Brennan, C.M., Stenberg, M.G., Swanson, M.S., Eversole, A., Maizels, N., and Steitz, J.A. (2000). HuR binding to cytoplasmic mRNA is perturbed by heat shock. Proc. Natl. Acad. Sci. U. S. A. *97*, 3073–3078.

Gamarnik, A. V, and Andino, R. (1997). Two functional complexes formed by KH domain containing proteins with the 5' noncoding region of poliovirus RNA. RNA *3*, 882–892.

Gao, M., Fritz, D.T., Ford, L.P., and Wilusz, J. (2000). Interaction between a poly(A)-specific ribonuclease and the 5' cap influences mRNA deadenylation rates in vitro. Mol. Cell. *5*, 479–488.

Garbarino-Pico, E., Niu, S., Rollag, M.D., Strayer, C.A., Besharse, J.C., and Green, C.B. (2007). Immediate early response of the circadian polyA ribonuclease nocturnin to two extracellular stimuli. RNA *13*, 745–755.

Garcia, J.F., and Parker, R. (2015). MS2 coat proteins bound to yeast mRNAs block 5' to 3' degradation and trap mRNA decay products: implications for the localization of mRNAs by MS2-MCP system. RNA *21*, 1393–1395.

Garcia, D., Garcia, S., and Voinnet, O. (2014). Nonsense-mediated decay serves as a general viral restriction mechanism in plants. Cell Host Microbe. *16*, 391–402.

Garneau, N.L., Sokoloski, K.J., Opyrchal, M., Neff, C.P., Wilusz, C.J., and Wilusz, J. (2008). The 3' Untranslated Region of Sindbis Virus Represses Deadenylation of Viral Transcripts in Mosquito and Mammalian Cells. J. Virol. *82*, 880–892.

Ge, Z., Quek, B.L., Beemon, K.L., and Hogg, J.R. (2016). Polypyrimidine tract binding protein 1 protects mRNAs from recognition by the nonsense-mediated mRNA decay pathway. Elife. *5*, e11155

Geerlings, T.H., Vos, J.C., and Raue, H.A. (2000). The final step in the formation of 25S rRNA in saccharomyces cerevisiae is performed by 5' ??? 3' exonucleases. RNA. *6*, 1698–1703.

Ghiringhelli, P.D., Rivera-Pomar, R. V., Lozano, M.E., Grau, O., and Romanowski, V. (1991). Molecular organization of Junin virus S RNA: complete nucleotide sequence, relationship with other members of the Arenaviridae and unusual secondary structures. J. Gen. Virol. *72*, 2129–2141.

Gilks, N., Kedersha, N., Ayodele, M., Shen, L., Stoecklin, G., Dember, L.M., and Anderson, P. (2004). Stress granule assembly is mediated by prion-like aggregation of TIA-1. Mol. Biol. Cell *15*, 5383–5398.

Gilmer, D., Bouzoubaa, S., Hehn, A., Guilley, H., Richards, K., and Jonard, G. (1992). Efficient cell-to-cell movement of beet necrotic yellow vein virus requires 3′ proximal genes located on RNA 2. Virology. *189*, 40–47.

Gilmer, D., Ratti, C., and Ictv Report Consortium, I.R. (2017). ICTV Virus Taxonomy Profile: Benyviridae. J. Gen. Virol. *98*, 1571–1572.

Giménez-Barcons, M., Alves-Rodrigues, I., Jungfleisch, J., Van Wynsberghe, P.M., Ahlquist, P., and Díez, J. (2013). The cellular decapping activators LSm1, Pat1, and Dhh1 control the ratio of subgenomic to genomic Flock House virus RNAs. J. Virol. *87*, 6192–6200.

Giorgi, C., Accardi, L., Nicoletti, L., Gro, M.C., Takehara, K., Hilditch, C., Morikawa, S., and Bishop, D.H.L. (1991). Sequences and coding strategies of the S RNAs of Toscana and Rift Valley fever viruses compared to those of Punta Toro, Sicilian sandfly fever, and Uukuniemi viruses. Virology. *180*, 738–753.

Goebel, S.J., Hsue, B., Dombrowski, T.F., and Masters, P.S. (2004a). Characterization of the RNA Components of a Putative Molecular Switch in the 3J Untranslated Region of the Murine Coronavirus Genome. J. Virol. *78*, 669–682.

Goebel, S.J., Taylor, J., and Masters, P.S. (2004b). The 3' cis-acting genomic replication element of the severe acute respiratory syndrome coronavirus can function in the murine coronavirus genome. J. Virol. *78*, 7846–7851.

Göertz, G.P., Fros, J.J., Miesen, P., Vogels, C.B.F., van der Bent, M.L., Geertsema, C., Koenraadt, C.J.M., van Rij, R.P., van Oers, M.M., and Pijlman, G.P. (2016). Noncoding Subgenomic Flavivirus RNA Is Processed by the Mosquito RNA Interference Machinery and Determines West Nile Virus Transmission by Culex pipiens Mosquitoes. J. Virol. *90*, 10145–10159.

Golden, J.W., Beitzel, B., Ladner, J.T., Mucker, E.M., Kwilas, S.A., Palacios, G., and Hooper, J.W. (2017). An attenuated Machupo virus with a disrupted L-segment intergenic region protects Guinea pigs against lethal Guanarito virus infection. Sci. Rep. *7*, 4679.

Gonzalez, J.P.J., Bowen, M.D., Nichol, S.T., and Rico-Hesse, R. (1996). Genetic characterization and phylogeny of Sabia virus, an emergent pathogen in Brazil. Virology. *221*, 318–324.

Goodman, N.C., and Spiegelman, S. (1971). Distinguishing reverse transcriptase of an RNA tumor virus from other known DNA polymerases. Proc. Natl. Acad. Sci. U. S. A. *68*, 2203–2206.

Grakoui, A., Mccourt, D.W., Wychowski, C., Feinstone, S.M., and Ric, C.M. (1993b). Characterization of the Hepatitis C Virus-Encoded Serine Proteinase: Determination of Proteinase-Dependent Polyprotein Cleavage Sites. J. Virol. *67*, 2832–2843.

Grakoui, A., Wychowski, C., Lin, C., Feinstone, S.M., and Rice, C.M. (1993a). Expression and identification of hepatitis C virus polyprotein cleavage products. J. Virol. *67*, 1385–1395.

Granneman, S., Petfalski, E., and Tollervey, D. (2011). A cluster of ribosome synthesis factors regulate pre-rRNA folding and 5.8S rRNA maturation by the Rat1 exonuclease. EMBO J. *30*, 4006–4019.

Green, C.B., and Besharse, J.C. (1996). Identification of a novel vertebrate circadian clock-regulated gene encoding the protein nocturnin. Proccedings Natl. Acad. Sci. United States Am. *93*, 14884–14888.

Green, C.B., Douris, N., Kojima, S., Strayer, C.A., Fogerty, J., Lourim, D., Keller, S.R., and Besharse, J.C. (2007). Loss of Nocturnin, a circadian deadenylase, confers resistance to hepatic steatosis and diet-induced obesity. Proc. Natl. Acad. Sci. U. S. A. *104*, 9888–9893.

Grima, D.P., Sullivan, M., Zabolotskaya, M. V., Browne, C., Seago, J., Wan, K.C., Okada, Y., and Newbury, S.F. (2008). The 5'-3' exoribonuclease pacman is required for epithelial sheet sealing in Drosophila and genetically interacts with the phosphatase puckered. Biol. Cell. *100*, 687–701.

Grò, M.C., Di Bonito, P., Fortini, D., Mochi, S., and Giorgi, C. (1997). Completion of molecular characterization of Toscana phlebovirus genome: Nucleotide sequence, coding strategy of M genomic segment and its amino acid sequence comparison to other phleboviruses. Virus Res. *51*, 81–91.

Grönke, S., Bickmeyer, I., Wunderlich, R., Jäckle, H., and Kühnlein, R.P. (2009). Curled encodes the Drosophila homolog of the vertebrate circadian deadenylase nocturnin. Genetics. *183*, 219–232.

Grousl, T., Ivanov, P., Frydlova, I., Vasicova, P., Janda, F., Vojtova, J., Malinska, K., Malcova, I., Novakova, L., Janoskova, D., et al. (2009). Robust heat shock induces eIF2 -phosphorylation-independent assembly of stress granules containing eIF3 and 40S ribosomal subunits in budding yeast, Saccharomyces cerevisiae. J. Cell Sci. *122*, 2078–2088.

Grzechnik, P., Szczepaniak, S.A., Dhir, S., Pastucha, A., Parslow, H., Matuszek, Z., Mischo, H.E., Kufel, J., and Proudfoot, N.J. (2018). Nuclear fate of yeast snoRNA is determined by co-transcriptional Rnt1 cleavage. Nat. Commun. *9*, 1783.

Grzela, R., Nasilowska, K., Lukaszewicz, M., Tyras, M., Stepinski, J., Jankowska-Anyszka, M., Bojarska, E., and Darzynkiewicz, E. (2018). Hydrolytic activity of human Nudt16 enzyme on dinucleotide cap analogs and short capped oligonucleotides. RNA. *24*, 633–642.

Gu, W., Gallagher, G.R., Dai, W., Liu, P., Li, R., Trombly, M.I., Gammon, D.B., Mello, C.C., Wang, J.P., and Finberg, R.W. (2015). Influenza A virus preferentially snatches noncoding RNA caps. RNA. *21*, 2067–2075.

Guarino, L.A., Ghosh, A., Dasmahapatra, B., Dasgupta, R., and Kaesberg, P. (1984). Sequence of the black beetle virus subgenomic RNA and its location in the viral genome. Virology. *139*, 199–203.

Guerra, M.A., Curns, A.T., Rupprecht, C.E., Hanlon, C.A., Krebs, J.W., and Childs, J.E. (2003). Skunk and raccoon rabies in the eastern United States: temporal and spatial analysis. Emerg. Infect. Dis. *9*, 1143–1150.

Guilligay, D., Tarendeau, F., Resa-Infante, P., Coloma, R., Crepin, T., Sehr, P., Lewis, J., Ruigrok, R.W.H., Ortin, J., Hart, D.J., et al. (2008). The structural basis for cap binding by influenza virus polymerase subunit PB2. Nat. Struct. Mol. Biol. *15*, 500–506.

Hagan, J.P., Piskounova, E., and Gregory, R.I. (2009). Lin28 recruits the TUTase Zcchc11 to inhibit let-7 maturation in mouse embryonic stem cells. Nat. Struct. Mol. Biol. *16*, 1021–1025.

El Hage, A., Koper, M., Kufel, J., and Tollervey, D. (2008). Efficient termination of transcription by RNA polymerase I requires the 5′ exonuclease Rat1 in yeast. Genes Dev. *22*, 1069–1081.

Halbach, F., Reichelt, P., Rode, M., and Conti, E. (2013). The yeast ski complex: Crystal structure and rna channeling to the exosome complex. Cell *154*, 814–826.

Hampson, K., Coudeville, L., Lembo, T., Sambo, M., Kieffer, A., Attlan, M., Barrat, J., Blanton, J.D., Briggs, D.J., Cleaveland, S., et al. (2015). Estimating the Global Burden of Endemic Canine Rabies. PLoS Negl. Trop. Dis. *9*, e0003709.

Hara, K., Schmidt, F.I., Crow, M., and Brownlee, G.G. (2006). Amino Acid Residues in the N-Terminal Region of the PA Subunit of Influenza A Virus RNA Polymerase Play a Critical Role in Protein Stability, Endonuclease Activity, Cap Binding, and Virion RNA Promoter Binding. J. Virol. *80*, 7789–7798.

Harigaya, Y., and Parker, R. (2012). Global analysis of mRNA decay intermediates in Saccharomyces cerevisiae. Proc. Natl. Acad. Sci. *109*, 11764–11769.

Harigaya, Y., Jones, B.N., Muhlrad, D., Gross, J.D., and Parker, R. (2010). Identification and Analysis of the Interaction between Edc3 and Dcp2 in Saccharomyces cerevisiae. Mol. Cell. Biol. *30*, 1446–1456.

Harris, D., Zhang, Z., Chaubey, B., and Pandey, V.N. (2006). Identification of Cellular Factors Associated with the 3′-Nontranslated Region of the Hepatitis C Virus Genome. Mol. Cell. Proteomics. *5*, 1006–1018.

Hass, M., Golnitz, U., Muller, S., Becker-Ziaja, B., and Gunther, S. (2004). Replicon System for Lassa Virus. J. Virol. *78*, 13793–13803.

Havrila, M., Stadlbauer, P., Islam, B., Otyepka, M., and Šponer, J. (2017). Effect of Monovalent Ion Parameters on Molecular Dynamics Simulations of G-Quadruplexes. J. Chem. Theory Comput. *13*, 3911–3926.

Hayashi, M., Nanba, C., Saito, M., Kondo, M., Takeda, A., Watanabe, Y., and Nishimura, M. (2012). Loss of XRN4 function can trigger cosuppression in a sequence-dependent manner. Plant Cell Physiol. *53*, 1310–1321.

Hayashi, T., Chaimayo, C., McGuinness, J., and Takimoto, T. (2016). Critical Role of the PA-X C-Terminal Domain of Influenza A Virus in Its Subcellular Localization and Shutoff Activity. J. Virol. *90*, 7131–7141.

He, S., Wurtzel, O., Singh, K., Froula, J.L., Yilmaz, S., Tringe, S.G., Wang, Z., Chen, F., Lindquist, E.A., Sorek, R., et al. (2010). Validation of two ribosomal RNA removal methods for microbial metatranscriptomics. Nat. Methods *7*, 807–812.

Heidel, G.B., Rush, C.M., Kendall, T.L., Lommel, S.A., and French, R.C. (1997). Characteristics of Beet Soilborne Mosaic Virus, a Furo-like Virus Infecting Sugar Beet. Plant Dis. *81*, 1070–1076.

Helfer, S., Schott, J., Stoecklin, G., and Förstemann, K. (2012). AU-rich element-mediated mRNA decay can occur independently of the miRNA machinery in mouse embryonic fibroblasts and Drosophila S2-cells. PLoS One. *7*, e28907.

Hengrung, N., El Omari, K., Serna Martin, I., Vreede, F.T., Cusack, S., Rambo, R.P., Vonrhein, C., Bricogne, G., Stuart, D.I., Grimes, J.M., et al. (2015). Crystal structure of the RNA-dependent RNA polymerase from influenza C virus. Nature *527*, 114–117.

Henry, Y., Wood, H., Morrissey, J.P., Petfalski, E., Kearsey, S., and Tollervey, D. (1994). The 5' end of yeast 5.8S rRNA is generated by exonucleases from an upstream cleavage site. EMBO J. *13*, 2452–2463.

Heo, I., Joo, C., Cho, J., Ha, M., Han, J., and Kim, V.N. (2008). Lin28 Mediates the Terminal Uridylation of let-7 Precursor MicroRNA. Mol. Cell. *32*, 276–284.

Heo, I., Joo, C., Kim, Y.K., Ha, M., Yoon, M.J., Cho, J., Yeom, K.H., Han, J., and Kim, V.N. (2009). TUT4 in Concert with Lin28 Suppresses MicroRNA Biogenesis through Pre-MicroRNA Uridylation. Cell. *138*, 696–708.

Heyer, W.D., Johnson, A.W., Reinhart, U., and Kolodner, R.D. (1995). Regulation and intracellular localization of Saccharomyces cerevisiae strand exchange protein 1 (Sep1/Xrn1/Kem1), a multifunctional exonuclease. Mol. Cell. Biol. *15*, 2728–2736.

Hidalgo, J., Richards, G.A., Jiménez, J.I.S., Baker, T., and Amin, P. (2017). Viral hemorrhagic fever in the tropics: Report from the task force on tropical diseases by the World Federation of Societies of Intensive and Critical Care Medicine. J. Crit. Care. *42*, 366–372.

Higashimoto, K., Maeda, T., Okada, J., Ohtsuka, Y., Sasaki, K., Hirose, A., Nomiyama, M., Takayanagi, T., Fukuzawa, R., Yatsuki, H., et al. (2013). Homozygous deletion of dis3l2 exon 9 due to non-allelic homologous recombination between line-1s in a japanese patient with perlman syndrome. Eur. J. Hum. Genet. *21*, 1316–1319.

Holcik, M., and Liebhaber, S.A. (1997). Four highly stable eukaryotic mRNAs assemble 3' untranslated region RNA-protein complexes sharing cis and trans components. Proc. Natl. Acad. Sci. U. S. A. *94*, 2410–2414.

Holloway, B.P., and Obijeski, J.F. (1980). Rabies virus-induced RNA synthesis in BHK21 cells. J. Gen. Virol. *49*, 181–195.

Houff, S.A., Burton, R.C., Wilson, R.W., Henson, T.E., London, W.T., Baer, G.M., Anderson, L.J., Winkler, W.G., Madden, D.L., and Sever, J.L. (1979). Human-to-human transmission of rabies virus by corneal transplant. N Engl J Med *300*, 603–604.

Howe, J.G., and Shu, M.D. (1988). Isolation and characterization of the genes for two small RNAs of herpesvirus papio and their comparison with Epstein-Barr virus-encoded EBER RNAs. J. Virol. *62*, 2790–2798.

Hsu, C.L., and Stevens, A. (1993). Yeast cells lacking 5'-->3' exoribonuclease 1 contain mRNA species that are poly(A) deficient and partially lack the 5' cap structure. Mol. Cell. Biol. *13*, 4826–4835.

Hsue, B., and Masters, P.S. (1997). A bulged stem-loop structure in the 3' untranslated region of the genome of the coronavirus mouse hepatitis virus is essential for replication. J. Virol. *71*, 7567–7578.

Hu, W., Sweet, T.J., Chamnongpol, S., Baker, K.E., and Coller, J. (2009). Co-translational mRNA decay in Saccharomyces cerevisiae. Nature. *461*, 225–229.

Hu, W., Petzold, C., Coller, J., and Baker, K.E. (2010). Nonsense-mediated mRNA decapping occurs on polyribosomes in Saccharomyces cerevisiae. Nat. Struct. Mol. Biol. *17*, 244–247.

Huang, C., Lokugamage, K.G., Rozovics, J.M., Narayanan, K., Semler, B.L., and Makino, S. (2011). SARS coronavirus nsp1 protein induces template-dependent endonucleolytic cleavage of mRNAs: Viral mRNAs are resistant to nsp1-induced RNA cleavage. PLoS Pathog. *7*, e1002433.

Hubstenberger, A., Courel, M., Bénard, M., Souquere, S., Ernoult-Lange, M., Chouaib, R., Yi, Z., Morlot, J.B., Munier, A., Fradet, M., et al. (2017). P-Body Purification Reveals the Condensation of Repressed mRNA Regulons. Mol. Cell *68*, 144–157.e5.

Hug, N., and Cáceres, J.F. (2014). The RNA Helicase DHX34 Activates NMD by promoting a transition from the surveillance to the decay-inducing complex. Cell Rep. *8*, 1845–1856.

Iapalucci, S., López, N., Rey, O., Zakin, M.M., Cohen, G.N., and Franze-Fernández, M.T. (1989). The 5′ region of Tacaribe virus L RNA encodes a protein with a potential metal binding domain. Virology *173*, 357–361.

Iapalucci, S., López, N., and Franze-Fernández, M.T. (1991). The 3′ end termini of the tacaribe arenavirus subgenomic RNAs. Virology *182*, 269–278.

Ikegami, T., Won, S., Peters, C.J., and Makino, S. (2007). Characterization of Rift Valley fever virus transcriptional terminations. J. Virol. *81*, 8421–8438.

Imai, M., Watanabe, T., Kiso, M., Nakajima, N., Yamayoshi, S., Iwatsuki-Horimoto, K., Hatta, M., Yamada, S., Ito, M., Sakai-Tagawa, Y., et al. (2017). A Highly Pathogenic Avian H7N9 Influenza Virus Isolated from A Human Is Lethal in Some Ferrets Infected via Respiratory Droplets. Cell Host Microbe *22*, 615–626.

Ingelfinger, D., Arndt-Jovin, D.J., Lührmann, R., and Achsel, T. (2002). The human LSm1-7 proteins colocalize with the mRNA-degrading enzymes Dcp1/2 and Xrnl in distinct cytoplasmic foci. RNA. *8*, 1489–1501.

Interthal, H., Bellocq, C., Bahler, J., Bashkirov, V.I., Edelstein, S., and Heyer, W.D. (1995). A role of Sep1 (= Kem1, Xrn1) as a microtubule-associated protein in Saccharomyces cerevisiae. EMBO J. *14*, 1057–1066.

Ishikawa, H., Yoshikawa, H., Izumikawa, K., Miura, Y., Taoka, M., Nobe, Y., Yamauchi, Y., Nakayama, H., Simpson, R.J., Isobe, T., et al. (2016). Poly(A)-specific ribonuclease regulates the processing of small-subunit rRNAs in human cells. Nucleic Acids Res. *45*, 3437–3447.

Ishikawa, H., Nobe, Y., Izumikawa, K., Taoka, M., Yamauchi, Y., Nakayama, H., Simpson, R.J., Isobe, T., and Takahash, N. (2018). Truncated forms of U2 snRNA (U2-tfs) are shunted toward a novel uridylylation pathway that differs from the degradation pathway for U1-tfs. RNA Biol. *15*, 261–268.

Ito, K., Takahashi, A., Morita, M., Suzuki, T., and Yamamoto, T. (2011). The role of the CNOT1 subunit of the CCR4-NOT complex in mRNA deadenylation and cell viability. Protein Cell. *2*, 755–763.

Iwakawa, H. -o., Mizumoto, H., Nagano, H., Imoto, Y., Takigawa, K., Sarawaneeyaruk, S., Kaido, M., Mise, K., and Okuno, T. (2008). A Viral Noncoding RNA Generated by cis-Element-Mediated Protection against 5'->3' RNA Decay Represses both Cap-Independent and Cap-Dependent Translation. J. Virol. *82*, 10162–10174.

Iwasaki, M., Ngo, N., Cubitt, B., and de la Torre, J.C. (2015). Efficient Interaction between Arenavirus Nucleoprotein (NP) and RNA-Dependent RNA Polymerase (L) Is Mediated by the Virus Nucleocapsid (NP-RNA) Template. J. Virol. *89*, 5734–5738.

Iwasaki, M., Cubitt, B., Sullivan, B.M., and de la Torre, J.C. (2016). The High Degree of Sequence Plasticity of the Arenavirus Noncoding Intergenic Region (IGR) Enables the Use of a Nonviral Universal Synthetic IGR To Attenuate Arenaviruses. J. Virol. *90*, 3187–3197.

Jaag, H.M., and Nagy, P.D. (2009). Silencing of Nicotiana benthamiana Xrn4p exoribonuclease promotes tombusvirus RNA accumulation and recombination. Virology. *386*, 344–352.

Jagger, B.W., Wise, H.M., Kash, J.C., Walters, K.A., Wills, N.M., Xiao, Y.L., Dunfee, R.L., Schwartzman, L.M., Ozinsky, A., Bell, G.L., et al. (2012). An overlapping protein-coding region in influenza A virus segment 3 modulates the host response. Science. *337*, 199–204.

Janda, M., and Ahlquist, P. (1993). RNA-dependent replication, transcription, and persistence of brome mosaic virus RNA replicons in S. cerevisiae. Cell *72*, 961–970.

Jartti, T., Lehtinen, P., Vuorinen, T., Österback, R., Van Den Hoogen, B., Osterhaus, A.D.M.E., and Ruuskanen, O. (2004). Respiratory picornaviruses and respiratory syncytial virus as causative agents of acute expiratory wheezing in children. Emerg. Infect. Dis. *10*, 1095–1101.

Jeeva, S., Cheng, E., Ganaie, S.S., and Mir, M.A. (2017). Crimean-Congo Hemorrhagic Fever Virus Nucleocapsid Protein Augments mRNA Translation. J. Virol. *91*, e00636-17.

Jennings, P.A., and Molloy, P.L. (1987). Inhibition of SV40 replicon function by engineered antisense RNA transcribed by RNA polymerase III. EMBO J. *6*, 3043–3047.

Jiang, S., Jiang, L., Yang, J., Peng, J., Lu, Y., Zheng, H., Lin, L., Chen, J., and Yan, F. (2018). Over-expression of Oryza sativa Xrn4 confers plant resistance to virus infection. Gene *639*, 44–51.

Jiao, X., Xiang, S., Oh, C., Martin, C.E., Tong, L., and Kiledjian, M. (2010). Identification of a quality-control mechanism for mRNA 5′-end capping. Nature. *467*, 608–611.

Jiao, X., Chang, J.H., Kilic, T., Tong, L., and Kiledjian, M. (2013). A Mammalian Pre-mRNA 5' End Capping Quality Control Mechanism and an Unexpected Link of Capping to Pre-mRNA Processing. Mol. Cell. *50*, 104–115.

Jiao, X., Doamekpor, S.K., Bird, J.G., Nickels, B.E., Tong, L., Hart, R.P., and Kiledjian, M. (2017). 5′ End Nicotinamide Adenine Dinucleotide Cap in Human Cells Promotes RNA Decay through DXO-Mediated deNADding. Cell *168*, 1015–1027.

Jinek, M., Coyle, S.M., and Doudna, J.A. (2011). Coupled 5' Nucleotide Recognition and Processivity in Xrn1-Mediated mRNA Decay. Mol. Cell. *41,* 600–608.

Johnson, A.W. (1997). Rat1p and Xrn1p are functionally interchangeable exoribonucleases that are restricted to and required in the nucleus and cytoplasm, respectively. Mol. Cell. Biol. *17*, 6122–6130.

Johnson, J.M., Thürich, J., Petutschnig, E.K., Altschmied, L., Meichsner, D., Sherameti, I., Dindas, J., Mrozinska, A., Paetz, C., Scholz, S.S., et al. (2018). A poly(A) ribonuclease controls the cellotriose-based interaction between Piriformospora indica and its host Arabidopsis. Plant Physiol. *176*, pp.01423.2017.

Jones, B.L., VanLoozen, J., Kim, M.H., Miles, S.J., Dunham, C.M., Williams, L.D., and Snell, T.W. (2013a). Stress granules form in Brachionus manjavacas (Rotifera) in response to a variety of stressors. Comp. Biochem. Physiol. - A Mol. Integr. Physiol. *166*, 375–384.

Jones, C.I., Grima, D.P., Waldron, J.A., Jones, S., Parker, H.N., and Newbury, S.F. (2013b). The 5′-3′ exoribonuclease Pacman (Xrn1) regulates expression of the heat shock protein Hsp67Bc and the microRNA miR-277-3p in Drosophila wing imaginal discs. RNA Biol. *10,* 1345–1355.

Jones, C.I., Pashler, A.L., Towler, B.P., Robinson, S.R., and Newbury, S.F. (2016). RNA-seq reveals post-transcriptional regulation of Drosophila insulin-like peptide dilp8 and the neuropeptide-like precursor Nplp2 by the exoribonuclease Pacman/XRN1. Nucleic Acids Res. *44*, 267–280.

Joshi, R.L., Joshi, S., Chapeville, F., and Haenni, A.L. (1983). tRNA-like structures of plant viral RNAs: conformational requirements for adenylation and aminoacylation. EMBO J. *2*, 1123–1127.

Jungfleisch, J., Chowdhury, A., Alves-Rodrigues, I., Tharun, S., and Díez, J. (2015). The Lsm1-7-Pat1 complex promotes viral RNA translation and replication by differential mechanisms. RNA. *21*, 1469–1479.

Kadaba, S., Krueger, A., Trice, T., Krecic, A.M., Hinnebusch, A.G., and Anderson, J. (2004). Nuclear surveillance and degradation of hypomodified initiator tRNA Met in S. cerevisiae. Genes Dev. *18*, 1227–1240.

Kadyrova, L.Y., Habara, Y., Lee, T.H., and Wharton, R.P. (2007). Translational control of maternal Cyclin B mRNA by Nanos in the Drosophila germline. Development *134*, 1519–1527.

Kamitani, W., Narayanan, K., Huang, C., Lokugamage, K., Ikegami, T., Ito, N., Kubo, H., and Makino, S. (2006). Severe acute respiratory syndrome coronavirus nsp1 protein suppresses host gene expression by promoting host mRNA degradation. Proc. Natl. Acad. Sci. *103*, 12885–12890.

Kamitani, W., Huang, C., Narayanan, K., Lokugamage, K.G., and Makino, S. (2009). A two-pronged strategy to suppress host protein synthesis by SARS coronavirus Nsp1 protein. Nat. Struct. Mol. Biol. *16*, 1134–1140.

Kang, D., Skalsky, R.L., and Cullen, B.R. (2015). EBV BART MicroRNAs Target Multiple Pro-apoptotic Cellular Genes to Promote Epithelial Cell Survival. PLoS Pathog. *11*, e1004979.

Kashima, I., Yamashita, A., Izumi, N., Kataoka, N., Morishita, R., Hoshino, S., Ohno, M., Dreyfuss, G., and Ohno, S. (2006). Binding of a novel SMG-1-Upf1-eRF1-eRF3 complex (SURF) to the exon junction complex triggers Upf1 phosphorylation and nonsense-mediated mRNA decay. Genes Dev. *20*, 355–367.

Kaushik, K., Sivadas, A., Vellarikkal, S.K., Verma, A., Jayarajan, R., Pandey, S., Sethi, T., Maiti, S., Scaria, V., and Sivasubbu, S. (2018). RNA secondary structure profiling in zebrafish reveals unique regulatory features. BMC Genomics. *19*, 147.

Kearse, M., Moir, R., Wilson, A., Stones-Havas, S., Cheung, M., Sturrock, S., Buxton, S., Cooper, A., Markowitz, S., Duran, C., et al. (2012). Geneious Basic: An integrated and extendable desktop software platform for the organization and analysis of sequence data. Bioinformatics. *28*, 1647–1649.

Kedersha, N. (2002). Evidence That Ternary Complex (eIF2-GTP-tRNAiMet)-Deficient Preinitiation Complexes Are Core Constituents of Mammalian Stress Granules. Mol. Biol. Cell. *13*, 195–210.

Kedersha, N.L., Gupta, M., Li, W., Miller, I., and Anderson, P. (1999). RNA-binding proteins TIA-1 and TIAR link the phosphorylation of eIF-2 alpha to the assembly of mammalian stress granules. J. Cell Biol. *147*, 1431–1442.

Kempf, B.J., and Barton, D.J. (2008). Poly(rC) Binding Proteins and the 5' Cloverleaf of Uncapped Poliovirus mRNA Function during De Novo Assembly of Polysomes. J. Virol. *82*, 5835–5846.

Kenna, M., Stevens, A., McCammon, M., and Douglas, M.G. (1993). An essential yeast gene with homology to the exonuclease-encoding XRN1/KEM1 gene also encodes a protein with exoribonuclease activity. Mol. Cell. Biol. *13*, 341–350.

Kerber, R., Rieger, T., Busch, C., Flatz, L., Pinschewer, D.D., Kummerer, B.M., and Gunther, S. (2011). Cross-Species Analysis of the Replication Complex of Old World Arenaviruses Reveals Two Nucleoprotein Sites Involved in L Protein Function. J. Virol. *85*, 12518–12528.

Khaperskyy, D.A., Emara, M.M., Johnston, B.P., Anderson, P., Hatchette, T.F., and McCormick, C. (2014). Influenza A Virus Host Shutoff Disables Antiviral Stress-Induced Translation Arrest. PLoS Pathog. *10*, e1004217.

Khaperskyy, D.A., Schmaling, S., Larkins-Ford, J., McCormick, C., and Gaglia, M.M. (2016). Selective Degradation of Host RNA Polymerase II Transcripts by Influenza A Virus PA-X Host Shutoff Protein. PLoS Pathog. *12*, e1005427.

Kim, J., and Kim, J. (2002). KEM1 is involved in filamentous growth of Saccharomyces cerevisiae. FEMS Microbiol. Lett. *216*, 33–38.

Kim, M., Krogan, N.J., Vasiljeva, L., Rando, O.J., Nedea, E., Greenblatt, J.F., and Buratowski, S. (2004). The yeast Rat1 exonuclease promotes transcription termination by RNA polymerase II. Nature. *432*, 517–522.

Kimball, S.R., Horetsky, R.L., Ron, D., Jefferson, L.S., and Harding, H.P. (2003). Mammalian stress granules represent sites of accumulation of stalled translation initiation complexes. Am. J. Physiol. Physiol. *284*, C273–C284.

Kiss, T., and Filipowicz, W. (1995). Exonucleolytic processing of small nucleolar RNAs from pre-mRNA introns. Genes Dev. *9*, 1411–1424.

Kitamura, N., Semler, B.L., Rothberg, P.G., Larsen, G.R., Adler, C.J., Dorner, A.J., Emini, E.A., Hanecak, R., Lee, J.J., Van Der Werf, S., et al. (1981). Primary structure, gene organization and polypeptide expression of poliovirus RNA. Nature. *291*, 547–553.

Klinck, R., Sprules, T., and Gehring, K. (1997). Structural characterization of three RNA hexanucleotide loops from the internal ribosome entry site of polioviruses. Nucleic Acids Res. *25*, 2129–2137.

Kojima, S., Gatfield, D., Esau, C.C., and Green, C.B. (2010). MicroRNA-122 modulates the rhythmic expression profile of the circadian deadenylase Nocturnin in mouse liver. PLoS One. *5*, e11264.

Koppstein, D., Ashour, J., and Bartel, D.P. (2015). Sequencing the cap-snatching repertoire of H1N1 influenza provides insight into the mechanism of viral transcription initiation. Nucleic Acids Res. *43*, 5052–5064.

Körner, C.G., and Wahle, E. (1997). Poly(A) tail shortening by a mammalian poly(A)-specific 3'- exoribonuclease. J. Biol. Chem. *272*, 10448–10456.

Korom, M., Wylie, K.M., and Morrison, L.A. (2008). Selective ablation of virion host shutoff protein RNase activity attenuates herpes simplex virus 2 in mice. J. Virol. *82*, 3642–3653.

Kowalinski, E., Kögel, A., Ebert, J., Reichelt, P., Stegmann, E., Habermann, B., and Conti, E. (2016). Structure of a Cytoplasmic 11-Subunit RNA Exosome Complex. Mol. Cell. *63*, 125–134.

Krishna, N.K., and Schneemann, A. (1999). Formation of an RNA heterodimer upon heating of nodavirus particles. J. Virol. *73*, 1699–1703.

Krug, R.M., Broni, B. a, LaFiandra, a J., Morgan, M. a, and Shatkin, a J. (1980). Priming and inhibitory activities of RNAs for the influenza viral transcriptase do not require base pairing with the virion template RNA. Proc. Natl. Acad. Sci. U. S. A. *77*, 5874–5878.

Kshirsagar, M., and Parker, R. (2004). Identification of Edc3p as an Enhancer of mRNA Decapping in Saccharomyces cerevisiae. Genetics. *166*, 729–739.

Kurilla, M.G., Cabradilla, C.D., Holloway, B.P., and Keene, J.D. (1984). Nucleotide sequence and host La protein interactions of rabies virus leader RNA. J. Virol. *50*, 773–778.

Kuzuoğlu-Öztürk, D., Bhandari, D., Huntzinger, E., Fauser, M., Helms, S., and Izaurralde, E. (2016). miRISC and the CCR4–NOT complex silence mRNA targets independently of 43S ribosomal scanning. EMBO J. *35*, 1186–1203.

Kwong, A.D., and Frenkel, N. (1987). Herpes simplex virus-infected cells contain a function(s) that destabilizes both host and viral mRNAs. Proc. Natl. Acad. Sci. U. S. A. *84*, 1926–1930.

Kwong, A.D., and Frenkel, N. (1989). The herpes simplex virus virion host shutoff function. J. Virol. *63*, 4834–4839.

Van Der Laan, A.M.A., Van Gemert, A.M.C., Dirks, R.W., Noordermeer, J.N., Fradkin, L.G., Tanke, H.J., and Jost, C.R. (2012). mRNA cycles through hypoxia-induced stress granules in live Drosophila embryonic muscles. Int. J. Dev. Biol. *56*, 701–709.

łabno, A., Warkocki, Z., Kulínski, T., Krawczyk, P.S., Bijata, K., Tomecki, R., and Dziembowski, A. (2016). Perlman syndrome nuclease DIS3L2 controls cytoplasmic non-coding RNAs and provides surveillance pathway for maturing snRNAs. Nucleic Acids Res. *44*, 10437–10453.

Lane, L.C. (1974). The bromoviruses. Adv. Virus Res. *19*, 151–220.

Lara, E., Billecocq, A., Leger, P., and Bouloy, M. (2011). Characterization of Wild-Type and Alternate Transcription Termination Signals in the Rift Valley Fever Virus Genome. J. Virol. *85*, 12134–12145.

Lardelli, R.M., Schaffer, A.E., Eggens, V.R.C., Zaki, M.S., Grainger, S., Sathe, S., Van Nostrand, E.L., Schlachetzki, Z., Rosti, B., Akizu, N., et al. (2017). Biallelic mutations in the 3' exonuclease TOE1 cause pontocerebellar hypoplasia and uncover a role in snRNA processing. Nat. Genet. *49*, 457–464.

Larimer, F.W., and Stevens, A. (1990). Disruption of the gene XRN1, coding for a 5′→3′ exoribonuclease, restricts yeast cell growth. Gene. *95*, 85–90.

Lauber, E., Guilley, H., Tamada, T., Richards, K.E., and Jonard, G. (1998). Vascular movement of beet necrotic yellow vein virus in Beta macrocarpa is probably dependent on an RNA 3 sequence domain rather than a gene product. J. Gen. Virol. *79*, 385–393.

Leach, N., and Johnson, N. (1939). Human Rabies, with special reference to virus distribution and titer. Am J Trop Med Hyg. *s1-20*, 335–340.

Lee, C.C., Lin, T.L., Lin, J.W., Han, Y.T., Huang, Y.T., Hsu, Y.H., and Meng, M. (2016). Promotion of bamboo mosaic virus accumulation in Nicotiana benthamiana by 5'→3' exonuclease NbXRN4. Front. Microbiol. *6*, 1508.

Lee, C.Y., Lee, A., and Chanfreau, G. (2003a). The roles of endonucleolytic cleavage and exonucleolytic digestion in the 5'-end processing of S. cerevisiae box C/D snoRNAs. RNA. *9*, 1362–1370.

Lee, H., Patschull, A.O.M., Bagnéris, C., Ryan, H., Sanderson, C.M., Ebrahimi, B., Nobeli, I., and Barrett, T.E. (2017a). KSHV SOX mediated host shutoff: The molecular mechanism underlying mRNA transcript processing. Nucleic Acids Res. *45*, 4756–4767.

Lee, H.J., Shieh, C.K., Gorbalenya, A.E., Koonin, E. V, La Monica, N., Tuler, J., Bagdzhadzhyan, A., and Lai, M.M.C. (1991). The complete sequence (22 kilobases) of murine coronavirus gene 1 encoding the putative proteases and RNA polymerase. Virology. *180*, 567–582.

Lee, J., Yu, H., Li, Y., Ma, J., Lang, Y., Duff, M., Henningson, J., Liu, Q., Li, Y., Nagy, A., et al. (2017b). Impacts of different expressions of PA-X protein on 2009 pandemic H1N1 virus replication, pathogenicity and host immune responses. Virology. *504*, 25–35.

Lee, K.J., Novella, I.S., Teng, M.N., Oldstone, M.B., and de La Torre, J.C. (2000). NP and L proteins of lymphocytic choriomeningitis virus (LCMV) are sufficient for efficient transcription and replication of LCMV genomic RNA analogs. J. Virol. *74*, 3470–3477.

Lee, L., Telford, E.B., Batten, J.S., Scholthof, K.B.G., and Rush, C.M. (2001). Complete nucleotide sequence and genome organization of Beet soilborne mosaic virus, a proposed member of the genus Benyvirus. Arch. Virol. *146*, 2443–2453.

Lee, N., Hui, D., Wu, A., Chan, P., Cameron, P., Joynt, G.M., Ahuja, A., Yung, M.Y., Leung, C.B., To, K.F., et al. (2003b). A Major Outbreak of Severe Acute Respiratory Syndrome in Hong Kong. N. Engl. J. Med. *348*, 1986–1994.

Lee, N., Pimienta, G., and Steitz, J.A. (2012). AUF1/hnRNP D is a novel protein partner of the EBER1 noncoding RNA of Epstein-Barr virus. RNA. *18*, 2073–2082.

Lefkowitz, E.J., Dempsey, D.M., Hendrickson, R.C., Orton, R.J., Siddell, S.G., and Smith, D.B. (2018). Virus taxonomy: The database of the International Committee on Taxonomy of Viruses (ICTV). Nucleic Acids Res. *46*, D708–D717.

Lehmann, M., Pahlmann, M., Jerome, H., Busch, C., Lelke, M., and Gunther, S. (2014). Role of the C Terminus of Lassa Virus L Protein in Viral mRNA Synthesis. J. Virol. *88*, 8713–8717.

Lelke, M., Brunotte, L., Busch, C., and Gunther, S. (2010). An N-Terminal Region of Lassa Virus L Protein Plays a Critical Role in Transcription but Not Replication of the Virus Genome. J. Virol. *84*, 1934–1944.

Lerner, M.R., Andrews, N.C., Miller, G., and Steitz, J.A. (1981). Two small RNAs encoded by Epstein-Barr virus and complexed with protein are precipitated by antibodies from patients with systemic lupus erythematosus. Proc. Natl. Acad. Sci. U. S. A. *78*, 805–809.

Leslie, M.J., Messenger, S., Rohde, R.E., Smith, J., Cheshier, R., Hanlon, C., and Rupprecht, C.E. (2006). Bat-associated rabies virus in skunks. Emerg. Infect. Dis. *12*, 1274–1277.

Li, C.H., Irmer, H., Gudjonsdottir-Planck, D., Freese, S., Salm, H., Haile, S., Estévez, A.M., and Clayton, C. (2006). Roles of a Trypanosoma brucei $5' \rightarrow 3'$ exoribonuclease homolog in mRNA degradation. RNA. *12*, 2171–2186.

Li, R., Yue, J., Zhang, Y., Zhou, L., Hao, W., Yuan, J., Qiang, B., Ding, J.M., Peng, X., and Cao, J.M. (2008). CLOCK/BMAL1 regulates human nocturnin transcription through binding to the E-box of nocturnin promoter. Mol. Cell. Biochem. *317*, 169–177.

Li, Y., Chen, Z.Y., Wang, W., Baker, C.C., and Krug, R.M. (2001). The mechanism and regulation of deadenylation: Identification and characterization of Xenopus PARN. RNA. *7*, 875–886.

Li, Y., Song, M., and Kiledjian, M. (2011). Differential utilization of decapping enzymes in mammalian mRNA decay pathways. RNA. *17*, 419–428.

Lin, W.J., Duffy, A., and Chen, C.Y. (2007). Localization of AU-rich element-containing mRNA in cytoplasmic granules containing exosome subunits. J. Biol. Chem. *282*, 19958–19968.

Liu, H., Rodgers, N.D., Jiao, X., and Kiledjian, M. (2002). The scavenger mRNA decapping enzyme DcpS is a member of the HIT family of pyrophosphatases. EMBO J. *21*, 4699–4708.

Liu, Q., Greimann, J.C., and Lima, C.D. (2006). Reconstitution, Activities, and Structure of the Eukaryotic RNA Exosome. Cell. *127*, 1223–1237.

Liu, S.W., Rajagopal, V., Patel, S.S., and Kiledjian, M. (2008). Mechanistic and kinetic analysis of the dcps scavenger decapping enzyme. J. Biol. Chem. *283*, 16427–16436.

Loh, B., Jonas, S., and Izaurralde, E. (2013). The SMG5-SMG7 heterodimer directly recruits the CCR4-NOT deadenylase complex to mRNAs containing nonsense codons via interaction with POP2. Genes Dev. *27*, 2125–2138.

Lokdarshi, A., Conner, W.C., McClintock, C., Li, T., and Roberts, D.M. (2016). Arabidopsis CML38, a Calcium Sensor That Localizes to Ribonucleoprotein Complexes under Hypoxia Stress. Plant Physiol. *170*, 1046–1059.

López, N., and Franze-Fernández, M.T. (2007). A single stem-loop structure in Tacaribe arenavirus intergenic region is essential for transcription termination but is not required for a correct initiation of transcription and replication. Virus Res. *124*, 237–244.

Lu, S., and Cullen, B.R. (2004). Adenovirus VA1 Noncoding RNA Can Inhibit Small Interfering RNA and MicroRNA Biogenesis. J. Virol. *78*, 12868–12876.

Lu, P., Jones, F.E., Saffran, H.A., and Smiley, J.R. (2001). Herpes simplex virus virion host shutoff protein requires a mammalian factor for efficient in vitro endoribonuclease activity. J. Virol. *75*, 1172–1185.

Lubas, M., Damgaard, C.K., Tomecki, R., Cysewski, D., Jensen, T.H., and Dziembowski, A. (2013). Exonuclease hDIS3L2 specifies an exosome-independent 3′-5′ degradation pathway of human cytoplasmic mRNA. EMBO J. *32*, 1855–1868.

Lukashevich, I.S., Djavani, M., Shapiro, K., Sanchez, A., Ravkov, E., Nichol, S.T., and Salvato, M.S. (1997). The Lassa fever virus L gene: Nucleotide sequence, comparison, and precipitation of a predicted 250 kDa protein with monospecific antiserum. J. Gen. Virol. *78*, 547–551.

Luo, J., Lu, G., Ye, S., Ou, J., Fu, C., Zhang, X., Wang, X., Huang, J., Wu, P., Xu, H., et al. (2018). Comparative pathogenesis of H3N2 canine influenza virus in beagle dogs challenged by intranasal and intratracheal inoculation. Virus Res.

Lykke-Andersen, J. (2002). Identification of a Human Decapping Complex Associated with hUpf Proteins in Nonsense-Mediated Decay. Mol. Cell. Biol. *22*, 8114–8121.

Lykke-Andersen, J., and Wagner, E. (2005). Recruitment and activation of mRNA decay enzymes by two ARE-mediated decay activation domains in the proteins TTP and BRF-1. Genes Dev. *19*, 351–361.

MacFadden, A., O'Donoghue, Z., Silva, P.A.G.C., Chapman, E.G., Olsthoorn, R.C., Sterken, M.G., Pijlman, G.P., Bredenbeek, P.J., and Kieft, J.S. (2018). Mechanism and structural diversity of exoribonuclease-resistant RNA structures in flaviviral RNAs. Nat. Commun. *9*, 119.

Malecki, M., Viegas, S.C., Carneiro, T., Golik, P., Dressaire, C., Ferreira, M.G., and Arraiano, C.M. (2013). The exoribonuclease Dis3L2 defines a novel eukaryotic RNA degradation pathway. EMBO J. *32*, 1842–1854.

Manokaran, G., Finol, E., Wang, C., Gunaratne, J., Bahl, J., Ong, E.Z., Tan, H.C., Sessions, O.M., Ward, A.M., Gubler, D.J., et al. (2015). Dengue subgenomic RNA binds TRIM25 to inhibit interferon expression for epidemiological fitness. Science. *350*, 217–221.

Mariën, J., Borremans, B., Gryseels, S., Soropogui, B., De Bruyn, L., Bongo, G.N., Becker-Ziaja, B., De Bellocq, J.G., Günther, S., Magassouba, N., et al. (2017). No measurable adverse effects of Lassa, Morogoro and Gairo arenaviruses on their rodent reservoir host in natural conditions. Parasites and Vectors. *10*, 210.

Mariën, J., Kourouma, F., Magassouba, N., Leirs, H., and Fichet-Calvet, E. (2018). Movement Patterns of Small Rodents in Lassa Fever-Endemic Villages in Guinea. Ecohealth. *15*, 1–12.

Marklewitz, M., Zirkel, F., Rwego, I.B., Heidemann, H., Trippner, P., Kurth, A., Kallies, R., Briese, T., Lipkin, W.I., Drosten, C., et al. (2013). Discovery of a Unique Novel Clade of Mosquito-Associated Bunyaviruses. J. Virol. *87*, 12850–12865.

van Marle, G., Dobbe, J.C., Gultyaev, A.P., Luytjes, W., Spaan, W.J., and Snijder, E.J. (1999). Arterivirus discontinuous mRNA transcription is guided by base pairing between sense and antisense transcription-regulating sequences. Proc. Natl. Acad. Sci. U. S. A. *96*, 12056–12061.

Marriott, A.C., Ward, V.K., and Nuttall, P.A. (1989). The S RNA segment of Sandfly fever Sicilian virus: Evidence for an ambisense genome. Virology. *169*, 341–345.

Mas-Moruno, C., Rechenmacher, F., and Kessler, H. (2010). Cilengitide: The First Anti-Angiogenic Small Molecule Drug Candidate. Design, Synthesis and Clinical Evaluation. Anticancer. Agents Med. Chem. *10*, 753–768.

Mas, A., Alves-Rodrigues, I., Noueiry, A., Ahlquist, P., and Díez, J. (2006). Host deadenylation-dependent mRNA decapping factors are required for a key step in brome mosaic virus RNA replication. J. Virol. *80*, 246–251.

Mathews, M.B. (1990). Control of translation in adenovirus-infected cells. Enzyme. *44*, 250–264.

Mazroui, R., Sukarieh, R., Bordeleau, M.-E., Kaufman, R.J., Northcote, P., Tanaka, J., Gallouzi, I., and Pelletier, J. (2006). Inhibition of ribosome recruitment induces stress granule formation independently of eukaryotic initiation factor 2alpha phosphorylation. Mol. Biol. Cell. *17*, 4212–4219.

Mccauley, J.W., and Mahy, B.W.J. (1983). Structure and function of the influenza virus genome. Biochem. J. *211*, 281–294.

McFleder, R.L., Mansur, F., and Richter, J.D. (2017). Dynamic Control of Dendritic mRNA Expression by CNOT7 Regulates Synaptic Efficacy and Higher Cognitive Function. Cell Rep. *20*, 683–696.

McInerney, G.M., Kedersha, N.L., Kaufman, R.J., Anderson, P., and Liljeström, P. (2005). Importance of eIF2alpha phosphorylation and stress granule assembly in alphavirus translation regulation. Mol. Biol. Cell. *16*, 3753–3763.

McQuiston, J.H., Yager, P.A., Smith, J.S., and Rupprecht, C.E. (2001). Epidemiologic characteristics of rabies virus variants in dogs and cats in the United States, 1999. J. Am. Vet. Med. Assoc. *218*, 1939–1942.

Menchaca-Armenta, I., Ocampo-Torres, M., Hernández-Gómez, A., and Zamora-Cerritos, K. (2018). Risk perception and level of knowledge of diseases transmitted by aedes aegypti. Rev. Inst. Med. Trop. Sao Paulo *60*, e10.

Mercer, T.R., Wilhelm, D., Dinger, M.E., Soldà, G., Korbie, D.J., Glazov, E.A., Truong, V., Schwenke, M., Simons, C., Matthaei, K.I., et al. (2011). Expression of distinct RNAs from 3′ untranslated regions. Nucleic Acids Res. *39*, 2393–2403.

Merret, R., Descombin, J., Juan, Y. ting, Favory, J.J., Carpentier, M.C., Chaparro, C., Charng, Y. yung, Deragon, J.M., and Bousquet-Antonelli, C. (2013). XRN4 and LARP1 are required for a heat-triggered mRNA decay pathway involved in plant acclimation and survival during thermal stress. Cell Rep. *5*, 1279–1293.

Miller, D., Brandt, N., and Gresham, D. (2018). Systematic identification of factors mediating accelerated mRNA degradation in response to changes in environmental nitrogen. PLoS Genet. *14*, 1–27.

Miller, W.A., Dreher, T.W., and Hall, T.C. (1985). Synthesis of brome mosaic virus subgenomic RNA in vitro by internal initiation on (-)-sense genomic RNA. Nature. *313*, 68–70.

Mishima, Y., Fukao, A., Kishimoto, T., Sakamoto, H., Fujiwara, T., and Inoue, K. (2012). Translational inhibition by deadenylation-independent mechanisms is central to microRNA-mediated silencing in zebrafish. Proc. Natl. Acad. Sci. *109*, 1104–1109.

Mitchell, P., Petfalski, E., Shevchenko, A., Mann, M., and Tollervey, D. (1997). The exosome: A conserved eukaryotic RNA processing complex containing multiple 3'→5' exoribonucleases. Cell. *91*, 457–466.

Mittal, S., Aslam, A., Doidge, R., Medica, R., and Winkler, G.S. (2011). The Ccr4a (CNOT6) and Ccr4b (CNOT6L) deadenylase subunits of the human Ccr4-Not complex contribute to the prevention of cell death and senescence. Mol. Biol. Cell *22*, 748–758.

Mizumoto, H., Tatsuta, M., Kaido, M., Mise, K., and Okuno, T. (2003). Cap-independent translational enhancement by the 3' untranslated region of red clover necrotic mosaic virus RNA1. J. Virol. *77*, 12113–12121.

Mochi, S., Gro, M.C., Di Bonito, P., Fortini, D., and Giorgi, C. (1997). Organization of the M genomic segment of Toscana phlebovirus. J. Gen. Virol. *78*, 77–81.

Mocquet, V., Neusiedler, J., Rende, F., Cluet, D., Robin, J.-P., Terme, J.-M., Duc Dodon, M., Wittmann, J., Morris, C., Le Hir, H., et al. (2012). The Human T-Lymphotropic Virus Type 1 Tax Protein Inhibits Nonsense-Mediated mRNA Decay by Interacting with INT6/EIF3E and UPF1. J. Virol. *86*, 7530–7543.

Mokas, S., Mills, J.R., Garreau, C., Fournier, M.-J., Robert, F., Arya, P., Kaufman, R.J., Pelletier, J., and Mazroui, R. (2009). Uncoupling Stress Granule Assembly and Translation Initiation Inhibition. Mol. Biol. Cell. *20*, 2673–2683.

Moncayo, A.C., Hice, C.L., Watts, D.M., Travassos De Rosa, A.P.A., Guzman, H., Russell, K.L., Calampa, C., Gozalo, A., Popov, V.L., Weaver, S.C., et al. (2001). Allpahuayo virus: A newly recognized arenavirus (Arenaviridae) from arboreal rice rats (Oecomys Bicolor and Oecomys Paricola) in Northeastern Peru. Virology. *284*, 277–286.

Montellese, C., Montel-Lehry, N., Henras, A.K., Kutay, U., Gleizes, P.E., and O'Donohue, M.F. (2017). Poly(A)-specific ribonuclease is a nuclear ribosome biogenesis factor involved in human 18S rRNA maturation. Nucleic Acids Res. *45*, 6822–6836.

Moon, D.H., Segal, M., Boyraz, B., Guinan, E., Hofmann, I., Cahan, P., Tai, A.K., and Agarwal, S. (2015a). Poly(A)-specific ribonuclease (PARN) mediates 3′-end maturation of the telomerase RNA component. Nat. Genet. *47*, 1482–1488.

Moon, S.L., Anderson, J.R., Kumagai, Y., Wilusz, C.J., Akira, S., Khromykh, A.A., and Wilusz, J. (2012). A noncoding RNA produced by arthropod-borne flaviviruses inhibits the cellular exoribonuclease XRN1 and alters host mRNA stability. RNA. *18*, 2029–2040.

Moon, S.L., Blackinton, J.G., Anderson, J.R., Dozier, M.K., Dodd, B.J.T., Keene, J.D., Wilusz, C.J., Bradrick, S.S., and Wilusz, J. (2015b). XRN1 stalling in the 5' UTR of Hepatitis C virus and Bovine Viral Diarrhea virus is associated with dysregulated host mRNA stability. PLoS Pathog. *11*, e1004708.

Moon, S.L., Dodd, B.J.T., Brackney, D.E., Wilusz, C.J., Ebel, G.D., and Wilusz, J. (2015c). Flavivirus sfRNA suppresses antiviral RNA interference in cultured cells and mosquitoes and directly interacts with the RNAi machinery. Virology. *485*, 322–329.

Mori, F., Tanji, K., Miki, Y., Toyoshima, Y., Sasaki, H., Yoshida, M., Kakita, A., Takahashi, H., and Wakabayashi, K. (2018). Immunohistochemical localization of exoribonucleases (DIS3L2 and XRN1) in intranuclear inclusion body disease. Neurosci. Lett. *662*, 389–394.

Morimoto, K., Patel, M., Corisdeo, S., Hooper, D.C., Fu, Z.F., Rupprecht, C.E., Koprowski, H., and Dietzschold, B. (1996). Characterization of a unique variant of bat rabies virus responsible for newly emerging human cases in North America. Proc. Natl. Acad. Sci. *93*, 5653–5658.

Morin, B., Coutard, B., Lelke, M., Ferron, F., Kerber, R., Jamal, S., Frangeul, A., Baronti, C., Charrel, R., de Lamballerie, X., et al. (2010). The N-terminal domain of the arenavirus L protein is an RNA endonuclease essential in mRNA transcription. PLoS Pathog. *6*, e1001038.

Mugridge, J.S., Tibble, R.W., Ziemniak, M., Jemielity, J., and Gross, J.D. (2018). Structure of the activated Edc1-Dcp1-Dcp2-Edc3 mRNA decapping complex with substrate analog poised for catalysis. Nat. Commun. *9*, 1152.

Muhlrad, D., and Parker, R. (1992). Mutations affecting stability and deadenylation of the yeast MFA2 transcript. Genes Dev. *6*, 2100–2111.

Muhlrad, D., and Parker, R. (2005). The yeast EDC1 mRNA undergoes deadenylation-independent decapping stimulated by Not2p, Not4p, and Not5p. EMBO J. *24*, 1033–1045.

Muhlrad, D., Decker, C.J., and Parker, R. (1994). Deadenylation of the unstable mRNA encoded by the yeast MFA2 gene leads to decapping followed by 5' → 3' digestion of the transcript. Genes Dev. *8*, 855–866.

Muller, M., and Glaunsinger, B.A. (2017). Nuclease escape elements protect messenger RNA against cleavage by multiple viral endonucleases. PLoS Pathog. *13*, e1006593.

Muller, M., Hutin, S., Marigold, O., Li, K.H., Burlingame, A., and Glaunsinger, B.A. (2015). A Ribonucleoprotein Complex Protects the Interleukin-6 mRNA from Degradation by Distinct Herpesviral Endonucleases. PLoS Pathog. *11*, e1004899.

Muller, R., Argentini, C., Bouloy, M., Prehaud, C., and Bishop, D.H.L. (1992). Completion of the genome sequence of rift valley fever phlebovirus indicates that the L RNA is negative sense or ambisense and codes for a putative transcriptase-replicase. Nucleic Acids Res. *20*, 6440.

Muller, R., Poch, O., Delarue, M., Bishop, D.H.L., and Bouloy, M. (1994). Rift Valley fever virus L-segment - correction of the sequence and possible functional-role of newly identified regions conserved in RNA-dependent polymerases. J. Gen. Virol. *75*, 1345–1352.

Müller, M., Padmanabhan, P.K., Rochette, A., Mukherjee, D., Smith, M., Dumas, C., and Papadopoulou, B. (2010). Rapid decay of unstable Leishmania mRNAs bearing a conserved retroposon signature 3'-UTR motif is initiated by a site-specific endonucleolytic cleavage without prior deadenylation. Nucleic Acids Res. *38*, 5867–5883.

Muramoto, Y., Noda, T., Kawakami, E., Akkina, R., and Kawaoka, Y. (2013). Identification of novel influenza A virus proteins translated from PA mRNA. J. Virol. *87*, 2455–2462.

Murray, K.E., Roberts, A.W., and Barton, D.J. (2001). Poly (rC) binding proteins mediate poliovirus mRNA stability. RNA. *7*, 1126–1141.

Mutua, E.N., Bukachi, S.A., Bett, B.K., Estambale, B.A., and Nyamongo, I.K. (2017). "We do not bury dead livestock like human beings": Community behaviors and risk of Rift Valley Fever virus infection in Baringo County, Kenya. PLoS Negl. Trop. Dis. *11*, e0005582.

Nagy, E., and Maquat, L.E. (1998). A rule for termination-codon position within intron-containing genes: When nonsense affects RNA abundance. Trends Biochem. Sci. *23*, 198–199.

Nakano, K., Ando, T., Yamagishi, M., Yokoyama, K., Ishida, T., Ohsugi, T., Tanaka, Y., Brighty, D.W., and Watanabe, T. (2013). Viral interference with host mRNA surveillance, the nonsense-mediated mRNA decay (NMD) pathway, through a new function of HTLV-1 Rex: Implications for retroviral replication. Microbes Infect. *15*, 491–505.

Nakouné, E., Kamgang, B., Berthet, N., Manirakiza, A., and Kazanji, M. (2016). Rift Valley Fever Virus Circulating among Ruminants, Mosquitoes and Humans in the Central African Republic. PLoS Negl. Trop. Dis. *10*, e0005082.

Narayanan, K., Huang, C., Lokugamage, K., Kamitani, W., Ikegami, T., Tseng, C.-T.K., and Makino, S. (2008). Severe Acute Respiratory Syndrome Coronavirus nsp1 Suppresses Host Gene Expression, Including That of Type I Interferon, in Infected Cells. J. Virol. *82*, 4471–4479.

Nderitu, L., Lee, J.S., Omolo, J., Omulo, S., O'Guinn, M.L., Hightower, A., Mosha, F., Mohamed, M., Munyua, P., Nganga, Z., et al. (2011). Sequential rift valley fever outbreaks in Eastern Africa caused by multiple lineages of the virus. J. Infect. Dis. *203*, 655–665.

Neira, V., Allerson, M., Corzo, C., Culhane, M., Rendahl, A., and Torremorell, M. (2018). Detection of influenza A virus in aerosols of vaccinated and non-vaccinated pigs in a warm environment. PLoS One *13*, e0197600.

Newton, C.A., Batra, K., Torrealba, J., Kozlitina, J., Glazer, C.S., Aravena, C., Meyer, K., Raghu, G., Collard, H.R., and Garcia, C.K. (2016). Telomere-related lung fibrosis is diagnostically heterogeneous but uniformly progressive. Eur. Respir. J. *48*, 1710–1720.

Ng, C.S., Jogi, M., Yoo, J.-S., Onomoto, K., Koike, S., Iwasaki, T., Yoneyama, M., Kato, H., and Fujita, T. (2013). Encephalomyocarditis Virus Disrupts Stress Granules, the Critical Platform for Triggering Antiviral Innate Immune Responses. J. Virol. *87*, 9511–9522.

Niedzwiecka, A., Nilsson, P., Worch, R., Stepinski, J., Darzynkiewicz, E., and Virtanen, A. (2016). Molecular recognition of mRNA 5′ cap by 3′ poly(A)-specific ribonuclease (PARN) differs from interactions known for other cap-binding proteins. Biochim. Biophys. Acta - Proteins Proteomics. *1864*, 331–345.

Nilsson, P., Henriksson, N., Niedzwiecka, A., Balatsos, N.A.A., Kokkoris, K., Eriksson, J., and Virtanen, A. (2007). A multifunctional RNA recognition motif in poly(A)-specific ribonuclease with cap and poly(A) binding properties. J. Biol. Chem. *282*, 32902–32911.

Nomoto, A., Kitamura, N., Golini, F., and Wimmer, E. (1977). The 5'-terminal structures of poliovirion RNA and poliovirus mRNA differ only in the genome-linked protein VPg. Proc. Natl. Acad. Sci. U. S. A. *74*, 5345–5349.

Noueiry, A.O., Diez, J., Falk, S.P., Chen, J., and Ahlquist, P. (2003). Yeast Lsm1p-7p/Pat1p deadenylation-dependent mRNA-decapping factors are required for brome mosaic virus genomic RNA translation. Mol Cell Biol. *23*, 4094–4106.

Nover, L., Scharf, K.D., and Neumann, D. (1989). Cytoplasmic heat shock granules are formed from precursor particles and are associated with a specific set of mRNAs. Mol. Cell. Biol. *9*, 1298–1308.

Oeffinger, M., Zenklusen, D., Ferguson, A., Wei, K.E., El Hage, A., Tollervey, D., Chait, B.T., Singer, R.H., and Rout, M.P. (2009). Rrp17p Is a Eukaryotic Exonuclease Required for 5′ End Processing of Pre-60S Ribosomal RNA. Mol. Cell. *36*, 768–781.

Oem, J.K., Kim, S.H., Kim, Y.H., Lee, M.H., and Lee, K.K. (2013). Complete genome sequences of three rabies viruses isolated from rabid raccoon dogs and a cow in Korea. Virus Genes. *47*, 563–568.

Ohnishi, T., Yamashita, A., Kashima, I., Schell, T., Anders, K.R., Grimson, A., Hachiya, T., Hentze, M.W., Anderson, P., and Ohno, S. (2003). Phosphorylation of hUPF1 induces formation of mRNA surveillance complexes containing hSMG-5 and hSMG-7. Mol. Cell. *12,* 1187–1200.

Okada-Katsuhata, Y., Yamashita, A., Kutsuzawa, K., Izumi, N., Hirahara, F., and Ohno, S. (2012). N-and C-terminal Upf1 phosphorylations create binding platforms for SMG-6 and SMG-5:SMG-7 during NMD. Nucleic Acids Res. *40*, 1251–1266.

Okuno, T., Hiruki, C., Rao, D. V, and Figueiredo, G.C. (1983). Genetic Determinants Distributed in Two Genomic RNAs of Sweet Clover Necrotic Mosaic, Red Clover Necrotic Mosaic and Clover Primary Leaf Necrosis Viruses. J. Gen. Virol. *64*, 1907–1914.

Olmedo, G., Guo, H., Gregory, B.D., Nourizadeh, S.D., Aguilar-Henonin, L., Li, H., An, F., Guzman, P., and Ecker, J.R. (2006). ETHYLENE-INSENSITIVE5 encodes a 5'-->3' exoribonuclease required for regulation of the EIN3-targeting F-box proteins EBF1/2. Proc. Natl. Acad. Sci. U. S. A. *103*, 13286–13293.

Opyrchal, M., Anderson, J.R., Sokoloski, K.J., Wilusz, C.J., and Wilusz, J. (2005). A cell-free mRNA stability assay reveals conservation of the enzymes and mechanisms of mRNA decay between mosquito and mammalian cell lines. Insect Biochem. Mol. Biol. *35*, 1321–1334.

Orban, T.I., and Izaurralde, E. (2005). Decay of mRNAs targeted by RISC requires XRN1, the Ski complex, and the exosome. RNA. *11*, 459–469.

Oroskar, A.A., and Read, G.S. (1989). Control of mRNA stability by the virion host shutoff function of herpes simplex virus. J. Virol. *63*, 1897–1906.

Oumard, A., Hennecke, M., Hauser, H., and Nourbakhsh, M. (2000). Translation of NRF mRNA Is Mediated by Highly Efficient Internal Ribosome Entry. Mol. Cell. Biol. *20*, 2755–2759.

Ozgur, S., Basquin, J., Kamenska, A., Filipowicz, W., Standart, N., and Conti, E. (2015). Structure of a Human 4E-T/DDX6/CNOT1 Complex Reveals the Different Interplay of DDX6-Binding Proteins with the CCR4-NOT Complex. Cell Rep. *13*, 703–711.

Pager, C.T., Schütz, S., Abraham, T.M., Luo, G., and Sarnow, P. (2013). Modulation of hepatitis C virus RNA abundance and virus release by dispersion of processing bodies and enrichment of stress granules. Virology. *435*, 472–484.

Palusa, S., Ndaluka, C., Bowen, R.A., Wilusz, C.J., and Wilusz, J. (2012). The 3′ untranslated region of the rabies virus glycoprotein mRNA specifically interacts with cellular PCBP2 protein and promotes transcript stability. PLoS One. *7*, e33561.

Park, J., Kang, M., and Kim, M. (2015). Unraveling the mechanistic features of RNA polymerase II termination by the 5'-3' exoribonuclease Rat1. Nucleic Acids Res. *43*, 2625–2637.

Parsley, T.B., Towner, J.S., Blyn, L.B., Ehrenfeld, E., and Semler, B.L. (1997). Poly (rC) binding protein 2 forms a ternary complex with the 5'-terminal sequences of poliovirus RNA and the viral 3CD proteinase. RNA. *3*, 1124–1134.

Pasternak, A.O., van den Born, E., Spaan, W.J., and Snijder, E.J. (2001). Sequence requirements for RNA strand transfer during nidovirus discontinuous subgenomic RNA synthesis. EMBO J. *20*, 7220–7228.

Pauli, E.K., Chan, Y.K., Davis, M.E., Gableske, S., Wang, M.K., Feister, K.F., and Gack, M.U. (2014). The ubiquitin-specific protease USP15 promotes RIG-I-mediated antiviral signaling by deubiquitylating TRIM25. Sci. Signal. *7*, ra3.

Pautus, S., Sehr, P., Lewis, J., Fortuné, A., Wolkerstorfer, A., Szolar, O., Guilligay, D., Lunardi, T., Décout, J.L., and Cusack, S. (2013). New 7-methylguanine derivatives targeting the influenza polymerase PB2 cap-binding domain. J. Med. Chem. *56*, 8915–8930.

Peabody, D.S. (1993). The RNA binding site of bacteriophage MS2 coat protein. EMBO J. *12*, 595–600.

Peccarelli, M., Scott, T.D., Wong, H., Wang, X., and Kebaara, B.W. (2014). Regulation of CTR2 mRNA by the nonsense-mediated mRNA decay pathway. Biochim. Biophys. Acta - Gene Regul. Mech. *1839*, 1283–1294.

Peltier, C., Klein, E., Hleibieh, K., D'Alonzo, M., Hammann, P., Bouzoubaa, S., Ratti, C., and Gilmer, D. (2012). Beet necrotic yellow vein virus subgenomic RNA3 is a cleavage product leading to stable non-coding RNA required for long-distance movement. J. Gen. Virol. *93*, 1093–1102.

Peng, J., Yang, J., Yan, F., Lu, Y., Jiang, S., Lin, L., Zheng, H., Chen, H., and Chen, J. (2011). Silencing of NbXrn4 facilitates the systemic infection of Tobacco mosaic virus in Nicotiana benthamiana. Virus Res. *158*, 268–270.

Peng, Y.H., Lin, C.H., Lin, C.N., Lo, C.Y., Tsai, T.L., and Wu, H.Y. (2016). Characterization of the role of hexamer AGUAAA and poly(A) tail in coronavirus polyadenylation. PLoS One *11*, e0165077.

Perchellet, E.M., Magill, M.J., Huang, X., Brantis, C.E., Hua, D.H., and Perchellet, J.P. (1999). Triptycenes: a novel synthetic class of bifunctional anticancer drugs that inhibit nucleoside transport, induce DNA cleavage and decrease the viability of leukemic cells in the nanomolar range in vitro. Anticancer. Drugs *10*, 749–766.

Perera, R., Daijogo, S., Walter, B.L., Nguyen, J.H.C., and Semler, B.L. (2007). Cellular Protein Modification by Poliovirus: the Two Faces of Poly(rC)-Binding Protein. J. Virol. *81*, 8919–8932.

Pérez-Vilaró, G., Scheller, N., Saludes, V., and Díez, J. (2012). Hepatitis C Virus Infection Alters P-Body Composition but Is Independent of P-Body Granules. J. Virol. *86*, 8740–8749.

Perrone, L.A., Narayanan, K., Worthy, M., and Peters, C.J. (2007). The S Segment of Punta Toro Virus (Bunyaviridae, Phlebovirus) Is a Major Determinant of Lethality in the Syrian Hamster and Codes for a Type I Interferon Antagonist. J. Virol. *81*, 884–892.

Petfalski, E., Dandekar, T., Henry, Y., and Tollervey, D. (1998). Processing of the precursors to small nucleolar RNAs and rRNAs requires common components. Mol. Cell. Biol. *18*, 1181–1189.

Pflug, A., Guilligay, D., Reich, S., and Cusack, S. (2014). Structure of influenza A polymerase bound to the viral RNA promoter. Nature. *516*, 355–360.

Picard-Jean, F., Brand, C., Tremblay-Létourneau, M., Allaire, A., Beaudoin, M.C., Boudreault, S., Duval, C., Rainville-Sirois, J., Robert, F., Pelletier, J., et al. (2018). 2'-O-methylation of the mRNA cap protects RNAs from decapping and degradation by DXO. PLoS One. *13*, e0193804.

Pijlman, G.P., Funk, A., Kondratieva, N., Leung, J., Torres, S., van der Aa, L., Liu, W.J., Palmenberg, A.C., Shi, P.Y., Hall, R.A., et al. (2008). A Highly Structured, Nuclease-Resistant, Noncoding RNA Produced by Flaviviruses Is Required for Pathogenicity. Cell Host Microbe. *4*, 579–591.

Pinschewer, D.D., Perez, M., and de la Torre, J.C. (2003). Role of the Virus Nucleoprotein in the Regulation of Lymphocytic Choriomeningitis Virus Transcription and RNA Replication. J. Virol. *77*, 3882–3887.

Pinschewer, D.D., Perez, M., and Carlos De La Torre, J. (2005). Dual Role of the Lymphocytic Choriomeningitis Virus Intergenic Region in Transcription Termination and Virus Propagation. J. Virol. *79*, 4519–4526.

Piotrowska, J., Hansen, S.J., Park, N., Jamka, K., Sarnow, P., and Gustin, K.E. (2010). Stable Formation of Compositionally Unique Stress Granules in Virus-Infected Cells. J. Virol. *84*, 3654–3665.

Pires, F.R., Franco, A.C.B.F., Gilio, A.E., and Troster, E.J. (2017). Comparison of enterovirus detection in cerebrospinal fluid with Bacterial Meningitis Score in children. Einstein (São Paulo) *15*, 167–172.

Pirouz, M., Du, P., Munafò, M., and Gregory, R.I. (2016). Dis3l2-Mediated Decay Is a Quality Control Pathway for Noncoding RNAs. Cell Rep. *16*, 1861–1873.

Piskounova, E., Polytarchou, C., Thornton, J.E., Lapierre, R.J., Pothoulakis, C., Hagan, J.P., Iliopoulos, D., and Gregory, R.I. (2011). Lin28A and Lin28B inhibit let-7 MicroRNA biogenesis by distinct mechanisms. Cell. *147*, 1066–1079.

Plotch, S.J., Bouloy, M., and Krug, R.M. (1979). Transfer of 5'-terminal cap of globin mRNA to influenza viral complementary RNA during transcription in vitro. Proc. Natl. Acad. Sci. *76*, 1618–1622.

Plotch, S.J., Bouloy, M., Ulmanen, I., and Krug, R.M. (1981). A unique cap(m7GpppXm)-dependent influenza virion endonuclease cleaves capped RNAs to generate the primers that initiate viral RNA transcription. Cell. *23*, 847–858.

Pompon, J., Manuel, M., Ng, G.K., Wong, B., Shan, C., Manokaran, G., Soto-Acosta, R., Bradrick, S.S., Ooi, E.E., Missé, D., et al. (2017). Dengue subgenomic flaviviral RNA disrupts immunity in mosquito salivary glands to increase virus transmission. PLoS Pathog. *13*, e1006535.

Poole, T.L., and Stevens, A. (1997). Structural modifications of RNA influence the 5' exoribonucleolytic hydrolysis by XRN1 and HKE1 of Saccharomyces cerevisiae. Biochem. Biophys. Res. Commun. *235*, 799–805.

Potuschak, T., Vansiri, A., Binder, B.M., Lechner, E., Vierstra, R.D., and Genschik, P. (2006). The Exoribonuclease XRN4 Is a Component of the Ethylene Response Pathway in Arabidopsis. The Plant Cell. *18*, 3047–3057.

Prévôt, D., Morel, A.P., Voeltzel, T., Rostan, M.C., Rimokh, R., Magaud, J.P., and Corbo, L. (2001). Relationships of the antiproliferative proteins BTG1 and BTG2 with CAF1, the human homolog of a component of the yeast CCR4 transcriptional complex: Involvement in estrogen receptor α signaling pathway. J. Biol. Chem. *276*, 9640–9648.

Price, B.D., Rueckert, R.R., and Ahlquist, P. (1996). Complete replication of an animal virus and maintenance of expression vectors derived from it in Saccharomyces cerevisiae. Proc. Natl. Acad. Sci. U. S. A. *93*, 9465–9470.

Puno, M.R., and Lima, C.D. (2018). Structural basis for MTR4–ZCCHC8 interactions that stimulate the MTR4 helicase in the nuclear exosome-targeting complex. Proc. Natl. Acad. Sci. *115*, E5506-E5515.

Putz, C. (1981). The Molecular Organization of Beet Necrotic. Virology. *438*, 428–438.

Qi, X., Lan, S., Wang, W., Schelde, L.M.L., Dong, H., Wallat, G.D., Ly, H., Liang, Y., and Dong, C. (2010). Cap binding and immune evasion revealed by Lassa nucleoprotein structure. Nature. *468*, 779–785.

Qiu, J., Cosmopoulos, K., Pegtel, M., Hopmans, E., Murray, P., Middeldorp, J., Shapiro, M., and Thorley-Lawson, D.A. (2011). A novel persistence associated EBV miRNA expression profile is disrupted in neoplasia. PLoS Pathog. *7*, e1002193.

Raaben, M., Groot Koerkamp, M.J.A., Rottier, P.J.M., and de Haan, C.A.M. (2007). Mouse hepatitis coronavirus replication induces host translational shutoff and mRNA decay, with concomitant formation of stress granules and processing bodies. Cell. Microbiol. *9*, 2218–2229.

Radhakrishnan, A., Chen, Y.H., Martin, S., Alhusaini, N., Green, R., and Coller, J. (2016). The DEAD-Box Protein Dhh1p Couples mRNA Decay and Translation by Monitoring Codon Optimality. Cell. *167*, 122–132.e9.

Raju, R., Raju, L., Hacker, D., Garcin, D., Compans, R., and Kolakofsky, D. (1990). Nontemplated bases at the 5′ ends of tacaribe virus mRNAs. Virology. *174*, 53–59.

Rao, P., Yuan, W., and Krug, R.M. (2003). Crucial role of CA cleavage sites in the cap-snatching mechanism for initiating viral mRNA synthesis. EMBO J. *22*, 1188–1198.

Rao, S., Amorim, R., Niu, M., Temzi, A., and Mouland, A.J. (2018). The RNA surveillance proteins UPF1, UPF2 and SMG6 affect HIV-1 reactivation at a post-transcriptional level. Retrovirology. *15*, 42.

Ratti, C., Hleibieh, K., Bianchi, L., Schirmer, A., Autonell, C.R., and Gilmer, D. (2009). Beet soil-borne mosaic virus RNA-3 is replicated and encapsidated in the presence of BNYVV RNA-1 and -2 and allows long distance movement in Beta macrocarpa. Virology. *385*, 392–399.

Reguera, J., Weber, F., and Cusack, S. (2010). Bunyaviridae RNA polymerases (L-protein) have an N-terminal, influenza-like endonuclease domain, essential for viral cap-dependent transcription. PLoS Pathog. *6*, e1001101.

Reguera, J., Gerlach, P., Rosenthal, M., Gaudon, S., Coscia, F., Günther, S., and Cusack, S. (2016). Comparative Structural and Functional Analysis of Bunyavirus and Arenavirus Cap-Snatching Endonucleases. PLoS Pathog. *12*, e1005636.

Reich, S., Guilligay, D., Pflug, A., Malet, H., Berger, I., Crepin, T., Hart, D., Lunardi, T., Nanao, M., Ruigrok, R.W.H., et al. (2014). Structural insight into cap-snatching and RNA synthesis by influenza polymerase. Nature. *516*, 361–366.

Reimão-Pinto, M.M., Manzenreither, R.A., Burkard, T.R., Sledz, P., Jinek, M., Mechtler, K., and Ameres, S.L. (2016). Molecular basis for cytoplasmic RNA surveillance by uridylation-triggered decay in Drosophila. EMBO J. *35*, 2417–2434.

Reineke, L.C., and Lloyd, R.E. (2015). The Stress Granule Protein G3BP1 Recruits Protein Kinase R To Promote Multiple Innate Immune Antiviral Responses. J. Virol. *89*, 2575–2589.

Reineke, L.C., Kedersha, N., Langereis, M.A., van Kuppeveld, F.J.M., and Lloyd, R.E. (2015). Stress granules regulate double-stranded RNA-dependent protein kinase activation through a complex containing G3BP1 and Caprin1. MBio. *6*, e02486.

Richner, J.M., Clyde, K., Pezda, A.C., Cheng, B.Y.H., Wang, T., Kumar, G.R., Covarrubias, S., Coscoy, L., and Glaunsinger, B. (2011). Global mrna degradation during lytic gammaherpesvirus infection contributes to establishment of viral latency. PLoS Pathog. *7*, e1002150.

Rietveld, K., Pleij, C.W.A., and Bosch, L. (1983). Three-dimensional models of the tRNA-like 3' termini of some plant viral RNAs. EMBO J. *2,* 1079–1085.

Robinson, S.R., Viegas, S.C., Matos, R.G., Domingues, S., Bedir, M., Stewart, H.J.S., Chevassut, T.J., Oliver, A.W., Arraiano, C.M., and Newbury, S.F. (2018). DIS3 isoforms vary in their endoribonuclease activity and are differentially expressed within haematological cancers. Biochem. J. *475*, 2091-2105.

Rohde, R.E., Neill, S.U., Clark, K.A., and Smith, J.S. (1997). Molecular epidemiology of rabies epizootics in Texas. Clin. Diagn. Virol. *8*, 209–217.

Romanowski, V., and Bishop, D.H.L. (1985). Conserved sequences and coding of two strains of lymphocytic choriomeningitis virus (WE and ARM) and Pichinde arenavirus. Virus Res. *2*, 35–51.

Rosenberg, R., Lindsey, N.P., Fischer, M., Gregory, C.J., Hinckley, A.F., Mead, P.S., Paz-Bailey, G., Waterman, S.H., Drexler, N.A., Kersh, G.J., et al. (2018). Morbidity and Mortality Weekly Report Vital Signs: Trends in Reported Vectorborne Disease Cases — United States and Territories, 2004–2016. MMWR. Morb. Mortal. Wkly. Rep. *67*, 496–501.

Rothenberger, S., Torriani, G., Johansson, M.U., Kunz, S., and Engler, O. (2016). Conserved endonuclease function of hantavirus L polymerase. Viruses. *8*, 108.

Rouault, J.P., Prévôt, D., Berthet, C., Birott, A.M., Billaud, M., Magaud, J.P., and Corbo, L. (1998). Interaction of BTG1 and p53-regulated BTG2 gene products with mCaf1, the murine homolog of a component of the yeast CCR4 transcriptional regulatory complex. J. Biol. Chem. *273*, 22563–22569.

Rozovics, J.M., Chase, A.J., Cathcart, A.L., Chou, W., Gershon, P.D., Palusa, S., Wilusz, J., and Semler, B.L. (2012). Picornavirus modification of a host mRNA decay protein. MBio. *3*, e00431-12.

Rymarquis, L.A., Souret, F.F., and Green, P.J. (2011). Evidence that XRN4, an Arabidopsis homolog of exoribonuclease XRN1, preferentially impacts transcripts with certain sequences or in particular functional categories. RNA. *17*, 501–511.

Sabin, L.R., Zheng, Q., Thekkat, P., Yang, J., Hannon, G.J., Gregory, B.D., Tudor, M., and Cherry, S. (2013). Dicer-2 Processes Diverse Viral RNA Species. PLoS One. *8*, e55458.

Sakamoto, J.M., Ng, T.F.F., Suzuki, Y., Tsujimoto, H., Deng, X., Delwart, E., and Rasgon, J.L. (2016). Bunyaviruses are common in male and female Ixodes scapularis ticks in central Pennsylvania. PeerJ. *4*, e2324.

Salvato, M.S., and Shimomaye, E.M. (1989). The completed sequence of lymphocytic choriomeningitis virus reveals a unique RNA structure and a gene for a zinc finger protein. Virology. *173*, 1–10.

Samanta, M., Iwakiri, D., and Takada, K. (2008). Epstein-Barr virus-encoded small RNA induces IL-10 through RIG-I-mediated IRF-3 signaling. Oncogene. *27*, 4150–4160.

Sandler, H., Kreth, J., Timmers, H.T.M., and Stoecklin, G. (2011). Not1 mediates recruitment of the deadenylase Caf1 to mRNAs targeted for degradation by tristetraprolin. Nucleic Acids Res. *39*, 4373–4386.

Sansó, M., Levin, R.S., Lipp, J.J., Wang, V.Y.F., Greifenberg, A.K., Quezada, E.M., Ali, A., Ghosh, A., Larochelle, S., Rana, T.M., et al. (2016). P-TEFb regulation of transcription termination factor Xrn2 revealed by a chemical genetic screen for Cdk9 substrates. Genes Dev. *30*, 117–131.

Sarma, N., Agarwal, D., Shiflett, L.A., and Read, G.S. (2008). Small interfering RNAs that deplete the cellular translation factor eIF4H impede mRNA degradation by the virion host shutoff protein of herpes simplex virus. J. Virol. *82*, 6600–6609.

Sayani, S., and Chanfreau, G.F. (2012). Sequential RNA degradation pathways provide a fail-safe mechanism to limit the accumulation of unspliced transcripts in Saccharomyces cerevisiae. RNA. *18*, 1563–1572.

Schäfer, I.B., Rode, M., Bonneau, F., Schüssler, S., and Conti, E. (2014). The structure of the Pan2-Pan3 core complex reveals cross-talk between deadenylase and pseudokinase. Nat. Struct. Mol. Biol. *21*, 591–598.

Scheller, N., Mina, L.B., Galao, R.P., Chari, A., Gimenez-Barcons, M., Noueiry, A., Fischer, U., Meyerhans, A., and Diez, J. (2009). Translation and replication of hepatitis C virus genomic RNA depends on ancient cellular proteins that control mRNA fates. Proc. Natl. Acad. Sci. *106*, 13517–13522.

Schnettler, E., Sterken, M.G., Leung, J.Y., Metz, S.W., Geertsema, C., Goldbach, R.W., Vlak, J.M., Kohl, A., Khromykh, A.A., and Pijlman, G.P. (2012). Noncoding flavivirus RNA displays RNA interference suppressor activity in insect and Mammalian cells. J. Virol. *86*, 13486–13500.

Schuller, J.M., Falk, S., Fromm, L., Hurt, E., and Conti, E. (2018). Structure of the nuclear exosome captured on a maturing preribosome. Science . *360*, 219–222.

Schutz, S., Noldeke, E.R., and Sprangers, R. (2017). A synergistic network of interactions promotes the formation of in vitro processing bodies and protects mRNA against decapping. Nucleic Acids Res. *45*, 6911–6922.

Scotti, P.D., Dearing, S., and Mossop, D.W. (1983). Flock House virus: a nodavirus isolated from Costelytra zealandica (White) (Coleoptera: Scarabaeidae). Arch. Virol. *75*, 181–189.

Sean, P., Nguyen, J.H.C., and Semler, B.L. (2009). Altered interactions between stem-loop IV within the 5′ noncoding region of coxsackievirus RNA and poly(rC) binding protein 2: Effects on IRES-mediated translation and viral infectivity. Virology. *389*, 45–58.

Sei, E., Wang, T., Hunter, O. V, Xie, Y., and Conrad, N.K. (2015). HITS-CLIP Analysis Uncovers a Link between the Kaposi's Sarcoma-Associated Herpesvirus ORF57 Protein and Host Pre-mRNA Metabolism. PLoS Pathog. *11*, e1004652.

Serquina, A.K.P., Das, S.R., Popova, E., Ojelabi, O.A., Roy, C.K., and Gottlinger, H.G. (2013). UPF1 Is Crucial for the Infectivity of Human Immunodeficiency Virus Type 1 Progeny Virions. J. Virol. *87*, 8853–8861.

Sethna, P.B., Hung, S.-L., and Briant, D.A. (1989). Coronavirus subgenomic minus-strand RNAs and the potential for mRNA replicons (kinetics of RNA synthesis/mRNA replication). Microbiology. *86*, 5626–5630.

Sethna, P.B., Hofmann, M.A., and Brian, D.A. (1991). Minus-strand copies of replicating coronavirus mRNAs contain antileaders. J. Virol. *65*, 320–325.

Severin, C., De Moura, T.R., Liu, Y., Li, K., Zheng, X., and Luo, M. (2016). The cap-binding site of influenza virus protein PB2 as a drug target. Acta Crystallogr. Sect. D Struct. Biol. *72*, 245–253.

Severini, F., Boccolini, D., Fortuna, C., Di Luca, M., Toma, L., Amendola, A., Benedetti, E., Minelli, G., Romi, R., Venturi, G., et al. (2018). Vector competence of Italian Aedes albopictus populations for the chikungunya virus (E1-226V). PLoS Negl. Trop. Dis. *12*, e0006435.

Shen, Y., Zhang, J., Calarco, J.A., and Zhang, Y. (2014). EOL-1, the Homolog of the Mammalian Dom3Z, Regulates Olfactory Learning in C. elegans. J. Neurosci. *34*, 13364–13370.

Shenton, D., Smirnova, J.B., Selley, J.N., Carroll, K., Hubbard, S.J., Pavitt, G.D., Ashe, M.P., and Grant, C.M. (2006). Global translational responses to oxidative stress impact upon multiple levels of protein synthesis. J. Biol. Chem. *281*, 29011–29021.

Sheth, U., and Parker, R. (2003). Decapping and decay of messenger RNA occur in cytoplasmic processing bodies. Science. *300*, 805–808.

Shiflett, L.A., and Read, G.S. (2013). mRNA Decay during Herpes Simplex Virus (HSV) Infections: Mutations That Affect Translation of an mRNA Influence the Sites at Which It Is Cleaved by the HSV Virion Host Shutoff (Vhs) Protein. J. Virol. *87*, 94–109.

Shih, S.R., and Krug, R.M. (1996). Surprising function of the three influenza viral polymerase proteins: Selective protection of viral mRNAs against the cap-snatching reaction catalyzed by the same polymerase proteins. Virology. *226*, 430–435.

Shu, M., Taddeo, B., and Roizman, B. (2015). Tristetraprolin Recruits the Herpes Simplex Virion Host Shutoff RNase to AU-Rich Elements in Stress Response mRNAs To Enable Their Cleavage. J. Virol. *89*, 5643–5650.

Shukla, S., and Parker, R. (2017). PARN modulates Y RNA stability, 3' end formation and its modification. Mol. Cell. Biol. *37*, MCB.00264-17.

Shukla, S., Schmidt, J.C., Goldfarb, K.C., Cech, T.R., and Parker, R. (2016). Inhibition of telomerase RNA decay rescues telomerase deficiency caused by dyskerin or PARN defects. Nat. Struct. Mol. Biol. *23*, 286–292.

Shwetha, S., Kumar, A., Mullick, R., Vasudevan, D., Mukherjee, N., and Das, S. (2015). HuR Displaces Polypyrimidine Tract Binding Protein To Facilitate La Binding to the 3′ Untranslated Region and Enhances Hepatitis C Virus Replication. J. Virol. *89*, 11356–11371.

Shyu, A.B., Greenberg, M.E., and Belasco, J.G. (1989). The c-fos transcript is targeted for rapid decay by two distinct mRNA degradation pathways. Genes Dev. *3*, 60–72.

Sidwa, T.J., Wilson, P.J., Moore, G.M., Oertli, E.H., Hicks, B.N., Rohde, R.E., and Johnston, D.H. (2005). Evaluation of oral rabies vaccination programs for control of rabies epizootics in coyotes and gray foxes: 1995–2003. J. Am. Vet. Med. Assoc. *227*, 785–792.

Sikora, D., Rocheleau, L., Brown, E.G., and Pelchat, M. (2017). Influenza A virus cap-snatches host RNAs based on their abundance early after infection. Virology. *509*, 167–177.

Silva, P.A.G.C., Pereira, C.F., Dalebout, T.J., Spaan, W.J.M., and Bredenbeek, P.J. (2010). An RNA pseudoknot is required for production of yellow fever virus subgenomic RNA by the host nuclease XRN1. J. Virol. *84*, 11395–11406.

Singh, M.K., Fuller-Pace, F. V., Buchmeier, M.J., and Southern, P.J. (1987). Analysis of the genomic L RNA segment from lymphocytic choriomeningitis virus. Virology. *161*, 448–456.

Skalsky, R.L., Corcoran, D.L., Gottwein, E., Frank, C.L., Kang, D., Hafner, M., Nusbaum, J.D., Feederle, R., Delecluse, H.J., Luftig, M.A., et al. (2012). The viral and cellular microRNA targetome in lymphoblastoid cell lines. PLoS Pathog. *8*, e1002484.

Smibert, C.A., Johnson, D.C., and Smiley, J.R. (1992). Identification and characterization of the virion-induced host shutoff product of herpes simplex virus gene UL41. J. Gen. Virol. *73*, 467–470.

Sokoloski, K.J., Wilusz, J., and Wilusz, C.J. (2008). The preparation and applications of cytoplasmic extracts from mammalian cells for studying aspects of mRNA decay. Methods Enzymol. *448*, 139–163.

Sokoloski, K.J., Dickson, A.M., Chaskey, E.L., Garneau, N.L., Wilusz, C.J., and Wilusz, J. (2010). Sindbis virus usurps the cellular HuR protein to stabilize its transcripts and promote productive infections in mammalian and mosquito cells. Cell Host Microbe. *8*, 196–207.

Son, A., Park, J.E., and Kim, V.N. (2018). PARN and TOE1 Constitute a 3′ End Maturation Module for Nuclear Non-coding RNAs. Cell Rep. *23*, 888–898.

Song, M.-G., Bail, S., and Kiledjian, M. (2013). Multiple Nudix family proteins possess mRNA decapping activity. RNA. *19*, 390–399.

Song, M.G., Li, Y., and Kiledjian, M. (2010). Multiple mRNA Decapping Enzymes in Mammalian Cells. Mol. Cell. *40*, 423–432.

Souret, F.F., Kastenmayer, J.P., and Green, P.J. (2004). AtXRN4 degrades mRNA in Arabidopsis and its substrates include selected miRNA targets. Mol. Cell *15*, 173–183.

Spagnolo, J.F., and Hogue, B.G. (2000). Host protein interactions with the 3' end of bovine coronavirus RNA and the requirement of the poly(A) tail for coronavirus defective genome replication. J. Virol. *74*, 5053–5065.

Spurrell, J.C., Wiehler, S., Zaheer, R.S., Sanders, S.P., and Proud, D. (2005). Human airway epithelial cells produce IP- 10 (CXCL10) in vitro and in vivo upon rhinovirus infection. Am J Physiol Lung Cell Mol Physiol. *289,* L85-95.

Sreenivasan, C.C., Jandhyala, S.S., Luo, S., Hause, B.M., Thomas, M., Knudsen, D.E.B., Leslie-Steen, P., Clement, T., Reedy, S.E., Chambers, T.M., et al. (2018). Phylogenetic analysis and characterization of a sporadic isolate of equine influenza a H3N8 from an unvaccinated horse in 2015. Viruses. *10*, 31.

Srinivasan, A., Burton, E.C., Kuehnert, M.J., Rupprecht, C., Sutker, W.L., Ksiazek, T.G., Paddock, C.D., Guarner, J., Shieh, W.-J., Goldsmith, C., et al. (2005). Transmission of Rabies Virus from an Organ Donor to Four Transplant Recipients for the Rabies in Transplant Recipients Investigation Team*. N Engl J Med *35211*, 1103–1111.

Stammler, S.N., Cao, S., Chen, S.J., and Giedroc, D.P. (2011). A conserved RNA pseudoknot in a putative molecular switch domain of the 3′-untranslated region of coronaviruses is only marginally stable. RNA. *17*, 1747–1759.

Steckelberg, A.-L., Akiyama, B.M., Costantino, D.A., Sit, T.L., Nix, J.C., and Kieft, J.S. (2018). A folded viral noncoding RNA blocks host cell exoribonucleases through a conformationally dynamic RNA structure. PNAS. *115*, 6404-6409.

Stenglein, M.D., Sanders, C., Kistler, A.L., Ruby, J.G., Franco, J.Y., Reavill, D.R., Dunker, F., and Derisi, J.L. (2012). Identification, characterization, and in vitro culture of highly divergent arenaviruses from boa constrictors and annulated tree boas: candidate etiological agents for snake inclusion body disease. MBio. *3*, e00180-12.

Streicker, D.G., Turmelle, A.S., Vonhof, M.J., Kuzmin, I. V, McCracken, G.F., and Rupprecht, C.E. (2010). Host phylogeny constrains cross-species emergence and establishment of rabies virus in bats. Science. *329*, 676–679.

Strom, T., and Frenkel, N. (1987). Effects of herpes simplex virus on mRNA stability. J. Virol. *61*, 2198–2207.

Stuart, G., Moffett, K., and Bozarth, R.F. (2004). A whole genome perspective on the phylogeny of the plant virus family Tombusviridae. Arch. Virol. *149*, 1595–1610.

Sun, M., Schwalb, B., Pirkl, N., Maier, K.C., Schenk, A., Failmezger, H., Tresch, A., and Cramer, P. (2013). Global analysis of Eukaryotic mRNA degradation reveals Xrn1-dependent buffering of transcript levels. Mol. Cell. *52*, 52–62.

Suzuki, A., Niimi, Y., and Saga, Y. (2014). Interaction of NANOS2 and NANOS3 with different components of the CNOT complex may contribute to the functional differences in mouse male germ cells. Biol. Open. *3*, 1207–1216.

Szankasi, P., and Smith, G.R. (1996). Requirement of S. pombe exonuclease II, a homologue of S. cerevisiae Sep1, for normal mitotic growth and viability. Curr. Genet. *30*, 284–293.

Szanto, A.G., Nadin-Davis, S.A., and White, B.N. (2008). Complete genome sequence of a raccoon rabies virus isolate. Virus Res. *136*, 130–139.

Taddeo, B., and Roizman, B. (2006). The virion host shutoff protein (UL41) of herpes simplex virus 1 is an endoribonuclease with a substrate specificity similar to that of RNase A. J. Virol. *80*, 9341–9345.

Taddeo, B., Zhang, W., and Roizman, B. (2006). The U(L)41 protein of herpes simplex virus 1 degrades RNA by endonucleolytic cleavage in absence of other cellular or viral proteins. Proc. Natl. Acad. Sci. U. S. A. *103*, 2827–2832.

Taddeo, B., Sciortino, M.T., Zhang, W., and Roizman, B. (2007). Interaction of herpes simplex virus RNase with VP16 and VP22 is required for the accumulation of the protein but not for accumulation of mRNA. Proc. Natl. Acad. Sci. U. S. A. *104*, 12163–12168.

Taddeo, B., Zhang, W., and Roizman, B. (2013). The Herpes Simplex Virus Host Shutoff RNase Degrades Cellular and Viral mRNAs Made before Infection but Not Viral mRNA Made after Infection. J. Virol. *87*, 4516–4522.

Talavera, S., Birnberg, L., Nuñez, A.I., Muñoz-Muñoz, F., Vázquez, A., and Busquets, N. (2018). Culex flavivirus infection in a Culex pipiens mosquito colony and its effects on vector competence for Rift Valley fever phlebovirus. Parasit. Vectors. *11*, 310.

Tamada, T., Schmitt, C., Saito, M., Guilley, H., Richards, K., and Jonard, G. (1996). High resolution analysis of the readthrough domain of beet necrotic yellow vein virus readthrough protein: A KTER motif is important for efficient transmission of the virus by Polymyxa betae. J. Gen. Virol. *77*, 1359–1367.

Tanaka, T., Kamitani, W., DeDiego, M.L., Enjuanes, L., and Matsuura, Y. (2012). Severe Acute Respiratory Syndrome Coronavirus nsp1 Facilitates Efficient Propagation in Cells through a Specific Translational Shutoff of Host mRNA. J. Virol. *86*, 11128–11137.

Tang, H.-B., Lu, Z.-L., Zhong, Y.-Z., He, X.-X., Zhong, T.-Z., Pan, Y., Wei, X.-K., Luo, Y., Liao, S.-H., Minamoto, N., et al. (2014). Characterization of the biological properties and complete genome sequence analysis of a cattle-derived rabies virus isolate from the Guangxi province of southern China. Virus Genes. *49*, 417–427.

Tang, X., Luo, M., Zhang, S., Fooks, A.R., Hu, R., and Tu, C. (2005). Pivotal role of dogs in rabies transmission, China. Emerg. Infect. Dis. *11*, 1970–1972.

Tharun, S., He, W., Mayes, A.E., Lennertz, P., Beggs, J.D., and Parker, R. (2000). Yeast Sm-like proteins function in mRNA decapping and decay. Nature. *404*, 515–518.

Thermann, R., Neu-Yilik, G., Deters, A., Frede, U., Wehr, K., Hagemeier, C., Hentze, M.W., and Kulozik, A.E. (1998). Binary specification of nonsense codons by splicing and cytoplasmic translation. EMBO J. *17*, 3484–3494.

Thi, N., Chinh, T., Ngoc, N., Minh, Q., Qui, P.T., Thi, T., Chau, H., Dang, H., Nghia, T., Anh, L., et al. (2018). Enterovirus serotypes in patients with central nervous system and respiratory infections in Viet Nam 1997 – 2010. Virol. J. *15*, 1–8.

Thiele, B.J., Doller, A., Kähne, T., Pregla, R., Hetzer, R., and Regitz-Zagrosek, V. (2004). RNA-binding proteins heterogeneous nuclear ribonucleoprotein A1, E1, and K are involved in post-transcriptional control of collagen I and III synthesis. Circ. Res. *95*, 1058–1066.

Thompson, J.R., Buratti, E., de Wispelaere, M., and Tepfer, M. (2008). Structural and functional characterization of the 5′ region of subgenomic RNA5 of cucumber mosaic virus. J. Gen. Virol. *89*, 1729–1738.

Thornton, J.E., Chang, H.-M., Piskounova, E., and Gregory, R.I. (2012). Lin28-mediated control of let-7 microRNA expression by alternative TUTases Zcchc11 (TUT4) and Zcchc6 (TUT7). RNA. *18*, 1875–1885.

Till, D.D., Linz, B., Seago, J.E., Elgar, S.J., Marujo, P.E., Elias, M.D.L., Arraiano, C.M., McClellan, J.A., McCarthy, J.E.G., and Newbury, S.F. (1998). Identification and developmental expression of a 5′-3′ exoribonuclease from Drosophila melanogaster. Mech. Dev. *79*, 51–55.

Tishkoff, D.X., Johnson, A.W., and Kolodner, R.D. (1991). Molecular and genetic analysis of the gene encoding the Saccharomyces cerevisiae strand exchange protein Sep1. Mol. Cell. Biol. *11*, 2593–2608.

Toczyski, D.P., Matera, A.G., Ward, D.C., and Steitz, J.A. (1994). The Epstein-Barr virus (EBV) small RNA EBER1 binds and relocalizes ribosomal protein L22 in EBV-infected human B lymphocytes. Proc. Natl. Acad. Sci. *91*, 3463–3467.

Tourrière, H., Chebli, K., Zekri, L., Courselaud, B., Blanchard, J.M., Bertrand, E., and Tazi, J. (2003). The RasGAP-associated endoribonuclease G3BP assembles stress granules. J. Cell Biol. *160*, 823–831.

Toyoda, H., Franco, D., Fujita, K., Paul, A. V, and Wimmer, E. (2007). Replication of poliovirus requires binding of the poly(rC) binding protein to the cloverleaf as well as to the adjacent C-rich spacer sequence between the cloverleaf and the internal ribosomal entry site. J. Virol. *81*, 10017–10028.

Tucker, M., Valencia-Sanchez, M.A., Staples, R.R., Chen, J., Denis, C.L., and Parker, R. (2001). The transcription factor associated Ccr4 and Caf1 proteins are components of the major cytoplasmic mRNA deadenylase in Saccharomyces cerevisiae. Cell. *104*, 377–386.

Tummala, H., Walne, A., Collopy, L., Cardoso, S., De La Fuente, J., Lawson, S., Powell, J., Cooper, N., Foster, A., Mohammed, S., et al. (2015). Poly(A)-specific ribonuclease deficiency impacts telomere biology and causes dyskeratosis congenita. J. Clin. Invest. *125*, 2151–2160.

Ukleja, M., Cuellar, J., Siwaszek, A., Kasprzak, J.M., Czarnocki-Cieciura, M., Bujnicki, J.M., Dziembowski, A., and M. Valpuesta, J. (2016). The architecture of the Schizosaccharomyces pombe CCR4-NOT complex. Nat. Commun. *7*, 10433.

Ustianenko, D., Hrossova, D., Potesil, D., Chalupnikova, K., Hrazdilova, K., Pachernik, J., Cetkovska, K., Uldrijan, S., Zdrahal, Z., and Vanacova, S. (2013). Mammalian DIS3L2 exoribonuclease targets the uridylated precursors of let-7 miRNAs. RNA. *19*, 1632–1638.

Ustianenko, D., Pasulka, J., Feketova, Z., Bednarik, L., Zigackova, D., Fortova, A., Zavolan, M., and Vanacova, S. (2016). TUT-DIS3L2 is a mammalian surveillance pathway for aberrant structured non-coding RNAs. EMBO J. *35*, 2179–2191.

Vindry, C., Marnef, A., Broomhead, H., Twyffels, L., Ozgur, S., Stoecklin, G., Llorian, M., Smith, C.W., Mata, J., Weil, D., et al. (2017). Dual RNA Processing Roles of Pat1b via Cytoplasmic Lsm1-7 and Nuclear Lsm2-8 Complexes. Cell Rep. *20*, 1187–1200.

Virtanen, A., Henriksson, N., Nilsson, P., and Nissbeck, M. (2013). Poly(A)-specific ribonuclease (PARN): An allosterically regulated, processive and mRNA cap-interacting deadenylase. Crit. Rev. Biochem. Mol. Biol. *48*, 192–209.

Vloet, R.P.M., Vogels, C.B.F., Koenraadt, C.J.M., Pijlman, G.P., Eiden, M., Gonzales, J.L., van Keulen, L.J.M., Wichgers Schreur, P.J., and Kortekaas, J. (2017). Transmission of Rift Valley fever virus from European-breed lambs to Culex pipiens mosquitoes. PLoS Negl. Trop. Dis. *11*, e0006145.

Vreeland, A.C., Yu, S., Levi, L., de Barros Rossetto, D., and Noy, N. (2014). Transcript Stabilization by the RNA-Binding Protein HuR Is Regulated by Cellular Retinoic Acid-Binding Protein 2. Mol. Cell. Biol. *34*, 2135–2146.

Wagner, E., Clement, S.L., and Lykke-Andersen, J. (2007). An Unconventional Human Ccr4-Caf1 Deadenylase Complex in Nuclear Cajal Bodies. Mol. Cell. Biol. *27*, 1686–1695.

Waldron, J.A., Jones, C.I., Towler, B.P., Pashler, A.L., Grima, D.P., Hebbes, S., Crossman, S.H., Zabolotskaya, M. V, and Newbury, S.F. (2015). Xrn1/Pacman affects apoptosis and regulates expression of hid and reaper. Biol. Open. *4*, 649–660.

Walter, B.L., Nguyen, J.H.C., Ehrenfeld, E., and Semler, B.L. (1999). Differential utilization of poly(rC) binding protein 2 in translation directed by picornavirus IRES elements. RNA. *5*, 1570–1585.

Wang, M., and Pestov, D.G. (2011). 5′-end surveillance by Xrn2 acts as a shared mechanism for mammalian pre-rRNA maturation and decay. Nucleic Acids Res. *39*, 1811–1822.

Wang, Z., and Kiledjian, M. (2001). Functional link between the mammalian exosome and mRNA decapping. Cell. *107*, 751–762.

Wang, B., Wu, M., Perchellet, E.M., McIlvain, C.J., Sperfslage, B.J., Huang, X., Tamura, M., Stephany, H.A., Hua, D.H., and Perchellet, J.P. (2001a). A synthetic triptycene bisquinone, which blocks nucleoside transport and induces DNA fragmentation, retains its cytotoxic efficacy in daunorubicin-resistant HL-60 cell lines. Int. J. Oncol. *19*, 1169–1178.

Wang, Y., Osterbur, D.L., Megaw, P.L., Tosini, G., Fukuhara, C., Green, C.B., and Besharse, J.C. (2001b). Rhythmic expression of Nocturnin mRNA in multiple tissues of the mouse. BMC Dev. Biol. *1*, 1–15.

Wang, Y., Perchellet, E.M., Ward, M.M., Lou, K., Zhao, H., Battina, S.K., Wiredu, B., Hua, D.H., and Perchellet, J.P.H. (2006). Antitumor triptycene analogs induce a rapid collapse of mitochondrial transmembrane potential in HL-60 cells and isolated mitochondria. Int. J. Oncol. *28*, 161–172.

Wang, Z., Jiao, X., Carr-Schmid, A., and Kiledjian, M. (2002). The hDcp2 protein is a mammalian mRNA decapping enzyme. Proc. Natl. Acad. Sci. *99*, 12663–12668.

Ward, L.D., and Kellis, M. (2012). Interpreting noncoding genetic variation in complex traits and human disease. Nat. Biotechnol. *30*, 1095–1106.

Wasmuth, E. V., and Lima, C.D. (2017). The Rrp6 C-terminal domain binds RNA and activates the nuclear RNA exosome. Nucleic Acids Res. *45*, 846–860.

Wasmuth, E. V, Zinder, J.C., Zattas, D., Das, M., and Lima, C.D. (2017). Structure and reconstitution of yeast Mpp6-nuclear exosome complexes reveals that mpp6 stimulates RNA decay and recruits the Mtr4 helicase. Elife. *6*, e29062.

Weber, C., Nover, L., and Fauth, M. (2008). Plant stress granules and mRNA processing bodies are distinct from heat stress granules. Plant J. *56*, 517–530.

Webster, M.W., Chen, Y.H., Stowell, J.A.W., Alhusaini, N., Sweet, T., Graveley, B.R., Coller, J., and Passmore, L.A. (2018). mRNA Deadenylation Is Coupled to Translation Rates by the Differential Activities of Ccr4-Not Nucleases. Mol. Cell. *70*, 1089–1100.

Weidmann, C.A., Raynard, N.A., Blewett, N.H., Van Etten, J., and Goldstrohm, A.C. (2014). The RNA binding domain of Pumilio antagonizes poly-adenosine binding protein and accelerates deadenylation. RNA. *20*, 1298–1319.

Weil, J.E., and Beemon, K.L. (2006). A 3' UTR sequence stabilizes termination codons in the unspliced RNA of Rous sarcoma virus. RNA. *12*, 102–110.

Weil, J.E., Hadjithomas, M., and Beemon, K.L. (2009). Structural characterization of the Rous sarcoma virus RNA stability element. J. Virol. *83*, 2119–2129.

Weiss, I.M., and Liebhaber, S. a (1994). Erythroid cell-specific determinants of alpha-globin mRNA stability. Mol. Cell. Biol. *14*, 8123–8132.

Weiss, I.M., and Liebhaber, S.A. (1995). Erythroid cell-specific mRNA stability elements in the alpha 2-globin 3' nontranslated region. Mol. Cell. Biol. *15*, 2457–2465.

van der Werf, S., Bregegere, F., Kopecka, H., Kitamura, N., Rothberg, P.G., Kourilsky, P., Wimmer, E., and Girard, M. (1981). Molecular cloning of the genome of poliovirus type 1. Proc. Natl. Acad. Sci. U. S. A. *78*, 5983–5987.

Wernet, M.F., Klovstad, M., and Clandinin, T.R. (2014). Generation of infectious virus particles from inducible transgenic genomes. Curr. Biol. *24*, 107–108.

Wery, M., Descrimes, M., Vogt, N., Dallongeville, A.S., Gautheret, D., and Morillon, A. (2016). Nonsense-Mediated Decay Restricts LncRNA Levels in Yeast Unless Blocked by Double-Stranded RNA Structure. Mol. Cell. *61*, 379–392.

Wery, M., Gautier, C., Descrimes, M., Yoda, M., Vennin-Rendos, H., Migeot, V., Gautheret, D., Hermand, D., and Morillon, A. (2018). Native elongating transcript sequencing reveals global anti-correlation between sense and antisense nascent transcription in fission yeast. RNA. *24*, 196–208.

West, S., Gromak, N., and Proudfoot, N.J. (2004). Human 5′ → 3′ exonuclease Xm2 promotes transcription termination at co-transcriptional cleavage sites. Nature. *432*, 522–525.

Westgeest, K.B., Russell, C.A., Lin, X., Spronken, M.I.J., Bestebroer, T.M., Bahl, J., van Beek, R., Skepner, E., Halpin, R.A., de Jong, J.C., et al. (2014). Genomewide Analysis of Reassortment and Evolution of Human Influenza A(H3N2) Viruses Circulating between 1968 and 2011. J. Virol. *88*, 2844–2857.

Wheeler, J.R., Matheny, T., Jain, S., Abrisch, R., and Parker, R. (2016). Distinct stages in stress granule assembly and disassembly. Elife. *5*, e18413.

Whipple, J.M., Lane, E.A., Chernyakov, I., D'Silva, S., and Phizicky, E.M. (2011). The yeast rapid tRNA decay pathway primarily monitors the structural integrity of the acceptor and T-stems of mature tRNA. Genes Dev. *25*, 1173–1184.

White, J.P., Cardenas, A.M., Marissen, W.E., and Lloyd, R.E. (2007). Inhibition of Cytoplasmic mRNA Stress Granule Formation by a Viral Proteinase. Cell Host Microbe. *2*, 295–305.

Williams, G., Chang, R., and Brian, D. (1999). A phylogenetically conserved hairpin-type 3' untranslated region pseudoknot functions in coronavirus RNA replication. J. Virol. *73*, 8349–8355.

Wilson, S.M., and Clegg, J.C.S. (1991). Sequence analysis of the S RNA of the African Arenavirus Mopeia: An unusual secondary structure feature in the intergenic region. Virology. *180*, 543–552.

Wilusz, J., Kurilla, M.G., and Keene, J.D. (1983). A host protein (La) binds to a unique species of minus-sense leader RNA during replication of vesicular stomatitis virus. Proc. Natl. Acad. Sci. U. S. A. *80*, 5827–5831.

de Wispelaere, M., and Rao, A.L.N. (2009). Production of cucumber mosaic virus RNA5 and its role in recombination. Virology. *384*, 179–191.

Withers, J.B., and Beemon, K.L. (2010). Structural features in the Rous sarcoma virus RNA stability element are necessary for sensing the correct termination codon. Retrovirology. *7*, 65.

Witwer, C., Rauscher, S., Hofacker, I.L., and Stadler, P.F. (2001). Conserved RNA secondary structures in Picornaviridae genomes. Nucleic Acids Res. *29*, 5079–5089.

Wolf, J., Valkov, E., Allen, M.D., Meineke, B., Gordiyenko, Y., Mclaughlin, S.H., Olsen, T.M., Robinson, C. V, Bycroft, M., Stewart, M., et al. (2014). Structural basis for Pan3 binding to Pan2 and its function in mRNA recruitment and deadenylation. EMBO J. *33*, 1514–1526.

Wong, G., Liu, W., Liu, Y., Zhou, B., Bi, Y., and Gao, G.F. (2015). MERS, SARS, and Ebola: The Role of Super-Spreaders in Infectious Disease. Cell Host Microbe. *18*, 398–401.

Wong, J., Si, X., Angeles, A., Zhang, J., Shi, J., Fung, G., Jagdeo, J., Wang, T., Zhong, Z., Jan, E., et al. (2013). Cytoplasmic redistribution and cleavage of AUF1 during coxsackievirus infection enhance the stability of its viral genome. FASEB J. *27*, 2777–2787.

Wu, J., and Hopper, A.K. (2014). Healing for destruction: TRNA intron degradation in yeast is a two-step cytoplasmic process catalyzed by tRNA ligase Rlg1 and 5′-to-3′ exonuclease Xrn1. Genes Dev. *28*, 1556–1561.

Wu, H., Yin, Q.F., Luo, Z., Yao, R.W., Zheng, C.C., Zhang, J., Xiang, J.F., Yang, L., and Chen, L.L. (2016). Unusual Processing Generates SPA LncRNAs that Sequester Multiple RNA Binding Proteins. Mol. Cell *64*, 534–548.

Wu, H.Y., Ke, T.Y., Liao, W.Y., and Chang, N.Y. (2013). Regulation of Coronaviral Poly(A) Tail Length during Infection. PLoS One *8*, e70548.

Wu, M., Nilsson, P., Henriksson, N., Niedzwiecka, A., Lim, M.K., Cheng, Z., Kokkoris, K., Virtanen, A., and Song, H. (2009). Structural Basis of m7GpppG Binding to Poly(A)-Specific Ribonuclease. Structure *17*, 276–286.

Wu, S., Wang, Y., Lin, L., Si, X., Wang, T., Zhong, X., Tong, L., Luan, Y., Chen, Y., Li, X., et al. (2014). Protease 2A induces stress granule formation during coxsackievirus B3 and enterovirus 71 infections. Virol. J. *11*, 192.

Wu, X., Franka, R., Velasco-Villa, A., and Rupprecht, C.E. (2007a). Are all lyssavirus genes equal for phylogenetic analyses? Virus Res. *129*, 91–103.

Wu, Y., Maruo, S., Yajima, M., Kanda, T., and Takada, K. (2007b). Epstein-Barr Virus (EBV)-Encoded RNA 2 (EBER2) but Not EBER1 Plays a Critical Role in EBV-Induced B-Cell Growth Transformation. J. Virol. *81*, 11236–11245.

Wunner, W.H., Curtis, P.J., and Wiktor, T.J. (1980). Rabies mRNA translation in Xenopus laevis oocytes. J. Virol. *36*, 133–142.

Wurm, J.P., Overbeck, J., and Sprangers, R. (2016). The S. Pombe mRNA decapping complex recruits cofactors and an Edc1-like activator through a single dynamic surface. RNA. *22*, 1360–1372.

Wylie, S.J., Luo, H., Li, H., and Jones, M.G.K. (2012). Multiple polyadenylated RNA viruses detected in pooled cultivated and wild plant samples. Arch. Virol. *157*, 271–284.

Xiao, S., Li, Y., Wong, T. wai, and Hui, D.S.C. (2017). Role of fomites in SARS transmission during the largest hospital outbreak in Hong Kong. PLoS One. *12*, e0181558.

Xu, G., Zhang, X., Sun, Y., Liu, Q., Sun, H., Xiong, X., Jiang, M., He, Q., Wang, Y., Pu, J., et al. (2016). Truncation of C-terminal 20 amino acids in PA-X contributes to adaptation of swine influenza virus in pigs. Sci. Rep. *6*, 21845.

Xue, Y., Bai, X., Lee, I., Kallstrom, G., Ho, J., Brown, J., Stevens, A., and Johnson, A.W. (2000). Saccharomyces cerevisiae RAI1 (YGL246c) is homologous to human DOM3Z and encodes a protein that binds the nuclear exoribonuclease Rat1p. Mol. Cell. Biol. *20*, 4006–4015.

Yajima, M., Kanda, T., and Takada, K. (2005). Critical role of Epstein-Barr Virus (EBV)-encoded RNA in efficient EBV-induced B-lymphocyte growth transformation. J. Virol. *79*, 4298–4307.

Yamaguchi, T., Suzuki, T., Sato, T., Takahashi, A., Watanabe, H., Kadowaki, A., Natsui, M., Inagaki, H., Arakawa, S., Nakaoka, S., et al. (2018). The CCR4-NOT deadenylase complex controls atg7-dependent cell death and heart function. Sci. Signal. *11*, eaan3638.

Yamaji, M., Jishage, M., Meyer, C., Suryawanshi, H., Der, E., Yamaji, M., Garzia, A., Morozov, P., Manickavel, S., McFarland, H.L., et al. (2017). DND1 maintains germline stem cells via recruitment of the CCR4-NOT complex to target mRNAs. Nature. *543*, 568–572.

Yamashita, A., Ohnishi, T., Kashima, I., Taya, Y., and Ohno, S. (2001). Human SMG-1, a novel phosphatidylinositol 3-kinase-related protein kinase, associates with components of the mRNA surveillance complex and is involved in the regulation of nonsense-mediated mRNA decay. Genes Dev. *15*, 2215–2228.

Yamashita, A., Chang, T.C., Yamashita, Y., Zhu, W., Zhong, Z., Chen, C.Y.A., and Shyu, A. Bin (2005). Concerted action of poly(A) nucleases and decapping enzyme in mammalian mRNA turnover. Nat. Struct. Mol. Biol. *12*, 1054–1063.

Yang, J., Koprowski, H., Dietzschold, B., and Fu, Z.F. (1999). Phosphorylation of rabies virus nucleoprotein regulates viral RNA transcription and replication by modulating leader RNA encapsidation. J. Virol. *73*, 1661–1664.

Yang, X., Fu, J., and Wei, X. (2017). Expression patterns of zebrafish nocturnin genes and the transcriptional activity of the frog nocturnin promoter in zebrafish rod photoreceptors. Mol. Vis. *23*, 1039–1047.

Yang, X., Hu, Z., Fan, S., Zhang, Q., Zhong, Y., Guo, D., Qin, Y., and Chen, M. (2018). Picornavirus 2A protease regulates stress granule formation to facilitate viral translation. PLoS Pathog. *14*, e1006901.

Yang, Y., Huang, Y., Gnanadurai, C.W., Cao, S., Liu, X., Cui, M., and Fu, Z.F. (2015). The Inability of Wild-Type Rabies Virus To Activate Dendritic Cells Is Dependent on the Glycoprotein and Correlates with Its Low Level of the De Novo -Synthesized Leader RNA. J. Virol. *89*, 2157–2169.

Ye, X., Pan, T., Wang, D., Fang, L., Ma, J., Zhu, X., Shi, Y., Zhang, K., Zheng, H., Chen, H., et al. (2018). Foot-and-mouth disease virus counteracts on internal ribosome entry site suppression by G3BP1 and inhibits G3BP1-mediated stress granule assembly via post-translational mechanisms. Front. Immunol. *9*, 1142.

Yoon, I., Suh, S.E., Barros, S.A., and Chenoweth, D.M. (2016). Synthesis of 9-Substituted Triptycene Building Blocks for Solid-Phase Diversification and Nucleic Acid Junction Targeting. Org. Lett. *18*, 1096–1099.

You, J., Li, H., Lu, X.-M., Li, W., Wang, P.-Y., Dou, S.-X., and Xi, X.-G. (2017). Effects of monovalent cations on folding kinetics of G-quadruplexes. Biosci. Rep. *37*, BSR20170771.

Yuan, P., Bartlam, M., Lou, Z., Chen, S., Zhou, J., He, X., Lv, Z., Ge, R., Li, X., Deng, T., et al. (2009). Crystal structure of an avian influenza polymerase PAN reveals an endonuclease active site. Nature. *458*, 909–913.

Zabolotskaya, M. V., Grima, D.P., Lin, M.-D., Chou, T.-B., and Newbury, S.F. (2008). The 5′–3′ exoribonuclease Pacman is required for normal male fertility and is dynamically localized in cytoplasmic particles in Drosophila testis cells. Biochem. J. *416*, 327–335.

Zakrzewska-Placzek, M., Souret, F.F., Sobczyk, G.J., Green, P.J., and Kufel, J. (2010). Arabidopsis thaliana XRN2 is required for primary cleavage in the pre-ribosomal RNA. Nucleic Acids Res. *38*, 4487–4502.

Zanluca, C., De Melo, V.C.A., Mosimann, A.L.P., Dos Santos, G.I.V., dos Santos, C.N.D., and Luz, K. (2015). First report of autochthonous transmission of Zika virus in Brazil. Mem. Inst. Oswaldo Cruz. *110*, 569–572.

Zhai, X., Wu, S., Lin, L., Wang, T., Zhong, X., Chen, Y., Xu, W., Tong, L., Wang, Y., Zhao, W., et al. (2018). Stress Granule Formation is One of the Early Antiviral Mechanisms for Host Cells Against Coxsackievirus B Infection. Virol. Sin. *4*, 314-322.

Zhang, R., and Wang, J. (2018). HuR stabilizes TFAM mRNA in an ATM/p38 dependent manner in ionizing irradiated cancer cells. Cancer Sci. *109*, 2446-2457

Zhang, F., Wang, S., Wang, Y., Shang, X., Zhou, H., and Cai, L. (2018a). Characterization of pseudoparticles paired with hemagglutinin and neuraminidase from highly pathogenic H5N1 influenza and avian influenza A (H7N9) viruses. Virus Res. *253*, 20–27.

Zhang, K., Dion, N., Fuchs, B., Damron, T., Gitelis, S., Irwin, R., Connor, M.O., Schwartz, H., Scully, S.P., Rock, M.G., et al. (2002). The human homolog of yeast SEP1 is a novel candidate tumor suppressor gene in osteogenic sarcoma. Gene. *298*, 121–127.

Zhang, R., Liu, C., Cao, Y., Jamal, M., Chen, X., Zheng, J., Li, L., You, J., Zhu, Q., Liu, S., et al. (2017). Rabies viruses leader RNA interacts with host Hsc70 and inhibits virus replication. Oncotarget. *8*, 43822–43837.

Zhang, Y., Si, B.Y., Kang, X.P., Hu, Y., Li, J., Wu, X.Y., Li, Y.C., Yang, Y.H., and Zhu, Q.Y. (2013). The confirmation of three repeated sequence elements in the 3′ untranslated region of Chikungunya virus. Virus Genes. *46*, 165–166.

Zhang, Y., Zhang, W., Liu, W., Liu, H., Zhang, Y., and Luo, B. (2018b). Epstein–Barr virus miRNA-BART16 modulates cell proliferation by targeting LMP1. Virus Res. *256*, 38–44.

Zhao, J., Wang, S., Zhang, S., Liu, Y., Zhang, J., Zhang, F., Mi, L., and Hu, R. (2014). Molecular characterization of a rabies virus isolate from a rabid dog in Hanzhong District, Shaanxi Province, China. Arch. Virol. *159*, 1481–1486.

Zinder, J.C., Wasmuth, E. V., and Lima, C.D. (2016). Nuclear RNA Exosome at 3.1 Å Reveals Substrate Specificities, RNA Paths, and Allosteric Inhibition of Rrp44/Dis3. Mol. Cell. *64*, 734–745.

Zúñiga, S., Sola, I., Alonso, S., and Enjuanes, L. (2004). Sequence Motifs Involved in the Regulation of Discontinuous Coronavirus Subgenomic RNA Synthesis. J. Virol. *78*, 980–994.

Zybura-Broda, K., Wolder-Gontarek, M., Ambrozek-Latecka, M., Choros, A., Bogusz, A., Wilemska-Dziaduszycka, J., and Rylski, M. (2018). HuR (Elavl1) and HuB (Elavl2) stabilize matrix metalloproteinase-9 mRNA during seizure-induced Mmp-9 expression in neurons. Front. Neurosci. *12*, 224.

APPENDICES

Appendix 1. The text alignment for the graphical alignment of XRN family from various species. Alignment of the amino acid sequence of XRNs from *Homo sapiens*, *Kluyveromyces lactis*, *Saccharomyces cerevisiae* XRN1, *Culex quinquefasciatus*, *Drosophila melanogaster*, *Mus musculus*, *Arabidopsis thaliana*, and *Saccharomyces cerevisiae* RAT1. Alignment was done using Geneious version 11.1.5 (Kearse et al., 2012)

Name	Species	NCBI accession number
5'-3' exoribonuclease 1 isoform a	*Homo sapiens*	NP_061874
KLLA0F22385p	*Kluyveromyces lactis*	CAG98788
5'-3' exoribonuclease	*Saccharomyces cerevisiae*	AAA35219
5'-3' exoribonuclease 1	*Culex quinquefasciatus*	EDS29953
pacman protein	*Drosophila melanogaster*	CAB43711
5'-3' exoribonuclease 1 isoform 1	*Mus musculus*	NP_036046
XRN4	*Arabidopsis thaliana*	AAG40731
ssRNA exonuclease RAT1	*Saccharomyces cerevisiae*	NP_014691

```
                                        1        10        20        30        40        50        60
                                        |         |         |         |         |         |         |

                  Homo sapiens XRN1    MGVPKFYRWISERYP-CLSEVVKEHQ--------IP-----------EFDNLYLDMNGII
                  Mus musculus XRN1    MGVPKFYRWISERYP-CLSEVVKEHQ--------IP-----------EFDNLYLDMNGII
   Drosophila melanogaster Pacman     MGVPKFFRYISERYP-CLSELAREHC--------IP-----------EFDNLYLDMNGIV
       Culex quinquefasciatus XRN1    MGVPKFFRYMSERYP-CLGELVRENQ--------VP-----------DFDNLYLDMNGII
      Saccharomyces cerevisiae XRN1   MGIPKFFRYISERWPMIL-QLIEGTQ--------IP-----------EFDNLYLDMNSIL
         Kluyveromyces lactis XRN1    MGIPKFFHFISERWPQ-ISQLIDGSQ--------IP-----------EFDNLYLDMNSIL
          Arabidopsis thaliana XRN4   MGVPAFYRWLADRYPKSISDVVEEEPTDGGRGDLIPVDITRPNPNGFEFDNLYLDMNGII
      Saccharomyces cerevisiae XRN2   MGVPSFFRWLSRKYPKIISPVLEEQPQIVDG-VILPLDYSASNPNG-ELDNLYLDMNGIV


                  Homo sapiens XRN1    HQCSHPNDDDVHFRISDDKIFTDIFHYLEVLFRIIKPRKVFFMAVDGVAPRAKMNQQRGR
                  Mus musculus XRN1    HQCSHPNDDDVHFRISDDKIFTDIFHYLEVLFRIIKPRKVFFMAVDGVAPRAKMNQQRGR
   Drosophila melanogaster Pacman     HNCSHPDDNNIHFHLEEEQIFQEIFNYVDKLFYLIKPQRLFFLSVDGVAPRAKMNQQRSR
       Culex quinquefasciatus XRN1    HNCSHPNDSDVFFRITEEQIFSDIFHYLEFLFRMIRPQKLFFIAVDGVAPRAKMNQQRGR
      Saccharomyces cerevisiae XRN1   HNCTHGNDDDVTKRLTEEEVFAKICTYIDHLFQTIKPKKIFYMAIDGVAPRAKMNQQRAR
         Kluyveromyces lactis XRN1    HNCTHGDGSEVNSRLSEEEVYSKIFSYIDHLFHTIKPKQTFYMAIDGVAPRAKMNQQRAR
          Arabidopsis thaliana XRN4   HPCFHPEGKPAPA--TYDDVFKSMFEYIDHLFTLVRPRKILYLAIDGVAPRAKMNQQRSR
      Saccharomyces cerevisiae XRN2   HPCSHPENKPPPE--TEDEMLLAVFEYTNRVLNMARPRKVLVMAVDGVAPRAKMNQQRAR


                  Homo sapiens XRN1    RFRSAKEA-------EDKIKKAIEKGETL----PTEARFDSNCITPGTEFMARLHEHLKY
                  Mus musculus XRN1    RFRSAKEA-------EDKIKKAIEKGETL----PTEARFDSNCITPGTEFMARLHEHLKY
   Drosophila melanogaster Pacman     RFRTAREA-------EQQEAKAAQRGEL-----REHERFDSNCITPGTEFMVRLQEGLRA
       Culex quinquefasciatus XRN1    RFRSAREA-------QEQVEQAEKKGDVL----PLEARFDSNCITPGTSFMVRLQRALEH
      Saccharomyces cerevisiae XRN1   RFRTAMDA-------EKALKKAIENGDEI----PKGEPFDSNSITPGTEFMAKLTKNLQY
         Kluyveromyces lactis XRN1    RFRTAMDA-------EKALQKAIENGDEL----PKGEPFDSNAITPGTEFMAKLTENLKY
          Arabidopsis thaliana XRN4   RFRAAKDAA-EAEAEEEERLRKDFEMEGQILSAKEKAETCDSNVITPGTPFMAILSVALQY
      Saccharomyces cerevisiae XRN2   RFRSARDAQIENEAREEIMRQREEVGEIIDDAVRNKKTWDSNAITPGTPFMDKLAAALRY


                  Homo sapiens XRN1    FVNMKISTDKSWQGVTIYFSGHETPGEGEHKIMEFIRSEKAKPDHDPNTRHCLYGLDADL
                  Mus musculus XRN1    FVNMKISTDKSWQGVTIYFSGHETPGEGEHKIMEFIRSEKAKPDHDPNTRHCLYGLDADL
   Drosophila melanogaster Pacman     FLKTKISTDPLWQRCTVILSGQEAPGEGEHKIMDYIRYMKTQPDYDPNTRHCLYGLDADL
       Culex quinquefasciatus XRN1    FIKVKVSTNPLWKHCKVVLSGHETPGEGEHKIMEYIRHAKASPGFDSNTRHCLYGLDADL
      Saccharomyces cerevisiae XRN1   FIHDKISNDSKWREVQIIFSGHEVPGEGEHKIMNFIRHLKSQKDFNQNTRHCIYGLDADL
         Kluyveromyces lactis XRN1    FIHDKITNDTRWQNVKVIFSGHEVPGEGEHKIMDYIRAIRAQEDYNPNTRHCIYGLDADL
          Arabidopsis thaliana XRN4   YIQSRLNHNPGWRYVKVILSDSNVPGEGEHKIMSYIRLQRNLPGFDPNTRHCLYGLDADL
      Saccharomyces cerevisiae XRN2   WTAFKLATDPGWKNLQVIISDATVPGEGEHKIMNFIRSQRADPEYNPNTTHCIYGLDADL


                  Homo sapiens XRN1    IMLGLTSHEAHFSLLREEVRFGG-------------------KKTQRVCA-----PEETT
                  Mus musculus XRN1    IMLGLTSHEAHFSLLREEVRF----------GG---------KKTQRVCAP-----EETT
   Drosophila melanogaster Pacman     IILGLCTHELHFVVLREEVKF--------------G-----RNVKRTS------VEETR
       Culex quinquefasciatus XRN1    IMLGLCTHERHFSLLREEVKF---------G--------KNDKKSSI-----VEETR
      Saccharomyces cerevisiae XRN1   IMLGLSTHGPHFALLREEVTF---------G--------RRNSEKKS-----LEHQN
         Kluyveromyces lactis XRN1    IILGLSTHDHHFCLLREEVTF---------G--------KRSSSVKT-----LETQN
          Arabidopsis thaliana XRN4   IMLSLATHEVHFSILREVITYPGQQEKCFVCGQTGHFASDCPGKSGSNNAAADIPIHKKK
      Saccharomyces cerevisiae XRN2   IFLGLATHEPHFKILREDVFAQ-D-------NRKRNNLKDTINMTEEEKQFLQKQNSEQP


                  Homo sapiens XRN1    FHLLHLSLMREYIDYEFSVLKEKITFKYDIERIIDDWILMGFLVGNDFIPHLPHLHINHD
                  Mus musculus XRN1    FHLLHLSLMREYIDYEFSALKEKITFKYDIEKIIDDWILMGFLVGNDFIPHLPHLHINHD
   Drosophila melanogaster Pacman     FFLLHLGLLREYLELEFDALRTD-EHKLDIAQLIDDWVLMGFLVGNDFIPHLPCLHISSN
       Culex quinquefasciatus XRN1    FYLLHLTLLREYLELEFAPVRDKLKFEFNPYKLIDDWVLMGYMVGNDFIPHLPNLHINEN
      Saccharomyces cerevisiae XRN1   FYLLHLSLLREYMELEFKEIADEMQFEYNFERILDDFILVMFVIGNDFLPNLPDLHLNKG
         Kluyveromyces lactis XRN1    FFLLHLSILREYLALEFEEITDSVQFEYDFERVLDDFIFVLFTIGNDFLPNLPDLHLKKG
          Arabidopsis thaliana XRN4   YQFLNIWVLREYLQYELAI--PDPPFMINFERIIDDFVFLCFFVGNDFLPHMPTLEIREG
      Saccharomyces cerevisiae XRN2   FLWLHINVLREYLSAELWV--PGLPFTFDLERAIDDWVFMCFFCGNDFLPHLPCLDVREN
```

187

```
             Homo sapiens XRN1    ALPLLYGTYVTILPELGGYINESGHLNLPRFEKYLVKLSDFDREHFSEVFVD----LKWF
              Mus musculus XRN1    ALPLLYGTYIAILPELGGYINESGHLNLPRFERYLVKLSDFDREHFSEVFVD----LKWF
   Drosophila melanogaster Pacman  ALPLLYRTYIGIYPTLGGNINENGKLNLRRLQIFISALTEVELDHFKEHADD----LKYM
      Culex quinquefasciatus XRN1  ALPTLFQAYMDVLPGLDGYINEGGILNLERLEVLMERLARFDRDIFLENYTD----LQYF
    Saccharomyces cerevisiae XRN1  AFPVLLQTFKEALLHTDGYINEHGKINLKRLGVWLNYLSQFELLNFEKDDID----VEWF
      Kluyveromyces lactis XRN1    AFPVLLQTFKEALQHMDGYINEQGKINLARFSIWLKYLSDFEYLNFEKKDID----VEWF
        Arabidopsis thaliana XRN4  AINLLMHVYRKEFTAMGGYLTDSGEVLLDRVEHFIQAVAVNEDKIFQKRTRI----KQSM
    Saccharomyces cerevisiae XRN2  SIDILLDIWKVVLPKLKTYMTCDGVLNLPSVETLLQHLGSREGDIFKTRHIQEARKKEAF

             Homo sapiens XRN1    ESKVGN-----K-------------------------------Y----------LNEAAG
              Mus musculus XRN1    ESKVGN---K---------------------------------Y------------LNEAAG
   Drosophila melanogaster Pacman  NNK--------S-------------------------------E-------------AFD
      Culex quinquefasciatus XRN1  KAKRGA---------N---------------------------D-------TEAFD
    Saccharomyces cerevisiae XRN1  NKQLENISLEGERKRQRVGKKLLVKQQKKLIGSIK-------PWLMEQLQEKLSPDLPD
      Kluyveromyces lactis XRN1    NQQLENISLEGERKRTRMGKKLLMKQQKKLIGAVK-------PWLLKTVQRKVTSELQD
        Arabidopsis thaliana XRN4  DNN------------------E--------------------------------------
    Saccharomyces cerevisiae XRN2  ERRKAQKNMSKGQDRHPTVATEQLQMYDTQGNLAKGSWNLTTSDMVRLKKELMLANEGNE

             Homo sapiens XRN1    VAAEEARNYKEKKKLKGQE--------------------------NSLCWTALDKNEG
              Mus musculus XRN1    AAAEEAKNCKEKRKPKGQE--------------------------NSLSWAALDKSEG
   Drosophila melanogaster Pacman  MDVGEITESQNLDSDLGA--------------------------LINKSMLLYDDDSE
      Culex quinquefasciatus XRN1  VTLEEIKADMDMDLSALIK-------------------------ASEDM-FLDDDED
    Saccharomyces cerevisiae XRN1  EEIPTLELPKDLDMKDHLEFLKEFAFDLGLFITHSKSKGSYSLKMDLDSINP-DETEEEF
      Kluyveromyces lactis XRN1    ADFEIFPLEDKELVRANLDFLKEFAFDLGLILAHSKSKDLYYFKLDLDSINV-QETDEEH
        Arabidopsis thaliana XRN4  ----EMKQRSRRDPSEV-------P-----------------------------------
    Saccharomyces cerevisiae XRN2  EAIAKVKQQSDKNNELMKDISKEEIDDAVSKANKTNFNLAEVMKQKIINKKHRLEKDNEE

             Homo sapiens XRN1    EMITSK--------D------NLEDETE----------------D--------------
              Mus musculus XRN1    EGVASR------D--------NFEDETE-------------D-----------------
   Drosophila melanogaster Pacman  EDCSDE---------------NAVLLKE----------------F--------------
      Culex quinquefasciatus XRN1  GGGERY---------------STEDIEN----------------------------D-P
    Saccharomyces cerevisiae XRN1  QNRVNSIRKTIKKYQNAIIVEDKEELET---------------------------E-K
      Kluyveromyces lactis XRN1    EARIHETRRSIKKYEQGIIIASEEELEE---------------------------E-R
        Arabidopsis thaliana XRN4  ----------------------PEPIDD---------------------------K--
    Saccharomyces cerevisiae XRN2  EEIAKDSKKVKTEKAESECDLDAEIKDEIVADVNDRENSETTEVSRDSPVHSTVNVSEGP

             Homo sapiens XRN1    -DDLFETEF------RQYKRTYYMTKMGVD--VVSDDFLADQAACYVQAIQWILHYYYHG
              Mus musculus XRN1    -DDLFETE------FRQYKRTYYMTKMGVD--VVSDEFLANQAACYVQAIQWILHYYYHG
   Drosophila melanogaster Pacman  ----------------QNYKRNFYRNKFKRD---PNDELIEELCHHYVNALQWVLDYYYRG
      Culex quinquefasciatus XRN1  -E-LFEKE------FAAYKRNYYMTKMGYG-DFN-EETRAEQAECYIRALQWTLLYYYRG
    Saccharomyces cerevisiae XRN1  -T-IYNER------FERWKHEYYHDKLKFT-TDS-EEKVRDLAKDYVEGLQWVLYYYRG
      Kluyveromyces lactis XRN1    -E-IYSER------FVEWKDQYYKDKLDFS-IND-TDSLKEMTENYVGGLQWVLYYYRG
        Arabidopsis thaliana XRN4  I----KLG------EPGYKERYYAEKFSTTNPEETEQIKQDMVLKYVEGLCWVCRYYYQG
    Saccharomyces cerevisiae XRN2  KNGVFDTDEFVKLFEPGYHERYYTAKFHVT-PQDIEQLRKDMVKCYIEGVAWVLMYYYQG

             Homo sapiens XRN1    VQSWSWYYPYHYAPFLSDIHNISTLKIHFELGKPFKPFEQLLAVLPAASKNLLPACYQHL
              Mus musculus XRN1    VQSWSWYYPYHYAPFLSDIRSISTLKIHFELGKPFKPFEQLLAVLPSASKNLLPTCYQHL
   Drosophila melanogaster Pacman  VQSWDWYYPFHYTPFISDLKNIEQVEIAFHMGTPFLPFQQLLAVLPAASAKLLPVAYHDL
      Culex quinquefasciatus XRN1  VSSWAWYYPHHYAPFISDVQNFKNIKLNFEMGKPFLPFQQLLSVLPAASKDHLPTAYHKL
    Saccharomyces cerevisiae XRN1  CPSWSWYYPHHYAPRISDLAKGLDQDIEFDLSKPFTPFQQLMAVLPERSKNLIPPAFRPL
      Kluyveromyces lactis XRN1    CPSWSWYYRYHYAPRISDVIKGIDQNIEFHKGQPFKPFQQLMAVLPERSKNLIPVVYRPL
        Arabidopsis thaliana XRN4  VCSWQWFYPYHYAPFASDLKNLPDLEITFFIGEPFKPFDQLMGTLPAASSNALPGEYRKL
    Saccharomyces cerevisiae XRN2  CASWNWFYPYHYAPLATDFHGFSHLEIKFEEGTPFLPYEQLMSVLPAASGHALPKIFRSL
```

188

```
            Homo sapiens XRN1  MTNEDSPIIEYYPPDFKTDLNGKQQEWEAVVLIPFIDEKRLLEAMETCNHSLKKEERKRN
            Mus musculus XRN1  MTSEDSPIIEYYPPDFKTDLNGKQQEWEAVVLIPFIDETRLLEAMETCNHSLKKEERKRN
  Drosophila melanogaster Pacman  MLLPTSPLAEFYPLEFESDLNGKKHDWEAVVLIPFIDEGRLLAAMLPCEAQLSLEERERN
      Culex quinquefasciatus XRN1  MTDPDSSVIDYYPENFGTDLNGKQQAWEAVVLIPFIDEKRLLKAMEPCDAFLTDEEKQRN
    Saccharomyces cerevisiae XRN1  MYDEQSPIHDFYPAEVQLDKNGKTADWEAVVLISFVDEKRLIEAMQPYLRKLSPEEKTRN
       Kluyveromyces lactis XRN1  MYDEHSPILDFYPNEVELDLNGKTADWEAVVKISFVDQKRLVEAMAPYDAKLSPDEKKRN
        Arabidopsis thaliana XRN4  MTDPSSPILKFYPADFELDMNGKRFAWQGIAKLPFIEEKLLLAATRKLEETLTVEEQQRN
    Saccharomyces cerevisiae XRN2  MSEPDSEIIDFYPEEFPIDMNGKKMSWQGIALLPFIDQDRLLTAVRAQYPLLSDAERARN

            Homo sapiens XRN1  QHSECLMCWYDRDTEFIYPSPWPEKFPAIE-RCCTRYKIISLDAWRVD--INKNKITRID
            Mus musculus XRN1  QHSECLMCWYDRDTEFTYSSPWPEKFPAIE-RCCTRYKMISLDAWRVD--INKNKITRVD
  Drosophila melanogaster Pacman  RHGP--MYVYKYSTVAQGPMPAYPPLRALPVLYCTEVAKWSHEIAVN---LPYSVCIELP
      Culex quinquefasciatus XRN1  VHGPMMLFQYDEQGSAFLGANYG--LDDVAELKVKEIPIYRDDLYVPENKLVLGPSKGAI
    Saccharomyces cerevisiae XRN1  QFGKDLIYSFNPQVDNLYKSPLGGIFSDIEHNHCVEKEYITIPLDSSE--IRYGLLPNAK
       Kluyveromyces lactis XRN1  SFGTDLIFIFNPQVDTVYKTPLAGLFNDIEHNHCIEREFIPESMENVK--FLFGLPKGAK
        Arabidopsis thaliana XRN4  SVMLDLLYVHPAHPLGQRILQYYHFYQHMPPHECLPWMIDPNSSQGMNGFLWFSERNGFQ
    Saccharomyces cerevisiae XRN2  IRGEPVLLISNKNANYERFSKKLYSKENNNNNVVVKFQHFKSGLSG----IVSKDVEGFE

            Homo sapiens XRN1  QKAL--YFCGFPTLKHIRHKFFLKKSGVQVFQQSSRGENMMLE--ILVDAESDELTVENV
            Mus musculus XRN1  QKAL--YFCGFPTLKHIKHKFFLKKSGVQVFQQSSRGENLMLE--ISVNAEPDELRIENI
  Drosophila melanogaster Pacman  NAARTVFFPGFPTMQHLPFDFELRNDRVKVFEQVSRNQNIVL----KPRKRQLEDTLTAV
      Culex quinquefasciatus XRN1  LDG---YIKGFPTMKHLKYHGILKEIRVKVFNFPSRNASMVV----AIDKEGDDKSTAQL
    Saccharomyces cerevisiae XRN1  LGAE--MLAGFPTLLSLPFTSSLEYNETMVFQQPSKQQSMVLQ--ITDIYKTNNVTLEDF
       Kluyveromyces lactis XRN1  LGAS--SLAGFPSLKTLPLTAELAYNSSVVFNFPSKQQSMVLH--IQDLYKENGISLSDL
        Arabidopsis thaliana XRN4  TRVDSP-VNGLPCIEQNRALNVTYLCPAKHSHISEPPRGAII-----PDKILTSVDIKPF
    Saccharomyces cerevisiae XRN2  LNGKIVCPIQGGSLPNLSTTLILKMS-YRLIPLPSRNKSIILNGFIPSEPVLTAYDLDSI

            Homo sapiens XRN1  ASSVLGKSVFVNWPHLEE-ARVVAVSDGETKFYLEEPPGTQKLYSGRTAPPSKVVHLGDK
            Mus musculus XRN1  ASAVLGKAVFVNWPHLEE-ARVVAVSDGETKFYIEEPPGTQKVYLGKTAPPSKVIQLTDK
  Drosophila melanogaster Pacman  ASQYLGKVIHVGWPHLVK-AIVVRVATRDQRVDSE----------------GITLNDSR
      Culex quinquefasciatus XRN1  AQELLGSIVYVSWPHLTE-AKVVKVADAKTVYEKD-----------REERPNN-----EK
    Saccharomyces cerevisiae XRN1  SKRHLNKVIYTRWPYLRE-SKLVSLTDGKTIYEYQESNDKKKFGFITKPAETQ----DKK
       Kluyveromyces lactis XRN1  AKRHMGKIVYSRWPFLRE-SKLLSLITEETVYEGV------KSGKLTKVIERKPQDFERK
        Arabidopsis thaliana XRN4  P-PLWHEDNSNRRRQARDRPQVVGAIAGPSLGEAAHRLIKNTLNMKSSTGAASGLIDPNG
    Saccharomyces cerevisiae XRN2  MYKYNNQNYSRRWNFGNDLKQNIVPVGPKGITQYKPRTGGYRAFFYFAELSRNNVQPAHN

            Homo sapiens XRN1  EQSNWAKEVQGISEHYLRRKG-----IIINETSAVVYAQLLTGRKYQINQNGEVRLEKQW
            Mus musculus XRN1  EQSNWTKEIQGISEQYLRRKG-----IIINETSAVVYAQLLTGRKYQISQNGEVRLEKQW
  Drosophila melanogaster Pacman  RFDSECKALQ---EHFITRMG-----IQFANYDVLVYVRTFAGNSTEFRDKGALMVRDSW
      Culex quinquefasciatus XRN1  FFGTCVKAIV---EHHSNRLA-----IDLGEIRQLVHVKTCVGSEY-VLKDDRYVLNKLW
    Saccharomyces cerevisiae XRN1  LFNSLKNSML---RMYAKQKA-----VKIGPMEAIATVFPVTG----LVRDSDGGYIKTF
       Kluyveromyces lactis XRN1  EFRELKMTLK---SNYQRTKA-----ILLDDISALAKVVPVNG----LVRNSDGSYSKSF
        Arabidopsis thaliana XRN4  YYRNVPGNYSYGGVNRPRAPGPSPYRKAYDDDSSYYYGKYNNSTQGTFNNGPRYPYPSNG
    Saccharomyces cerevisiae XRN2  YGRNSYNSQPG--FNNSRYDGGNNNYRQNSNYRNNNYSGNRNSGQYSGNSYSRNNKQSRY

            Homo sapiens XRN1  SKQVVPFVYQTIVKDIRAFDSRFS--NIKTLDDLFPLRSMVFMLGTPYYGCTGEVQDSGD
            Mus musculus XRN1  SKQILPFVYQTIVKDIRAFDSRFS--NIKTLDDLFPPRTMVFMLGTPYYGCTGEVQDSGD
  Drosophila melanogaster Pacman  SSSVTGYPAQGVVADLTVWERMRK--NFLNVEHYFPVGSTIFLITDPYYGSEGTVQDPRL
      Culex quinquefasciatus XRN1  NQGETMYPVQAIVTDLR--EALRTLKPYQEVQEMFPENCVVFLRATQWYGSMGHVVDVTA
    Saccharomyces cerevisiae XRN1  SPTPDYYPLQLVVESVVNEDERYKERGPIPIEEEFPLNSKVIFLGDYAYGGETTI-DGYS
       Kluyveromyces lactis XRN1  NETIEYYPLQLIVEDVKNKDERYIEKEPLPINKEFPKGSKVVFLGDYAYGGEATV-DGYN
        Arabidopsis thaliana XRN4  SQDYNRNYNSKIVAEQHNRGGLGAGMSGLSIEDNGRSKQLYSSYTEAANANLNPLPSPPT
    Saccharomyces cerevisiae XRN2  DNSRANRR----------------------------------------------------
```

189

```
             Homo sapiens XRN1  VPTQVPTKDDDEFCNIWQSLQGSGKMQYFQPTIQEKGAVLPQEISQVNQHHKSGFNDNSV
             Mus musculus XRN1  LPTQVPTKGDDEFCNIWQSLQGAGKIQHLQPTVQEKGAVLPQEISQVTEGHKSGFTDHSV
 Drosophila melanogaster Pacman  MKTQISDEFVKTRSSPIARTDSYKPSSEPKPVPVPEQITNWRERVSTPTNKPQPAPNNWR
      Culex quinquefasciatus XRN1  VKPSKPTAKSESIKKRLNERIEKNPNPMKAFVMANRKPLEENGANSQAGCDFEKVWNKLR
    Saccharomyces cerevisiae XRN1  RAHDLLNFIKKDTNEKNSESVDNKSMGSQKDSKPAKKVLLKRPAQKSSENVQVDLANFEK
         Kluyveromyces lactis XRN1  LNHIKKDNAESNTESGSAPQIAVNTLNPSAANNVFNAVLNQIKPGSQQQIQPPPANSLPY
        Arabidopsis thaliana XRN4  ------------------------------------------------------------
    Saccharomyces cerevisiae XRN2  ------------------------------------------------------------

             Homo sapiens XRN1  KYQQRKHDPHR--KFKEECKSPKAECWSQKMSNKQPNS--G--------------------
             Mus musculus XRN1  RHQQRKHDSQR--KFKEEYKSPKAECQSQKLSSKQTSGGSARCSIKLLKRNESPGTSEAQ
 Drosophila melanogaster Pacman  INRSSSRQQGGSIFVAPPTKTPDAAASTASTAFTAASSATL---------TPLDQTLAL-
      Culex quinquefasciatus XRN1  EPNQTTTTTLDERDIKSFLANAAPAAQESAPVPTNPLAPSS---------DPTDMLKKM-
    Saccharomyces cerevisiae XRN1  APLDNPTVAGSIFNAVANQYSDGIGSNLNIPTPPHPMNVVG---------GPIPGANDVA
         Kluyveromyces lactis XRN1  NFTVPPHMVPGGIPHPLMMQPPFIPNNEHIAYAAPPQSQPV---------QNPPLDKEA-
        Arabidopsis thaliana XRN4  ------------------------------------------------------------
    Saccharomyces cerevisiae XRN2  ------------------------------------------------------------

             Homo sapiens XRN1  ----------------IENFLASLNISKENEVQSSHHGEPPSEEHLSPQSFAMG---TRM
             Mus musculus XRN1  KVVTSYPNAVHKPPSGIENFLASLNLSKENEAQLPHHGEPPDEADLSPQSFAMKG--TRM
 Drosophila melanogaster Pacman  -M-----SVLGVGEDQSSPPLQEAVQQQRPPLLQQQRAPFPGQMPNLPKPPLFWQQEAQK
      Culex quinquefasciatus XRN1  ---L-KISADQEPAVQTPPQLNIPMPKNLPKPPSSWRSDHKSAKDTVKQQHPADKPQQKQ
    Saccharomyces cerevisiae XRN1  D-V-GLPYNIPPGFMTHPNGLHPLHPHQMPYPNMNGMSIPPPAPHGFGQPISFPPPPPMT
         Kluyveromyces lactis XRN1  --S-RNLKNLLIRDENGRTANVENKDSDDTKRSSHSRGGRRGRSNRGRGASGRGGHFKNS
        Arabidopsis thaliana XRN4  ------------------------------------------------------------
    Saccharomyces cerevisiae XRN2  ------------------------------------------------------------

             Homo sapiens XRN1  LKEILKIDGSNTVDHKNEIKQIANEIPV--SSNRRDEYGLPSQPKQNKKLASYMNKPHS-
             Mus musculus XRN1  LKEILKIDSPDTRDSKNDMKKSDNEATV---SSRRDERGVSAHPKPSKKLTCHMNKPHG-
 Drosophila melanogaster Pacman  QEALQQEAQQQEAQKKQQQAHAQMEPERINSQHFYRSGQTGAALNQPPLGAPSKRQWHEW
      Culex quinquefasciatus XRN1  NHQMPMPPQPFAQFQPYQLAHQQNRYQPPPGQFLPNQYQPMPRYQPQMPMPPQKNNNHS-
    Saccharomyces cerevisiae XRN1  NVSDQGSRIVVNEKESQDLKKFINGKQHSNGSTIGGETKNSRKGEIKPSSGTNSTECQS-
         Kluyveromyces lactis XRN1  PKKTET------------------------------------------------------
        Arabidopsis thaliana XRN4  ------------------------------------------------------------
    Saccharomyces cerevisiae XRN2  ------------------------------------------------------------

             Homo sapiens XRN1  -ANEYHNVQSMDNMCWPAPSQIPPVSTPVTELSRICSLVGMPQPDFSFLRMPQTMTVCQV
             Mus musculus XRN1  -TNEFQNVASVDSVCWPG--QMPPVSTPVTELSRICSLVGMPQPDFSFLRTTQTMTVCQV
 Drosophila melanogaster Pacman  VHPRMQHANAFHAGVNNGYQMRPKKNIAAQSTFNNNVHMHLQQPYYPNQQQQQQQQQPLQ
      Culex quinquefasciatus XRN1  -AYQQFNQHHQQLQQQLYRPQYYPGNGPQNNNNNNQHHLRQRGPNGPQNLSFNRNTPAGT
    Saccharomyces cerevisiae XRN1  -PKSQSNAADRDNKKDEST-----------------------------------------
         Kluyveromyces lactis XRN1  ------------------------------------------------------------
        Arabidopsis thaliana XRN4  ------------------------------------------------------------
    Saccharomyces cerevisiae XRN2  ------------------------------------------------------------

             Homo sapiens XRN1  KLSNGLLVHGPQCHSENEAKEKAALFALQQLGSLGMNFPLPSQVFANYPSAVPP--GTIP
             Mus musculus XRN1  KLSNGLLVHGPQCHSESEAKERAALFALQQLGSLGVSFPLPPPIFTNYPPAVPP------
 Drosophila melanogaster Pacman  LTEINNAPPRYSTIQDFVPIQAYRPKKLNRVQPAGRQDVDATKNPSRSPVLQQPTNETID
      Culex quinquefasciatus XRN1  GAFVPLQAIIKSKTRPNGGGNKSNKAGSSNANSTGFAQKNAELRQKVEQKQQENKQDFAS
    Saccharomyces cerevisiae XRN1  ------------------------------------------------------------
         Kluyveromyces lactis XRN1  ------------------------------------------------------------
        Arabidopsis thaliana XRN4  ------------------------------------------------------------
    Saccharomyces cerevisiae XRN2  ------------------------------------------------------------
```

```
                 Homo sapiens XRN1   VITEGRIRV-IFSIPCEPNLDALIQNQHKYSIKYNPGYVLASRLGVSGYLVSRFTGSIFI
                 Mus musculus XRN1   LITEGRIRV-VFSIPCEPNLDALIQNQHKYSIKYNPGYVLAGRLGVSGYLVSRFTGSIFI
  Drosophila melanogaster Pacman    AYTNGRIQVSIM-VRPEPKVNAARQLQEERDRDYLSTFQVCNLLRISGRTLGRLSGTVWV
       Culex quinquefasciatus XRN1   GHKRIKTR---FEIYEEPNLDTVLKIDDEARSHYLTTYDAASSIGISANLLSRLSSTIYM
     Saccharomyces cerevisiae XRN1   SDRRLKITVEKKFLDSEPTIGKERLQMDHQAVKYYPSYIVSKNMHLHPLFLSKITSKFMI
         Kluyveromyces lactis XRN1   SETRLKLTVKKGSLRAEPNIGKVRAKLDSQALRFYPTQVFSKIARVHPLFLSKITSRYLV
          Arabidopsis thaliana XRN4   QWIGTQPGGNFVGGYYRDGVGYSETNGKSVKKVIYQAKTQPSHRGANL------------
     Saccharomyces cerevisiae XRN2   ------------------------------------------------------------

                 Homo sapiens XRN1   GRGSRRN--PHGDHKANVGLNLKFNKKNEEVPGYTKKVGSEWMYSSAAEQLLAEYLERAP
                 Mus musculus XRN1   GRGSRRN--PHGDHKANVGLNLKFNKKNEEVPGYTKKVGNEWMYSSAAEQLLAEYIERAP
  Drosophila melanogaster Pacman    VLGPRRQ-KMENVDQAQHWPAAQVSAAERGACRILLPHEQPVVLLQPGRGSDAQLLPALP
       Culex quinquefasciatus XRN1   VTGGRRSLNVDEKGKMNIGLQLRLVSQDIETVGYTRKMAKNWMYSDKAIELVKAYYDKVP
     Saccharomyces cerevisiae XRN1   TDATGK--------HINVGIPVKFEARHQKVLGYARRNPRGWEYSNLTLNLLKEYRQTFP
         Kluyveromyces lactis XRN1   NDSKKK--------SHNVGLMIKFKARNQKVLGYARCSSNKWEYSDVALGLLEQFRSTFP
          Arabidopsis thaliana XRN4   ------------------------------------------------------------
     Saccharomyces cerevisiae XRN2   ------------------------------------------------------------

                 Homo sapiens XRN1   ELFSYIAKNSQEDVFYEDDIWPGENENGAEKV-QEIITWLKGHPVSTLSRSSCDLQILDA
                 Mus musculus XRN1   ELFSYIAKNSQEDVFYEDDIWPGENENGAEKV-QEIITWLKGHPVSTLSRSSCDLHILDA
  Drosophila melanogaster Pacman    RRYRLLWRLQRSRRVRIRT--GRVPQCGWPSPRRGMANWVRQQPHMKVERISCGSKTVCR
       Culex quinquefasciatus XRN1   QVFEKLESFGNRDVLFEDEIFGEKREEG--SGLKELVAWIKAQDHAKAEKRSCGTKILEP
     Saccharomyces cerevisiae XRN1   DFFFRLSKVGN-DIPVLEDLFPDTSTKDAMNLLDGIKQWLK-YVSSKFIAVSLESDSLTK
         Kluyveromyces lactis XRN1   EFFAKLSNSKEQAIPSITDLFPNKSSAEADSILKTVADWLS-EARKPFVVVSLESDSLTK
          Arabidopsis thaliana XRN4   ------------------------------------------------------------
     Saccharomyces cerevisiae XRN2   ------------------------------------------------------------

                 Homo sapiens XRN1   AIVEKIEEEVEKCKQRKNNKKVRVTVK-PHLLYRPLEQQHGVIPDRDAEFCLFDRVVNVR
                 Mus musculus XRN1   AIVEKIEEEVEKCKQRKSNKKVRVTVK-PHLLYRPLEQQHGVIPDRDAEFRLFDRVVNVR
  Drosophila melanogaster Pacman    ETIELLIAAVDE-LRSLPVKHVKLQVK-PHLLIKPNVTLPDVY-RSKRPVRLFDRVVIVR
       Culex quinquefasciatus XRN1   AAVEELVKIRAESVRQLPTMQTMFVH--PKDLYKPGMKQARSI-DYMANYELLDRVIIAR
     Saccharomyces cerevisiae XRN1   TSIAAVEDHIMKYAANIEGHERKQLAKVPREAVLNPRSSFALL--RSQKFDLGDRVVYIQ
         Kluyveromyces lactis XRN1   ASMAAVESEIIKYVSLPDSSEQKKLAKVPREAILNAESSYVLL--RSQRFHLGDRVMYIQ
          Arabidopsis thaliana XRN4   ------------------------------------------------------------
     Saccharomyces cerevisiae XRN2   ------------------------------------------------------------

                 Homo sapiens XRN1   ENFSVPVGLRGTIIGIKGAN----------READVLFEVLFDEEFPGGLTIRCSP---GR
                 Mus musculus XRN1   ESFSVPVGLRGTVIGIKGAS----------READVLFEVLFDEEFPGGLTIRCSP---GR
  Drosophila melanogaster Pacman    TIYMVPVGTKGTVIGIHPVTDPNPVRLECVHAVDTFCKVLFDSPVPNCNNIHGIAE--DR
       Culex quinquefasciatus XRN1   ETEVVPLGYRGTIIGIHLAKDPNPVRQESVSKEDKYFDILFDKQFPNGTHIFGIEQTRNR
     Saccharomyces cerevisiae XRN1   DSGKVPIFSKGTVVGYTTLSS------------SLSIQVLFDHEIVAGNNFGGRLRT-NR
         Kluyveromyces lactis XRN1   DSGKVPLHSKGTVVGYTSIGK------------NVSIQVLFDNEIIAGNNFGGRLQT-RR
          Arabidopsis thaliana XRN4   ------------------------------------------------------------
     Saccharomyces cerevisiae XRN2   ------------------------------------------------------------

                 Homo sapiens XRN1   GYRLPTSALVNLSHGSRSETGNQKLTAIVKPQPAVHQHSSSSSVSSGHLGALNHSPQSLF
                 Mus musculus XRN1   GYRLPTSALVNLSHGSRCETGNQKLTAIVKPQPSV---SHCSAAPSGHLGGLNHSPQSPF
  Drosophila melanogaster Pacman    VYKVPEIALVIIKTDEEGKKQNDCELPVRDPQPNQAQDEPVRATSSRYVTAAGSTSVPIT
       Culex quinquefasciatus XRN1   VVRVAEGAILNISFGVADFEYKQVDPAQPIMLPA---EEFCPGGLASKQPSTVRSVETIR
     Saccharomyces cerevisiae XRN1   GLGLDASFLLNITNRQFIYHSKASKKALEKKKQSNNRNNNTKTAHKTPSKQQSEEKLRKE
         Kluyveromyces lactis XRN1   GLGLDSSFLLNLSDRQLVYHSKASKSADKKPK-AVPNDKQVALAKKKRVEELKKKQAHEL
          Arabidopsis thaliana XRN4   ------------------------------------------------------------
     Saccharomyces cerevisiae XRN2   ------------------------------------------------------------
```

191

Appendix 1. Continued.

```
              Homo sapiens XRN1    PAFPPPTGWDHYGSNYALGAANIMPSSSHLFGSMPWGPSVPVPGKPFHHTLYSGTMPMAG
              Mus musculus XRN1    ----GAVP-----PVFTQPTANIMPSSSHLFGSVSWRPPVPVAGNAFHYPSYPGTMPLAG
   Drosophila melanogaster Pacman  TKASSSLPVQSAGEQVIGLMQTLEIKQPAASQSESDGVSTGSANAPTATTSSQAVNRRKH
       Culex quinquefasciatus XRN1  FLGGAGKSVEAAAAAVVTTADEKCDKPERKKDDGGDGVQKTASTSPKPPKVRQMRIAANF
    Saccharomyces cerevisiae XRN1   ----------------------------------------------------------
          Kluyveromyces lactis XRN1 ----------------------------------------------------------
          Arabidopsis thaliana XRN4 ----------------------------------------------------------
    Saccharomyces cerevisiae XRN2   ----------------------------------------------------------

              Homo sapiens XRN1    GIPGGVHNQFIPLQVTKKRVANKKNFENKEAQSSQATPVQTSQPDSSNIVKVSPRESSSA
              Mus musculus XRN1    GVPGGVHSQFIPLQVTKKRVANRKNFENKEAQSSQATPLQTNKPGSSEATKMTPQESPPA
   Drosophila melanogaster Pacman  RVPRIGAKFDLEYILPDSPHPT------------------------------------
       Culex quinquefasciatus XRN1  SQAD------------------------------------------------------
    Saccharomyces cerevisiae XRN1   ----------------------------------------------------------
          Kluyveromyces lactis XRN1 ----------------------------------------------------------
          Arabidopsis thaliana XRN4 ----------------------------------------------------------
    Saccharomyces cerevisiae XRN2   ----------------------------------------------------------

              Homo sapiens XRN1    SLKSSPIAQPASSFQVETASQGHSISHHKSTPISSSRRKSRKLAVNFGVSKPSE
              Mus musculus XRN1    SSSSSQAAQPVSSHVETASQGHVGSQPRSAPSSSKRKSRKLAVNFSVSKPSE--
   Drosophila melanogaster Pacman  ----------------------------------------------------
       Culex quinquefasciatus XRN1  ----------------------------------------------------
    Saccharomyces cerevisiae XRN1   ----------------------------------------------------
          Kluyveromyces lactis XRN1 ----------------------------------------------------
          Arabidopsis thaliana XRN4 ----------------------------------------------------
    Saccharomyces cerevisiae XRN2   ----------------------------------------------------
```

Appendix 2. Radiolabeled, 5' monophosphorylated RNAs containing the 5' half of 3' UTR of DENV-2 were incubated with recombinant XRN1 in the presence of 250 µM of the indicated triptycene derivative for two minutes. Reaction products were separated on a 5% polyacrylamide gel containing urea and visualized by phosphorimaging. The decay intermediates generated by XRN1 stalling are indicated by the black arrow on the right. The gel is representative of at least three independent experiments.